Simultaneous identification of nucleotide-modified aptamers with different properties by multiplexed click-SELEX

Dissertation

zur
Erlangung des Doktorgrades (Dr. rer. nat.)
der
Mathematisch-Naturwissenschaftlichen Fakultät
der
Rheinischen Friedrich-Wilhelms-Universität Bonn
vorgelegt von

Olga Plückthun, geb. Wolter

aus

Rostow-am-Don (Russland)

Bonn 2019

Angefertigt mit Genehmigung der Mathematisch-Naturwissenschaftlichen Fakultät der

Rheinischen Friedrich-Wilhelms-Universität Bonn

1. Gutachter: Prof. Dr. Günter Mayer

2. Gutachter: Prof. Dr. Heinz Beck

Tag der Promotion: 26.05.2020

Erscheinungsjahr: 2020

Danksagung

Ein besonderer Dank gilt *Herrn Prof. Dr. Günter Mayer* für die Vergabe des überaus spannenden Themas, seiner hilfreichen Diskussionsbereitschaft, seinem Enthusiasmus sowie den vielreichen Ermutigungen während der gesamten Promotion.

Ich bedanke mich bei allen Mitgliedern meiner Prüfungskommision, *Herrn Prof. Dr. Heinz Beck*, *Frau PD Dr. Gerhild van Echten-Deckert* und *Herrn Prof. Dr. Ulrich Ettinger*, dafür, dass sie sich bereit erklärt haben die vorliegende Arbeit zu begutachten.

Ein großer Dank richtet sich an die Mitglieder der Kollaboration, insbesondere an *Herrn Dr. Dominik Holtkamp*, *Herrn Dr. Thoralf Opitz* und *Frau Sabine Opitz*.

Die vorliegende Arbeit wurde von SFB1089 gefördert. Ich danke Ihnen für die Ermöglichung dieser Arbeit.

Next-generation Sequencing (NGS) hat einen großen Teil zur der vorliegenden Arbeit beigetragen. Ich möchte mich bei allen bedanken, die daran beteiligt waren, insbesondere bei *Herrn Dr. Kristian Händler* und *Frau Kathrin Klee*, die die Sequenzierung durchgeführt haben. Des Weiteren gilt der Dank *Herrn Dr. Michael Blank* und *Herrn Dr. Carsten Gröber* von AptaIT GmbH für die NGS-Analysen. I would like to thank *Laura Lledo Bryant* for the final NGS-analysis and the discussions.

I would like to thank *Dr. Laia Civit* for the patient advice and helpfulness at the beginning of this work, who introduced me to cell culture technology.

Weiterhin möchte ich mich bei den gesamten aktuellen und ehemaligen Mitgliedern der Arbeitsgruppen Mayer, Famulok und Kath-Schorr für die großartige Zeit im Labor bedanken. Danke für die vielen Diskussionen, Ratschläge und Unterstützung. Ein spezieller Dank gilt an *Frau Dr. Silvana Haßel*, *Frau Dr. Franziska Pfeiffer (Ersoy)* und *Frau Julia Siegl* für das Korrekturlesen dieser Arbeit.

Ich möchte mich von Herzen bedanken bei meinen Eltern und meiner Schwester, die mir durch Ihre Unterstützung das Studium der Chemie und somit die Doktorarbeit ermöglicht haben. (Я хотела бы искренне поблагодарить моих родителей и мою сестру за их поддержку в предоставлении мне возможности изучать химию и, таким образом, получить докторскую степень.)

Ein großer Dank gilt meinen Schwiegereltern für ihre großartige Unterstützung und Begeisterung für das Projekt der vorliegenden Arbeit.

Zuletzt möchte ich mich bei meinem geliebten Eheman *Marius Konstantin Plückthun* bedanken, Du gibst mir die Kraft auch die schwierigen Zeiten positiv zu sehen und sie willkommen zu heißen.

Contents

1. Abstract

Voltage-gated sodium channels (VGSC) are important key regulators in excitable tissue that initiate and propagate the action potential in specifically excitable tissue such as brain nerves or muscle. In order to understand the impact of VGSC on the complex nerve system, specific molecular tools are required that enable the spatial-temporal control of VGSC function. These tools shall recognize and modulate VGSC with high affinity and utmost specificity.

Aptamers are short oligo(deoxy)nucleotides that are able to interact with target molecules in a highly affine and specific way. Aptamers are identified by an *in vitro* selection procedure known as SELEX (Systematic Evolution of Ligands by EXponential enrichment).

The present study investigated whether the SELEX methods allow the generation of aptamers targeting voltage-gated sodium channels. Several selection methods such as cell-SELEX, click-SELEX, or SELEX targeting small peptides were investigated using the different subtypes of VGSC ($Na_v1.1$, $Na_v1.2$, $Na_v1.4$, $Na_v1.5$, $Na_v1.6$). All selections led to an enrichment of aptamers targeting the VGSC-presenting HEK293 cells or the peptide immobilization matrix, but not VGSC or VGSC-peptides. One possible cause might be the limited chemical diversity in the subjected library. Click-SELEX, which uses copper(I)-catalyzed alkyne–azide cycloaddition (CuAAC) for DNA functionalization, promises a higher chemical diversity in the library compared to DNA libraries, but allows only one modification per library. The present study established a multiplexed click-SELEX approach. This unique method allows the selection of clickmers from several libraries containing different modifications in one procedure, *e.g.*, by using five different azides for DNA functionalization.

The multiplexed click-SELEX method has been validated in two selections targeting two different proteins, Cycle 3 Green Fluorescent Protein (C3-GFP) and streptavidin. Both selections led to the generation of highly affine and specific clickmers with slow dissociation (k_{off} rate). The clickmers depend on the correct functionalization for interaction with the protein.

Now that multiplexing of modified nucleobases has been established in a SELEX, the procedure in this proof of concept study can be applied to a variety of other targets. The simple applicability of the multiplexed click-SELEX approach will benefit all *in vitro* selection methods and allow the generation of clickmers targeting “difficult” target molecules such as VGSC.

2. Zusammenfassung

Spannungsgesteuerte Natriumkanäle (VGSC) sind wichtige Schlüsselregulatoren im erregbaren Gewebe, die das Aktionspotenzial in spezifisch erregtem Gewebe wie Hirnnerven oder Muskeln initiieren und propagieren. Um die Auswirkungen von VGSC auf das komplexe Nervensystem zu verstehen, sind spezifische molekulare Werkzeuge erforderlich, die eine räumlich-zeitliche Kontrolle der VGSC-Funktion ermöglichen. Diese Werkzeuge sollen VGSC mit hoher Affinität und höchster Spezifität erkennen und modulieren.

Aptamere sind kurze Oligo(desoxy)nucleotide, die in der Lage sind, mit Zielmolekülen auf hochaffine und spezifische Weise zu interagieren. Aptamere werden durch ein *in vitro* Selektionsverfahren namens SELEX (Systematic Evolution of Ligands by EXponential enrichment) identifiziert.

Die vorliegende Studie untersuchte, ob die SELEX-Methoden die Erzeugung von Aptameren ermöglichen, die auf spannungsgesteuerte Natriumkanäle abzielen. Mehrere Selektionsmethoden wie cell-SELEX, click-SELEX oder SELEX, die auf kleine Peptide abzielen, wurden mit den verschiedenen Subtypen von VGSC ($Na_v1.1$, $Na_v1.2$, $Na_v1.4$, $Na_v1.5$, $Na_v1.6$) untersucht. Alle Selektionen führten zu einer Anreicherung von Aptameren, die auf die VGSC-präsentierenden HEK293-Zellen oder die Peptidimmobilisierungsmatrix abzielen, aber nicht auf VGSC oder VGSC-Peptide. Eine mögliche Ursache könnte die begrenzte chemische Vielfalt in der untersuchten Bibliothek sein. Click-SELEX, die die kupfer(I)-katalysierte Alkinazid-Cycloaddition (CuAAC) zur DNA-Funktionalisierung einsetzt, verspricht eine höhere chemische Vielfalt in der Bibliothek im Vergleich zu DNA-Bibliotheken, erlaubt aber nur eine Modifikation pro Bibliothek. Die vorliegende Studie etablierte einen multiplexten click-SELEX-Ansatz. Diese einzigartige Methode ermöglicht die Selektion von Clickmeren aus mehreren Bibliotheken mit unterschiedlichen Modifikationen in einem Verfahren, z.B. durch die Verwendung von fünf verschiedenen Aziden zur DNA-Funktionalisierung.

Die multiplexierte click-SELEX-Methode wurde in zwei Selektionen validiert, die auf zwei verschiedene Proteine abzielen, Cycle 3 Green Fluorescent Protein (C3-GFP) und Streptavidin. Beide Selektionen führten zur Erzeugung von hochaffinen und spezifischen Clickmeren mit langsamer Dissoziation (k_{off} rate). Die Clickmere zeigten eine kritische Abhängigkeit von der korrekten Funktionalisierung für die Interaktion mit dem Protein.

Nachdem das Multiplexing von modifizierten Nukleobasen in einem SELEX etabliert wurde, kann das Verfahren dieser Konzeptbeweis-Studie auf eine Vielzahl anderer Ziele angewendet werden. Die einfache Anwendbarkeit des multiplexen click-SELEX-Ansatzes wird allen *In-vitro*-Selektionsmethoden zugutekommen und die Erzeugung von Clickmeren ermöglichen, die auf "schwierige" Zielmoleküle wie VGSC abzielen.

3. Introduction

One goal of modern neuroscience is to analyse and understand the localization of the various functions in the brain. In order to understand "how" the brain functions, it is necessary to know "where" the various functions are located. Early experimental studies on the brain led to the realization that the electrical stimulation of certain areas of the cortex causes certain parts of the body to move. In addition, injuries to the same areas have impeded the execution of these movements[1]. It has been a long way to find out that this electrical signal in our body is triggered and spread by specific voltage-gated ion channels (VGIC) in excitable tissue.

According to the guidelines of the International Union of Basic and Clinical Pharmacology (IUPHAR) Guides to Pharmacology[2], 145 VGIC[3] are known in the human genome. For the diagnosis and therapy of diseases, all these channels are attractive for drugs, *e.g.* local anaesthetics or neurotoxins. Gene mutations in the channels cause so-called channelopathies, *e.g.* various forms of epilepsy, long or short QT syndrome. It is obvious that a detailed understanding of VGIC function promises improved therapeutic treatment of channelopathies.

A new generation drug could be aptamers (defined in **section 3.1**). With their unique properties, such as the modulation of protein activity through interaction with it[4], aptamers represent a promising way to investigate VGIC functions in the complex nervous system on a new scientific level.

3.1. Aptamers

Aptamers are a diverse class of molecular tools used in chemical biology. They are short oligo(deoxy)nucleotides (RNA and ssDNA) that fold into complex three-dimensional structures and bind to target molecules with high affinity and specificity[5-9]. This specificity is achieved by precise stacking of aptamer bases and side chains of proteins (target molecule), specific hydrogen binding and electrostatic interactions[10-13]. All these interactions are strongly influenced by interaction conditions such as buffer composition, pH or temperature, which may influence the aptamer structure and affinity to the target molecule[14].

Aptamers were selected for different target molecules of small molecules[15], peptides[16], proteins[17,18], with K_D values from nanomolar to picomolar[4,19]. Aptamers are selected in a repetitive process called SELEX (Systematic Evolution of Ligands by Exponential Enrichment) (**section 3.1.1**). This process was developed three decades ago by three independent research groups[5,6,8].

The advantages of aptamers are that they can be synthesized enzymatically or by chemical synthesis. They can be functionalized with a variety of modifications, *e.g.* radioactivity, fluorophores, or affinity markers[7]. In addition, aptamers can be equipped with photolabile groups, so-called cages, at strategic positions. This enables photocontrol of their affinity to the target molecule[20-22]. These unique

properties of aptamers represent a great opportunity to study the functions of VGIC in the complex nervous system that are not accessible to other biological tools.

3.1.1. Introduction to SELEX

This section gives an overview of the SELEX process in general as well as the main methods used in this work.

Selection begins with the incubation of the target molecule with a starting library of 10^{14}-10^{15} single-stranded deoxyribonucleic acid (ssDNA) molecules (**Figure 3.1**). The starting library contains ssDNA molecules with a random region flanked by primer binding sites, which are required for enzymatic amplification[23,24]. After removal of the unbound sequences, the bound sequences are recovered and amplified by polymerase chain reaction (PCR). The generation of ssDNA (for a DNA-SELEX) is then performed, *e.g.* by enzymatic cleavage of the phosphorylated strand or by biotin streptavidin interaction[23]. The enzymatic cleavage requires phosphor modifications of the reverse DNA strand, which is introduced during PCR using a phosphorylated reverse primer. A biotinylated reverse primer is used for biotin streptavidin interaction. In the case of RNA-SELEX, the PCR product is transcribed to RNA. The enriched ssDNA or RNA library is then subjected to the next selection cycle[23].

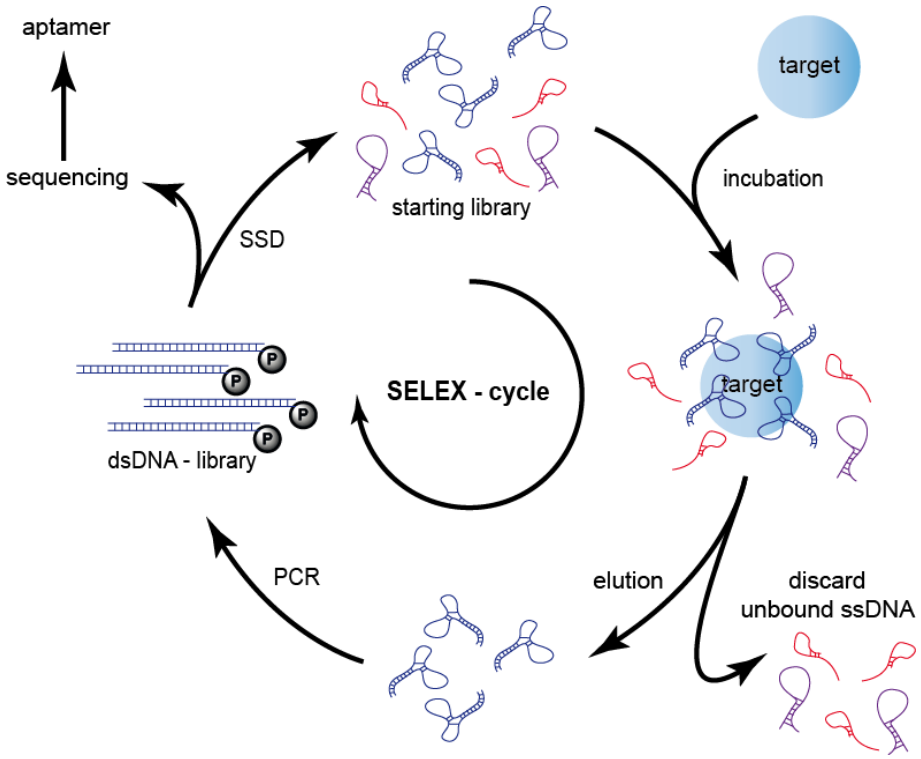

Figure 3.1 Systematic Evolution of Ligands by Exponential enrichment.

Schematic representation of the Systematic Evolution of Ligands by Exponential enrichment (SELEX) process. The starting library is incubated with the target molecule. After removal of unbound ssDNA by washing, the bound sequences are recovered and amplified by PCR. The single strand is generated *e.g.* by enzymatically digestion (SSD) and the enriched library is used for the next selection cycle.

An important step of a successful SELEX is the efficient separation of unbound and bound sequences. This is usually done by washing the target molecule-aptamer complex. For the first selections, nitrocellulose membrane was used to immobilize the target molecule-aptamer complex. Because the nitrocellulose membrane interacts only with proteins and not with nucleic acids[6,25], the unbound sequences were washed away. Today, various immobilization techniques are available, including sepharose[26,27], agarose-based resin[28] or magnetic beads[29,30]. The latter are coated with *e.g.* streptavidin to immobilize biotinylated proteins or functionalized with cobalt or nickel to immobilize His-tagged protein targets. In addition, the immobilization of small molecules can be achieved by covalent bonding by chemical functionalization[31,32]. The immobilization technique used depends on both the target molecule of interest and the selection protocol.

Selection is performed by several selection cycles. On the one hand, it is important to generate a suitable high selection pressure in order to select an aptamer with desired properties. On the other hand, the selection pressure must not be too high to allow amplification of the recovered sequences. After several cycles, the DNA of the last SELEX cycle is examined for binding to the target molecule. If there is a clear difference compared to the DNA starting library, the DNA of the last SELEX cycle is cloned and sequenced. The sequences are sorted into similar motifs and arranged into families. Finally, the most frequently occurring sequences are examined for their affinity and specificity. The identification of the most frequently occurring sequences is presented in **section 3.1.2**.

3.1.1.1. Cell-SELEX

Cell surface proteins such as membrane proteins are the most commonly used drug targets for diagnostic and therapeutic approaches[33]. Several selections targeting membrane proteins have been performed for the generation of specific aptamers[34-37]. One of the most promising selection approaches for identifying aptamers targeting cell surface proteins is cell-SELEX[35]. Living cells are used as target molecules. Most frequently, the target protein is overexpressed on cells which do not naturally express this target protein.

At cell-SELEX, the cells are incubated with the aptamer library. The unbound sequences are removed by washing. In most cases, the bound sequences are recovered by breaking up the cell membrane, *e.g.* using heat, and subsequent phenol-chloroform extraction. The amplification of these sequences and the single strand generation are similar to those of the standard SELEX procedure (**section 3.1.1**).

The advantage of cell-SELEX is that the cell surface proteins are addressed in their native conformation.

A disadvantage of cell-SELEX is the non-specific binding to dead cells[38], which increases the number of selection cycles required to enrich certain sequences. To overcome this limitation, it is recommended to perform several washing steps before incubating the library with the cells to remove the dead cells. Another disadvantage is the large number of different proteins present on the cell

surface. All these proteins form a potential target molecule for aptamers. This disadvantage can be overcome by introducing negative selection. The library is first incubated with a cell line that does not express the target protein, and then all unbound sequences are incubated with the target protein cell line[39].

3.1.2. Identification of aptamers

As mentioned in **section 3.1.1**, enrichment must be confirmed after selection. If the selection was successful, the DNA of the enriched SELEX cycle is cloned and sequenced. Today, there are two approaches to library sequencing, Sanger sequencing and Next Generation sequencing (NGS), which are explained in the next two sections. The decision as to which sequencing method to use depends on the goal of the selection and the required information about the enriched sequences. However, the resulting sequences are grouped into families according to homology in their random region. The most frequently occurring sequences are tested for binding affinity and specificity to the target molecule.

3.1.2.1. Sanger sequencing

Sanger sequencing is the traditional approach for the identification of aptamers[23]. The DNA of the enriched selection cycle is cloned into a plasmid. This plasmid is converted into competent bacteria for amplification. After individual bacterial colonies have been formed and amplified, the plasmids are purified and sequenced according to the Sanger sequencing procedure[40]. Due to the high workload, Sanger sequencing enables the sequencing of 50-100 clones per selection cycle. For this reason, the last SELEX cycle should be highly enriched for accurate aptamer identification.

3.1.2.2. Next-generation sequencing (NGS)

The ability to generate large sequencing data has revolutionized SELEX technology. Next-generation sequencing (NGS) has become very attractive to the SELEX community[41,42] due to its high sequencing power and reduced costs over the last ten years. An NGS experiment enables the sequencing of up to 100 million sequences. This allows a detailed analysis of the selection process and an improved identification of aptamers. Even slightly enriched selection cycles can be analyzed by NGS. The selection analysis benefits from the possibility of higher sequence coverage as well as the verification of library diversity and the possibility to obtain sequence information from all selection cycles[43]. Therefore, NGS enables the tracking of the development of individual sequences and their amplification behavior over several selection cycles and provides information on the enrichment process[44,45]. This large amount of bioinformatics knowledge for the identification of aptamers must be evaluated and correctly interpreted. Today, several NGS analysis programs are available[46-50]. However, it is still a challenge and requires further improvement of the NGS analysis technique with respect to SELEX.

Furthermore, NGS is limited by relatively high error rates[51], depending on the sequencing method and platform used. The average error rate of the most widely used sequencing method, sequencing by synthesis, is about 0.1%-0.25% per nucleotide[51,52]. These error rates are mainly caused by phasing, the incorporation of zero or more than one nucleotide per sequencing cycle[52]. It is recommended by Pfeiffer *et al*. to sequence individual sequences in order to gain a deeper understanding of the error rate and the type of setup used[52].

3.1.3. Chemically modified aptamers

DNA aptamers have four natural bases - thymine, cytosine, adenine and guanine. These four bases achieve a diverse chemical repertoire in a nucleic acid library and can be used for the successful selection of aptamers with promising properties. The aptamer uses various interactions for binding to a target molecule, *e.g.* hydrogen binding, van der Waals and electrostatic binding[53]. However, aptamers can be provided with certain features that improve their properties, *e.g.* to reduce nuclease degradation or increase thermal stability[54-60]. The modifications can be made at three different sites of the natural nucleosides - nucleobase, phosphodiester binding and ribofuranose[61]. A further modification at the 3'- or 5'-end of the aptamer can reduce renal filtration and increase serum half-life, *e.g.* by adding a high molecular weight PEG)[62]. A schematic representation of the common modifications is shown in **Figure 3.2**. The two main categories of changes are explained in detail in the following sections.

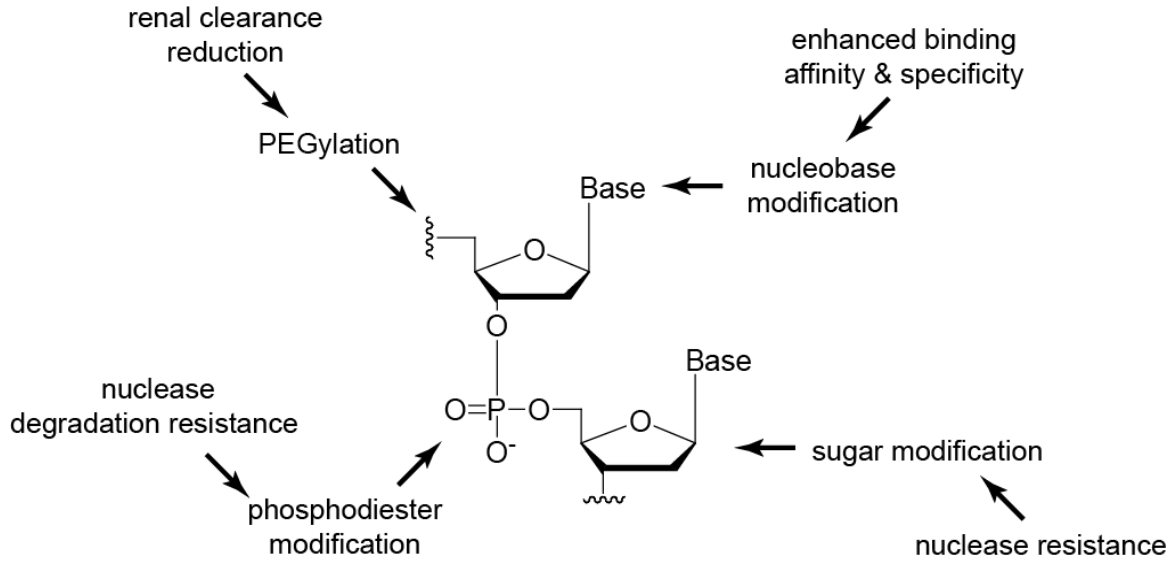

Figure 3.2. Schematic representation of chemical modifications of nucleic acids.

Common chemical modifications of aptamers to increase the stability or affinity and specificity. The modifications can be introduced as PEGylation, base-, phosphodiester-, or sugar modifications.

3.1.3.1. Backbone modification

The following is a brief overview of the backbone modifications with phosphate or sugar units to stabilize the aptamer.

Most sugar modifications concentrate on the 2'-position of deoxyribose sugar, such as 2'-amino[63], 2'-fluorine[64] or 2' methoxy nucleotides[65] (**Figure 3.3 A).** A large number of aptamers for different target molecules have been equipped with these modifications[54].

A methylene bridge between 2'-O and C4, which leads to a "locked" ribofuranose ring, leads not only to an increase in nuclease resistance, but also to duplex stabilization (**Figure 3.3 B**) [66]. This enables the selection of short and highly stable closed nucleic acid aptamers (LNA aptamers)[67-69].

In addition, the phosphates, which turn DNA into a polyanion, can be modified. The backbone modification of the triphosphate must be located at α-P atom[54]. The most promising is phosphorothioate (**Figure 3.3 C**), which is well established and used for higher stability against nucleases[70].

The so-called "spiegelmer" (**Figure 3.3 D**) offer an elegant way to increase nuclease defence. Here the chirality of the molecules is exploited. First, a D-aptamer is selected against an unnatural mirror image target molecule. Then the mirror image L-aptamer is synthesized, which interacts with the naturally occurring target molecule. The advantage of L-aptamers is that they are not recognised by nucleases.

Another modification is xenonucleic acid (XNA), a genetic polymer[71] in which the sugar residue and/or phosphodiester backbone bonds are modified[66]. However, these XNAs require the development of new polymerases for the amplification of XNA aptamers[72,73]. Several XNA aptamers and catalysts have since been selected[71,74-76].

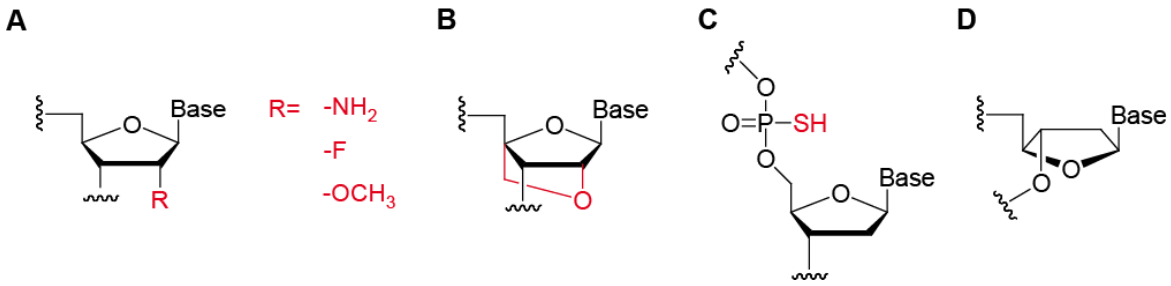

Figure 3.3 Chemical structures of common backbone modifications.

A) 2'-amino, 2'-fluoro, and 2'-methoxy modifications. **B**) Locked nucleic acids (LNA) modification. **C**) Phosphorothioate backbone modification. **D**) D-aptamer-backbone in "spiegelmer".

3.1.3.2. Nucleobase modification

In order to increase chemical diversity, various nucleobase modifications for aptamer selection[53] have been developed. These modifications allow the introduction of innovative chemical groups that increase the interaction possibilities between the modified nucleic acid and the target molecule. This in turn increases the selection probability of an aptamer for the desired target molecule[77,78]. For example, in the case of Slow Off-Rate Modified Aptamers (SOMAmers) it has been shown that the success rate of selections is increased to 84%[79].

Most modifications were introduced at the C5 position of the pyrimidine (**Figure 3.4 A**). The reason for this is that modifications at the C5 position do not inhibit the hydrogen binding necessary for the hybridization of DNA strands and are accepted by polymerases. The acceptance of the polymerases is important for the amplification step in a SELEX process with modified nucleotides[80]. The main contribution to this topic was published by Bruce E. Eaton *et al*., with an emphasis on the introduction of functional groups that mimic amino acid side chains. The group aimed to achieve slow, adjustable off-rates for the dissociation of the aptamer-protein complex[81]. This led to the development of Slow Off-Rate Modified Aptamers (SOMAmers)[79]. SOMAmers have significantly improved binding affinities and kinetics compared to conventional DNA aptamers[79,82-84]. In addition, the selection success could be increased by the use of hydrophobic modifications, in particular tryptamino, naphthyl, isobutyl or benzyl residues[79]. The main advantage of SOMAmers is that the functional groups mimic the amino acid side chains of protein-protein interactions and thus extend the chemical repertoire of aptamers. In antibody-protein interactions, tryptophan, phenylalanine and tyrosine[85,86] are the most common amino acids. SOMAlogic® integrated one of these groups at the 5-position of dUTPs (**Figure 3.4**) and performed several selections with these modified libraries[79]. The chemical groups give the aptamers more hydrophobicity, which leads to a higher probability of selection success in "difficult" target proteins (**section 3.2**). Several crystal structures confirmed that the modified nucleobases are involved in the SOMAmer[87-90] protein interaction.

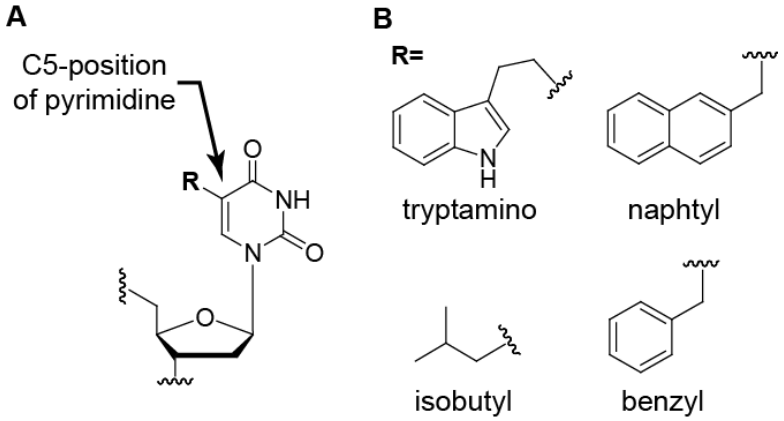

Figure 3.4 Nucleobase modifications in SOMAmers.

A) Chemical structure of the modified deoxyuridine analog. B) Chemical modifications used for the selection of SOMAmers[33].

The next improvement in SELEX is the above-mentioned SomaLogic® approach to the introduction of several protein-like modifications. Gawande *et al*. inserted two different modifications at the C5 position on the pyrimidines (dU and dC). This allows the selection of ligands with higher affinity due to the expanded chemical diversity to the target molecule compared to a single modification. In addition, the second modification improved nuclease resistance and the target epitope spectrum[91].

A major disadvantage of this technique is the complex synthesis of the desired modified nucleotides. This is because phosphoramidite (for library synthesis) and triphosphate (for PCR) are required for selection, as well as a two-stage PCR process to obtain the completely modified library[91].

3.1.3.3. Click-SELEX

The last mentioned disadvantage of the SOMAmers (**section 3.1.3.2**) led to the development of clickmers by Tolle *et al.*[29,57]. Clickmers are modified aptamers selected by click-SELEX. By using copper(I)-catalyzed alkynazide cycloaddition (CuAAC or click chemistry)[92-95] the ssDNA can be functionalized with any residue as long as it can be synthesized or commercially purchased. This functionalization, which for example contributes more hydrophobicity to the clickmer, increases the target molecule spectrum[26,57]. The first clickmer, C12, was selected in 2015 by Tolle *et al*. and targets cycle 3 GFP with 3-(2-azidoethyl)indole as DNA functionalization[29]. Until then, only RNA[96] and no DNA[97]-aptamer was selected for GFP, which shows that the click-SELEX approach increases selection success in target molecules that are not accessible with conventional SELEX methods. In 2019, another clickmer, C11.41, was published for a small molecule, (-) Δ9 Tetrahydrocannabinol (THC)[98]. To maximize DNA interaction with THC, the DNA was functionalized with benzylazide. No aptamer has been published for THC either. While the C12 clickmer shows no binding with other aromatic modifications, but only with indole[29], benzofuran[26] and benzothiophen[26], the C11.41 clickmer interacts with THC via a number of aromatic modifications, but no interaction with non-aromatic units[98].

A click selection cycle involves one more step compared to conventional DNA-SELEX. The initial library consists of four nucleotides, whereby dT is exchanged for EdU (5-ethynyl-2'-deoxyuridine) (**Figure 3.5**). EdU contains an ethynyl group that allows modification by cycloaddition through CuAAC[93,99].

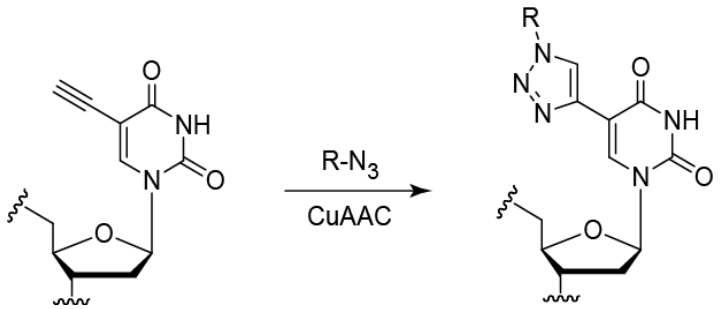

Figure 3.5 Schematic representation of the copper (I)-catalyzed alkyne-azide cycloaddition on EdU-modified DNA.
Functionalization of an EdU-modified DNA library by CuAAC using an azide-containing compound ($R\text{-}N_3$).

The click-SELEX starts with the functionalization of an EdU-modified ssDNA library with the desired azide-containing compound. The next steps, incubation with the target molecule, separation of unbound and bound sequences, amplification of the latter and single strand generation are the same as

in the common SELEX protocol (**Figure 3.1**, **Figure 3.6**). A significant change is performed during PCR: EdUTP must be used instead of dTTP to allow functionalization to be reintroduced after single-strand generation. The finally generated enriched ssDNA library can be functionalized and used for the next selection cycle. A detailed protocol was recently published by Pfeiffer *et al.*[26].

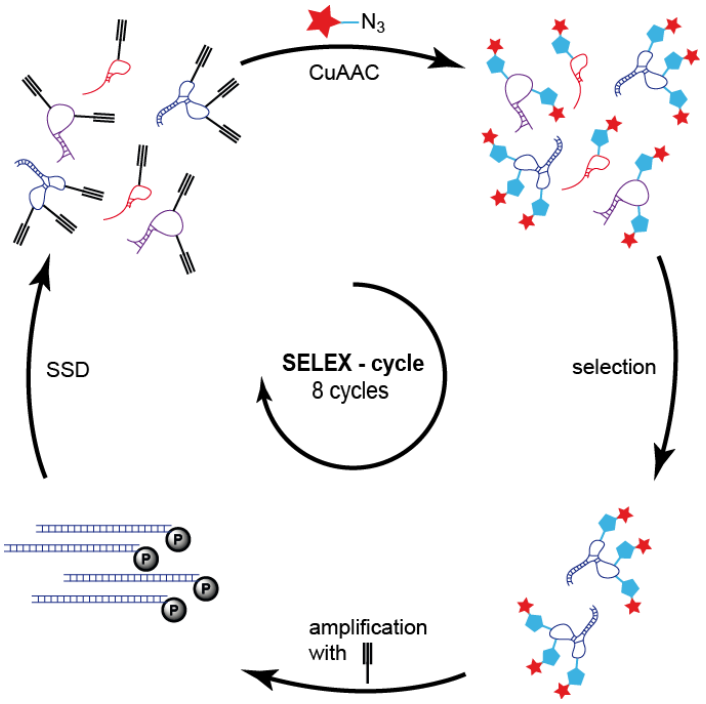

Figure 3.6: Schematic representation of the click-SELEX process.

An alkyne modified ssDNA-library is functionalized with an azide-containing entity by click-chemistry (CuAAC). After incubation with the target molecule, the non-bound sequences are removed (selection) and the bound sequences recovered and amplified by PCR using 5-ethynyl-2'-deoxyuridine (EdUTP) instead of thymidine (TTP). In the next step, the single-stranded DNA (ssDNA) is generated by λ-exonuclease digestion (SSD). Finally, the ssDNA is functionalized by CuAAC and subjected to the next selection cycle.

3.2. SELEX adjustments for "difficult" target molecules

For each target molecule of interest and the final application, a SELEX protocol can be modified in small but important details to allow successful aptamer selection. For example, the influence of ionic strength on aptamer conformation must be taken into account, as any change in environmental conditions can lead to a loss of aptamer binding to the target molecule. It is therefore recommended to apply the end-use conditions already during the selection procedure[100].

Even at the best settings of a SELEX process, the process may still fail[101]. The greatest limitation is the uncertain prediction of selection success[100], i.e. the generation of an aptamer with desired properties such as high affinity or specificity or even any aptamer. This situation could be caused by the limited set of canonical nucleotides, i.e. too little chemical diversity. Recent developments, such as the modification of nucleotides such as SOMAmers (**section 3.1.3.2**), have overcome this limitation and increased selection success from 30% to 90%[79]. However, a restriction remains for the modified

nucleotides that they must not influence polymerase activity to allow library amplification during SELEX[102].

So far, SOMAmers and clickmers allow the introduction of a modification of one[29,79] or two [91] in a SELEX. Gewande *et al*. showed that the introduction of two modified bases into a SELEX approach significantly improves affinity, metabolic stability and inhibitory potency compared to single modifications[91].

If the attempt to select an aptamer fails, the molecules addressed are referred to as "difficult" target molecules[79]. SOMAlogic® has subjected several such "difficult" targets to different selections. They showed that selections with unmodified DNA against "difficult" target molecules did not lead to the enrichment of binding sequences. In contrast, the selections with modified DNA were successful[79].

Since the VGIC has to be integrated into a membrane in order to function optimally, the VGIC can be classified as a "difficult" target molecule. The cell-SELEX approach makes sense because the VGIC is integrated into a cell membrane and remains fully functional. However, it should be mentioned that although cell-SELEX opened up the possibility of generating aptamers that target cell surface proteins in their native form, no aptamer could be selected for numerous target molecules[103]. Here it would be useful to combine the click-SELEX procedure with the cell-SELEX in order to increase the success rate of the selection.

3.3. Voltage-gated ion channels

The lipid bilayer contains channels, the so-called intergral membrane proteins with transmembrane pores. These membrane channels enable the regulated flow of certain ions or small molecules through the cellular and intracellular membranes along their electrochemical gradient. The first step of this channel concept was taken in 1952 with four publications by Nobel Prize winners Alan Lloyd Hodgkin and Andres Fielding Huxley. They used the voltage clamping technique to analyze the action potential of the squid axon[104-107]. Inspired by this electrical signalling mechanism, Bertil Hille and Clay Armstrong came up with the idea of specific ion channels conducting sodium and potassium currents in the 1960s. While Hille presented a detailed model of the sodium channel and its sodium ion selectivity filter[108-110], Armstrong developed the model of the intracellular mouth of the pore[111]. Hille summarized all studies that led to the development of the conceptual model of sodium channel function in one book[112]. Over the years, the diversity of the channels and their functions has been investigated by inhibiting them, *e.g.* with complementary DNA (cDNA), toxins and drugs[112,113]. The following general functions of the channels became known: First, the regulation of cell volume by the transport of water and ions through the cell membrane. Secondly, the regulation of electrical potential across the membranes and the production of membrane potential. This leads to a coordinated action potential, which is used by nerve and muscle cells for high-speed communication[114]. However, the

diversity of the channels (145 VGIC: **section 3**) illustrates the complexity of the channel functions and the difficulty of fully understanding the neuronal system.

3.3.1. Voltage-gated sodium channel

Voltage-gated sodium channels (VGSC) are present in various species from bacteria to humans. They generate the action potential in excitable cells such as neurons or muscles[112]. The decisive function of the channels is the rapid membrane depolarisation during the generation of action potentials. Furthermore, the channels play a decisive role in drug treatment. The main function of VGSC is the elimination of sodium ions (Na^+) via potassium (K^+) and other monovalent ions. By the penetration of sodium ions into the cell with the help of VGSC, the action potential is expanded[115].

Although the understanding of VGSC is still lacking, several VGSC inhibitors are used today to treat pain[116], *e.g.* local anesthetics such as lidocaine[117,118] and procaine[119] in dental treatments[120].

3.3.1.1. Discovery and structure of VGSC

In the 1950-1970s, early physiological development confirmed the existence of VGSC, although there was no information about its structure. It was known that the channels initiate and propagate the action potential in excitable cells[112]. However, it took a decade longer to identify the large α-subunits of 260 kDa and the smaller β-subunits of 30-40 kDa[121] using a photoaffinity labelled scorpion toxin[121]. Further investigations of α-subunits of sodium channels from eel electroplax[122] and a complex of α- and β-subunits from rat skeletal muscle[123] contributed to the first reconstruction of a voltage-gated ion channel (**Figure 3.7 A**).

The studies by Noda *et al.*[124,125] and Goldin *et al.*[126] showed that the mRNA coding for the α-subunit is sufficient for the expression of functional sodium channels. The α-subunit consists of about 2000 amino acids coordinated in four homologous domains (I-IV). It has been predicted that each of these domains contains six transmembrane segments (S1-S6)[125] (**Figure 3.7 B**). With the help of further structure-function studies, it was predicted that the segments S1-S4 form the voltage sensor module. In addition, S4 contains four to seven positively charged arginine or lysine residues and serves as a voltage sensor[127,128]. The mutation of the arginine residues in segment S4 confirmed this prediction of the gating mechanism[129,130]. The pore domain is formed by the segments S5 and S6, while the P loop between them serves as an ion selectivity filter[131]. The activation gate[131] is located between the segments S6 and S1 on the intracellular side.

Long before the development of crystal structures, functional analysis of VGSC was performed by modeling the gating and using toxins in electrophysiological imaging. The detailed understanding of voltage-dependent gating, ion selectivity and drug blockade was obtained from the recent crystal structure of bacterial VGSC. The VGSC is dissolved in a detergent such as digitonin and crystallized in a lipid-based bicyte system[132]. Payandeh *et al*. published in 2011 a crystal structure of a closed form

of the sodium channel, the Na_vAb of *Arcobacter butzleri*[132]. It has been shown that the four P loops between S5 and S6 in each of the four domains form a ring of glutamates which form an ion selectivity gate. This ion selectivity gate is located near the extracellular site of the pore and directs the hydrated sodium ion through the pore[132].

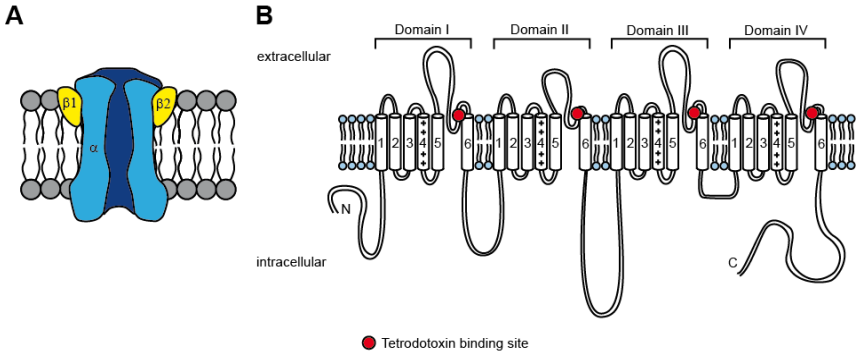

Figure 3.7 Structure of voltage-gated sodium channels.

A) Schematic representation of the brain sodium channel based on biochemical data[114], incorporated into a planar bilayer. B) Polypeptide chain of the α-subunit from VGSC. The cylinders illustrate α-helical segments. The cylinders 4 represent the voltage sensors S4. The binding sites of tetrodotoxin, which is a specific blocker of the pore, are shown as red circles. Adapted from Catterall 2000[133].

In 2012 Zhang *et al*. showed the crystal structure of an inactive channel, the Na_vRh from the marine bacterium *Rickettsiales*[134]. In comparison to Na_vAb, new information on conformational rearrangements during the electromechanical mechanism of voltage-gated channels was discovered[134]. Another crystal structure of an open conformation of the Na_vM channel with the marine bacterium *Magnetococcus* provides a more detailed insight into the channel characteristics, *e.g.* gate and selectivity mechanism[135]. The study of the activation gate in two conformations of the Na_vAb allows an accurate modeling of the gate and the comparison of the segment S6 in the closed and open state of the channel (**Figure 3.8 A, B**)[136].

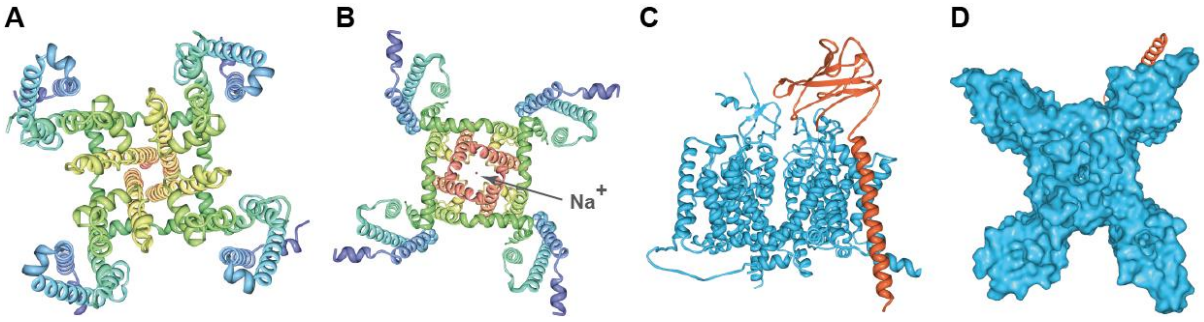

Figure 3.8 Structure of the human $Na_v1.4$-β1 complex.

A) The crystallographic structure of the Na_vAb voltage-gated sodium channel in the closed (PDB ID: 5VB2) and open (**B**) conformation (PDB ID: 5VB8). The structures were modified after Lenaeus *et al.* 2017[136] with the freeware program RCSB PDB Protein Workshop 4.2.0[137,138]. **C**) The side view of the human $Na_v1.4$-β1 complex in ribbon cartoon is depicted. The α-subunit is colored in blue and the β-subunit in orange. **D**) The surface presentation of the human $Na_v1.4$-β1 complex is depicted from the bottom. The structure (PDB ID: 6AGF) was modified with the freeware program RCSB PDB Protein Workshop 4.2.0[137,138] after Catterall *et al.* 2005[139].

Further structural analyses in 2018 provided molecular details on the blocking mechanism with neurotoxins such as tetrodotoxin (TTX) or saxitoxin (STX) on the Na_vPaS channel[140]. The crystal structure of human VGSCs remained unclear until Pan *et al*. showed the structure of the human $Na_v1.4$-β1 complex using cryoelectron microscopy[139] (**Figure 3.8 C, D**).

3.3.1.2. Gating of VGSC

The VGSC pass through three states - open, closed and inactivated (**Figure 3.9**)[116]. When the membrane potential is at rest, i.e. the intracellular space is negatively charged, the channels are in the non-conductive closed conformation. Starting with depolarization, the voltage sensor (S4 segment) moves outward, resulting in a conformational change (open) that allows opening of the pore and inflow of Na^+ for less than a millisecond. This rapid inflow of sodium ions depolarizes the membrane and causes a voltage increase across the neuronal membrane, increasing the action potential. Following inactivation, the inactivation gate blocks (inactivates) the pore. Finally, the channel recovers to the non-conductive inactivated conformation, with the activation gate closing the pore (closed).

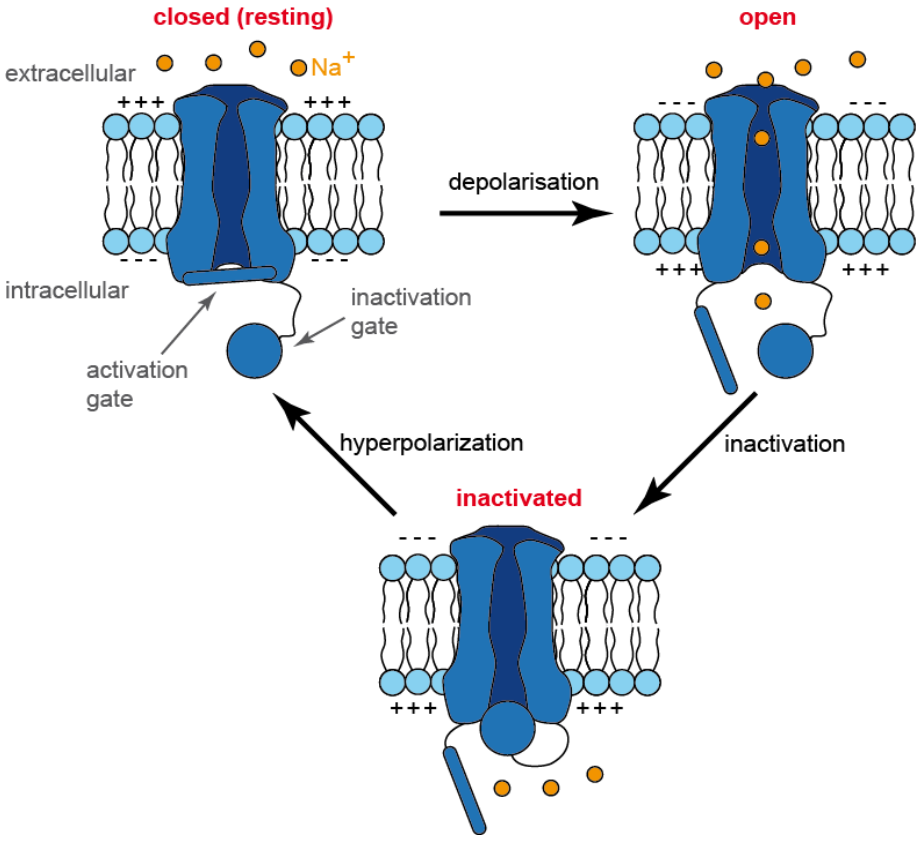

Figure 3.9 Schematic representation of the gating of the voltage-gated sodium channel.

Depicted are the three states of VGSC, closed, open, and inactivated. At the resting membrane potential, the channel is closed. The depolarisation forces the channel into the open conformation, allowing the permission of sodium ions (yellow). Finally, the inactivation gate occludes the channel in the inactivated conformation. After the hyperpolarization, the channel returns into the closed conformation.

3.3.1.3. Diversity of VGSC

As already mentioned, VGSC are responsible for the initiation and spread of action potential in excitable cells such as muscle or nerve cells. Nevertheless, these channels are also localized in non-irritable cells with low expression. The physiological role of this expression is unclear[141].

The primary sodium channels in the central nervous system are $Na_v1.1$, $Na_v1.2$, $Na_v1.3$ and $Na_v1.6$. The skeletal muscle is dominated by $Na_v1.4$ and the heart by $Na_v1.5$. $Na_v1.7$, $Na_v1.8$ and $Na_v1.9$ are expressed in the peripheral nervous system. The 10th sodium channel is not voltage-gated[142]. Although the channels have different expression profiles, their protein sequence is very similar and their mechanisms of ion selectivity and conductivity are the same. Their biophysical properties and pharmacological sensitivities, *e.g.* to local anesthetics and neurotoxins, differ slightly[141]. Despite all structural and functional information about VGSC, there are some open questions, *e.g*. why the sodium channels in neurons cannot replace their equivalent in skeletal muscle.

3.3.1.4. Tetrodotoxin

Several drugs interact with VGSC, *e.g.* by blocking the channel. These drugs are used clinically, *e.g.* local anesthetics, antiepileptics or antiarrhythmics. They bind to a receptor site in the pore and prevent permeation of sodium ions[142].

Tetrodotoxin (TTX) is a naturally occurring marine neurotoxin. It inhibits neuronal electrical activity by preventing permeation of sodium ions by VGSC[143,144]. TTX is a heterocyclic guanidinium compound isolated from the Japanese buffer fish[145]. Due to the fact that VGSC is highly sensitive to TTX, it was used to study the structural and functional properties of VGSC. The crystal structure of TTX was triggered by Woodward in 1964[146] (**Figure 3.10**). TTX was then used by Narahashi *et al*. He observed a TTX effect on the neuronal sodium ion current when applied only at the extracellular site. After intracellular application no effect could be observed[119,147]. Furthermore, TTX was used in 1975 by Hille *et al*.[143] to predict the diameter of the sodium ion channel pore.

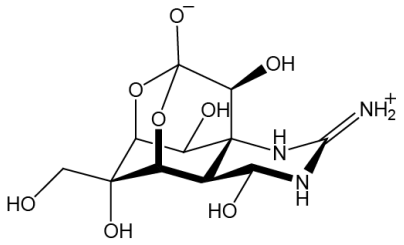

Figure 3.10 Chemical structure of tetrodotoxin (TTX).

Today, VGSC are divided into TTX-sensitive ($Na_v1.1$-$Na_v1.4$, $Na_v1.6$-$Na_v1.7$) and TTX-resistant ($Na_v1.8$, $Na_v1.9$) channels. This means that the required concentration of TTX varies from nanomolar to millimolar for a completely blocked channel[141]. The complete inhibition of $Na_v1.5$ (TTX-highly

resistant) requires a micromolar TTX concentration[133]. It is important to note that the binding affinity of TTX has a low dependence on membrane potential, which can be explained by the binding site of TTX. This is located on the extracellular side of the membrane[113]. In addition, the mutation of individual amino acids alters TTX sensitivity[148]. Terlau *et al*. showed a loss of TTX affinity by mutation of the S5-S6 segment region in one of the four domains[149].

3.3.1.5. Prospect of VGSC drug development

Despite the great progress in understanding VGSC in recent decades, there is still room for improvement. Information on the binding of drugs to VGSC enables the design of new drugs. There is great interest in drugs that are capable of targeting individual sodium channel subtypes. The new generation of drugs should be able to differentiate between these different subtypes expressed in the brain, skeleton or heart muscle to enable safe and highly effective treatment of channel epilepsy or cardiac arrhythmia[114]. However, most of the anti-epileptic or antiarrhythmic drugs used today are painkillers, such as carbamazepine or phenytoin[113] and lidocaine[116]. These drugs target the same binding site in domain IV on segment S6[150] and therefore have low selectivity for individual VGSC, leading to side effects. The studies on the exact structure of VGSC open the way for the design of the new generation of drugs specifically designed for individual VGSC.

4. Aim of the study

Within the past decades, voltage-gated sodium channels (VGSC) have been identified as integral membrane proteins that form pores that conduct sodium ions through the cell membrane. As a result, VGSC initiate and propagate the action potential in excitable tissue, such as neurons or muscles. Mutations in the VGSC gene cause several channelopathies, like epilepsy or arrhythmic diseases, which are nowadays treated with drugs, such as antiepileptics or antiarrhythmics, albeit with differing degrees of success.

The aim of this thesis was to investigate the potential applicability of aptamers as a novel tool for specific regulation of the VGSC gating mechanism. In particular, we were interested in the following question:

Is it possible to select aptamers specifically targeting different subtypes of VGSC? To our knowledge, there is no specific tool for the regulation of the VGSC gating process. Toxins or local anesthetics block the VGSC pore but are not subtype-specific. Hence, there is an urgent need for the discovery of new drugs targeting the specific subtypes of VGSC. To achieve this, the aim of this study was to implement a specialized selection scheme and next-generation sequencing (NGS) to identify the desired aptamers. We were interested in aptamer characterization, especially regarding affinity and specificity but also towards their impact on VGSC function.

5. Results

This chapter describes the investigations on the potential of aptamers and clickmers as molecular tools for voltage-gated sodium channels (VGSC), α-amino-3-hydroxy-5-methyl-4-isoxazolepropionic acid receptor (GluR1), cycle3-green fluorescent protein (C3-GFP) and streptavidin.

In the first part, several selection procedures for the identification of aptamers or clickmers for VGSC and GluR1 are investigated (**Section 5.1-5.4**). The second part of this chapter extends the click-SELEX concept and describes the split-combine procedure for the selection of clickmers from an agreed library functionalized with different modifications (**Section 5.5-5.9**).

5.1. Selections of VGSC targeting aptamers

The selection of aptamers targeting cell-surface proteins such as VGSC requires their introduction into a membrane to ensure their native conformation and thus their functionality. A protocol for cell-SELEX approach[37,151] was chosen because it allows the identification of aptamers targeting membrane proteins with living cells. Prof. Holger Lerche from the Hertie Institute for Clinical Brain Research in Tübingen was kind enough to donate these VGSC-HEK293 cells to us. In this way, the VGSC are expressed in their native conformation in HEK293 cells.

In order to ensure the enrichment of sequences targeting VGSC only, a negative selection step was implemented with HEK293 cells without VGSC.

Cell-SELEX (**Figure 5.1**) was started with the negative selection step. The single-stranded DNA (ssDNA) library, containing 10^{14} unique sequences (500pmol), was incubated with HEK293 cells at 37°C (**Figure 5.1**). The unbound sequences remained in the supernatant and were transferred to VGSC-HEK293 cells expressing a type of VGSC ($Na_v1.5$ or $Na_v1.6$), which were also incubated at 37°C. The separation of the unbound from the bound sequences was performed by washing the cells. To avoid those sequences that might interact with VGSC from the intracellular side are lost, all bound sequences were recovered and amplified. Finally, the double-stranded DNA (dsDNA) was digested into ssDNA (SSD) using the λ exonuclease. The enriched ssDNA library was used for the next selection cycle.

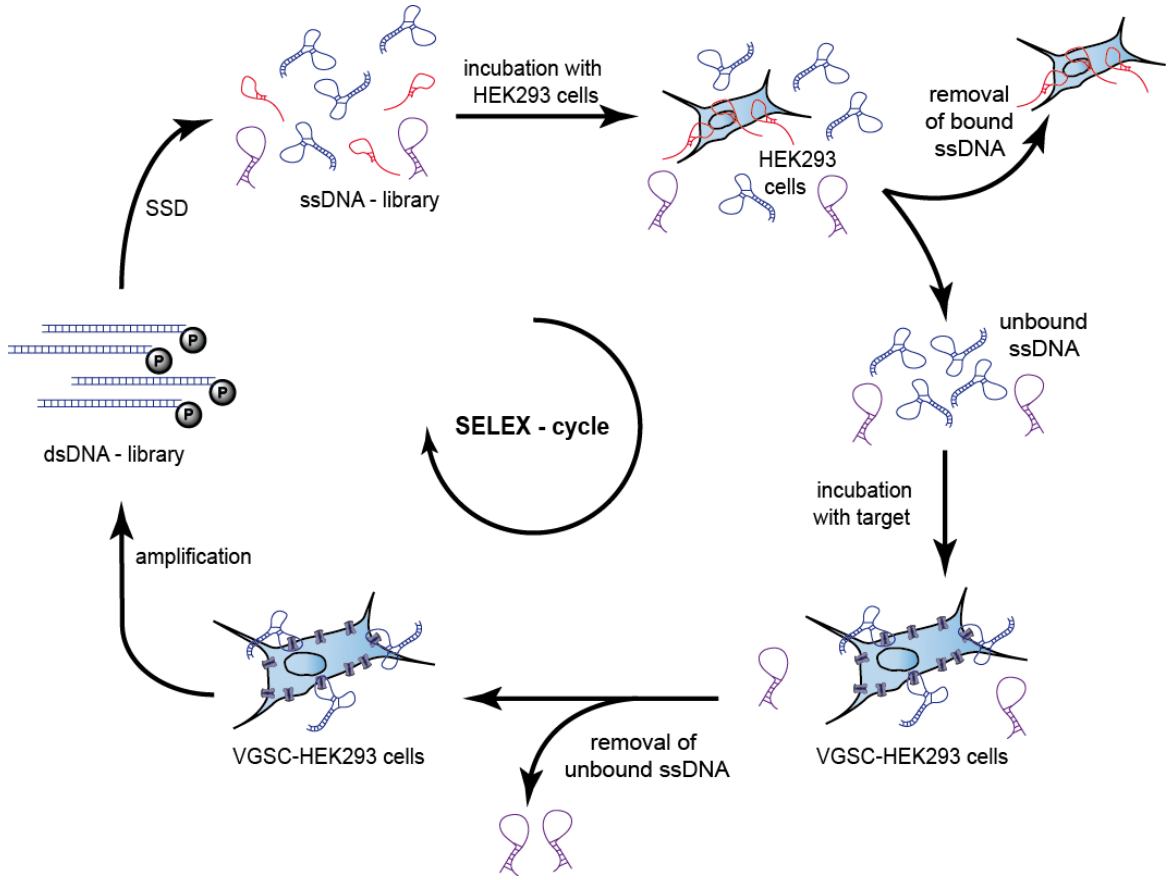

Figure 5.1: Schematic representation of a DNA cell-SELEX process.

The ssDNA library is first incubated with the non-target cell line (HEK293 cells) and the unbound sequences are used for incubation with the target cell line (VGSC-HEK293 cells). The bound sequences are obtained by PCR and amplified. The dsDNA is then subjected to a single strand displacement (SSD) to obtain a single-stranded DNA (ssDNA). The enriched ssDNA library is then subjected to the next selection cycle. After several selection cycles (8-15), the DNA of the enriched library is cloned and sequenced.

The expression of transmembrane proteins, such as ion channels in mammalian cells, is very low. If the expression of VGSC is compared with other cell surface proteins, it becomes clear that VGSC are inferior. Since the aptamers also bind to all other cell-surface proteins that are in clear excess (compared to VGSC), the probability of selecting an aptamer targeting VGSC is low. For this reason, we have decided to include a branch in the selection process (**Figure 5.2**). For the first two selection cycles, a common cell-SELEX approach was applied, followed by a branching point, which allows to divide the enriched library into two aliquots and to perform two separate selections with different target molecules. One aliquot was used for HEK293 cells and the second for VGSC-HEK293 cells. After successful enrichment of both selections, the DNA of the selection cycles should be sequenced in order to compare both selections in the subsequent analysis. All sequences not present in the selection target HEK293 cells but present in the selection target VGSC-HEK293 cells should be examined for specificity to VGSC.

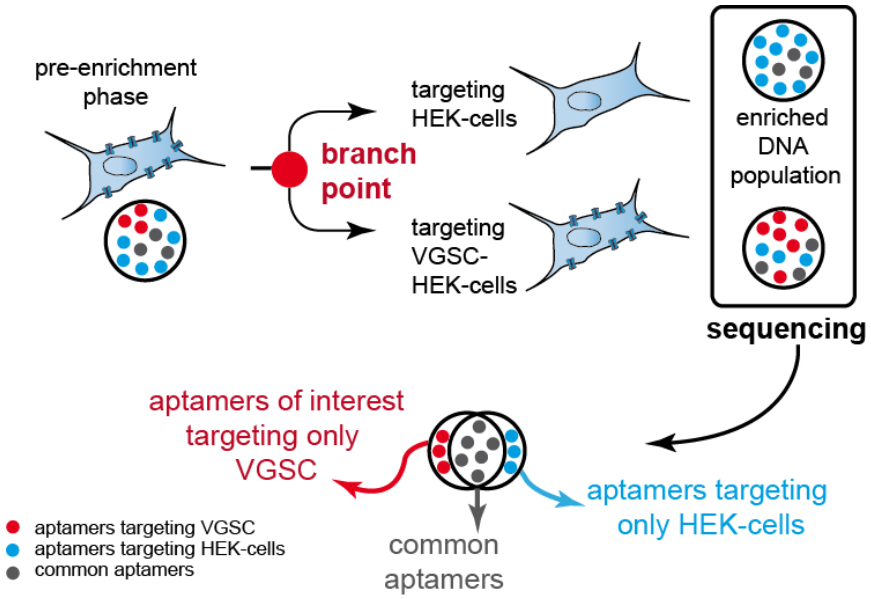

Figure 5.2: Schematic representation for the branch point SELEX hypothesis.

All sequences enriched in the pre-enrichment phase should have an affinity to both cell lines. Then the enriched library is separated and used for two different selections targeting the two cell lines. Both selections generate different enriched sequences. The comparison of the enriched DNA populations should lead to the detection of three aptamer groups: Aptamers of interest for VGSC, common aptamers and aptamers for HEK cells.

5.1.1. SELEX using DNA libraries targeting $Na_v1.5$ and $Na_v1.6$

The group around Prof. Heinz Beck (Life&Brain Center, Bonn) analyzed the expression profile as well as the functionality of the expressed VGSC by patch-clamp technique. The results showed that $Na_v1.5$ and $Na_v1.6$ had the highest expression with 3000 channels per cell. Therefore, these channels were selected for the first SELEX to increase the probability of successful selection.

The selections for VGSC ($Na_v1.5$ and $Na_v1.6$) were performed with an ssDNA library called D3 as shown in **Figure 5.1**. The selections were initiated by incubating the conventional ssDNA library. Prior to the third selection cycle, the pre-enriched library was subdivided according to **Figure 5.2** and two selections were continued in parallel. One selection focused on VGSC-HEK293 cells and the other on HEK293 cells. A total of ten selection cycles were performed. Two further selection cycles (twelve in total) were performed to align the branching point selection with HEK293 to increase enrichment. Selection to $Na_v1.5$ was performed without branching points. We assumed that selection at the branching point against HEK293 cells would enrich the same sequences as the former selection target $Na_v1.6$. After ten or twelve selection cycles, the DNA of the enriched libraries was analyzed for its affinity to the different cell lines HEK293, $Na_v1.5$-HEK293, and $Na_v1.6$-HEK293 using radioactive binding assays. The γ32P-DNA was incubated with the cells and the amount of γ32P-DNA bound to the cells was measured by liquid scintillation counting (**Figure 5.3**).

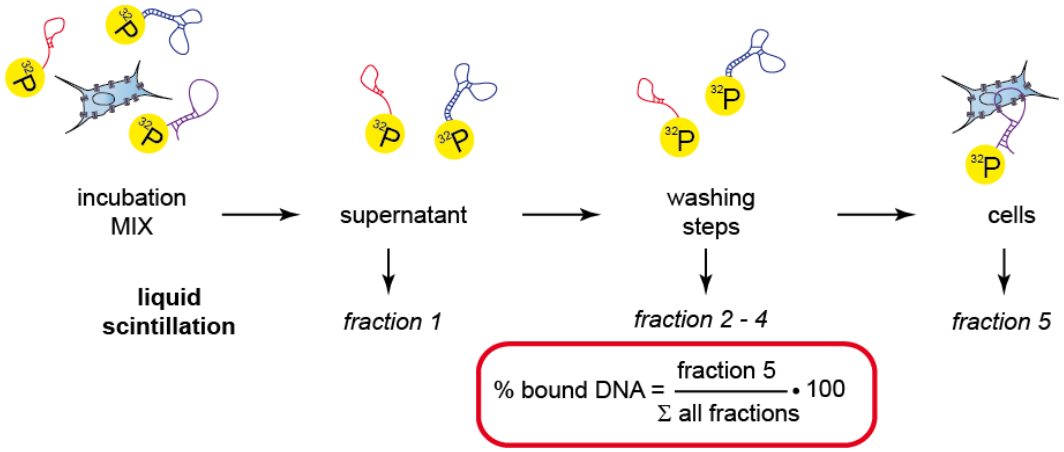

Figure 5.3: Schematic representation of the radioactive Cherenkov binding assay.

The HEK293 cells, $Na_v1.5$-HEK293 cells, or $Na_v1.6$ HEK293 cells, were incubated at 37°C with γ32P DNA. The supernatant (fraction 1) and the three wash fractions (fraction 2-4) were collected. The cells were separated and collected as fraction 5. The radioactivity of all fractions was measured by liquid scintillation counting. The percentage of bound DNA was calculated according to the formula shown.

All three selections showed increased binding of the DNA of the selection cycles compared to the DNA of the start library (SL). Selection targeting $Na_v1.5$ showed enrichment in the 8th selection cycle with 11% of DNA binding to $Na_v1.5$-HEK293 cells (**Figure 5.4 A**). The selection target $Na_v1.6$ showed a binding of 3.5% of the DNA from the 10th selection cycle to $Na_v1.6$-HEK293 cells (**Figure 5.4 B**). Both selections were promising because the binding to HEK293 cells was lower than to $Na_v1.5$- or $Na_v1.6$-HEK293. Selection on HEK293 cells resulted in 6.5% binding DNA in the last selection cycle (**Figure 5.4 C**). Therefore, DNA from the enriched libraries was used for further analysis.

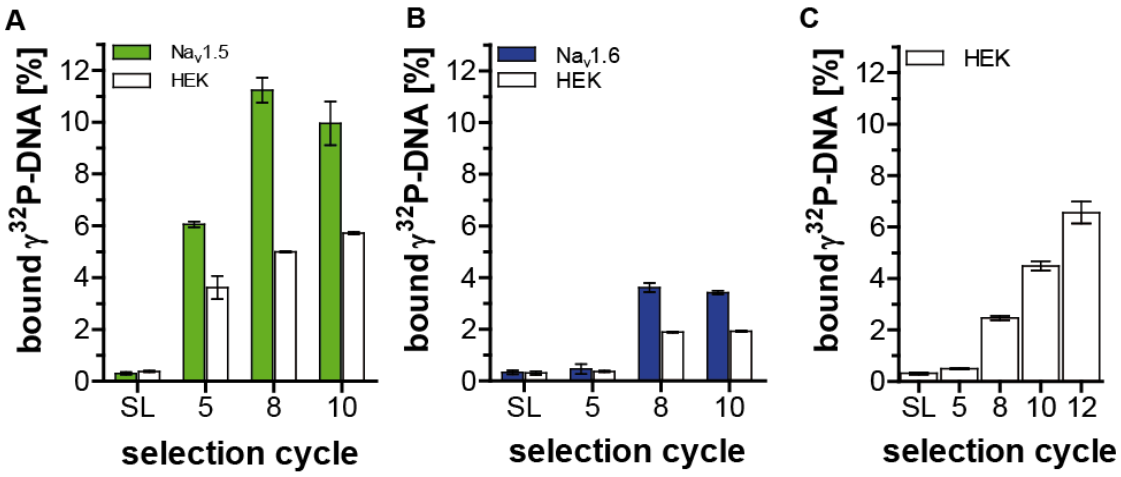

Figure 5.4: Radioactive binding assays of cell-selections targeting HEK293-cells expressing $Na_v1.5$ and $Na_v1.6$, as well as HEK293-cells.

γ32P-DNA of the start library (SL), selection cycles 5, 8, 10 and 12 was incubated with VGSC-HEK293. The selection target $Na_v1.5$-HEK293 is shown in (**A**), the selection target $Na_v1.6$-HEK293 in (**B**) and the selection target only HEK293 cells in (**C**). The radioactivity retained on or in the cells was determined by liquid scintillation counting (n=2, duplicates, mean ± SD).

5.1.2. Identification of aptamer candidates from cell-SELEX by Sanger sequencing

The DNA of the enriched libraries of the 10th and 12th selection cycle of all three cell selections was cloned. The sequencing revealed 39 DNA sequences for $Na_v1.5$, 34 DNA sequences for $Na_v1.6$ and 22 DNA sequences for HEK293. The most frequently occurring sequences can be grouped into three sequence patterns (Sa, Sb, and Sc) (**Table 5.1**). These three most common sequences were analyzed for their affinity to the cell lines using the radioactive binding test (**Section 5.1.3**). All sequences not found in HEK293-SELEX were also analyzed. All sequences are listed in the appendix (**Supp. table 1**, **Supp. table 2**, **Supp. table 3**, **Supp. table 4**).

Table 5.1: DNA sequences selected in cell-SELEX targeting $Na_v1.5$-/$Na_v1.6$-HEK293. Listed are the sequence and their frequency according to the selections.

The nomenclature of the sequences was random.

Name	Random region	SELEX $Na_v1.5$	SELEX $Na_v1.6$	SELEX HEK
H1	CGTGGGTGGGTTTATATTCGGTGGTGGTGGGGGTGGTACTGTT	-	1/34	11/22
S1	CCGTGGCCGTTAGGCGTATCGTCCCCCACTACTACTTTGGGTT	1/39	-	-
S2	GCTGAGTTCCTCTCCTCCGAAGTGTTGTGCGGTTTAATCGTGG	1/39	-	-
Sa	TGGGGGGTTGGGGAGTTGGGGATCCTTTGGTAGAGATTGAGTT	22/39	8/34	1/22
Sb	CCTCGAAGAAGGCGTCCCCCACTCATTCCTCCTTATACGAGG	13/39	4/34	1/22
Sc	CGAGACGGATCTTTAGTCCCCCACTCGCCCCATCCGTTCGAGG	1/39	4/34	1/22
2	CGTAGACGAATCGATGGAAGGTTGCGTTCCTTTATTCACCGGG	-	1/34	-
4	GCCCATCGGATTCCTTCGTTCCTCTCAGCCGGGAAAGTTTCCA	-	1/34	-
5	CCAACCCTCGTATGTCAACTAATGTGGGGGTCTTTTATCGTTG	-	1/34	-
6	CCAAGAAGAAATCCCAACGAAAGAAAGGCATCTGGATCTATTG	-	1/34	-
10	GGACGGCACTTCTCATTTACTCCTGCGATGGTCATGGTGAGGG	-	1/34	-
14	CGAGACTTTTGCATAAATTGAAGAGCAGTCAGTAAAATCGGGGG	-	1/34	-
22	CCCCGGGTCTTTCGTTTTTACCTATCCCCTTTGTTAGCGTTGG	-	1/34	-
28	GGGAGGTTCGGAGTGTTTAGGGGATCATTACATGTGGGTGTGG	-	1/34	-

5.1.3. Validation of selected DNA sequences

The binding capacity of the selected sequences to the three cell lines was analyzed with the radioactive Cherenkov assay (**Figure 5.3**). The start library (SL) was used as a non-binding control. Since the sequence H1 was present in the selection target HEK293 as the most abundant sequence, it was assumed that this sequence only targets HEK293 and not VGSC. H1 was not considered in further analysis. Sequences S1 and S2 were only present in $Na_v1.5$-HEK293 SELEX. Sequences Sa, Sb and Sc were present in all three selections. We assume that these sequences bind to all three cell lines ("common aptamer" according to **Figure 5.2**). Sequences 2-28 were only present in the $Na_v1.6$-HEK293 selection. All tested sequences showed binding to all three cell lines (**Figure 5.5**). Only sequence 28 showed stronger binding to $Na_v1.6$-HEK293 than to HEK293.

Since each sequence investigated bound to both HEK293 and VGSC-HEK293 cells, a deeper insight into selection was required. For this reason, Next-Generation sequencing (NGS) was performed for these selections.

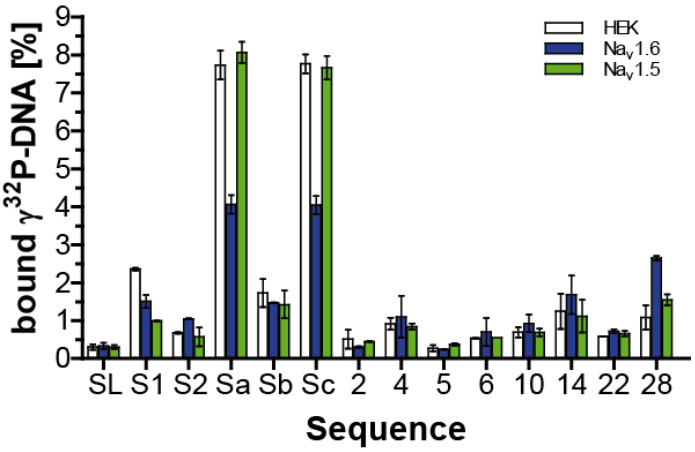

Figure 5.5: Binding of DNA sequences of the selection targeting $Na_v1.5$-HEK293 and $Na_v1.6$-HEK293 to different cell lines.

The γ32P-DNA of the start library (SL) and the different sequences was incubated with HEK293 cells (white), $Na_v1.5$-HEK293 cells (green) and $Na_v1.6$-HEK293 cells (blue). The radioactivity retained on/in the cells was determined by liquid scintillation counting (n=1, duplicates, mean ± SD).

5.1.4. Analysis of the cell-SELEX by Next-Generation sequencing (NGS)

As mentioned above, an NGS[152] analysis was performed using Illumina sequencing[153] to gain a better understanding of the cell SELEX process targeting VGSC. The DNA of selection cycles 2, 3, 4, 5, 6, 7, 8, 9, 10 and 12 for HEK293 and $Na_v1.6$-HEK293 was sequenced by NGS. The DNA of selection cycles 4, 6, 8 and 10 of the selection target $Na_v1.5$-HEK293 was also sequenced.

100 bp single-ended readings were performed on an Illumina HiSeq 1500 device in collaboration with Prof. Joachim Schultze (LIMES, Bonn). The raw data analysis was performed by Dr. Carsten Gröber at AptaIT GmbH with the COMPAS software[46].

The first indicator for the enrichment is the reduction of unique sequences in the library via selection. **Figure 5.6 A** shows the percentage of the unique sequences over the selection for all three selections. The start library (SL) contained about 100% unique sequences. This number decreased during the selection process. While the selections for HEK293 and $Na_v1.6$-HEK293 showed a similar decrease over cycles 6 to 9, the selection for $Na_v1.5$ showed a stronger and faster reduction, leading to only 5% unique sequences already in the 6th cycle.

Another indicator of enrichment is the change in nucleotide distribution in the random region. The nucleotide distribution of SL and the last selection cycles 10 and 12 for the three selections HEK293, $Na_v1.6$-HEK293 and $Na_v1.5$-HEK293 are shown in **Figure 5.6 B-E**. The SL contained a relatively even distribution of all four nucleobases over the entire random region. Whereby A is represented with 20%, while C, T, and G with more than 25%. During selection, the nucleobase distribution of the last selection cycles for all three selections was changed in different ways. The selections against HEK293 and $Na_v1.5$-HEK293 were strongly G-rich. These results suggest that certain sequences were enriched

during the selection procedure. The nucleotide distribution for all sequenced selection cycles is in **Supp. figure 1**, **Supp. figure 2**, and **Supp. figure 3**.

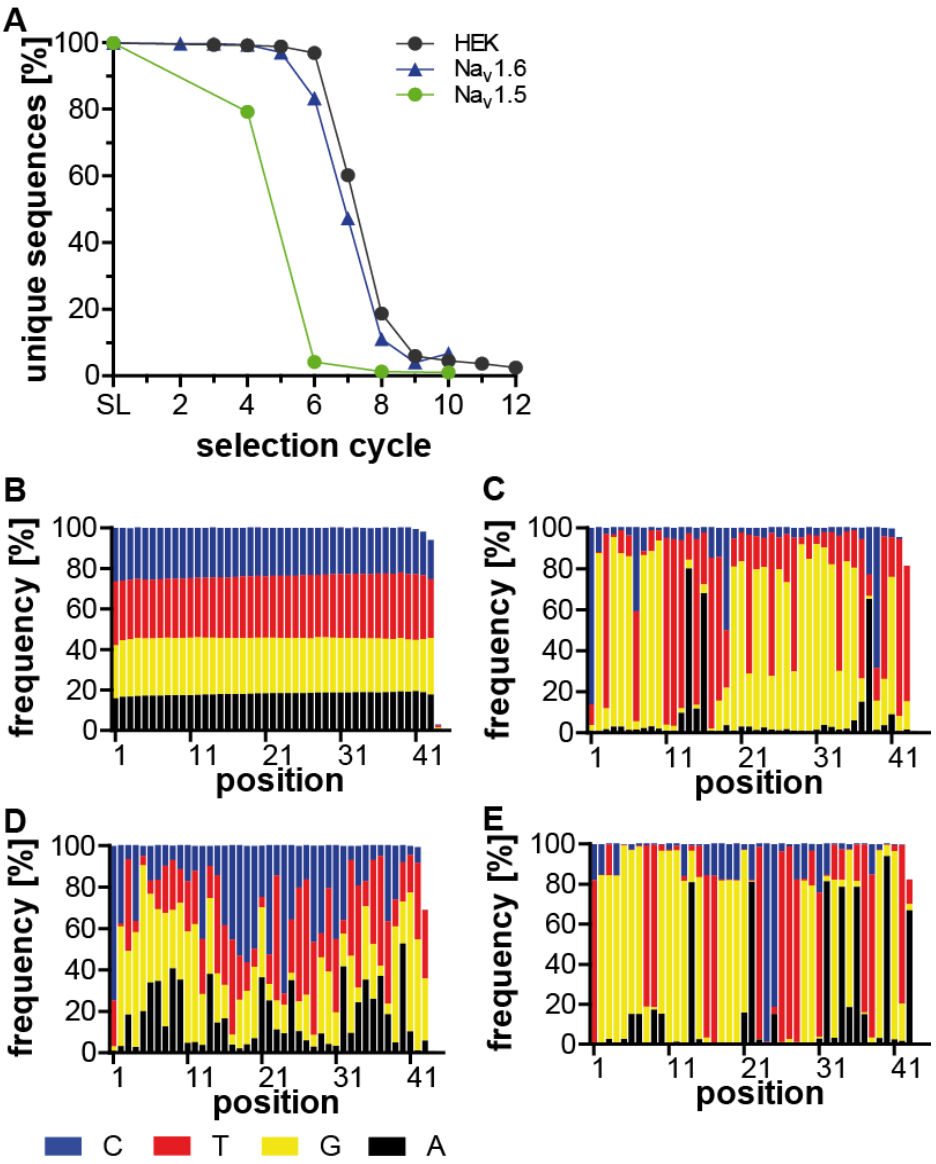

Figure 5.6: Unique sequences and nucleotide distribution of the NGS analyses of cell-selections targeting $Na_v1.5$-HEK293, $Na_v1.6$-HEK293, or HEK293 cells.

(**A**) The unique sequence frequency of the start library (SL) and all selection cycles for the selections targeting HEK293 cells (black), $Na_v1.6$-HEK293 cells (blue) or $Na_v1.5$-HEK293 cells (green). Nucleotide distribution at the different positions of the random region in the DNA of the initial library (**B**) and the final selection cycle 12 of HEK293 cell-SELEX (**C**) and cycle 10 of $Na_v1.6$-HEK293 (**D**) and $Na_v1.5$-HEK293 (**E**). The changes in the nucleotide distribution were investigated with the software COMPAS (COMmonPAtternS) of AptaIT GmbH (Planegg-Martinsried, Germany).

In addition, the COMPAS software bundles similar sequences into "patterns" and tracks their frequency over the selection cycles. The most common sequence patterns of all three selections were identical to those of Sanger sequencing (**Table 5.1**). Their frequencies in all three selections are shown in **Figure 5.7**. For the selection targeting HEK293, the pattern H1 increases continuously during selection. All patterns found in one of the selections for $Na_v1.5$-HEK293 or $Na_v1.6$-HEK293 were also

observed in the selection for HEK293. The patterns Sa, Sb, and Sc increased during the first selection cycles but decreased in the latter. Selection targeting $Na_v1.6$-HEK293 showed a strong accumulation of pattern Sa up to the 8th selection cycle, followed by a strong decrease. The patterns Sb and Sc showed a slow increase in their frequency. In addition, the selection on $Na_v1.5$-HEK293 showed a strong frequency enrichment of up to 50% for the pattern Sa and a slower increase for the patterns Sb and Sc (**Figure 5.7 B-C**).

From these data, it can be seen that the enrichment of the sequences only starts after the selection cycles 4-6. For these selections, the branching point was already introduced in the third selection cycle. The data from **Figure 5.7** clearly showed that the branching point should be introduced much later, *e.g.* in cycle 8.

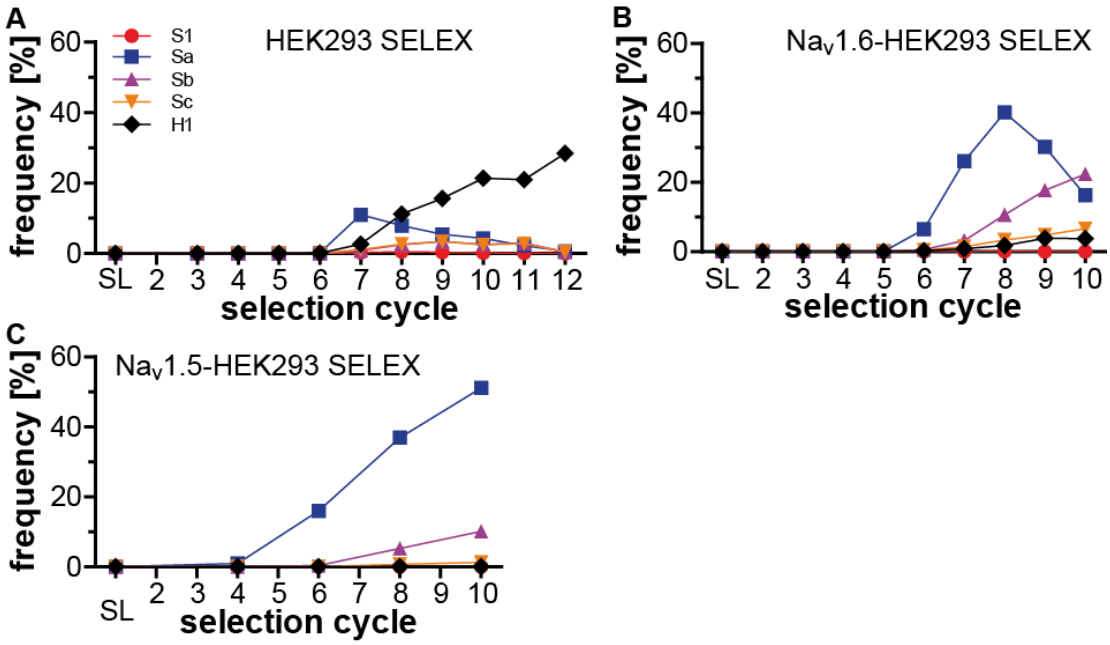

Figure 5.7: Frequency in NGS analyses of the most abounded sequences on the used target in the selections targeting HEK293-cells, $Na_v1.5$-, and $Na_v1.6$-HEK293-cells.

Frequency of the most frequent sequences in the selections targeting HEK293 cells (**A**), $Na_v1.6$-HEK293 cells (**B**) and $Na_v1.5$-HEK293 cells (**C**).

Another advantage of the COMPAS software is the ability to hide patterns during analysis. From now on, all sequences present in the selection target cells HEK293 were excluded from the analysis of the selection target cells $Na_v1.5$-HEK293 or $Na_v1.6$-HEK293. The remaining sequence patterns are listed in **Supp. table 8** and **Supp. table 9**. Compared to sequence Sa (which is used as a positive control for binding to HEK293), all other sequence patterns are slightly enriched. The binding capacity of these remaining sequences was analyzed in a Cherenkov assay (**Figure 5.8**). All investigated sequences showed minimal binding to all tested cell lines. There was no difference between HEK293 cells and $Na_v1.5$-HEK293 or $Na_v1.6$-HEK293 cells.

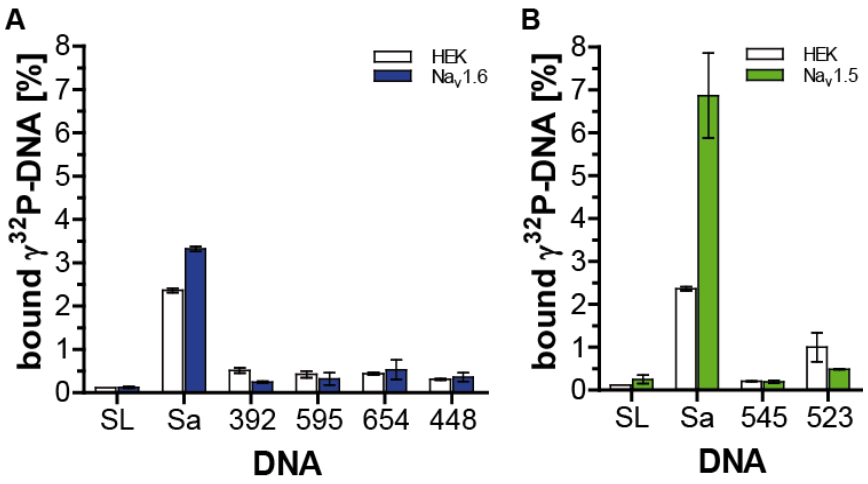

Figure 5.8: Binding of DNA sequences obtained from NGS analyses, all sequences were not present in the SELEX targeting HEK293, but Sa.

γ32P DNA of the start library (SL) and the various sequences obtained from NGS analyses in the SELEX targeting $Na_v1.6$-HEK293 (**A**) and $Na_v1.5$-HEK293 (**B**) but not present in the SELEX targeting HEK293 were analyzed with HEK293 cells (white), $Na_v1.6$-HEK293 cells (blue) and $Na_v1.5$-HEK293 cells (green), the radioactivity retained on or in the cells was determined by liquid scintillation counting (n=1, duplicates, mean ± SD).

Since the conventional cell-SELEX approach does not allow the selection of a sequence-specific to $Na_v1.5$ or $Na_v1.6$, the selection protocol must be changed. To exclude the possibility that $Na_v1.5$ or $Na_v1.6$ are not bound by aptamers, we have decided to use $Na_v1.1$ or $Na_v1.2$ for the next selection. The expression profile of these channels was investigated in collaboration with Prof. Heinz Beck (Life&Brain Center, Bonn). For both channels an expression of about 2500 channels per cell was determined.

5.1.5. Enrichment of DNA libraries targeting $Na_v1.1$ and $Na_v1.2$ with a multitude negative cell-SELEX

The first selections described above led to the conclusion that aptamers to the cell surface proteins of HEK293 cells are very easy to select using the conventional cell-SELEX approach. This means that the accumulation of sequences targeting these cell surface proteins must be suppressed during selection targeting VSGC. As a result, the selection process has been extended by a large number of negative selection steps. After incubation of the DNA library with HEK293 cells, the supernatant was transferred to the next flask with HEK293 cells, etc. (ten times in total). Finally, the supernatant was transferred to $Na_v1.1$-HEK293 or $Na_v1.2$-HEK293 cells (**Figure 5.9**).

After eight selection cycles, the DNA of the enriched libraries was analyzed with the Cherenkov assay (**Figure 5.10 A-B**).

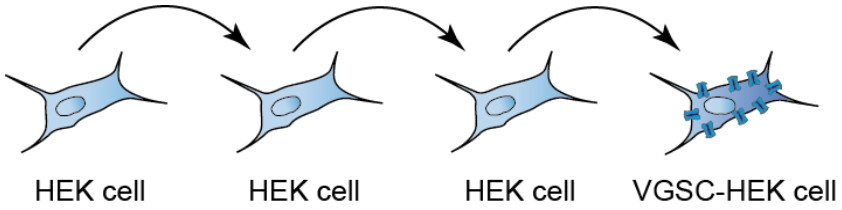

Figure 5.9: Schematic representation of the multiple negative incubation step SELEX.

After the first incubation with HEK293 cells, the supernatant is transferred to the next flask with HEK293 cells. After several incubations with new HEK293 cells, the supernatant is added to the HEK293 cells underexpression of VGSC.

Selection targeting $Na_v1.2$-HEK293 showed enrichment and a small difference in binding to HEK293 or $Na_v1.2$-HEK293 cells. For this reason, the selection target $Na_v1.2$-HEK293 was not further investigated. The selection target $Na_v1.1$-HEK293 showed in the 8th selection cycle an enrichment with a higher signal for $Na_v1.1$-HEK293 compared to HEK293 cells. For this reason, the selection target $Na_v1.1$-HEK293 was further analyzed in a radioactive Cherenkov assay with multiple negative selections according to the scheme in **Figure 5.9**.

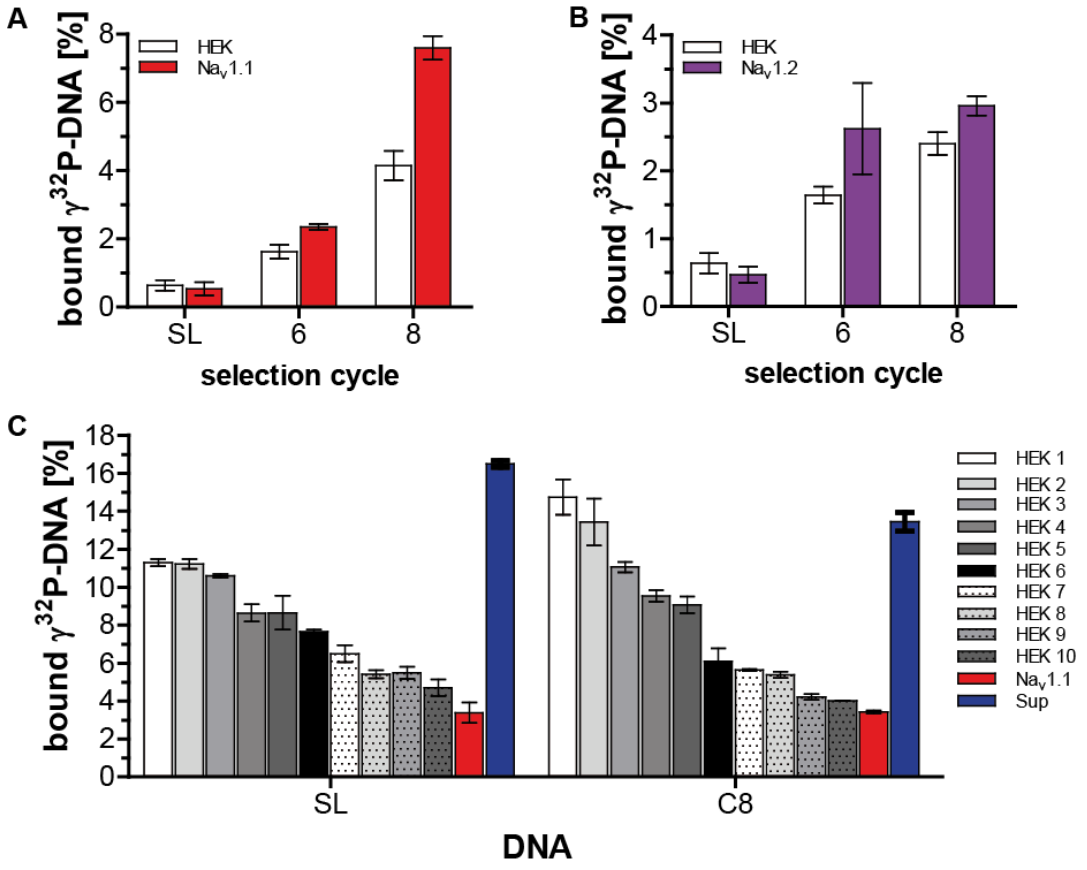

Figure 5.10: Radioactive binding assays of selections targeting $Na_v1.1$-HEK293-cells and $Na_v1.2$-HEK293-cells.

The γ32P DNA of the start library (SL), the selection cycles 6 and 8 of the selections for $Na_v1.1$ (**A**) and $Na_v1.2$-HEK293 cells (**B**) were incubated with HEK293, $Na_v1.1$-HEK293 or $Na_v1.2$-HEK293 cells, the radioactivity retained at the cells was determined by liquid scintillation (n=2, duplicates, mean ± SD). (**C**) The γ32P-DNA of the starting library (SL) and the selection cycle 8 (C8) was incubated with ten consecutive HEK293 cells (HEK 1 - 10), then the supernatant was transferred to $Na_v1.1$-HEK293 cells and the radioactivity retained on the cells and in the remaining supernatant (Sup) was determined by liquid scintillation (n=1, duplicates, mean ± SD).

After ten incubations with HEK293 cells (HEK 1 - HEK 10) no difference in the binding of the DNA of the SL to $Na_v1.1$-HEK293 ($Na_v1.1$) compared to the DNA of selection cycle 8 could be observed (**Figure 5.10 C**). This difference could be caused by the different expression profiles of HEK293 cell surface proteins on both cell lines. Consequently, the two selections for $Na_v1.1$-HEK293 and $Na_v1.2$-HEK293 were not further investigated.

One possible explanation could be that VGSC are "difficult" target molecules that cannot interact with DNA aptamers[79]. The chemical repertoire of canonical DNA containing four building blocks (dA, dT, dG, and dC) is limited compared to the high diversity of antibodies with 21 amino acids[57]. The novel click-SELEX[29] approach allows the increase of chemical diversity through the use of click chemistry and the functionalization of DNA with any desired residue. This leads to higher success in the selection of an aptamer[98], which is called a "clickmer" compared to DNA SELEX (**section 3.1.3.3**). For this reason, the click-SELEX approach was investigated for the next selection targeting VGSC.

5.2. Selections of clickmers targeting VGSC

Clickmers are a new generation of aptamers that contain chemical substances. The copper(I)-catalyzed alkyne azide cycloaddition (CuAAC)[29] modifies the DNA libraries carrying alkyne-modified nucleotides (EdU instead of dT) (**Figure 3.9**) (**section 3.1.3.3**). In our laboratory, several azides were synthesized or commercially purchased and tested for the functional ability and amplifiability (**Figure 5.11**).

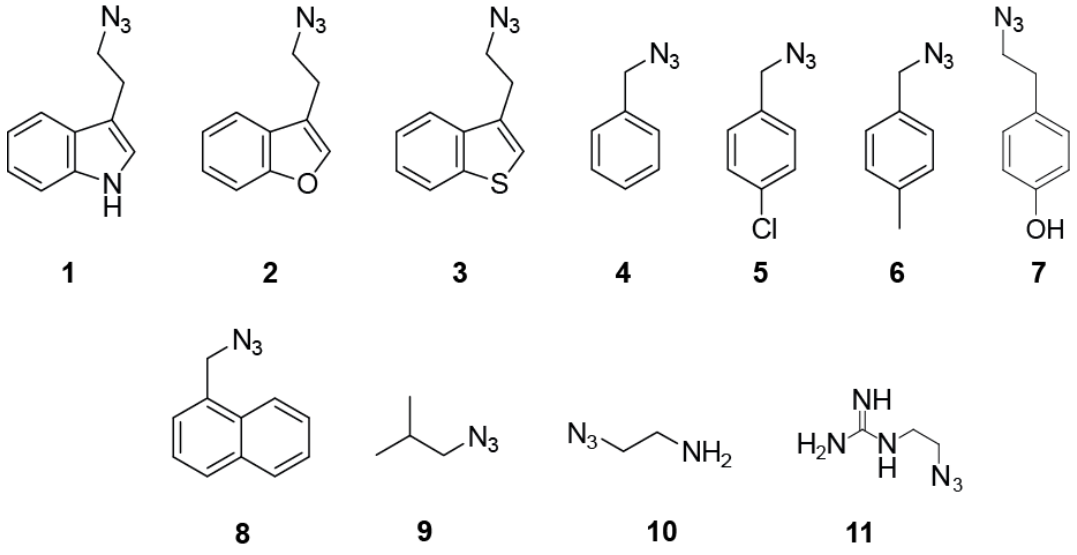

Figure 5.11 Chemical structure of the azides available for click-SELEX.

Chemical structures of the azides used for DNA functionalization: (**1**) 3-(2-azidoethyl)-1*H*-indole, (**2**) 3-(2-azidoethyl)-benzofuran, (**3**) 3-(2-azidoethyl)-benzo[*b*]thiophene, (**4**) 1-(azidomethyl)-benzene, (**5**) 1-(azidomethyl)-4-chlorobenzene, (**6**) 1-(azidomethyl)-4-methylbenzene, (**7**) 4-(2-Azido-ethyl)-phenol, (**8**) 1-(2-azidomethyl)naphthalene, (**9**) 1-azido-2-methylpropane, (**10**) 2-azidoethanamine, and (**11**) *N*-(2-Azido-ethyl)-guanidine.

The first click-SELEX was performed on $Na_v1.6$-HEK293 cells as they show a high expression of VGSC compared to the other cell lines ($Na_v1.1$-HEK293, $Na_v1.2$-HEK293, $Na_v1.4$-HEK293, $Na_v1.5$-HEK293 (**section 5.1.1**)). The DNA of the FT2 library (an alkyne-containing library) was functionalized with guanidine azide (**11**) according to **Figure 3.9**. Guanidine azide (**11**) was used due to its chemical similarity to tetrodotoxin (TTX) (**Figure 5.12**). TTX is an extreme neurotoxin as it blocks VGSC. TTX binds via its guanidine residue to the extracellular domain of VGSC[154]. Guanidine azide (**11**) was selected to increase the probability of selecting a clickmer as it could interact with the same binding site as TTX.

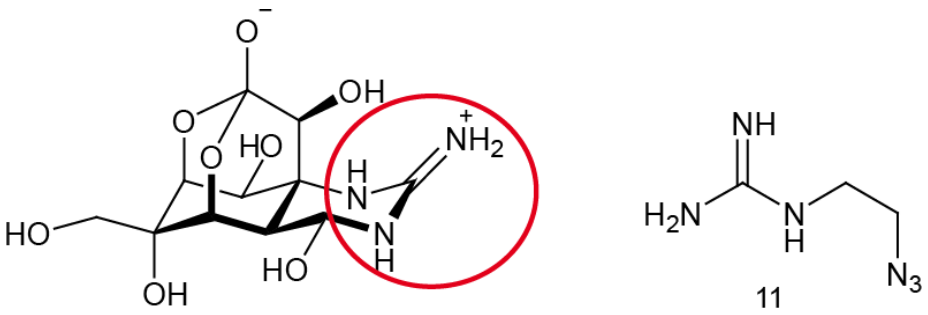

Figure 5.12 Chemical structure of tetrodotoxin (TTX) and guanidine azide (11).

The chemical structures of the VGSC-binding guanidinium residue of tetrodotoxin (red circle) and *N*-(2-azido-ethyl)-guanidine (**11**) are shown.

HEK293 cells were used for negative selection (**section 5.1.1**). The bound sequences were recovered in the elution buffer containing TTX (20µM). TTX should specifically elute only sequences bound to VGSC. After selection cycle 7, a Cherenkov assay was performed. It was expected that 7 selection cycles would be sufficient for enrichment due to all previously performed selections (**Figure 5.4**, **Figure 5.10 A-B**) which had an enrichment between selection cycles of 5 to 8. However, no enrichment was observed for both cell lines, neither for HEK293 nor for $Na_v1.6$-HEK293 cells (**Figure 5.13**). A possible explanation could be that elution with TTX did not work properly. Another possibility is the fact that the FT2 library contains about ten random EdUs. In the event that the EdUs are close together in the random range, the remainders of the final functionalization may interfere with each other due to steric obstacles in order to interact properly with VGSC.

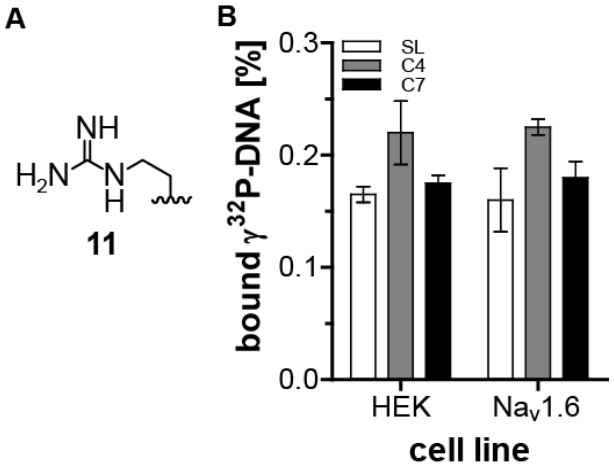

Figure 5.13: Binding assay of click-selection targeting $Na_v1.6$-HEK293 cells.

(**A**) Chemical structure of *N*-ethylguanidine (**11**). (**B**) γ32P-click DNA of the start library (SL - white), selection cycle 4 (C4 - grey) and cycle 7 (C7 - black) were functionalized with guanidine azide (**11**) and incubated with HEK293 (HEK) or $Na_v1.6$-HEK293 ($Na_v1.6$) cells. The radioactivity retained on or in the cells was determined by liquid scintillation counting (n=1, duplicates, mean ± SD).

For this reason, another library, FT2-0.35, was chosen for the second click-SELEX. This library contains about four EdUs in the random range instead of ten, *e.g.* FT2. Fewer functionalizations could ensure the interaction of the chemical unit with the VGSC due to fewer steric obstacles. Two selections were made in parallel using indole (**1**) and guanidine azide (**11**) for DNA functionalization.

Both selections targeted $Na_v1.6$-HEK293 cells. After performing eight selection cycles with a negative selection with HEK293 cells, a branching point as shown in **Figure 5.2** was introduced. After a total of 12 selection cycles, a Cherenkov assay was performed with DNA from selection cycles 1, 8 and 12 (**Figure 5.14**). Both selections showed enrichment in comparison of the binding of the DNA of SL and the last selection cycle C12. Nevertheless, the unfunctionalized DNA (w/o) of selection cycles 8 and 12 showed a signal similar to that of the functionalized DNA (**11** and **1**). Accordingly, both selection and binding were not dependent on DNA functionalization. With regard to enrichment, however, both selections were sequenced using NGS.

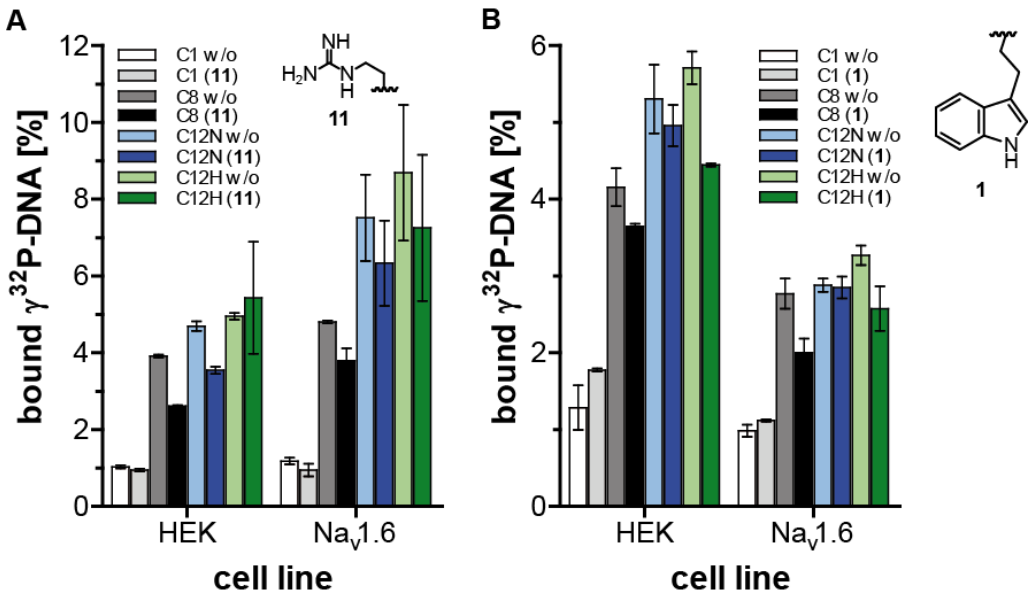

Figure 5.14: Binding assay of the cell-click-selections targeting $Na_v1.6$-HEK293-cells using guanidine azide (11) or indole (1) for DNA functionalization.

γ32P-click DNA of selection cycles 1 (C1), 8 (C8), 12 of HEK293-SELEX (C12H) and 12 of $Na_v1.6$-HEK293-SELEX (C12N) were functionalized with guanidine (**11**) (**A**) or indole azide (**1**) (**B**). The unmodified (w/o) and modified click DNA were incubated with HEK293 and $Na_v1.6$-HEK293 cells. The radioactivity retained on or in the cells was determined by liquid scintillation counting (n=1, duplicates, mean ± SD).

The change of the nucleotide distribution in the random region confirmed the enrichment of both selections. As expected, the initial library FT2-0.35 contained about 30% of the nucleotides C, G, and A, but 10% T. For the last selection cycle 12 a change of the nucleotide distribution was observed. No difference could be observed between the nucleotide distribution of cycle 12 $Na_v1.6$-HEK293 or HEK293 (**Figure 5.15 B-E**). But the comparison of the nucleotide distribution for the two different azides showed a different pattern. The analysis of the nucleotide distribution for all sequenced selection cycles is in **Supp. figure 4** and **Supp. figure 5** shown. The reduction of unique sequences in the library via selection also indicated enrichment (**Figure 5.15 F-G**). A strong reduction can be observed in the selection for $Na_v1.6$-HEK293. While the fourth selection cycle contained more than 95% unique sequences, the amount in the eighth selection cycle decreased to below 20% for guanidine and below 10% for indole azide. The introduction of branching points led to an increase in unique sequences for selection to HEK293.

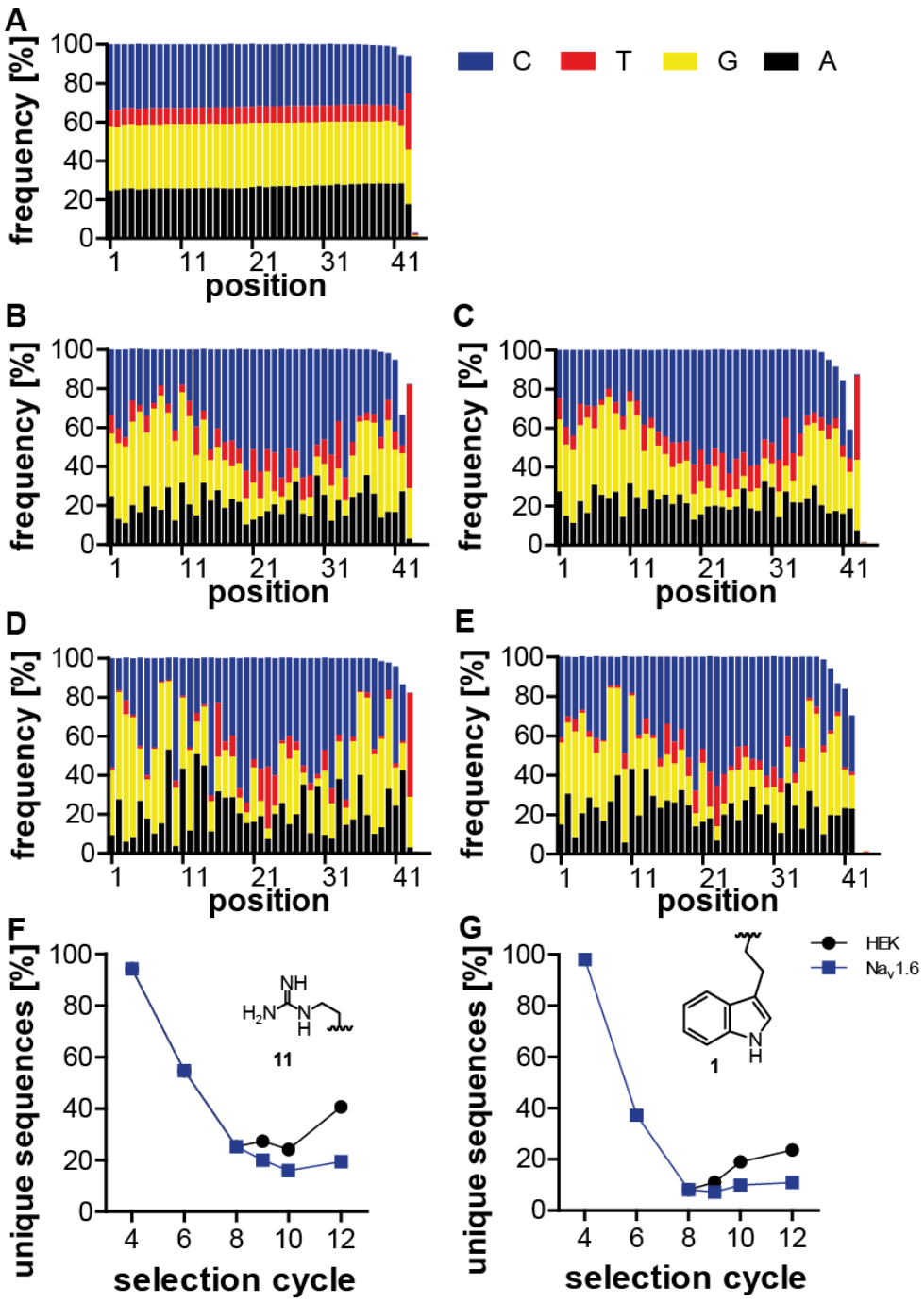

Figure 5.15: Nucleotide distribution and unique sequences of the NGS analyses of the click-selections using guanidine (11) and indole (1) azides for DNA functionalization targeting $Na_v1.6$-HEK293 and HEK293 cells.

Nucleotide distribution at the different positions of the random region in the DNA of the initial library FT2-0.35 (**A**) and the final selection cycle 12 using guanidine (**11**) for DNA functionalization for $Na_v1.6$-HEK293 (**B**) and cycle 12 for HEK293 cell SELEX (**C**). Selection cycle 12 using indole (**1**) for DNA functionalization targeting $Na_v1.6$-HEK293 (**D**) and HEK293 cell-SELEX (**E**). The unique sequences of both selections are presented in (**F**) with guanidine (**11**) and (**G**) with indole (**1**) for DNA functionalization.

With the COMPAS software, all sequences enriched with the selection target HEK293 (HEK sequences) were hidden during the analysis of the selection target $Na_v1.6$-HEK293. No sequence was left for indole azide (**1**). All enriched sequences target cell surface proteins of HEK293 cells, not

$Na_v1.6$. For guanidine azide (**11**) selection, however, a promising sequence, GN1, was selected for further investigation. GN1 was the only most abundant sequence after all sequences found in the HEK selection were hidden. The frequency of the most frequent sequence Sa in the cell selections performed with the ssDNA library D3 was about 40-50% in the last selection cycles (**Figure 5.7**), while the frequency of GN1 is very low at 0.8%. Nevertheless, GN1 was examined for VGSC binding in a Cherenkov assay. The eighth selection cycle was used as binding control. In both cell lines, no difference was found between DNA from selection cycle 1 (C1) and GN1 (**Figure 5.16 B**).

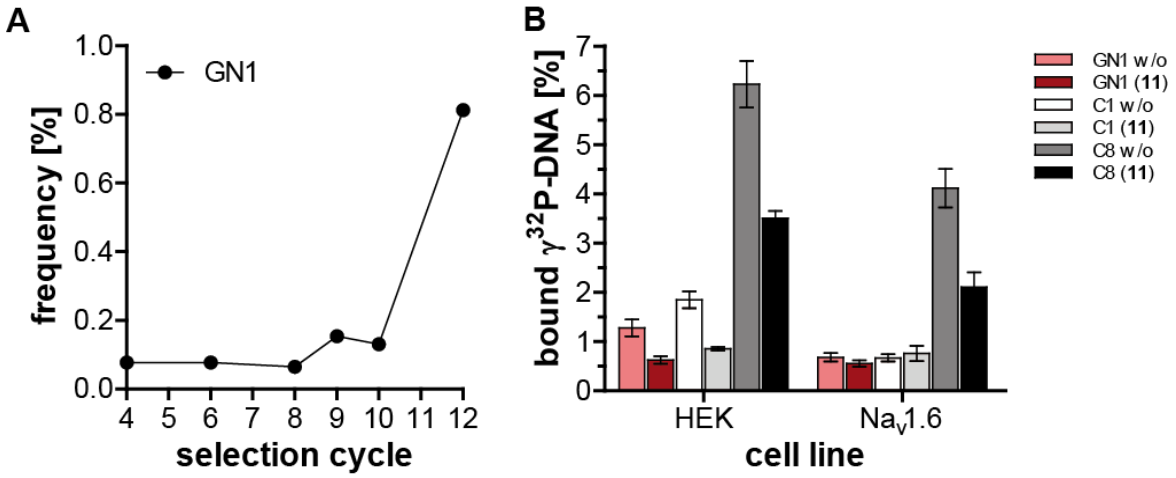

Figure 5.16: NGS frequency and binding analysis of the sequence GN1.

(**A**) Shown is the frequency of the selected sequence GN1 in the relevant selection cycles of the click-SELEX targeting $Na_v1.6$-HEK293 cells. (**B**) Unfunctionalized (w/o) and guanidine azide functionalized (**11**) γ32P-click DNA of sequence GN1, selection cycle 1 (C1) and cycle 8 (C8) was incubated with HEK293 and $Na_v1.6$-HEK293 cells. The radioactivity retained on or in the cells was determined by liquid scintillation counting (n=1, duplicates, mean ± SD).

5.3. Library design of the OW1 library

All selections carried out so far support the assumption that the low expressed proteins (VGSC) on the cell surface are difficult to bind by aptamers or clickmers. The main problem is the high expression of other membrane proteins, which are good targets for aptamers or clickmers. To solve this problem, it is important to suppress all sequences targeting proteins other than the target molecule, *e.g.* by negative selection. Under these circumstances, the number of eluted sequences can be very small due to the small number of target proteins. Therefore, SELEX requires a library that allows a high number of PCR cycles to amplify the eluted sequences without the generation of by-products such as shortened or prolonged PCR products. Many selections fail due to such by-products[155].

Previously, the FT2-click library was used because it already led to the successful selection of clickmeren in two click selections[29,98]. However, the FT2-click library only allows about 22 PCR cycles without amplification of by-products. For this reason, a new click library was developed: OW1: 5'- AGCCACGGAAGAGAAGAACCAGA -N44- GCAGAAGCGACAGCAACA -3' (N= dA:dC:dG:EdU = 1:1:1:1:1). It consists of a 44 nucleotide (nt) random region with the same

nucleotide distribution. This random region is flanked by two 18 nt primer binding sites that do not contain EdU or T to avoid polymerase problems during amplification or the false annealing of the primers[26]. In addition, about 20% EdU oxidizes during deprotection during solid-phase synthesis, resulting in a unfunctionalizable ketone[156]. If the primer binding sites contained such a ketone, this could lead to an unspecific binding or inhibit the binding of the clickmer to the target molecule due to the lack of functionalization. Although some syntheses solve this problem, such as protection with triisopropyl silyl ether (TIPS) or the click-on solid-phase approach[156], they are much more expensive.

5.3.1. Functionalization of the OW1 library using click chemistry

The quantitative functionalization of the OW1 library was investigated. Therefore, the OW1 and FT2 libraries were functionalized with two different azides and enzymatically digested to the nucleotides as described in **section 8.2.3**. The sample was then analyzed by HPLC. Both libraries were quantitatively functionalized (**Figure 5.17**).

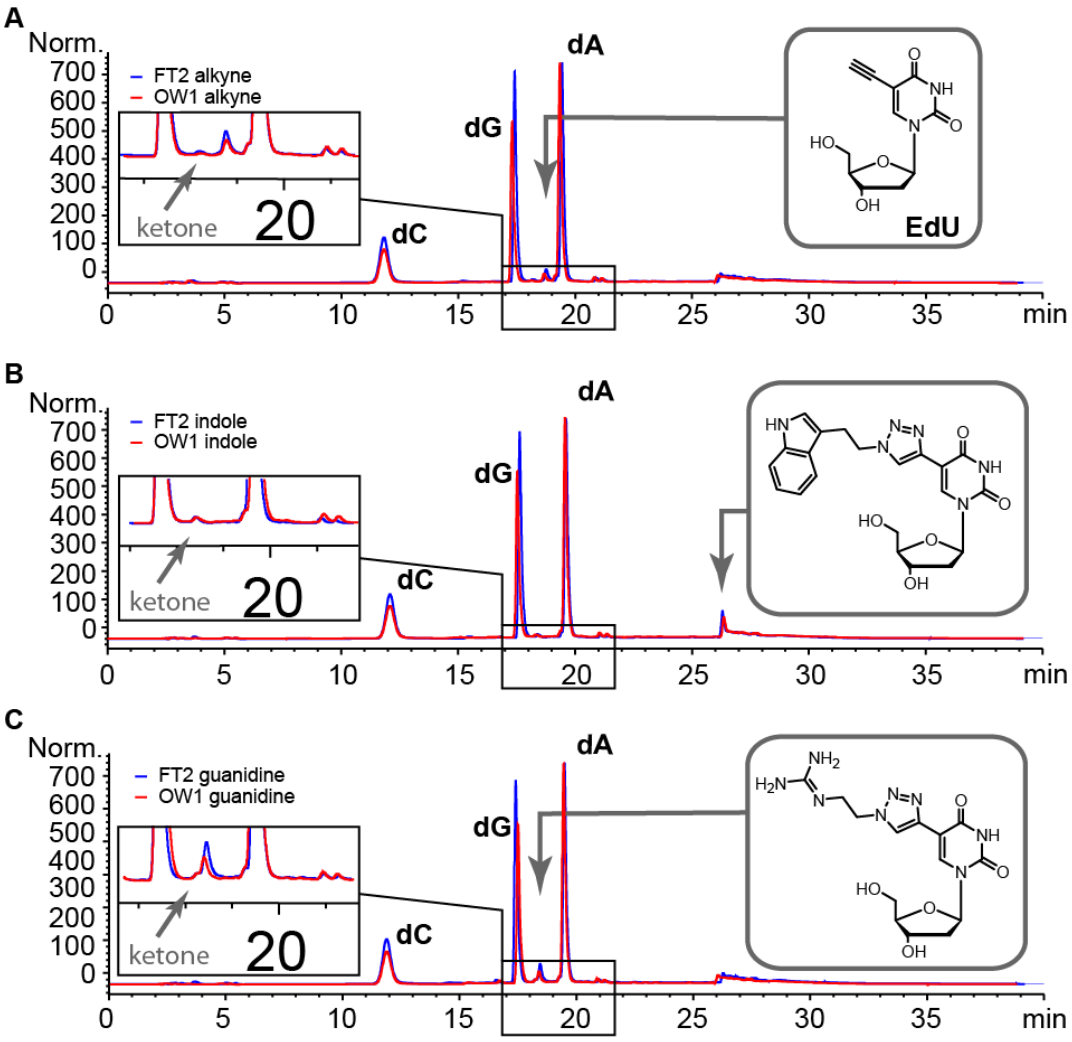

Figure 5.17: HPLC analyses of the functionalization with OW1 and FT2 libraries using indole azide (1) and guanidine azide (11).

HPLC analyses of libraries FT2 and OW1. The libraries were digested to the nucleotides as unfunctionalized DNA (**A**) and DNA functionalized with indole (**1**) (**B**) or guanidine azide (**11**) (**C**).

Figure 5.17 A shows the unfunctionalized libraries. The nucleotides dC, dG, and dA are clearly recognizable with a strong signal. EdU, as well as ketone, are not as well visible due to low UV activity. The functionalized libraries are shown in **Figure 5.17 B** and **C**. Here you can clearly see that the signal for EdU is gone and another one for the functionalized nucleotide appears. The signal for the guanidine functionalized nucleotide is in the same range as for the ketone and EdU. Therefore, HPLC purification was performed and the functionalized nucleotide was examined for mass by LCMS. The calculated mass of the nucleotide functionalized with guanidine was confirmed.

5.4. Selections of clickmers targeting GluR1

5.4.1. Generation of a stable cell line expressing GluR1

In order to validate the selection strategy, it is important to have a positive control. For this reason, we have decided to generate a stable cell line that expresses a protein that is known to be ligated by aptamers. Recently, an RNA aptamer targeting glutamate receptor 1 (GluR1) was published[157].

HEK293 was selected as the cell line for transfection. The fusion plasmid (pEGFPC1-GluR1Ctail[158]) was purchased from Addgen (**Supp. figure 6**). The transfected cells were sorted according to their EGFP expression and compared with unsorted or non-transfected cells by flow cytometry. Since it is a fusion plasmid, the expression of GluR1 can be confirmed by EGFP expression, since EGFP is only expressed when GluR1 has been expressed. The results are shown in **Figure 5.18**. When comparing the non-transfected (HEK) with the transfected cells (GluR1-HEK), a shift in fluorescence intensity was observed. This showed that the expression of the proteins EGFP and GluR1 was successful. The sorted cells (GluR1-HEK sorted) showed a high fluorescence intensity, which means that all cells express EGFP and GluR1.

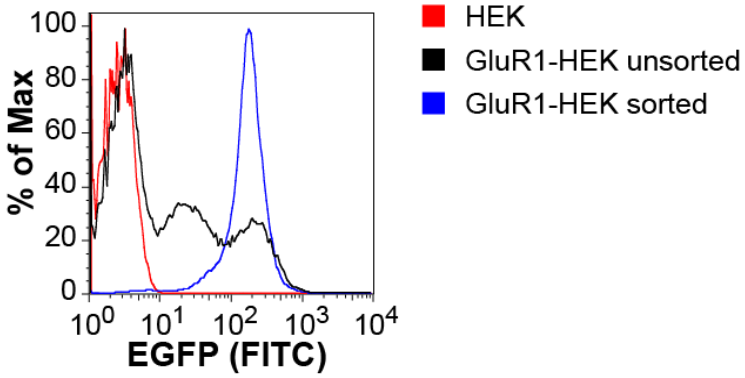

Figure 5.18: EGFP fluorescence of unsorted and sorted cells HEK293, GluR1-HEK.

The mean fluorescence intensities (MFI) of FITC were determined. The representative flow cytometry histograms of HEK293 (red), GluR1-HEK293 unsorted (black) and sorted (blue) are displayed (one representative is shown).

Confocal microscopy was performed to evaluate the membrane localization of both expressed proteins. The cells were stained with DAPI (nucleus) and the lipophilic membrane dye Dil. DAPI

catches the nucleus blue and Dil catches the membrane red. The superposition of green (**Figure 5.19 A**) and red fluorescence (**Figure 5.19 B**) shows that EGFP (green) is expressed on the membrane (red). Since GluR1 is expressed as EGFP fusion protein, we can assume that GluR1 is also present on the membrane.

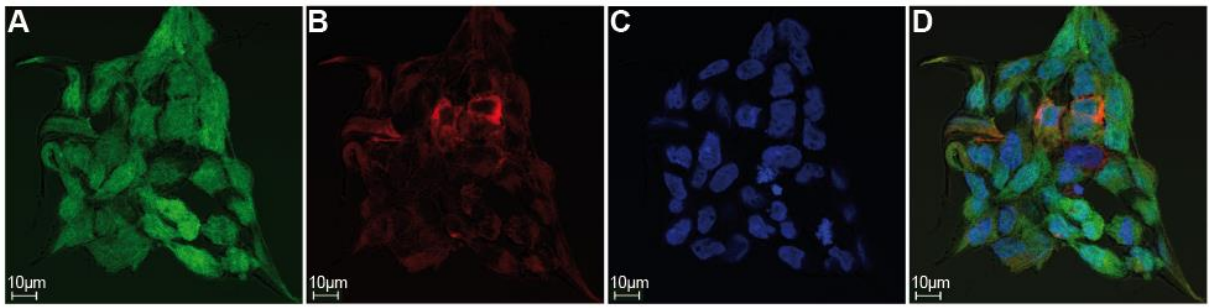

Figure 5.19: Confocal microscopy of the sorted GluR1-HEK293 cells.

GluR1-HEK293 cells were stained with DAPI and the lipophilic membrane dye Dil. **A**) represents the green fluorescence of EGFP, **B**) the membrane in red (lipophilic membrane dye Dil), **C**) the nucleus in blue (DAPI) and **D**) the combined image (one representative is shown).

5.4.2. Click-SELEX targeting GluR1

Indole (**1**), benzyl (**4**) and guanidine (**11**) azides were selected for click-selection targeting GluR1-HEK293 cells. Indole and benzyl were used because they were the modification in the two successful click-SELEX[29,98]. Indole and benzyl are chemically similar to the amino acids most commonly involved in protein-protein interactions (tryptophan and phenylalanine)[85,86]. Guanidine was selected due to the fact that it should be used in the selection for VGSC.

Click-selection for GluR1-HEK293 cells was performed with a negative selection step on non-transfected HEK293 cells, as described in **section 8.5.1.5**. Unfortunately, selection had to be stopped for all three functionalizations before ten selection cycles were completed as no PCR products could be obtained. Three selection cycles could be performed for indole functionalization, four for benzyl and five for guanidine. The DNA of the last selection cycle of each click-SELEX was marked with γ32P and analyzed for binding to GluR1-HEK293 cells in a Cherenkov binding test (**Figure 5.20**). A small enrichment was observed only for SELEX with guanidine azide. Here the DNA of the selection cycle five (C5) showed a higher signal to HEK cells than to cells expressing GluR1, this selection was not further analyzed since we assume that only sequences targeting HEK293 cells, but not GluR1, could be obtained from it.

The Cherenkov assay also showed that the binding properties of the source library depend on the functionalization used. The indole (**1**) functionalized DNA of the initial library has a much higher background than the DNA functionalized with benzyl (**4**) or guanidine (**11**) (**Figure 5.20**). One possible explanation might be that indole functionalization has a higher affinity to the cell surface proteins of HEK293 cells, leading to a higher binding signal.

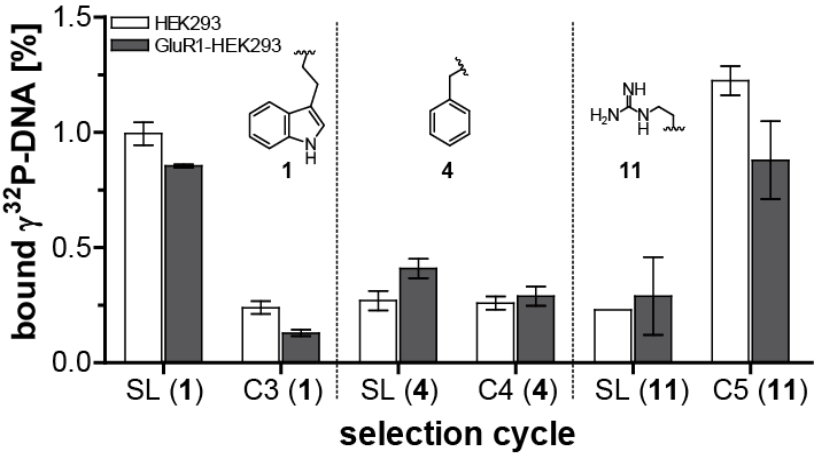

Figure 5.20: Binding analyses of the click-selections targeting GluR1-HEK293 cells using indole (1), benzyl (4), or guanidine (11) for DNA functionalization.

γ32P-click DNA of the start library (SL), selection cycle 3 (C3), 4 (C4) and 5 (C5) were functionalized with indole (**1**), benzyl (4) or guanidine azide (**11**) and subsequently incubated with HEK293 (white) or GluR1-HEK293 cells (grey). The radioactivity retained on or in the cells was determined by liquid scintillation counting (n=1, duplicates, mean ± SD).

The failed click-selections targeting GluR1-HEK293 cells with indole and benzyl azides show that the selection strategy does not allow targeting of a specific cell surface protein. However, selection with guanidine azide shows clear enrichment. This means that the new start library (OW1) works correctly, i.e. it allows the generation of aptamers/clickmers by SELEX. However, because the selection was not further investigated, the functionality of the OW1 library was demonstrated in a separate selection (see **section 5.5**).

5.5. Identification of clickmers targeting cycle3-GFP

To our knowledge, only two clickmers, C12, and C11.41 were released. C12 targets C3-GFP[29] proteins and C11.41 targets a small molecule target, the (-)-Δ9-tetrahydrocannabinol (THC)[98]. While the C12 has functionalized with indole azide (**1**), the C11.41 was selected with benzyl azide (**4**). Further analyses showed that functionalization also led to interaction of the clickmers with other azides. The C12 interacts with C3-GFP also with benzofuran (**2**) or benzothiophene (**3**) functionalization, but not with aliphatic functionalizations. Clickmer C11.41 also showed that it interacts with aromatic side-chain functionalizations other than benzyl functionalization with THC. We asked ourselves whether the functionalisation had an influence on the click-SELEX and, if so, which one. For this reason, we first decided to investigate the click-SELEX approach with different functionalizations in order to understand their effects on the selection process. Since a cell is a complex system with a large number of cell surface proteins, a protein target was used to simplify the selection model.

5.5.1. Click-SELEX using different azides

To illustrate the effects of the chemical residue used for DNA functionalization in click-SELEX, we performed eight click selections with a representative collection of azides. Since cycle3-GFP (C3-GFP) was successfully targeted with click-SELEX[29], it was selected as the target protein to test the OW1 library's ability to select clickmers. Eight azides were selected for the selections (**Figure 5.21**). The selection was performed as published by Tolle *et al.*[29].

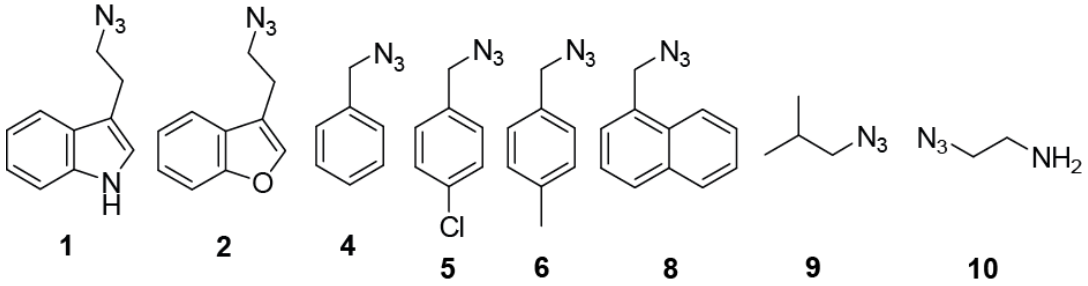

Figure 5.21 Azides used for DNA functionalization in click-selections targeting C3-GFP.

Chemical structures of the azides used in the click-selections for C3-GFP. (**1**) 3-(2-azidoethyl)-1*H*-indole, (**2**) 3-(2-azidoethyl)-benzofuran, (**4**) 1-(azidomethyl)-benzene, (**5**) 1-(azidomethyl)-4-chlorobenzene, (**6**) 1-(azidomethyl)-4-methylbenzene, (**8**) 1-(2-azidomethyl)naphthalene, (**9**) 1-azido-2-methylpropane, and (**10**) 2-azidoethanamine.

Five click selections using azides **5**, **6**, **8**, **9**, and **10** for DNA functionalization could not be successfully completed due to PCR by-product formation and were stopped (**Supp. figure 8**). The by-products in PCR are a sign of failure as the enrichment of certain target sequences is prohibited[155]. One explanation could be that these five azides reject interaction with the target protein C3-GFP and no binding sequence can be recovered for amplification after incubation with the target protein. Furthermore, functionalization may have an effect on DNA folding, which does not lead to DNA-protein interaction. The more exact reason cannot be determined at this point with the generated data.

Three other click-selections, in which azides **1**, **2**, and **4** were used for DNA functionalization, were successfully completed. After ten selection cycles for indole azide (**1**) and eight selection cycles each for the functionalization of benzofuran (**2**) and benzyl azide (**4**), the Cy5-labeled DNA of the last selection cycles was examined for its binding to C3-GFP by flow cytometry (**Figure 5.22**). The DNA from the selection cycles ten for indole, eight for benzofuran and benzyl azide showed binding to C3-GFP. No binding to the functionalized DNA of SL and to the unfunctionalized DNA of selection cycles and SL was detected.

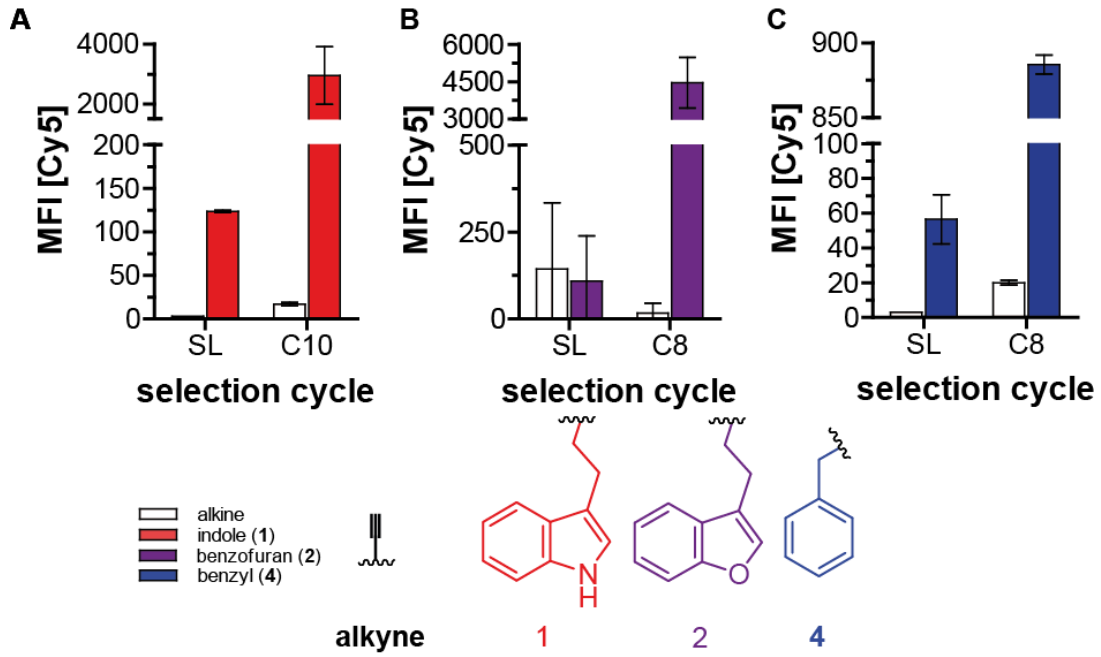

Figure 5.22: Interaction analysis of the click-selections targeting cycle3-GFP functionalized with indole (1), benzofuran (2), and benzyl azide (4).

500 nM Cy5-labeled DNA from the initial library (SL), selection cycles 8 (C8) and 10 (C10) were incubated with unchanged magnetic beads and cycle3-GFP (C3-GFP) with magnetic beads. The Cy5 fluorescence retained on the beads was determined by flow cytometry (n=2, singlets, mean ± SD). The mean fluorescence intensity (MFI) at the C3-GFP beads is shown after subtraction of the respective values at the unmodified beads and the chemical structures of functionalization, alkyne, indole (**1**), benzofuran (**2**) and benzyl (**4**). The selection with the indole (**1**) functionalization is illustrated in (**A**), with benzofuran (**2**) in (**B**), and with benzyl (**4**) in (**C**).

5.5.2. NGS analyses of C3-GFP click-selections

The three successful selections were analyzed by NGS with a dNTP mix containing dTTP instead of EdUTP. **Figure 5.23 A** shows the frequency of the unique sequences over the three successful click-selections. All selections showed a strong decrease (to below 6%) of the frequency of the unique sequences. The strongest effect can be seen with benzofuran, ready in the fourth selection cycle the frequency of the unique sequences is very much reduced.

The nucleotide distribution of the start library and each last selection cycle differ with respect to DNA functionalization (**Figure 5.23 B-E**). In the start library, all nucleotides are distributed almost evenly at each position of the random region. The NGS measurement shows a higher error rate the longer the oligonucleotide to be sequenced[52]. Therefore, the measurements in **Figure 5.23 B**, **D**, and **E** from position 41 show a reduction in the nucleotide sequence.

The indole selection is so highly enriched that it enables the most frequently occurring sequence to be read out from the random region (**Figure 5.23 C**). The selections of benzyl or benzofuran azide (**Figure 5.23 D**, **E**) were enriched with several sequences, resulting in a mixed distribution of nucleotides. In summary, both unique sequences and the distribution of nucleotides showed a high

enrichment of all three selections and a difference in the sequence pattern of the most common sequences.

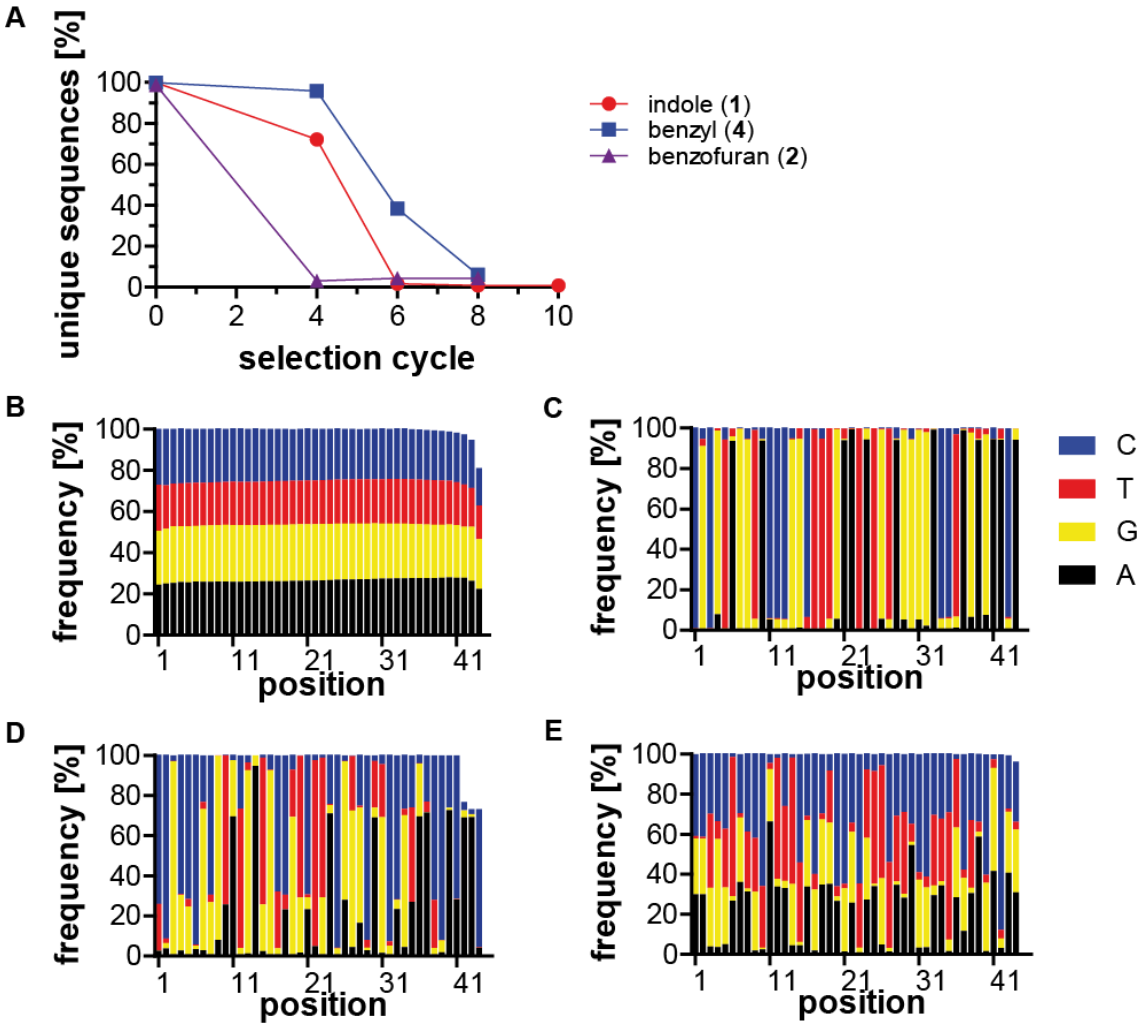

Figure 5.23: NGS analyses of click-DNA sequences in click-selections targeting C3-GFP.

(**A**) The unique sequences of the click selections are shown with indole (**1**) in red, benzofuran (**2**) in violet and benzyl azide (**4**) in blue. Nucleotide distribution at the different positions of the random region in the DNA of the initial library OW1 (**B**), the final selection cycle 10 with indole azide (**1**) for DNA functionalization (**C**), cycle 8 with benzofuran (**2**) (**C**) and cycle 8 with benzyl azide (**4**) (**D**).

Figure 5.24 A shows the frequency of the most common sequences present in the NGS analyses from the click-selections for C3-GFP. I10 was selected with indole azide (**1**), B33, B15, and B10 were selected using benzyl azide (**4**), F20 and F8 with benzofuran azide (**2**). The frequency in the final selection cycle was between 9-60% for all sequences (**Table 5.2**). These six sequences were tested for binding to C3-GFP by flow cytometry (**Figure 5.24 B**). All sequences showed a high mean fluorescence intensity (MFI) when functionalized with the respective azide, except B10.

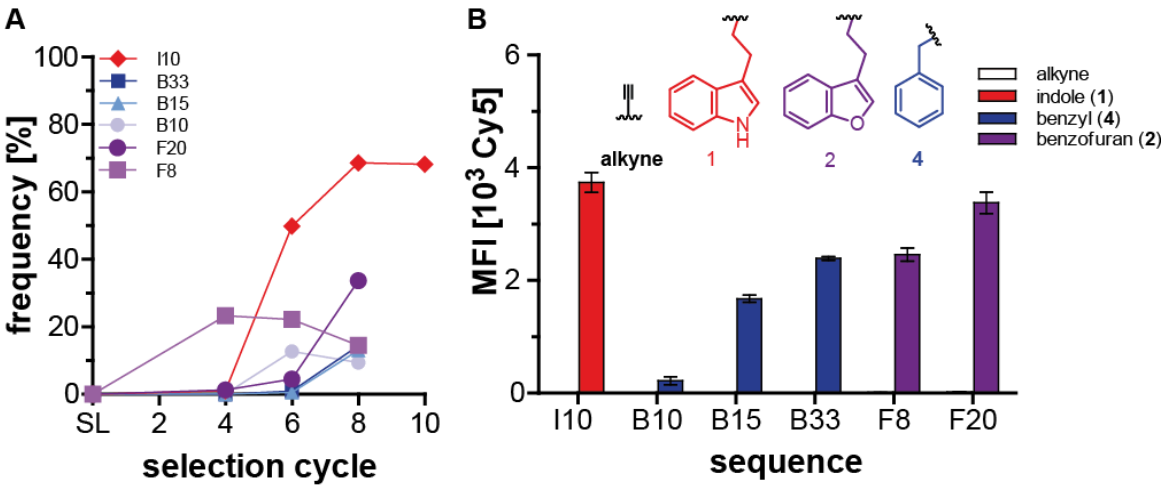

Figure 5.24: Frequency in the NGS and flow cytometry analyses of the most abundant sequences in click-selections targeting C3-GFP.

(**A**) The frequency of the most frequent sequences I10, B33, B15, B20, F20 and F8 in the relevant click-selection cycles for C3-GFP is shown. (**B**) The amount of Cy5-labeled un-/functionalized DNA bound to C3-GFP-modified magnetic beads was analyzed by flow cytometry. The DNA was either unfunctionalized (alkyne) or functionalized with indole (**1**), benzofuran (**2**) or benzyl azide (**4**) (n=2, singlets, mean ± SD). The mean fluorescence intensity (MFI) at the C3-GFP beads is shown after subtraction of the respective values at the unmodified beads and the chemical structures of functionalization, alkyne, indole (**1**), benzofuran (**2**) and benzyl (**4**).

Table 5.2 Sequences identified by NGS analysis in the single azide click-SELEX. Their copy number according to Sanger sequencing and frequency in the last selection cycle is listed. The primer binding sites were omitted.

The nomenclature of the sequences was random.

Name	Random region (44 nt; X=EdU)	Sanger	NGS (%)
I10	CGCGXAGGXACCCGGCXXXGAAXAXGXAGGGGACCXAGAGAACA	45/47	60.4
B10	CCXCCXACCCAXXXXACAACCCCXAGXACCCCXAXGGCACACAC	12/42	9.4
B15	AAGGGXGAGCAAAACCGGGCGGXGXXCCXAGGCXXXCACGGCGG	12/42	13.1
B33	GGCGXGCXXXGXCXCACCXACACAXXCXAACCACCACXACGCCA	14/42	14.4
F8	XCGGGCCGGAGCGAGGXAXGAXGCCAXCCXXCACAGCXCCA	3/21	14.5
F20	CCGCCCGCGXAXGAXGCCGXCXXACGGGCAGCCGXAACCACAAC	3/21	33.7

5.5.3. Characterization of clickmers targeting C3-GFP

5.5.3.1. Analyses regarding the clickmers functionalization

I10, F8, F20, B33, and B15 have been selected for further characterization. B10 was not further characterized due to the lower signal in the binding analysis shown in **Figure 5.24 B**.

A concentration-dependent analysis was performed for B15 and B33. The DNA was labeled with Cy5 and functionalized with benzyl azide (**4**). The binding of the functionalized DNA to C3-GFP was measured by flow cytometry. As shown in **Figure 5.25**, it was assumed that B15 had a lower affinity to C3-GFP than B33. For this reason, B15 was not further characterized.

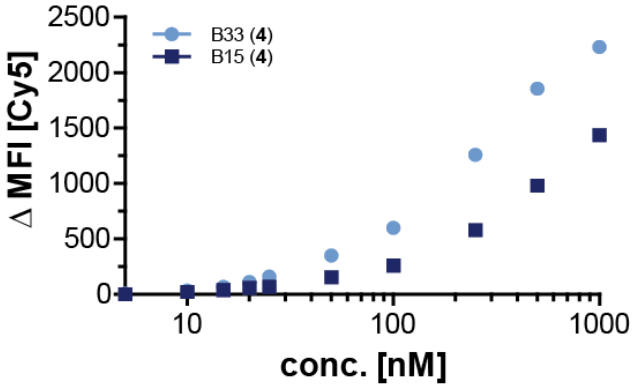

Figure 5.25: Concentration-dependent flow cytometry analysis of B15 and B33.

Shown is a concentration-dependent binding curve of the Cy5-labeled sequences B15 and B33, which are functionalized with benzyl azide (**4**) to C3-GFP and analyzed by flow cytometry (n=1, singlet). The MFI of the non-binding control (SL) was subtracted from the MFI of the sequences.

Sequences I10, B33, F8, F20, and F20sc were examined for binding by flow cytometry with regard to functionalization with different azides. F20sc was used as the non-binding control. Additional azides were used for sequence modification (**Figure 5.26**). The values were normalized to the original azide of the sequences, i.e. indole (**1**) functionalization for I10, benzyl (**4**) functionalization for B33 and benzofuran (**2**) functionalization for F20. I10 has a bond of about 20% with all aromatic units and B33 has a bond of about 30%. Nevertheless, both sequences, I10 and B33, reached their full binding potential compared to the other functionalizations only when they were functionalized with the original modification. F8 and F20 show a bond only with benzofuran and the very similar aromatic group benzothiophene (**3**). All sequences show no binding without functionalization. The control F20sc showed no binding with functionalization. This shows the high specificity regarding functionalization with the original azide for sequence binding.

Sequences I10, F8, and F20 show a clear difference in behavior with regard to the specificity with regard to functionalization. I10 selected with indole (**1**) is not as specific as F8 or F20 selected with benzofuran (**2**). Looking at the chemical structures of indole and benzofuran (**Figure 5.26**), it becomes clear that both benzofuran and benzothiophene are electron pairs donors in contrast to indole, which is an acceptor. This small difference has an influence on the sequence selected by click-SELEX and thus on the properties of this sequence. The characterization of the sequences is done in the next chapters (**section 5.5.4**).

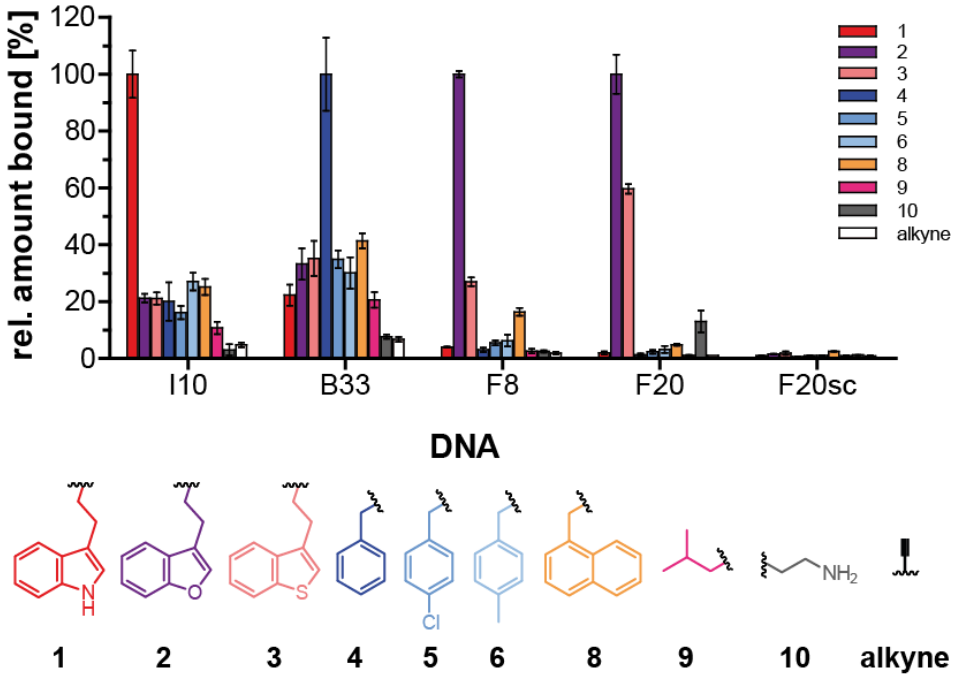

Figure 5.26: Impact of different functionalizations on the binding of selected clickmers targeting C3-GFP.

The amount of 500 nM Cy5-labeled DNA functionalized with various azides bound to C3-GFP and analyzed by flow cytometry is shown. The sequences were either unfunctionalized (alkyne) or functionalized with (**1**) 3-(2-azidoethyl)-1*H*-indole, (**2**) 3-(2-azidoethyl)benzofuran, (**3**) 3-(2-azidoethyl)benzo[*b*]thiophene, (**4**) 1-(azidomethyl)benzene, (**5**) 1 (azidomethyl)-4-chlorobenzene, (**6**) 1-(azidomethyl)-4-methylbenzene, (**8**) 1 (2 azidomethyl)naphthalene, (**9**) 1-azido-2-methylpropane, and (**10**) 2-azidoethanamine. The values were normalized to the original residues, I10 functionalized to indole (**1**), B33 functionalized to benzyl (**4**) and F20 functionalized to benzofuran (**2**) (n=3, singlets, mean ± SD).

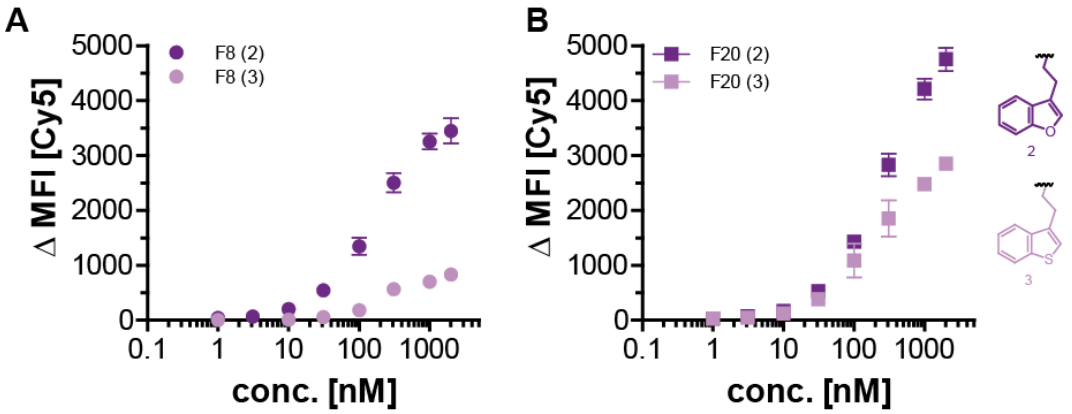

Figure 5.27: Flow cytometry analyses of the sequences F8 and F20 binding to C3-GFP modified with two functionalizations.

A concentration-dependent binding analysis of the sequences F8 (**A**) and F20 (**B**) to C3-GFP is shown. F20 and F8 were functionalized with benzofuran (**2**) and benzothiophene (**3**) and analyzed by flow cytometry (n=3, singlets, mean ± SD). The MFI of the non-binding control (F20sc (**2**), F20sc (**3**)) was subtracted from the MFI of the sequences.

Since the sequences F8 and F20 showed binding with benzothiophene (**3**) functionalization, we were interested in analyzing the difference in the binding to C3-GFP when modified with this functionalization and with benzofuran (**2**). Accordingly, the sequences F8 and F20 were functionalized with benzofuran (**2**) and benzothiophene (**3**). The binding affinity to C3-GFP was investigated by flow

cytometry depending on the concentration. Both sequences showed a lower signal with benzothiophene (**3**) compared to benzofuran (**2**) (**Figure 5.27**). Under these circumstances, further characterization was concentrated only on benzofuran (**2**).

5.5.4. Surface plasmon resonance spectroscopy analyses of C3-GFP clickmers

To study the K_D, k_{on} and k_{off} rate of the sequences, measurements of surface plasmon resonance spectroscopy (SPR) were performed. A representative value for each clickmer is shown in **Figure 5.28**. For the sequences I10, F8 and F20 a stable stationary state could not be achieved even with long injection times. For cost reasons, shorter injection times were chosen (80-150 µL = 120-225 s). Additional measurements are can be found in **Supp. figure 9**, **Supp. figure 10**, **Supp. figure 11**, and **Supp. figure 12**. The corresponding values are listed in **Table 5.3** and summarized in **Figure 5.29**.

The k_{on} rate of F20 is the highest of all investigated sequences for both temperatures. The sequence-protein complex is generated faster than with the other sequences. Interestingly, B33 and I10 have similar k_{on} rates at 37°C. The k_{off} rates of sequences I10, F8 and F20 are identical and slower compared to B33, which has a much faster k_{off} rate. The K_D value for I10 is slightly higher at 37C. While F8 and F20 have much lower K_D values than B33, all three are temperature independent.

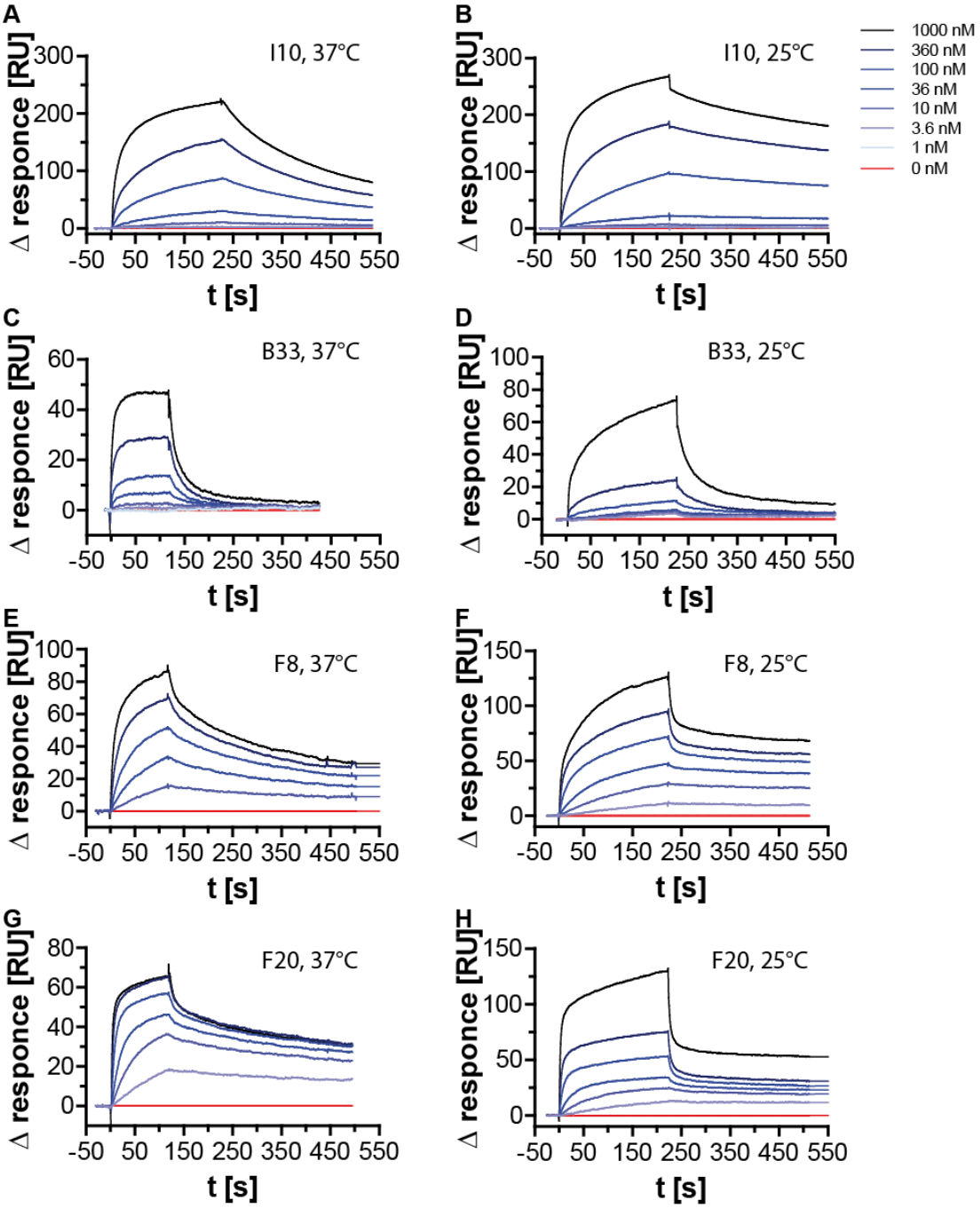

Figure 5.28 Surface plasmon resonance spectroscopy (SPR) measurements of the sequences I10 (1), B33 (4), F8 (2), and F20 (2) targeting C3-GFP at 37°C and 25°C.

The biotinylated sequences were immobilized on a streptavidin-coated SPR sensor chip and C3-GFP was used as an analyte in various concentrations. The measurements were performed at 37°C and 25°C. Buffer injection values were subtracted.

Table 5.3 K_{on} rate, k_{off} rate, and K_D of functionalized clickmers targeting C3-GFP as identified by SPR analysis at 25°C and 37°C.

		I10 (1)	F8 (2)	F20 (2)	B33 (4)
k_{on} rate [10^5 $M^{-1}s^{-1}$]	25°C	14.0 ± 1.1	7.5 ± 1.9	31.2 ± 19.2	3.3 ± 0.8
	37°C	13.5 ± 4.8	62.7 ± 24.5	181.0 ± 41.1	22.8 ± 4.4
k_{off} rate [10^{-4} s^{-1}]	25°C	7.2 ± 0.5	6.7 ± 0.6	9.6 ± 2.0	60.1 ± 3.4
	37°C	33.9 ± 7.6	31.8 ± 12.8	39.9 ± 9.8	350.3 ± 156.9
K_D [nM]	25°C	5.2 ± 0.8	9.4 ± 2.8	4.7 ± 3.7	191.2 ± 45.1
	37°C	26.5 ± 5.9	6.2 ± 4.1	2.3 ± 0.6	153.8 ± 68.4

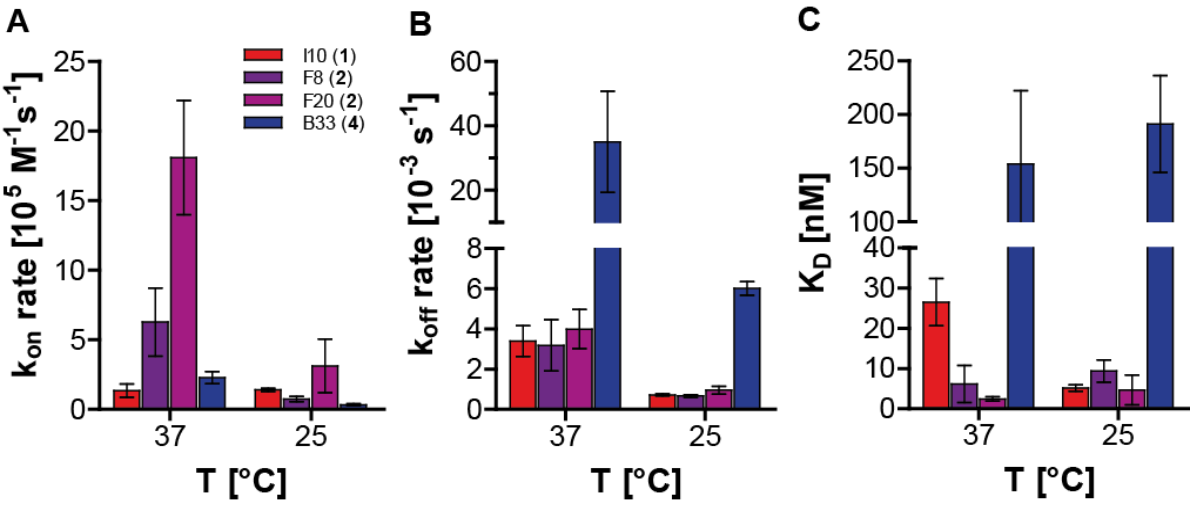

Figure 5.29 SPR data of the clickmers targeting C3-GFP.

Shown are k_{on} rate, k_{off} rate and K_D of the investigated clickmers I10 (**1**), B33 (**4**), F8 (**2**) and F20 (**2**), which respond to C3-GFP at two temperatures, 25°C and 37°C (n=5, singlets, mean ± SD).

The specificity of the clickmers was investigated by flow cytometry. A large number of proteins were coupled to magnetic beads. No binding was detected for a specific protein other than C3-GFP (**Figure 5.30**). Surprisingly, no clickmer showed binding to mE-GFP, which is very homologous to C3-GFP and differs in only nine point mutations.

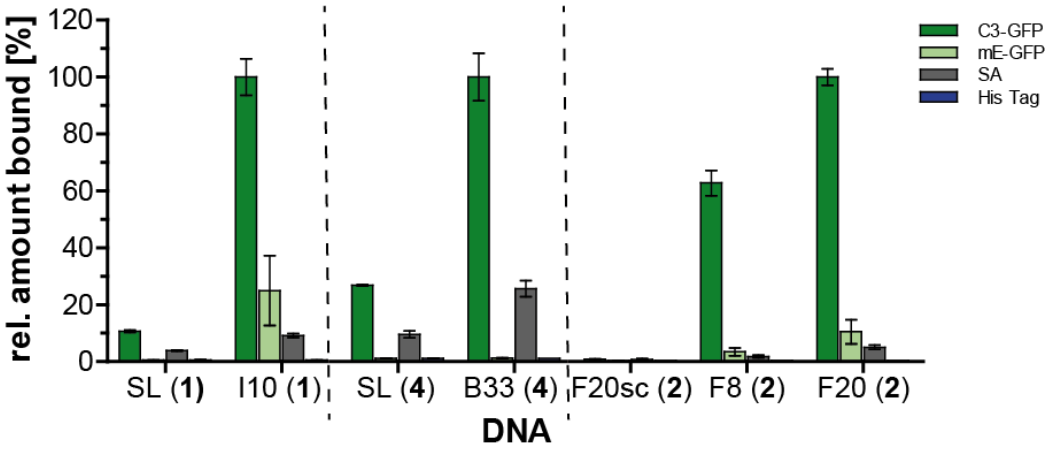

Figure 5.30: Specificity determination for the starting library SL (1) and SL (4), and I10 (1), B33 (4), F8 (2), F20 (2), and F20sc (2).

The relative amount of 500 nM Cy5-labelled functionalized DNA bound to different proteins as analyzed by flow cytometry is shown. The values of SL (**1**) and I10 (**1**) were normalized to I10 (**1**), the values of SL (**4**) and B33 (**4**) to B33 (**4**) and the values of F20sc (**2**), F8 (**2**) and F20 (**2**) to F20 (**2**) (n=2, singlets, mean ± SD).

5.6. Multiplexed click-SELEX targeting C3-GFP

Executing eight different click selections was time-consuming and costly, not to mention that only three out of eight selections were successful, *i.e.* generation of a clickmer. For this reason, a new approach was explored. In addition, the probability of a successful selection was to be increased.

Ideally, the concept of multiplexing the functionalized DNA libraries should improve click-selections ability to generate the most affine clickmer.

The multiplexed click-SELEX makes it possible to perform several click-selections in parallel. The multiplexing of libraries modified with different chemical units greatly increases the diversity of the library. The clickmers adaptation is improved, time and costs are reduced. A schematic representation of a multiplexed click-SELEX can be found in **Figure 5.31 A**. For example, the non-functionalized alkyne-modified library is divided into five aliquots. The aliquots are functionalized separately by CuAAC with five different azides. These functionalized libraries are then mixed and applied in a selection cycle. After PCR amplification of the bound sequences and single-strand displacement (SSD), the enriched library is aliquoted and again functionalized separately, followed by the mixing of the aliquots and their application in the next selection cycle.

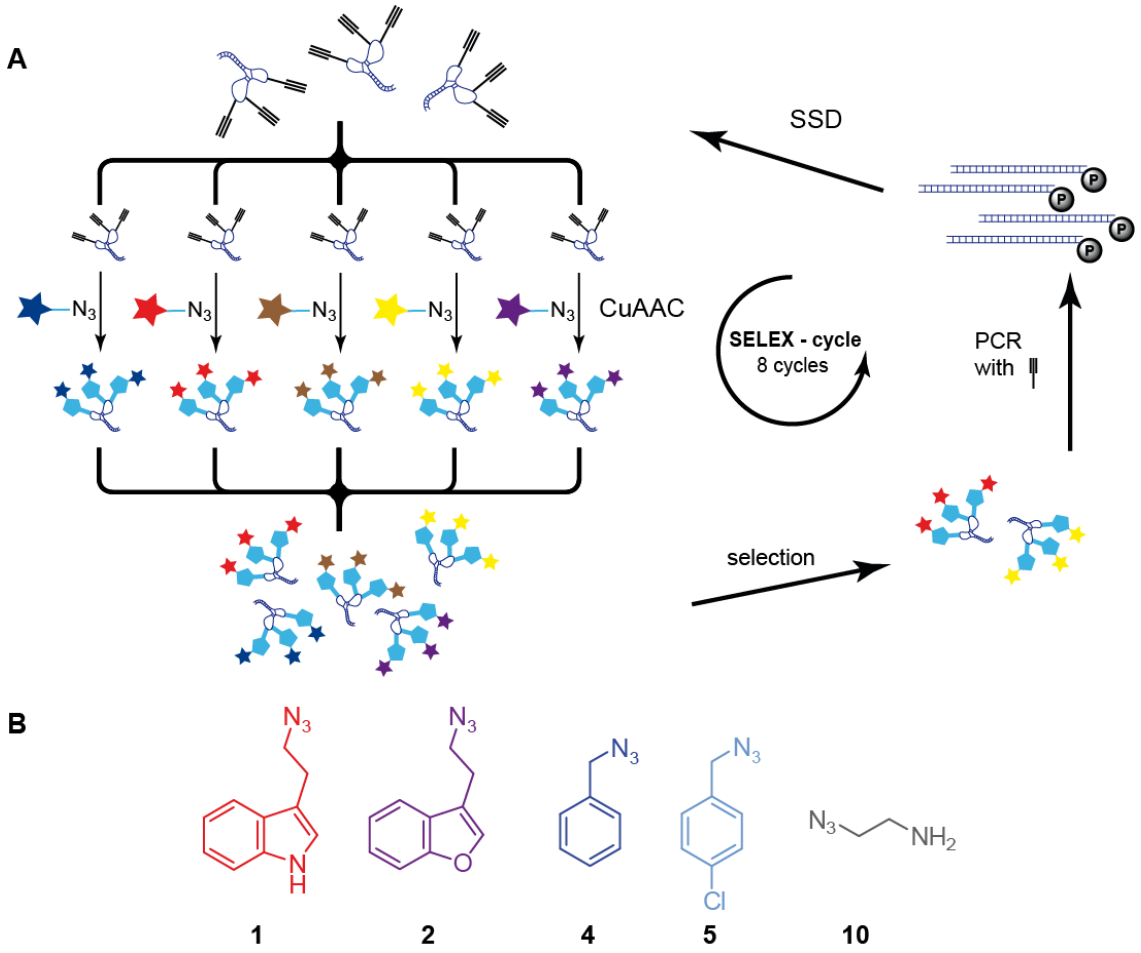

Figure 5.31: Schematic representation of the multiplexed click-SELEX process.

(**A**) An alkyne-modified ssDNA library is divided into five aliquots, each functionalized with a different azide by click chemistry (CuAAC). The functionalized libraries are then combined. After incubation with the target molecule, the unbound sequences are removed and the bound sequences are obtained (selection) and amplified by PCR with 5-ethynyl-2'-deoxyuridine (EdU) instead of thymidine. In the next step, the single-stranded DNA is generated by the λ exonuclease degradation of the 5'-phosphorylated antisense strand (SSD). Finally, the ssDNA is aliquoted and functionalized by CuAAC and subjected to the next selection cycle. (**B**) Chemical structures of the azide-containing compounds used in multiplexed click-SELEX targets on C3-GFP. (**1**) 3-(2-azidoethyl)-1*H*-indole, (**2**) 3-(2-azidoethyl)-benzofuran, (**4**) 1-(azidomethyl)-benzene, (**5**) 1-(azidomethyl)-4-chlorobenzene, and (**10**) 2-azidoethanamine.

C3-GFP was selected as the target molecule for the first multiplexed click-SELEX and five different azide-containing compounds were investigated (**Figure 5.31 B**). For three of these azides (**1**, **2**, **4**) a successful click-SELEX was previously performed, for two (**5** and **10**) the click-SELEX could not be completed due to by-product formation during PCR amplification (**Supp. figure 7**). The latter were included to show that functionalization with these azides does not interfere with the multiplexed click-SELEX process. After performing eight multiplexed click-selection cycles, the DNA of the enriched library was examined for its binding to C3-GFP by flow cytometry separately for each azide (**Figure 5.32**).

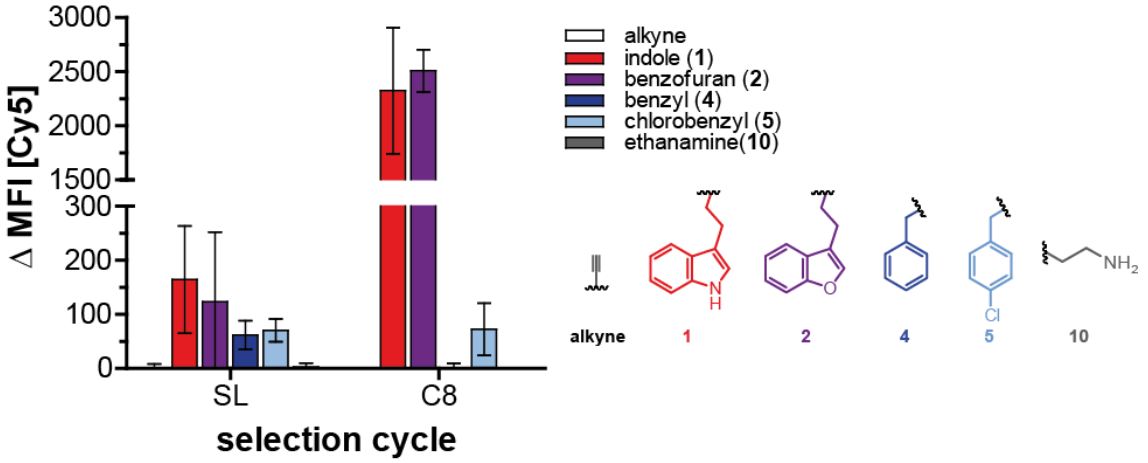

Figure 5.32: Binding analysis of the multiplexed click-SELEX targeting C3-GFP using click-DNA-libraries functionalized with indole (1), benzofuran (2), benzyl (4), chlorobenzyl (5), and 2-azidoethanamine (10).

500 nM Cy5-labeled un-/functionalized DNA from the start library (SL) and selection cycle 8 (C8) were incubated with unmodified beads and C3-GFP. The Cy5 fluorescence retained on the beads was determined by flow cytometry (n=2, singlets, mean ± SD). The mean fluorescence intensity (MFI) at the C3-GFP beads after subtraction of the MFI from unmodified beads is shown.

We have assumed that a further selection cycle, the deconvolution cycle, is required to assess which functionalization is necessary for each enriched sequence to bind (**Figure 5.33**). The enriched library of the selection cycle eight is aliquotted and functionalized separately with the various azides. After that, these functionalized libraries are no longer mixed. For each of the enriched functionalized libraries, a single click-selection cycle is performed according to **Figure 3.1**. The deconvolution cycle is followed by the NGS analysis (**Figure 5.33 A**). By performing the deconvolution cycle, we assume that the sequence composition of this cycle will change, as shown in **Figure 5.33 B**. If only one azide is used for functionalization, only sequences that need this azide for binding are obtained. Thus, the number of binding sequences increases, while the number of all other sequences decreases. This makes it possible to predict which sequence which azide needs to interact with the target molecule.

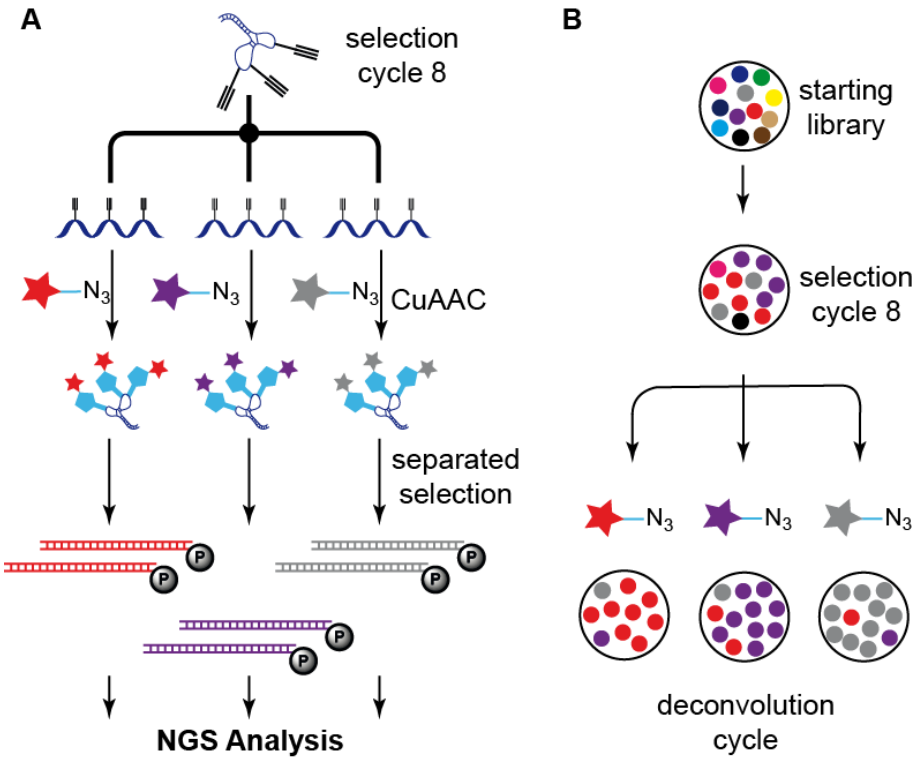

Figure 5.33: Schematic representation of the deconvolution cycle and the NGS analysis.

(**A**) The deconvolution cycle is shown in a multiplexed click-SELEX with three different azides (for simplification). The alkyne-modified DNA library of an enriched selection cycle is divided into three aliquots and each aliquot is functionalized with a different azide by click chemistry (CuAAC). The functionalized libraries are then no longer combined. A click selection cycle is performed for each functionalized library (separate SELEX). After completion of the PCR with 5-ethynyl-2'-deoxyuridine (EdU) instead of thymidine, the DNA of the different selection cycles is sequenced *e.g.* by NGS. (**B**) Schematic representation of the sequence frequency during the deconvolution cycle in a multiplexed click-SELEX with three different azides. The start library (SL) contains almost unique sequences represented by different colors. In contrast, selection cycle 8 has a high frequency for two sequence patterns (red and violet), while other sequences are reduced or disappeared. After the deconvolution cycle, the sequence composition changed depending on the azide used for functionalization.

After performing a deconvolution cycle, NGS analyzed the multiplexed click-SELEX with a dNTP mix containing dTTP instead of EdUTP.

Figure 5.34 shows the relative number of unique sequences plotted over the selection cycles of the multiplexed click-SELEX targeting C3-GFP. Over the first eight selection cycles, the number of unique sequences decreased to less than 3%. In the deconvolution cycle, this amount changes depending on the azide used for DNA functionalization. While indole (**1**) and benzofuran azide (**2**) led to further reduced unique sequences, the use of benzyl- (**4**) and ethanamine (**10**) led to a higher amount of unique sequences by 4%. The amount of chlorobenzyl azide (**5**) even increased to 8%. How exactly the number of unique sequences can increase is still unclear. Obviously, it is caused by the lack of binding sequences, which require other functionalizations to bind to the protein.

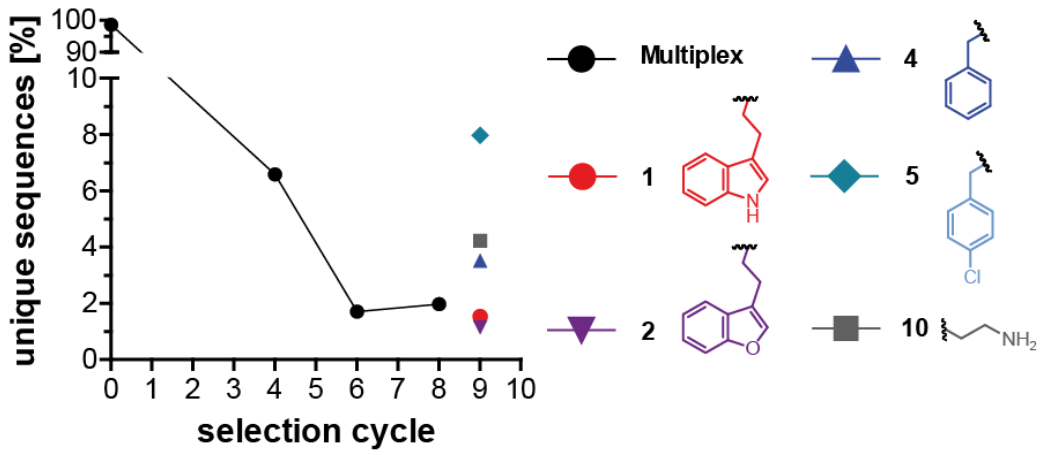

Figure 5.34: Unique sequences in different cycles of the multiplexed click-SELEX targeting C3-GFP.

During the first eight selection cycles, the number of individual sequences fell sharply from around 100% to 2%. Cycle 9 was performed as a deconvolution cycle and showed a decrease for indole (**1**) and benzofuran azide (**2**) in the unique sequences, but an increase for the other three azides (benzyl (**4**), chlorobenzyl (**5**), 2-azidoethanamine (**10**)).

The nucleotide distribution of the NGS analysis confirmed the enrichment of the multiplexed click-SELEX targeting C3-GFP. In the start library, all four nucleotides are distributed almost evenly over the random range (**Figure 5.35 A**), which indicates a high diversity of the library. This distribution changed during selection cycles 4, 6 and 8 (**Figure 5.35 B-D**). The most significant changes were observed in the deconvolution cycle. The nucleotide distribution for indole (**1**) and benzofuran azide (**2**) shows almost a single sequence. For benzyl (**4**) or ethanamine (**10**) azide the results are very similar to the 8th selection cycle. The distribution for chlorobenzyl azide (**5**) also showed almost one sequence (**Figure 5.35 H**), suggesting an enrichment of one sequence.

As mentioned above (**section 5.5.2**) NGS measurements have a higher error the longer the sequence to be analyzed. Therefore, the intrinsic nucleotide distribution shows a lower frequency from position 41 (**Figure 5.35**).

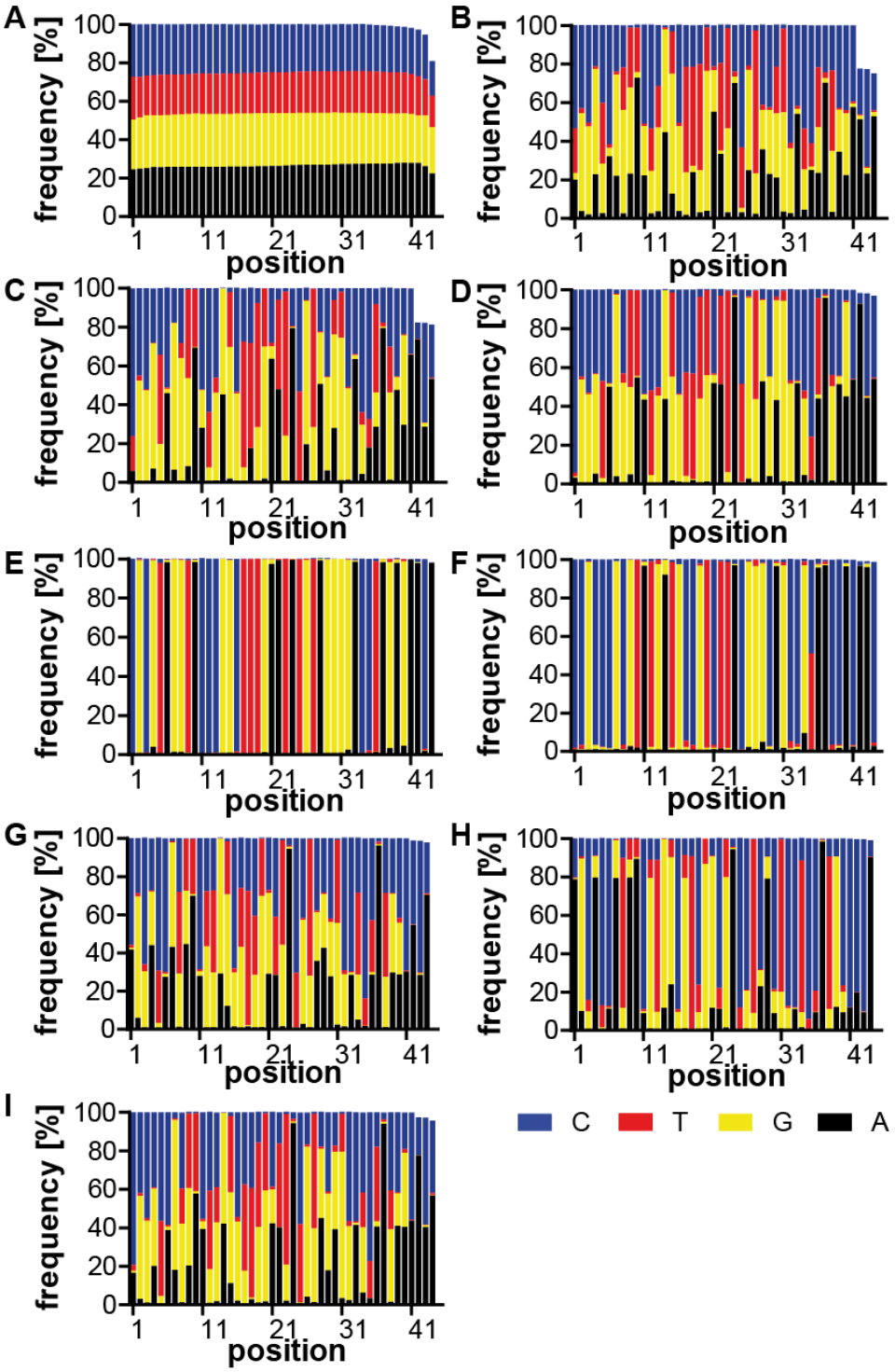

Figure 5.35: Nucleotide distribution of the NGS analysis of multiplexed click-SELEX targeting C3-GFP.

Nucleotide distribution at the different positions of the random region in the DNA of the initial library OW1 (**A**), selection cycle 4 (**B**), cycle 6 (**C**), cycle 8 (**D**) and deconvolution cycle 9 using the azides indole (**1**) (**E**), benzofuran (**2**) (**F**), benzyl (**4**) (**G**), chlorobenzyl (**5**) (**H**) and ethanamine (**10**) (**I**).

The frequency of the sequences was then analyzed. **Figure 5.36** illustrates the frequency of the most abundant sequences over the selection cycles. Over the first eight selection cycles, I10 was the most abundant sequence, with a frequency of about 35% in the eighth selection cycle. F20 was the second

most frequent sequence with 13%. All other sequences, F8, B33, B15, and C1, were below 1%. The deconvolution cycle clearly showed which sequence required which azide to interact with the target molecule. When indole azide (**1**) was used for DNA functionalization, the frequency of all sequences decreased but increased to over 65% at I10 (**Figure 5.36 B**). This indicates that I10 requires indole azide for interaction with C3-GFP. A similar effect is observed in the use of benzofuran azide (**2**) for DNA functionalization. I10, the most abundant sequence in the 8th selection cycle, decreased from 35% to almost 0%, while F20 increased from 13% to 30% (**Figure 5.36 C**). This suggests that F20 needs benzofuran for interaction with C3-GFP. I10 loses its binding properties when DNA is functionalized with benzofuran. When benzyl or chlorobenzyl azide was used, the frequency of the most abundant sequences decreased significantly. For benzyl azide, the sequences B33 and B15 increased slowly (**Figure 5.36 D**, **E** zoomed), suggesting that they were suppressed by other sequences before, such as I10 or F20. Another sequence, C1, increased dramatically from 0.9% to 13% (**Figure 5.36 D**). This sequence was also found in the deconvolution cycle of chlorobenzyl, where the frequency increased even more to 24% (**Figure 5.36 F**). Ethanamine led to a decrease in all most abundant sequences and showed that no sequence of this azide was required for functionalization (**Figure 5.36 G**).

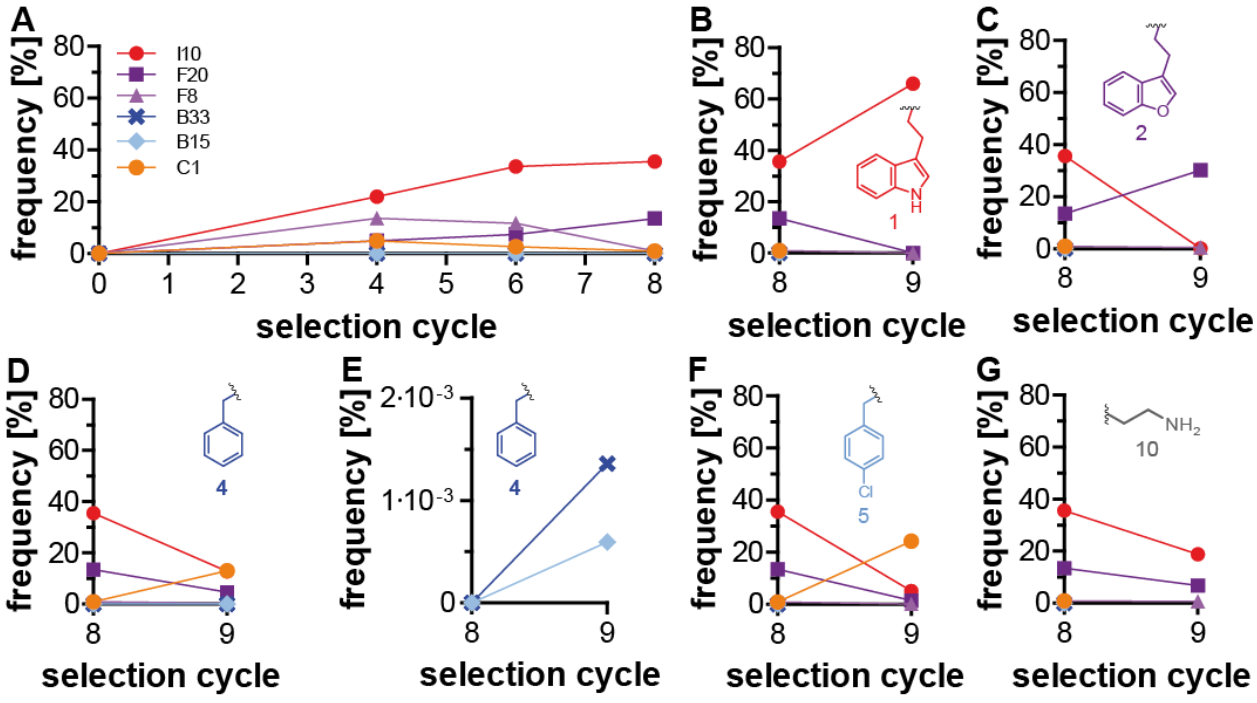

Figure 5.36: Frequency of the most abundant sequences for multiplexed click-SELEX targeting C3-GFP.

The frequency of the most frequent sequences I10, B33, B15, F20, F20, F8 and C1 in the relevant selection cycles of the multiplex click-SELEX targeting C3-GFP is shown. For the first eight multiplexed selection cycles, I10 is the dominant sequence with 35% (**A**). The deconvolution cycle 9 for indole azide (**1**) showed a higher enrichment for I10 to 65%, while all other sequences fell below 1% (**B**). Benzofuranazide (**2**) led to a decrease from I10 to almost 0%, while F20 increased to 30% (**C**). For benzyl (**4**) (**D**, **E** zoomed) and chlorobenzyl azide (**5**) (**F**), all most abundant sequences decreased in frequency. Instead, C1 increased from almost 0% to 15% and 25%, respectively. All of the most abundant sequences decreased when 2-azidoethanamine (**10**) (**G**) was used.

The NGS data, the nucleotide distribution as well as the frequency of the sequences, showed surprising results, which can be explained by the characterization of the clickmer. The SPR data of the sequences I10, F20, F8, and B33 (**section 5.5.4**) clearly show why B33 could not be enriched in the first eight selection cycles. Since B33 has a high k_{off} rate and a high K_D value compared to I10 and F20, B33 was obviously displaced in the first eight selection cycles. Or B33 has been washed away in the step of separating the unbound sequences by washing due to its fast decomposition rate.

Furthermore, it is very interesting that the selection using chlorobenzyl for DNA functionalization failed as a single click-SELEX (**section 5.5**), but led to enrichment in the multiplexed click-SELEX in the deconvolution cycle. Both benzyl and chlorobenzyl enriched the sequence C1 to high frequency. Due to time constraints, this sequence was not further characterized. We assume that C1, similar to B33, has a fast k_{on} rate, but also a fast k_{off} rate, and thus by the other affinate clickmere, I10, and F20, during the first eight selection cycles was displaced and therefore could not be strongly enriched.

5.7. Multiplexed click-SELEX targeting peptide $Na_v1.6$

To keep the target molecule simple, we decided to use a short peptide of $Na_v1.6$ instead of the complex cell system like $Na_v1.6$-HEK293 with all the different targets on its membrane to apply the multiplexed click-SELEX approach (s**ection 5.6**). The idea of using a peptide came from the recent publication of Lee *et al*. on monoclonal antibodies acting on the voltage sensor paddle of $Na_v1.7$[159]. The group selected a peptide corresponding to the voltage sensor paddle located in domain II (S3 - S4 loop)[159] (**Figure 3.7 B**). Based on this strategy, we chose the same peptide sequence of $Na_v1.6$ (**section 9.7**).

For the multiplexed click-SELEX approach, we used five azides for DNA functionalization: indole (**1**), benzyl (**4**), phenol (**7**), methylpropane (**9**) and guanidine (**11**). The *N*-terminal biotinylated peptide $Na_v1.6$ (**section 9.7**) was immobilized on streptavidin coupled magnetic beads (SA). The selection was made as described in **section 8.5.3**. A negative selection step with streptavidin-coupled beads without peptide was used to suppress the accumulation of sequences recognizing the immobilization matrix (SA). Eight selection cycles were performed and the binding was analyzed by flow cytometry. The DNA of the start library (SL) and the selection cycle 8 (C8) were labeled with Cy5 and functionalized separately. Each functionalized DNA was analyzed for binding to empty (SA) and peptide carrying $Na_v1.6$ (peptide) beads (**Figure 5.37**).

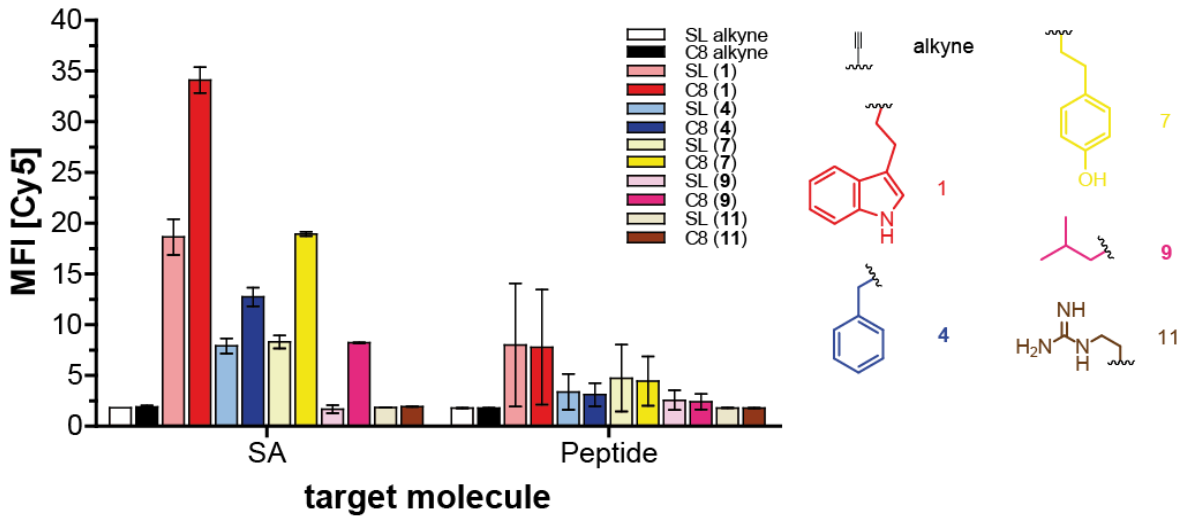

Figure 5.37: Binding analysis of the multiplexed click-SELEX targeting peptide $Na_v1.6$.

500 nM Cy5-labeled DNA of the start library (SL) and selection cycle 8 (C8) was functionalized with the various azides (**1**, **4**, **7**, **9**, **11**) and incubated with unmodified (SA) and peptide $Na_v1.6$ (peptide) storage beads. The fluorescence signal on the beads was determined by flow cytometry (n=2, singlets, mean ± SD).

A binding not to the peptide $Na_v1.6$ but to SA was observed. Four azides (**1**, **4**, **7** and **9**) showed an accumulation of SA binding sequences when comparing DNA from cycle 8 with SL. No enrichment with guanidine (**11**) as DNA functionalization was observed. Under these circumstances, it was interesting to perform the deconvolution step targeting streptavidin instead of the peptide $Na_v1.6$. The deconvolution cycle was performed as described in **section 5.6**. The DNA of the SL and the selection cycles 4, 6, 8 and the deconvolution cycle were then sequenced by NGS.

The unique sequences are the main indication for the enrichment of a selection. **Figure 5.38** illustrates the unique sequences of the multiplexed click-SELEX, which first targets the peptide $Na_v1.6$ and in the deconvolution cycle SA. Until the eighth selection cycle, the unique sequences decrease from about 100% to 25%. This reduction indicated that the diversity of the library was decreasing. The deconvolution cycle showed a dependence on the azide used. For azides **1**, **4**, **7** and **9** the unique sequences decreased even more compared to the selection cycle eight. Azide **11** led to an increase to over 30%.

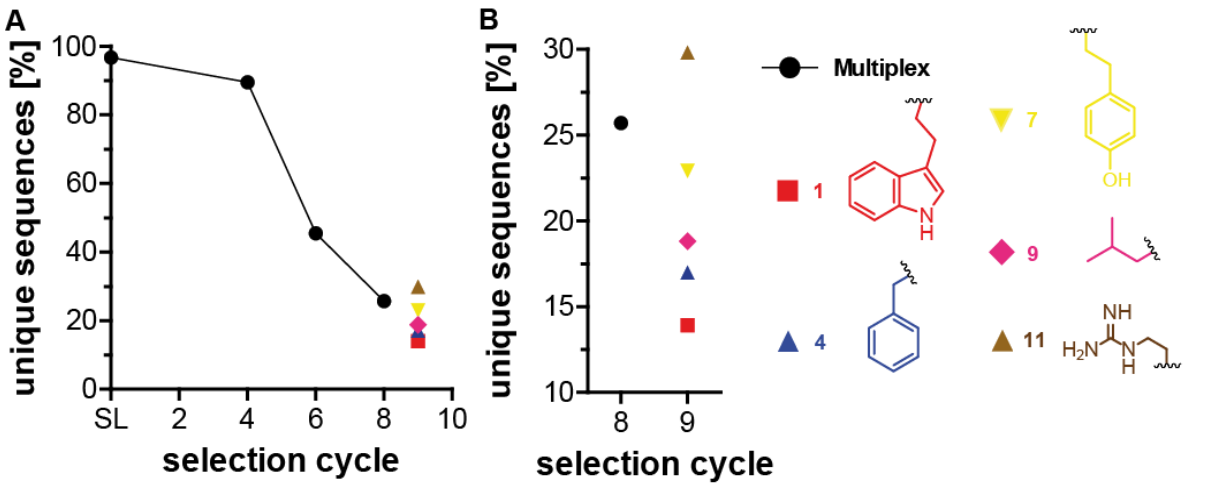

Figure 5.38: The unique sequences of multiplexed click-SELEX targeting peptide $Na_v1.6$ and SA.

(**A**) Shown are the unique sequences of the multiplexed click-SELEX targeting peptide Nav1.6 and SA, magnified in (**B**). During the first eight selection cycles the number of unique sequences decreased from about 100% to 25%. Cycle 9 was carried out as a deconvolution cycle focused only on SA.

The nucleotide distribution of the multiplexed click-SELEX targeting the first peptide $Na_v1.6$ and then in the ninth selection cycle SA is shown in **Figure 5.39**. The initial library showed a homogeneous distribution of the four nucleotides (A, T, and C about 20%, G 40%). This distribution changed over the selection cycles starting in the 4^{th} to 8^{th} selection cycle. The strongest change was observed for indole (**1**) and benzyl (**4**) in the deconvolution cycle (**Figure 5.39 E**, **F**). This corresponds to the data of unique sequences. For the other three azides (**7**, **9** and **11**) almost no difference in nucleotide distribution was observed (**Figure 5.39 G-I**).

The deconvolution cycle for each azide was analyzed and the most common sequences determined. As shown in **Figure 5.40**, the most common sequence over the first eight selection cycles was I1 with 2.4%. This sequence increased to 15% in the deconvolution cycle with indole (for DNA functionalization), while all other sequences were below 2%. This showed that I1 requires indole functionalization for interaction with SA. When benzyl was used for DNA functionalization, the sequences Ben1 and Ben2 were most enriched with 5.4 and 4.1%, respectively. This led to the assumption that Ben1 and Ben2 require benzyl functionalization for interaction with SA. The use of the other three azides (**7**, **9** and **11**) did not result in significant sequence enrichment.

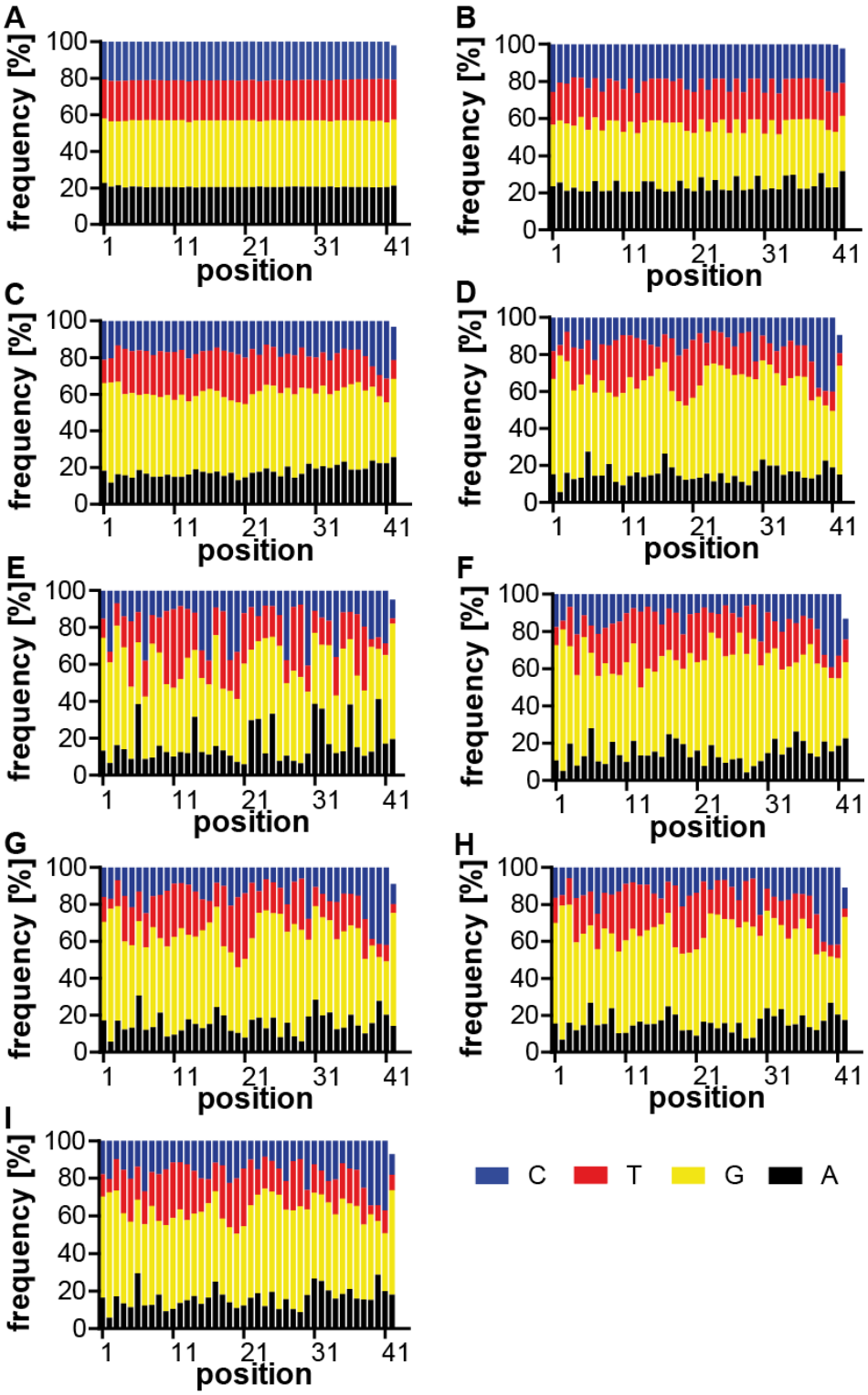

Figure 5.39: Nucleotide distribution of the NGS analysis of multiplexed click-SELEX targeting peptide $Na_v1.6$ and SA.

Nucleotide distribution at the different positions of the random region in the DNA of the initial library FT2 (**A**), the selection cycle 4 (**B**), 6 (**C**), 8 (**D**) and the deconvolution cycle 9, which addresses SA with the azides indole (**1**) (**E**), benzyl (**4**) (**F**), phenol (**7**) (**G**), methylpropane (**9**) (**H**) and guanidine (**11**) (**I**).

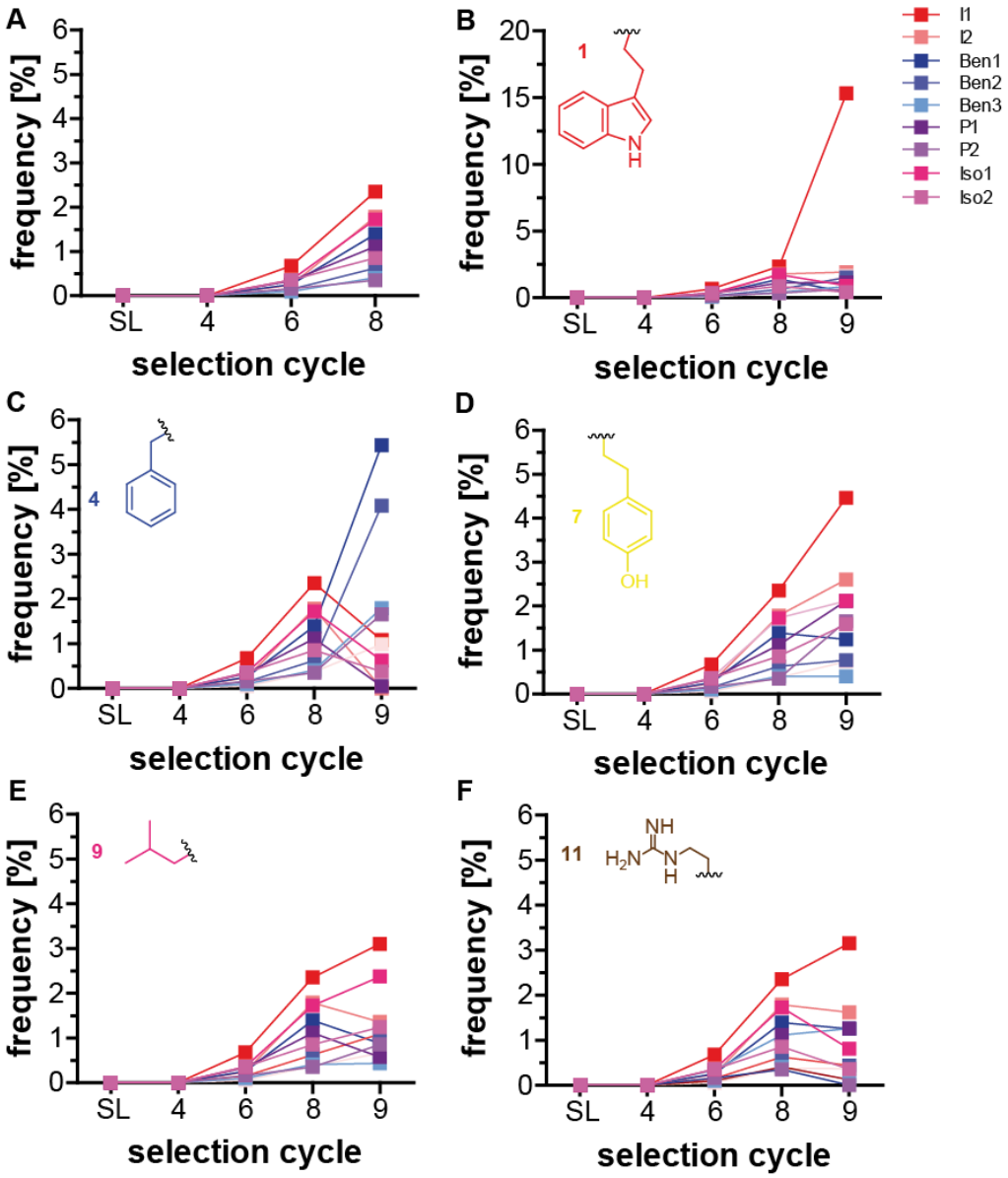

Figure 5.40: Frequency of the most abundant sequences in the NGS analysis for multiplexed click-SELEX targeting peptide Nav1.6 and SA.

Shown is the frequency of the most abundant sequences I1, I2, Ben1, Ben2, Ben2, Ben3, P1, P2, Iso1 and Iso2 in the first eight selection cycles of the multiplexed click-SELEX target peptide $Na_v1.6$ and SA (**A**) as well as the deconvolution cycle for indole (**1**) (**B**), benzyl (**4**) (**C**), phenol (**7**) (**D**), methylpropane (**9**) (**E**) and guanidine azide (**11**) (**F**).

Since sequences I1, Ben1, Ben2, Ben2, P1, P2, and Iso1 had the highest frequency increase in the deconvolution cycle, these sequences were selected for further analysis. They were functionalized with the corresponding azide and tested for binding by flow cytometry. The start library (SL) and the selection cycle 8 (C8) served as non-binding and binding controls. All tested sequences showed a binding to streptavidin as functionalized DNA (**Figure 5.41**). No binding was observed without any functionalization (alkyne). Since Ben2, P1 and Iso1 showed the lowest binding signal, these sequences were not further analyzed.

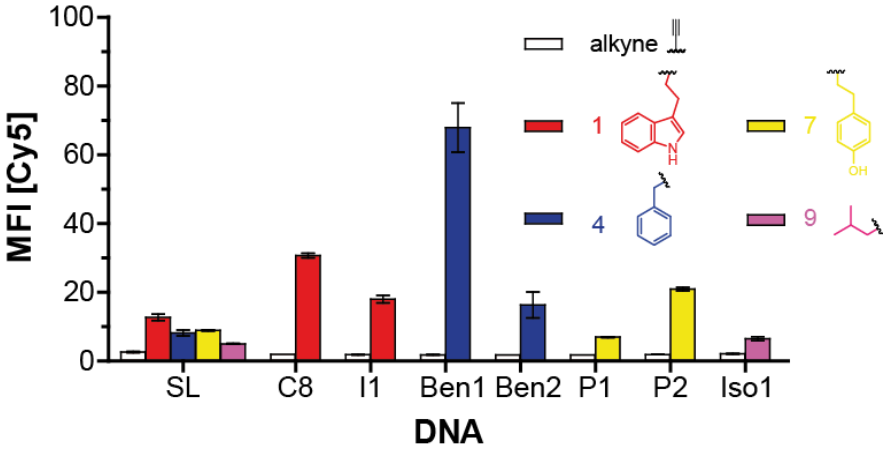

Figure 5.41: Binding analysis of the most abundant sequences in the multiplexed click-SELEX targeting streptavidin.

500 nM Cy5-labeled DNA of the starting library (SL) and the selection cycle 8 (C8), and the sequences I1, Ben1, Ben2, P1, P2 and Iso1 were either unfunctionalized (alkyne) or functionalized with indole (**1**), benzyl (**4**), phenol (**7**), or methylpropane (**9**) and incubated with streptavidin magnetic beads. The fluorescence signal on the beads was determined by flow cytometry (n=2, singlets, mean ± SD).

In addition, sequences I1, Ben1, and P2 were analyzed for their need for a specific azide for DNA functionalization. The DNA of these sequences was functionalized with eleven different azides and analyzed for binding to streptavidin. Unexpectedly, all sequences showed binding with all functionalizations, but no binding as unfunctionalized DNA (alkyne) (**Figure 5.42**). Since no specific functionalization is required, the triazole, which is formed by the click reaction and serves as the link between the chemical entity and the DNA (**Figure 3.5**), may be responsible for the interaction with streptavidin. The fact that multiplexed click-SELEX targeting streptavidin had an enrichment convinced us to perform multiplexed click-SELEX targeting streptavidin from the beginning. This selection should prove the concept of multiplexed click-SELEX.

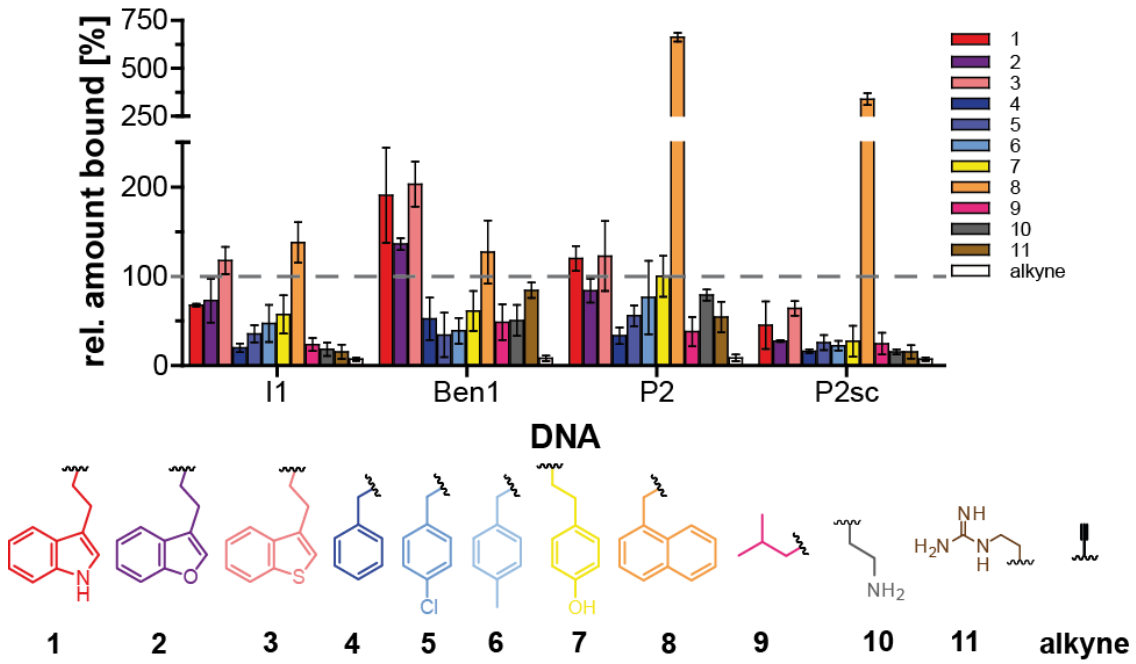

Figure 5.42: The impact of different functionalizations on the binding of selected sequences targeting streptavidin.

500 nM Cy5-labeled DNA was functionalized with various azides and incubated with streptavidin (SA) and analyzed by flow cytometry. The sequences were either unfunctionalized (alkyne) or functionalized with (**1**) 3-(2-azidoethyl)-1*H*-indole, (**2**) 3-(2-azidoethyl)benzofuran, (**3**) 3-(2-azidoethyl)benzo[*b*]thiophene, (**4**) 1-(azidomethyl)benzene, (**5**) 1 (azidomethyl)-4-chlorobenzene, (**6**) 1-(azidomethyl)-4-methylbenzene, (**7**) 4-(2-azido-ethyl)-phenol, (**8**) 1 (2 azidomethyl)naphthalene, (**9**) 1-azido-2-methylpropane, (**10**) 2-azidoethanamine, and (**11**) *N*-(2-azido-ethyl)-guanidine. The values were normalized to phenol-functionalized P2 (**7**) (n=2, singlets, mean ± SD).

5.8. Multiplexed click-SELEX targeting streptavidin

Unsatisfactory results for the selection target peptide $Na_v1.6$ led to the conclusion to change the target to streptavidin for the proof of concept multiplexed click-SELEX at pH7.4. Therefore, we performed a multiplexed click-SELEX targeting streptavidin with five azides: Indole (**1**), benzyl (**4**), phenol (**7**), methylpropane (**9**) and guanidine (**11**). SELEX was performed as described in **section 8.5.4**.

After eight multiplexed click-selection cycles, the DNA of the start library and the eighth selection cycle were analyzed for binding to the target molecule streptavidin by flow cytometry. As shown in **Figure 5.43**, the unfunctionalized DNA (alkyne) did not bind to streptavidin either in the start library (SL) or in the eighth selection cycle (C8). In contrast, the functionalized DNA with indole, benzyl, phenol, or methylpropane showed a higher signal of the DNA from the eighth selection cycle compared to SL, which indicates an enrichment. Functionalization with guanidine led to no difference between SL and the eighth selection cycle, indicating that no enriched sequence requires guanidine for interaction with streptavidin. If all functionalized DNAs are mixed equally (mix), then a higher signal is observed for the eighth selection cycle than for the SL, which also speaks for enrichment.

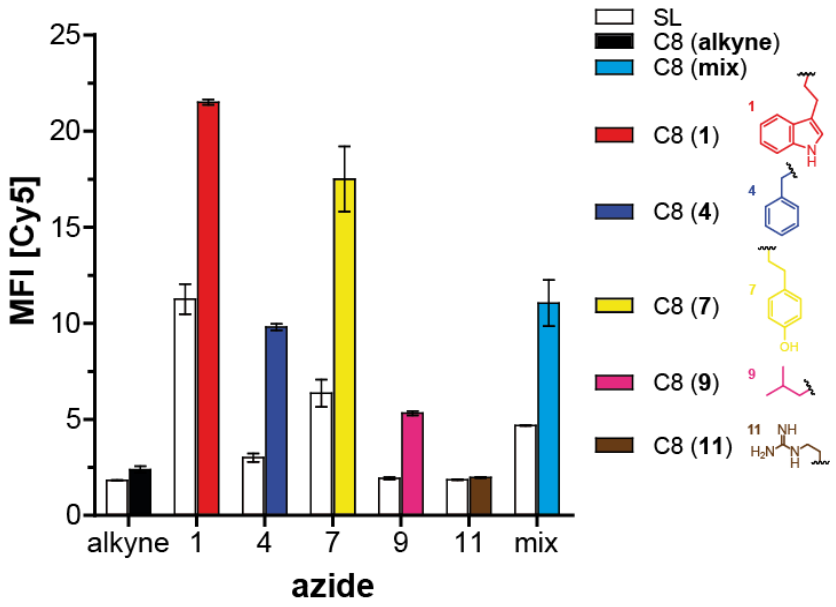

Figure 5.43: Binding analysis of the multiplexed click-SELEX targeting streptavidin.

500 nM Cy5-labeled DNA from the start library (SL) and selection cycle 8 (C8) were incubated with unmodified beads (SA). The DNA was used as unfunctionalized (alkyne) or functionalized with indole (**1**), benzyl (**4**), phenol (**7**), methylpropane (**9**) and guanidine (**11**). In addition, all functionalizations were equally mixed and also analyzed for binding (mix). The Cy5 fluorescence retained on the beads was determined by flow cytometry (n=2, singlets, mean ± SD).

After the enrichment of the eighth selection cycle was confirmed, two deconvolution cycles were performed for each azide in order to obtain a clear hypothesis on the need for azide. This was followed by NGS analysis of selection cycles 6, 8, 9 and 10. The unique sequences in selection cycles 6 and 8 are below 10%, while this number increases or decreases depending on the azide used for DNA functionalization in cycles 9 and 10 (**Figure 5.44**). When the DNA was functionalized with indole (**1**), benzyl (**4**), or phenol azide (**7**), the number of individual sequences remained at about 12%. The use of methylpropan azide (**9**) led to an increase in unique sequences, suggesting that none of the enriched sequences required this modification for interaction with streptavidin. On the contrary, the modification with guanidine azide (**11**) led to a decrease of the unique sequences below 2%.

The analysis of the nucleotide distributions supported the results of the unique sequence analysis (**Supp. figure 13**). The start library (SL) can be found in **Figure 5.39 A**. After eight selection cycles, there was a strong change in the nucleotide distribution, clear evidence of a decrease in library diversity. In the deconvolution cycle, this nucleotide distribution changes depending on the azide used for DNA functionalization. For example, indole and benzyl azide changed the respective nucleotide distribution, while the use of phenol and methylpropan azide caused almost no change. The functionalization of guanidine azide led to a dramatic change.

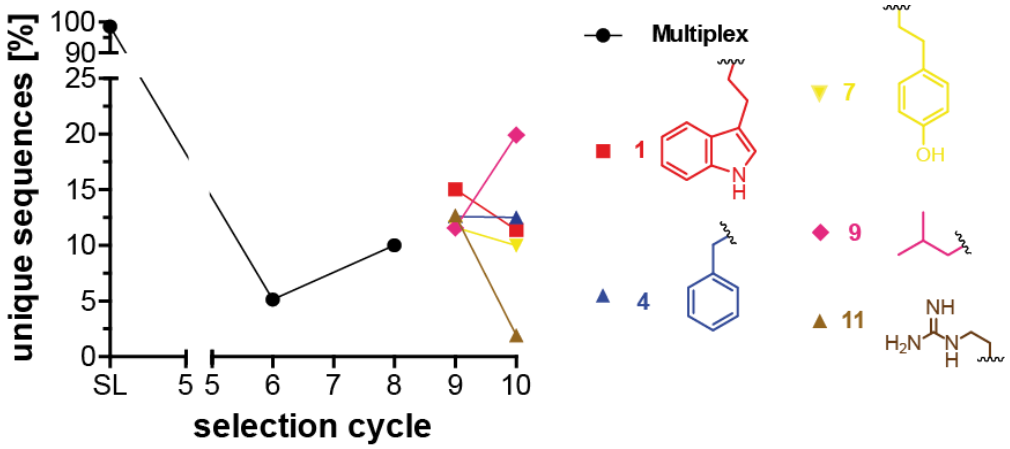

Figure 5.44: The unique sequences of multiplexed click-SELEX targeting streptavidin.

The unique sequences of the multiplexed click-SELEX targeting streptavidin are shown. Cycles 6 and 8 were performed as multiplexed click-SELEX (black). Cycles 9 and 10 were performed as deconvolution cycles and DNA was functionalized with indole (**1**) (red), benzyl (**4**) (blue), phenol (**7**) (yellow), methylpropane (**9**) (pink) and guanidine (**11**) (brown).

The tracking of the most abundant sequences is shown in **Figure 5.45**. In the first eight selection cycles, P2 was the most enriched sequence with about 22% in the eighth selection cycle. All other sequences were about 1%. In the deconvolution cycles, sequences with low frequency increased depending on functionalization. When indole azide (**1**) was used for DNA functionalization, the most abundant sequence P2 decreased from 22% to 7%, while I1 and I2 increased to 5-7.5%. A similar effect was observed in benzyl functionalization. P2 decreased to below 3%, while B1 increased to above 15%. Phenol functionalization resulted in a stable frequency of P2, suggesting that P2 requires phenol, not indole or benzyl, for interaction with streptavidin. For methylpropane functionalization, no sequence was more enriched than that which occurred most frequently in the eighth selection cycle. For guanidine functionalization, the most abundant sequences of the eighth selection cycle were reduced to below 0.2%, while two other sequences, G1 and G2, increased dramatically to 39 and 6%, respectively. The most abundant sequences P2, B1, and G1 were selected for further characterization. P2 was selected because it is the dominant sequence through the first selection cycles, B1 and G1 because they were highly enriched in the deconvolution step.

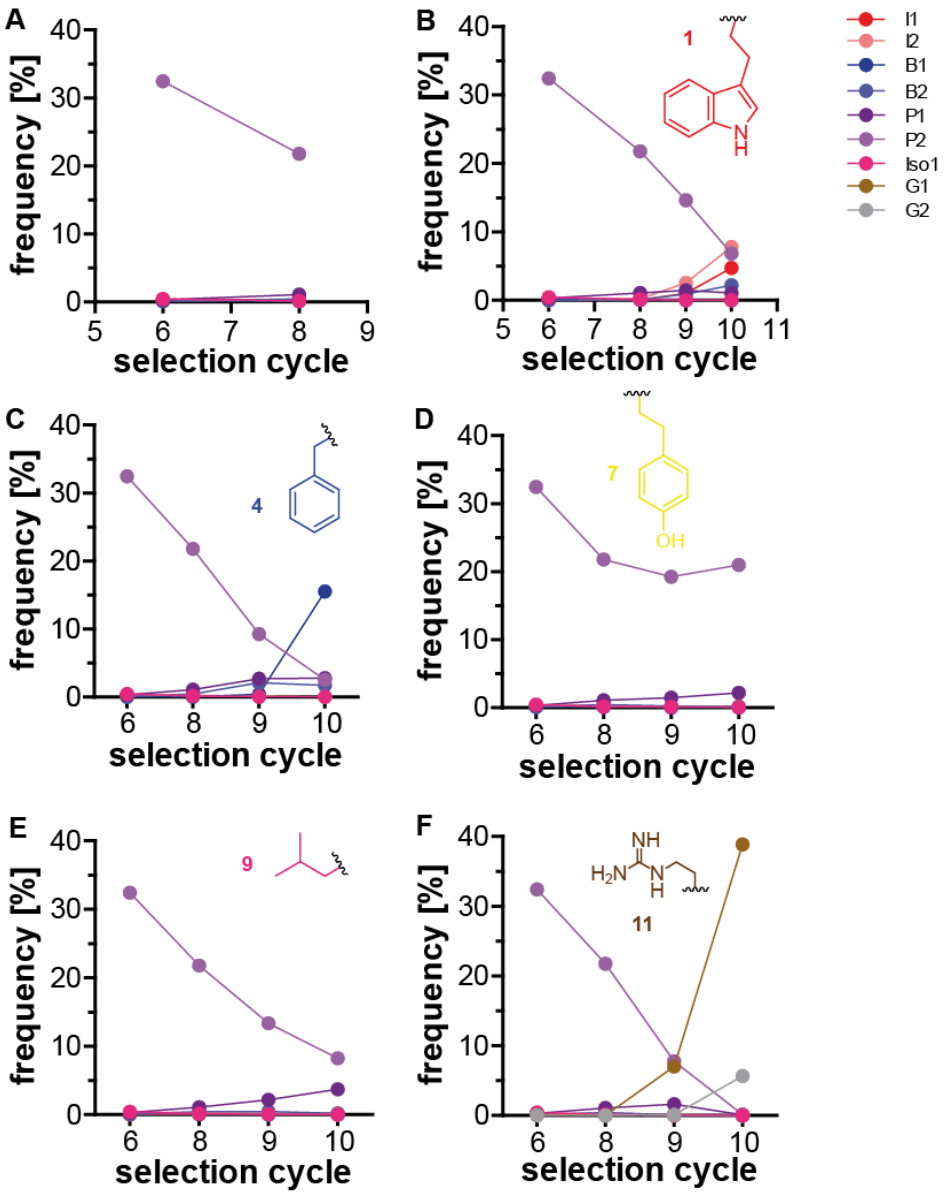

Figure 5.45: Frequency of the most abundant sequences in the NGS analysis for the multiplexed click-SELEX targeting streptavidin.

Shown is the frequency of the most abundant sequences I1, I2, B1, B2, P1, P2, Iso1, G1 and G2 in the relevant selection cycles of the multiplexed click-SELEX targeting SA. (**A**) Multiplexed click-selection and the deconvolution cycles 9 and 10 for indole (**1**) (**B**), benzyl (**4**) (**C**), phenol (**7**) (**D**), methylpropane (**9**) (**E**) and guanidine (**11**) (**F**).

5.9. Characterization of clickmers targeting streptavidin

5.9.1. Analyses of binding towards streptavidin

The binding capabilities of the three most abundant sequences were analyzed by flow cytometry. The DNA was labeled with Cy5 and tested un- (alkyne) and functionalized with the original modification regarding the deconvolution cycle (**1**, **4**, **7**, **11**). The eighth selection cycle was functionalized with indole (**1**) as the previous binding test with this modification yielded the highest signal (**Figure 5.46**). Sequences B1 and P2 showed binding to streptavidin only if they were functionalized (**Figure 5.46**).

The sequence G1 binds unfunctionalized and functionalized, suggesting that G1 is a DNA aptamer and not a clickmer. Sequence G1sc is an scramble version of G1 and does serve as a non-binding control.

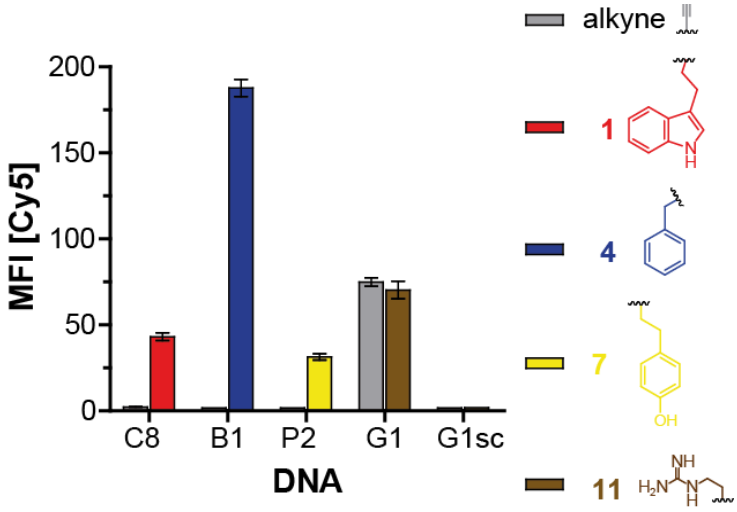

Figure 5.46: Binding analysis of the most abundant sequences in multiplexed click-SELEX targeting streptavidin by flow cytometry.

500 nM Cy5-labeled DNA of selection cycle 8 (C8) and sequences B1, P2, G1, and G1sc were incubated with streptavidin beads (SA). The Cy5 fluorescence retained on the beads was determined by flow cytometry. All sequences were unfunctionalized (alkyne) and functionalized with indole (**1**) (C8), benzyl (**4**) (B1), phenol (**7**) (P2) or guanidine (**11**) (G1 and G1sc) (n=2, singlets, mean ± SD).

The specificity of sequences P2, G1 and B1 was investigated by flow cytometry. The binding data are summarized in **Figure 5.47**. A control sample without protein immobilization (w/o) was used to exclude non-specific binding to the beads matrix. No binding was found for a tested protein other than streptavidin.

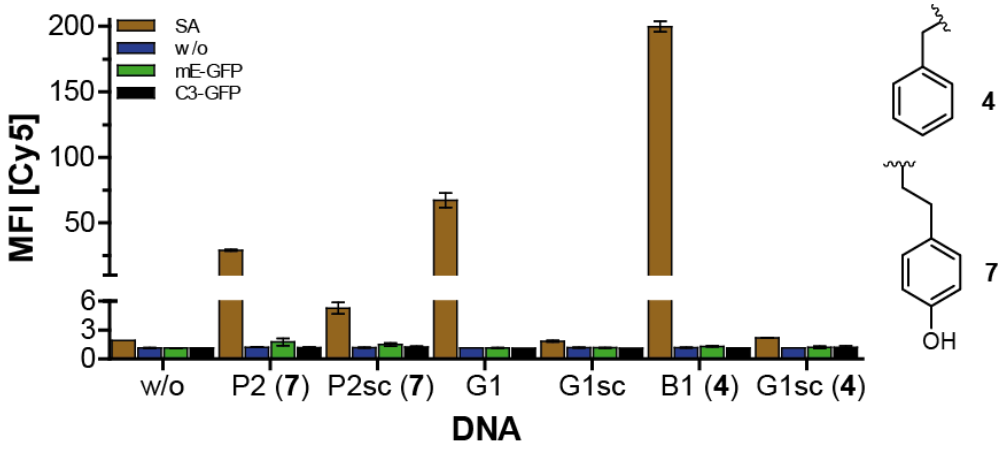

Figure 5.47 Specificity determination for the clickmers P2 (7), P2sc (7), G1, G1sc, B1 (4), and G1sc (4).

500 nM Cy5-labeled functionalized DNA of P2 (**7**), G1, and B1 (**4**) sequences bound to different proteins was analyzed by flow cytometry. Sequences P2sc (**7**), G1sc and G1sc (**4**) served as non-binding controls (n=3, singlets, mean ± SD).

Subsequently, concentration-dependent binding analyses were performed using flow cytometry **Figure 5.48**. It is shown that B1 (**4**) is more affine than G1 or P2 (**7**). For this reason, we have concentrated our further characterization on B1.

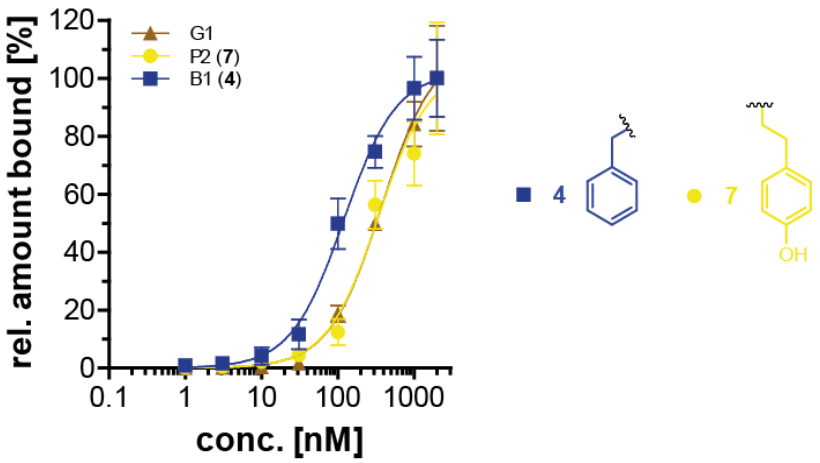

Figure 5.48 Concentration-depending binding analysis of the sequences G1, P2 (7), and B1 (4).

Different concentrations of DNA of sequences B1 (**4**), P2 (**7**), and G1 were incubated with streptavidin and analyzed by flow cytometry. G1 was used as a DNA sequence, P2 (7) was functionalized with phenol (**7**) and B1 (**4**) with benzyl (**4**). The non-binding control was subtracted from the values. The values for each sequence were normalized to the 2000 nM value (n=3, singlets, mean ± SD).

5.9.2. Analyses of the clickmer functionalization

B1 was investigated for binding to streptavidin with eleven different azides for DNA functionalization and analyzed by flow cytometry (**Figure 5.49 A**). B1 showed a specific requirement for functionalization with benzyl (**4**), chlorobenzyl (**5**), and methylbenzyl azide (**6**) to obtain binding to streptavidin. All other functionalizations tested did not result in binding.

Since B1 showed binding with three functionalizations, the binding capabilities were verified with these three modifications. Functionalization with benzyl (**4**) led to a slightly higher signal compared to chlorobenzyl (**5**) or methylbenzyl azide (**6**), which indicates a better affinity when modified with benzyl (**Figure 5.49 B**). Therefore, further characterization of B1 was concentrated on benzyl functionalization.

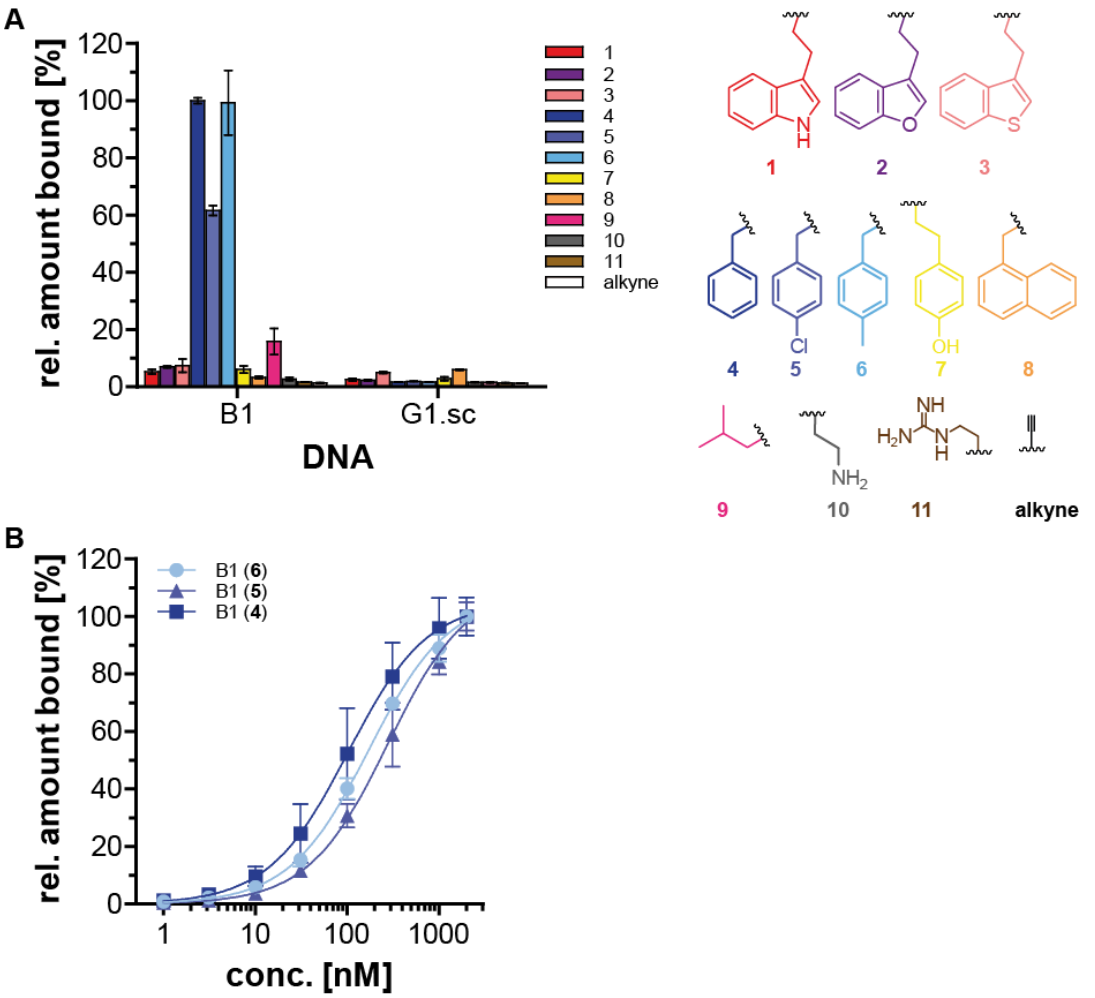

Figure 5.49: Binding analysis on the impact of the different functionalizations on the binding of B1 to streptavidin.

(**A**) 500 nM Cy5-labeled DNA functionalized with various azides were incubated with SA and analyzed by flow cytometry. B1 and G1sc were either unfunctionalized (alkyne) or functionalized with (**1**) 3-(2-azidoethyl)-1*H*-indole, (**2**) 3-(2-azidoethyl)benzofuran, (**3**) 3-(2-azidoethyl)benzo[*b*]thiophene, (**4**) 1-(azidomethyl)benzene, (**5**) 1 (azidomethyl)-4-chlorobenzene, (**6**) 1-(azidomethyl)-4-methylbenzene, (**7**) 4-(2-azido-ethyl)-phenol, (**8**) 1 (2 azidomethyl)naphthalene, (**9**) 1-azido-2-methylpropane, (**10**) 2-azidoethanamine and (**11**) N-(2-azido-ethyl)-guanidine. The values were normalized to the benzyl-functionalized B1 (**4**) (n=2, singlet, mean ± SD). (**B**) The concentration-dependent binding behavior of B1 functionalized with three different azide units (**4**, **5**, **6**) was determined by flow cytometry. The non-binding control G1sc was subtracted from the values. The values for each sequence were normalized to the 2000 nM value (n=3, singlet mean ± SD).

5.9.3. Surface plasmon resonance spectroscopy (SPR) analyses of streptavidin aptamers and clickmer

For the study of the K_D, k_{on} and k_{off} rate from B1 to streptavidin SPR was studied. Since several DNA aptamers targeting streptavidin are published, we also measured the aptamer 33 (Apt33)[17] and the DNA aptamer G1 (selected in multiplexed click-SELEX targeting SA, **section 5.9**) for comparison. The measurements were performed at different temperatures, 21°C and 37°C, and with two buffer systems, since Apt33 was selected at 21°C in a TRIS buffer system. The multiplexed click-SELEX was performed at 37°C in a PBS-based buffer. A representative measurement for each clickmer/aptamer and each condition is shown in **Figure 5.50**. Since a stable state could not be

achieved even with long injection times, a shorter injection time (80 µL = 120 s) was chosen for cost reasons. A selection of further measurements can be found in **Supp. figure 14**, **Supp. figure 15**, **Supp. figure 16**, **Supp. figure 17**, **Supp. figure 18**. The corresponding thermodynamic properties are listed in **Table 5.4** and shown in **Figure 5.51**.

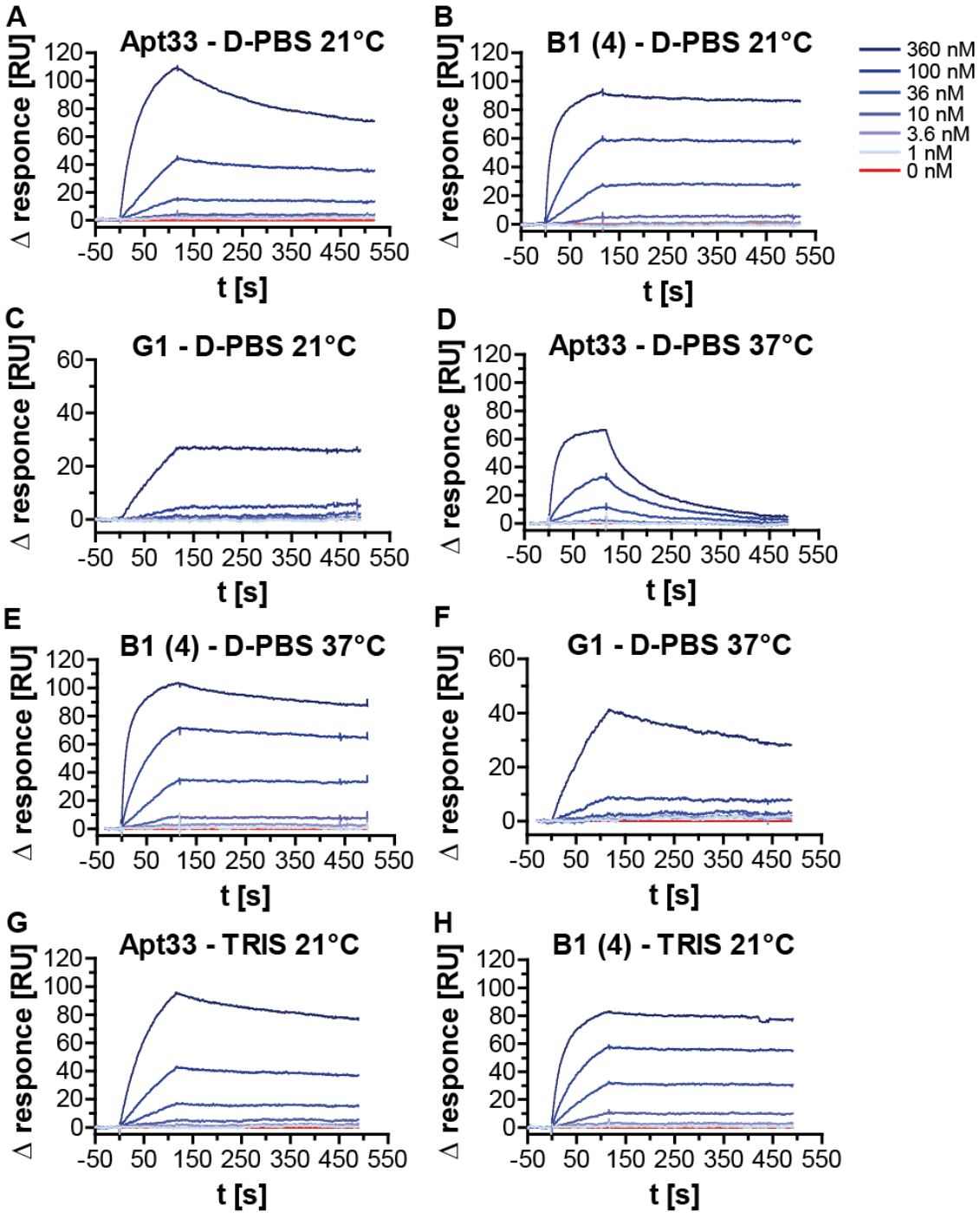

Figure 5.50: SPR kinetic analyses of the clickmer B1 and the DNA aptamers Apt33 and G1.

The kinetic analysis of the benzyl functionalized clickmer B1 (**4**) and the DNA aptamers Apt33 and G1, which bind to streptavidin, is shown. Superimposed sensorgrams for six concentrations of clickmer or aptamers are presented. The measurements were first performed at 21°C in the D-PBS buffer for Apt33 (**A**), B1 (**4**) (**B**) and G1 (**C**), then at 37°C in the D-PBS buffer for Apt33 (**D**), B1 (**4**) (**E**) and G1 (**F**). Finally, the interaction was measured at 21°C in the TRIS buffer for Apt33 (**E**) and B1 (**4**) (**F**).

Table 5.4 K_{on} rate, k_{off} rate, and K_D of benzyl functionalized B1 (4), G1, and Apt33 targeting streptavidin as identified by SPR analysis and measured at 21 and 37°C (n=5, singlets, mean ± SD).

		B1 (4)	G1	Apt33
k_{on} rate [10^4 $M^{-1}s^{-1}$]	37°C D-PBS	22.42 ± 1.53	2.04 ± 0.28	17.04 ± 0.86
	21°C D-PBS	19.42 ± 0.5	0.75 ± 0.26	7.23 ± 0.18
	21°C TRIS	13.28 ± 0.44	not measured	4.39 ± 0.08
k_{off} rate [10^{-4} s^{-1}]	37°C D-PBS	3.09 ± 0.4	10.75 ± 0.79	74.62 ± 3.34
	21°C D-PBS	0.66 ± 0.32	0.57 ± 0.43	10.34 ± 0.57
	21°C TRIS	0.64 ± 0.28	not measured	5.16 ± 0.27
K_D [nM]	37°C D-PBS	1.4 ± 0.2	53.28 ± 5.89	43.84 ± 3.08
	21°C D-PBS	0.34 ± 0.16	8.92 ± 8.2	14.30 ± 0.73
	21°C TRIS	0.49 ± 0.23	not measured	11.76 ± 0.73

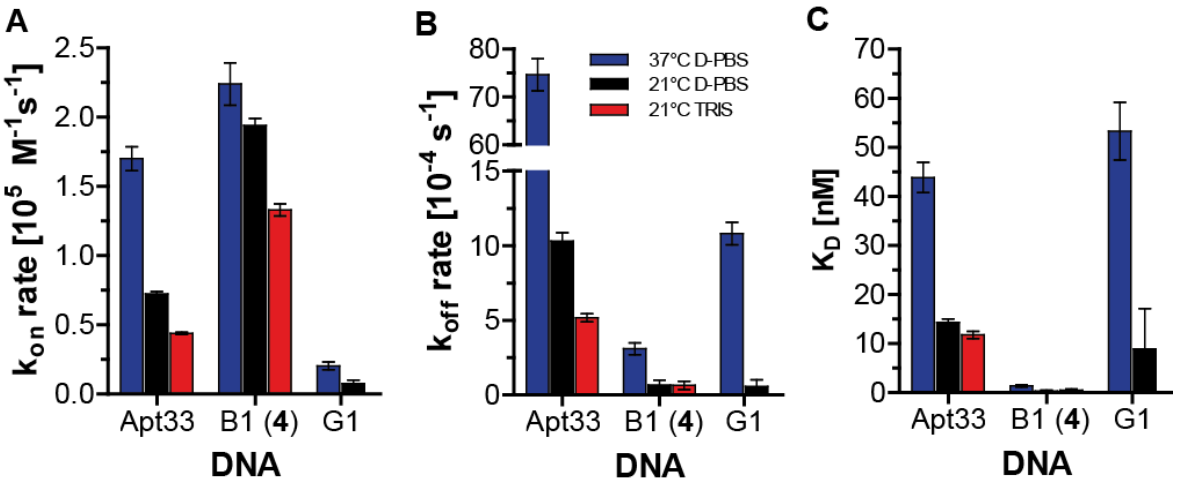

Figure 5.51: Thermodynamic properties of the Apt33, B1(4), and G1 targeting streptavidin.

The following are shown: the k_{on} rate (**A**), the k_{off} rate (**B**), and the K_D (**C**) of the clickmer B1 (**4**) as well as the DNA aptamers Apt33 and G1, which target streptavidin at different temperatures and in different buffer systems (n=5, singlets, mean ± SD).

B1 (**4**) has the fastest k_{on} rate compared to the other two aptamers. In addition, at a value of max. 3.09 ± 0.4 · 10-4 s^{-1}, B1 (**4**) has a slow k_{off} rate (at 37°C). The aptamers Apt33 and G1 have clearly higher values (**Table 5.4**) so that the complex B1(**4**)-SA is more stable compared to Apt33-SA and G1-SA. With a K_D of 0.49 to 1.4 nM, B1(**4**) has the highest affinity to SA of all aptamers investigated, independent of temperature and buffer system. The aptamers Apt33 and G1 have comparable values to each other, although they have no similarity in their sequence.

6. Discussion

With the ability to interact highly specific and affine with a defined target molecule, aptamers have proven to be powerful tools in molecular biology. However, not every target molecule can be addressed by the common selection approaches. To overcome these limitations, several new techniques have recently been published, *e.g.* modified nucleotide aptamers[53,57], clickmers[26,29], SOMAmer[79].

The present study aimed at the selection of aptamers for voltage-gated sodium channels (VGSC). S**ection 6.1.1** deals with different selection methods such as DNA-SELEX, cell-SELEX and click-SELEX, which were investigated for this purpose. Since none of these selections led to aptamers or clickers binding to VGSC, the following selections focused on the effects of DNA modification on the click-SELEX approach. The validation of the click selection for C3-GFP is discussed in **section 6.2**. This is followed by the discussion on multiplexed click-SELEX (**section 6.3**). Two different target proteins were addressed with this method, resulting in highly specific and affine clickmers for C3-GFP and streptavidin.

6.1. Selections targeting cell-surface proteins

6.1.1. VGSC selections with non-nucleobase-modified nucleic acids

Voltage-gated sodium channels (VGSC) are transmembrane proteins that must be inserted into a membrane for full functionality. For this reason, the VGSC-HEK293 cells were used, which express the different VGSC types. The functionality of the individual VGSCs was analyzed using patch clam technology.

In order to select a DNA aptamer for VGSC, the cell-SELEX approach was investigated (**section 5.1**). Cell-SELEX uses whole cells as target molecules, so that all molecules on the cell surface serve as potential target molecules[9,151,160]. In order to increase selection strength, salmon sperm DNA was used as a competitor. This salmon sperm DNA is not amplified because of the primers used, which hybridize with the library during PCR and not with salmon sperm DNA. The competitor (salmon sperm DNA) interacts with all potential targets and competes with the non-specific binding sequences of the library so that only specific binding sequences are used for amplification. The cell selections performed led to the generation of DNA aptamers targeting other proteins on the surface of HEK293 cells, but not VGSC (**Figure 5.5**, **Figure 5.8**). This may be due to the very low expression of VGSC in host cells[161]. So far, a large number of aptamers targeting overexpressed proteins in host cells have been selected[9,162,163], but to our knowledge no aptamer targeting a low expressed voltage-gated channel has been selected. Furthermore, it is not known whether VGSC can be addressed by DNA aptamers at all.

When calculating the approximate theoretical number of proteins on the cell surface of the HEK293 cell, it becomes clear that the chance of selecting an aptamer for VGSC is very low. A HEK293 cell has a radius (r) of 6.5 µm[164], and assuming that the cell is a sphere, this cell has a cell surface (O) of $5.3 \cdot 10^{-10}$ m² ($O=4 \cdot \pi \cdot r^2$). An average protein has a radius (r) of about 7.5 nm[164], and thus an area (A) on the surface membrane of a cell of about $1.8 \cdot 10^{-16}$ m² ($A= \pi \cdot r^2$). If now the cell surface and the surface of the average protein are set in relation, this results in approx. $3 \cdot 10^6$ proteins per cell. This is of course a theoretically assumed number, calculated under a very simplified model. Nevertheless, when comparing the number of channels per cell calculated by the Platch-clamp method (**section 5.1.1** - 3000 for $Na_v1.6$) with this theoretical number, a ratio of 1000 proteins per channel results. What does this mean for the selection of an aptamer for VGSC? Since the cell-SELEX addresses all possible target molecules, including the 1000 proteins, it is very difficult to filter out the VGSC because all binding sequences are amplified in the amplification step of the SELEX. This means that all potential aptamers that bind to the 1000 proteins must be suppressed so that they are not amplified. This was investigated using the multiple negative cell-SELEX approach (**section 5.1.5**). It included several counter selection steps to suppress all potential aptamers against the target molecules on the host cell. The library is incubated with several successive HEK293 cells before the depleted library is incubated with the VGSC-HEK293. However, this technique did not produce aptamers targeting VGSC (**Figure 5.10**). It is plausible that the selected selection conditions in this study negatively influenced the results. The introduction of the counter step in the 4th selection cycle was chosen too late. The already enriched sequences that attack other proteins on the HEK293 cell may already have been strongly enriched at the beginning of the counterselection. Due to this excess, the sequences targeting HEK293 can no longer be suppressed with the multiple negative cell selection approach. It makes sense to introduce this counting step from the very beginning.

The click-SELEX approach was established to improve selection success for difficult targets through chemical modifications such as indole (**section 5.2**). Indole provides hydrophobicity to the DNA aptamer and mimics the amino acid side chains in protein-protein interaction, making DNA-protein interactions stronger compared to unmodified DNA. Indole is chemically similar to tryptophan, which is one of the most common amino acids in antibody-protein interactions[85,86]. Unfortunately, this DNA functionalization leads to greater DNA affinity to all potential target molecules (proteins) that have hydrophobic epitopes, including undesired target molecules on the cell surface. One way to suppress this non-specific binding is to use competitors. The first click selection showed that the addition of a double-stranded, indole-modified DNA competitor leads to a higher selection strength[26]. In the present study, a solid phase synthesized single-stranded DNA, the click competitor (5'-N42-A-3') was used, which contains EdU and how the library can be modified[26]. This modification enables the competitor to compete with the library used and suppress the non-specific interaction with the target molecule.

In addition, guanidine modification was studied due to its chemical similarity to tetrodotoxin (TTX), an extremely neurotoxic agent by blocking VGSC (**Figure 5.12**). TTX binds via its guanidine residue to the extracellular domain of VGSC[154]. We chose guanidine-modified DNA to mimic the interaction of TTX with VGSC (**section 5.2**).

Unfortunately, click-SELEX did not lead to the selection of clickmers targeting VGSC, but HEK293 proteins (**section 5.2, Figure 5.14**).

All cell selections performed led to the conclusion that the expression of VGSC in HEK293 cells is too low compared to all other potential target proteins to be targeted during a SELEX. To prove the expression hypothesis, another target (GluR1) was chosen for a click-SELEX. This will be explained in the next **section 6.1.2**.

6.1.2. Click-SELEX for GluR1

Numerous published selection processes show the possibility of successful DNA/RNA aptamer selection for cell surface proteins[37,151,165,166]. Nevertheless, the large number of different target molecules on the cell surface complicates the suppression of aptamers, which do not target VGSC but other accessible molecules on the cell surface. HEK293 cells have a large variety of proteins on their cell surface. To ensure that the chosen selection method is the right one for the selection of clickmers targeting a channel on the cell surface, we have used the same technique to select a target molecule that is known to be addressed by aptamers. A publication in 2009 showed that it is possible to select RNA aptamers for glutamate receptor 1 (GluR1)[157]. At the beginning of this part of the study, no DNA aptamer, clickmer, or other nucleotide-modified aptamer targeting a voltage-gated channel expressed in a cell was published. We investigated click-SELEX for GluR1 expressed in HEK293 cells. Confocal microscopy showed that the stable cell line produced contains GluR1 in the cell membrane (**Figure 5.19**). In this way, the VGSC-HEK293 cell line can be compared with the GluR1-HEK293 cell line. However, GluR1 is presumably present on the cell surface in much larger quantities than VGSC, i.e. the ratio of all proteins to GluR1 is smaller.

Unfortunately, we could not select a clickmer for GluR1 with multiple negative cells-SELEX (**section 5.4.2**). It is plausible that the click-SELEX conditions are not optimal for cell-SELEX. Another reason might be that the azide-containing compounds selected for DNA functionalization (indole, benzyl and guanidine azide) are not optimal modifications for the GluR1 target. Gold *et al.* has shown for protein targets that not every modification leads to successful selection[79]. Indole and benzylazide were chosen because of their chemical similarity to the amino acids (tryptophan and phenylalanine) most commonly found in protein-protein interactions[85,86]. This should increase the interaction between protein and clickmer. But since all potential proteins are addressed, these azide compounds may increase clickmer cell-surface-protein interaction, i.e. the initial library interacts with all potential

proteins on the cell surface except GluR1. The same problematic situation as with VGSC (**section 6.1.1**).

In addition, it is known that SELEX success depends on several factors, including the complexity of the source library and its background binding to the target molecule, selection severity, structural properties of the target, and buffer composition[167]. The possibility to select a high affinity aptamer is very low at high background binding because the sequences have a high non-specific binding. This is the case with the binding to the versatile proteins on the cell surface observed in the cell selections with indole azide for DNA functionalization (**Figure 5.20**). Despite the addition of competitors such as salmon sperm DNA and click competitor (**section 6.1.1**), this background binding could not be suppressed.

Based on the different background binding of the three differently functionalized start libraries to the GluR1-HEK293 and HEK293 (**Figure 5.20**), we decided to understand the effects of functionalization during the click-SELEX approach. This was investigated with a simplified model, a protein (**sections 5.5 and 6.2**).

6.2. Click-SELEX targeting C3-GFP

At the beginning of this part of the work was the click-SELEX for C3-GFP, published by Tolle et al., the only successful implementation of the technique[29]. The selected clickmer C12 used indoles azid for DNA functionalization[29]. Recently a second clickmer, C11.41, for a small molecule, (−)-Δ^9-tetrahydrocannabinol (THC) was published[98]. THC is a difficult target molecule due to its high hydrophobicity. In order to maximize the interaction of the modified DNA with THC, the DNA was functionalized with benzylazide. While the C12-clickmer shows no binding with other aromatic modifications, but only with indole[29], benzofuran[26] and benzothiophen[26], the C11.41-clickmer develops an interaction with THC via a number of aromatic modifications, but no interaction with non-aromatic units[98]. In addition, for protein targets Gold *et al*. have been shown that not all modifications function adequately[79]. Furthermore, the group has shown that not all modifications lead to the selection of a SOMAmer for protein targets[79]. These examples show how important the strategic choice of the modification used can be in influencing the selection. Due to the similarity of the modifications of the nucleotides, it can be assumed that this also applies to click-SELEX. An indication is provided by the recent publication on the partial loss of binding to the target molecule using other clicked-in modifications[26,29].

For this reason, in this part of the study, we have discussed the effects of azide functionalization on the SELEX process. The selection was as similar as possible to the first published GFP-SELEX. The main changes were the inclusion of a click competitor (**section 6.1**) and the use of another library. In order to exclude that the library has an influence on the selection success, we designed a new library

(**section 5.3**), which contains EdU instead of dT and allows functionalization via CuAAC. After making eight identical click selections targeting C3-GFP with different azides (**section 5.5**), we can assume that the choice of azide will dramatically affect SELEX's success. Only three out of eight modifications lead to successful selections of clickmers. Interestingly, the properties of the clickmer also depend on the modification described in section 6.3.3. For C3-GFP, only the selections with indole, benzyl and benzofuranazide led to the selection of clickmers (**section 5.5** and **5.5.3**, **Figure 5.22**). The SELEX could not be completed with chlorobenzyl, methylbenzyl, naphthalene, methylpropane or ethylamine azide due to PCR by-products (**Supp. figure 7**). One possible explanation is that only indole, benzyl and benzofuran are able to interact with C3-GFP and thus positively influence its binding to the functionalized DNA. These results are comparable with Gold *et al.*[79]. The group compared selections with unmodified and modified nucleotides targeting thirteen different proteins. Twelve selections with unmodified nucleotides failed[79]. Furthermore, not all selections using the three different modifications 5-benzylaminocarbonyl-dU, 5-tryptaminocarbonyl-dU and 5-isobutylaminocarbonyl-dU were successful in generating SOMAmers[79]. Another indication of the importance of correct modification was given by Gelinas *et al*. The group published a crystal structure of an IL-6 – SOMAmer-complex and demonstrated that the chemical modification of the SOMAmer is strongly linked to the contact with the protein (IL-6) [89].

To confirm the hypothesis that the clickmer modification is involved in the binding to the protein, a further analysis such as a dissolved crystal structure is required, which was not possible during this work due to time constraints. So far no clickmer structures have been published.

6.3. Multiplexed click-SELEX

After having determined that functionalization has an influence on the success of click-SELEX, we established the multiplexed click-SELEX procedure (**Figure 5.31 A**). Each individual functionalization increases the selection pressure in this method because the individual functionalized libraries compete with each other for binding to the target molecule through greater diversity. The selection pressure can, for example, be additionally increased by harder washing steps, higher volumes or longer washing times[26]. The use of competitors during the selection process is another possibility to increase the selection pressure, since unspecifically binding sequences are suppressed (**section 6.1.1**). In addition, multiplexed click-SELEX offers the possibility to perform multiple click selections in one, which is less time-consuming and cheaper. The great advantage of multiplexed click-SELEX is that the chance of a successful selection is greatly increased.

Before sequencing the enriched library, this multiplexed click selection procedure requires a deconvolution cycle. After performing several multiplexed selection cycles, the enrichment of the library is usually confirmed by a binding test to compare the initial library and the last selection cycle.

For the multiplexed click-SELEX it is important to investigate this binding for each functionalization. Therefore, it is not sufficient to use only the azide that showed binding to the target molecule in the deconvolution cycle. It is essential to perform this deconvolution cycle for each functionalization in order to ensure perfect assignment of the functionalization required for clickmer interaction with protein after sequencing. The sequencing by NGS ensures the deep information of all sequences, the information generated by the Sanger sequencing could not provide sufficient information about the increase/decrease of the sequences over the selection cycles in multiplexed click-SELEX. It may be possible to functionalize a sequence with more than one chemical unit without losing its ability to interact with the target molecule. This can be explained by the separation into different aliquots of the library prior to functionalization. Each aliquot theoretically contains the same sequences and is functionalized with different azides. Thus the same sequences are prepared with different functionalizations. In addition, the published clickmer C11.41 (**section 6.2**) develops an interaction with THC via a series of aromatic modifications[98]. This example is an indication of the possibility of multiplexed click-SELEX to generate clickmers which can be equipped with different functionalizations without losing the binding to the target molecule and without losing affinity.

The first published clickmer for C3-GFP[29] and the successful click selections showed that C3-GFP can be targeted by clickmers (**section 5.5**). For this reason, and for comparison with click-SELEX, it was selected as the target molecule for the first multiplexed click-SELEX. To maximize the chances of success, the azides indole, benzofuran and benzylazide (**section 5.5**) were included as click selections with these azides led to the generation of clickmers. In addition, the use of all three azides allows the hypothesis of clickmers competition to be investigated. Furthermore, we also included two other azides where click selection was not successful (**Supp. figure 7**) to show that functionalizations with these azides do not interfere with the multiplexed click-SELEX process.

The second multiplexed click-SELEX targeted the peptide $Na_v1.6$. This is explained in **section 6.3.4**. This selection led to the third multiplexed click-SELEX targeting streptavidin (**section 5.8**). Since numerous selections were made leading to DNA aptamers with high affinity to streptavidin[17,168,169], it was selected as the target molecule. To maximize the chances of success, indole, benzyl and phenol azides were selected for DNA functionalizations because they are similar to the most abundant amino acids (tryptophan, phenylalanine and tyrosine) in antibody-protein interactions[85,86]. We have also included two non-aromatic azides, methylpropane and guanidine. Since Gold *et al*. have shown that SOMAMers using the methylpropane modification can respond to some protein targets[79]. And the guanidine modification was used as a hydrophilic modification.

In the case of C3-GFP, indole and benzofuranazide showed binding to C3-GFP in the 8th selection cycle (**Figure 5.32**). The deconvolution cycle (9th selection cycle) showed that the most frequent sequences require one of the azides (indole or benzofuran) for interaction with C3-GFP (**Figure 5.36 B**, **C**). In addition, multiplexed click selection towards streptavidin showed a binding for four out of

five azides (**Figure 5.43**). Here it was important to perform the deconvolution cycle for all azides used for two cycles. The NGS analysis confirmed this, showing that a deconvolution cycle resulted in a small change for the individual sequences (**Figure 5.44**) compared to the 8th selection cycle and the 10th deconvolution cycle. The frequency of the most frequent sequences has the same tendency: the frequency for sequences B1 and G1 was increased in the 9th, but more strongly in the 10th selection cycle (**Figure 5.45**). This could be explained by the higher number of sequences that are able to shape the interaction with the target molecule by various modifications, such as the clickmer C11.41, which targets THC[98]. An indication of how many deconvolution cycles a selection requires, however, could be the binding analysis of the last multiplexed click selection cycle. The more modifications show binding, the more deconvolution cycles may be necessary for a clear hypothesis about optimal sequence functionalization. Both multiplexed click selections confirm this as four modifications showed binding to streptavidin in the 8th selection cycle (**Figure 5.43**) and only two modifications showed binding to C3-GFP (**Figure 5.32**).

6.3.1. Identification of clickmers targeting C3-GFP

Next-generation sequencing (NGS) gives a deep insight into the selections[26]. The percentage of unique sequences in each selection cycle allows a very fast and easy analysis of the selection (**Figure 5.23 A, Figure 5.34**). The more the number of individual sequences decreases, the greater the enrichment of the individual sequences. Probably due to the different DNA functionalization, all three click selections and the multiplexed click-SELEX for C3-GFP developed different enrichment profiles with respect to the unique sequences (**Figure 5.23 A, Figure 5.34**). Benzofuran functionalization already shows a frequency below 3% for unique sequences in the 4th selection cycle, while indoles and benzyl functionalizations are still at 72% and 96%, respectively. Since all selections were carried out completely the same, except for the functionalization, this effect can be traced back to the functionalization. After the characterization of the selected sequences (**section 5.5.3-5.5.4**), this can also be explained as follows. The clickmer F20 was selected with benzofuran functionalization and has better kinetic properties compared to I10 (indole functionalization) and B33 (benzyl functionalization) (**section 5.5.4**, **Table 5.3**, **Figure 5.29**). When comparing I10 to B33 again, the frequency of the unique sequences can also be explained as I10 is more affine than B33 (**section 5.5.4**, **Table 5.3**, **Figure 5.29**). In other words, the more affinier the sequence, the faster it can be enriched, which can be read from the frequency of the unique sequences. Whether benzofuran functionalization also allows successful selections for other target molecules must be checked by means of further selections. Consequently, the percentage of unique sequences is the first indication of successful selection[46], but other analytical methods, such as the distribution of nucleotides and the frequency of unique sequences, should be used for selection analysis.

The nucleotide distribution showed a different enrichment profile for the three click selections. It is interesting to note that the click-SELEX with indole functionalization yielded almost only one sequence, I10, with a frequency of 60.4% in the last selection cycle (**Figure 5.24**). The next most frequent sequence I27 has 2.8% in the last selection cycle. The motif of the most frequent sequence I10 is visible in the nucleotide distribution of the last selection cycle (**Figure 5.23 C**). Obviously, the highest possible selection strength was used for selection with indole azid. This result is different from the first clickmer C12 targeting C3-GFP[29]. It was selected under similar conditions, but with a different library and competitor[26]. In the study presented, a solid phase synthesized single-stranded DNA, the click competitor (5'-N42-A-3') was used, which contains EdU and how the library used can be modified (**section 6.1**). The results of the presented study showed the importance of the click competitor during click-SELEX. With the help of the click competitor, binding sequences are enriched more quickly.

Furthermore, the difference between the published clickmer C12 and I10 lies not only in the selection process, but also in the clickmer properties. This will be explained in the next section **section 6.3.3**).

The other two click selections with benzofuran and benzyl azide were enriched with several sequences. The mixed nucleotide distributions reflect these mixed sequences (**Figure 5.35**). Several clickmers could be identified for both selections: F8 and F20 containing benzofuran azide and B10, B15, B33 containing benzyl azide. Since all selections used the same target molecule (C3-GFP), but different azide-containing compounds for DNA functionalization, it is surprising that sequences I10 and B33, with the exception of "CXXXG" (**Table 6.1**), have no sequence similarity. Similarly, sequences F20, F8, and I10 with a small pattern "GXAXGAXGCC" show sequence similarity. It is surprising that despite this similarity, F20 does not show a binding to C3-GFP at indole functionalization (**Figure 5.26**), but I10 shows a reduced binding (~20%) to C3-GFP at benzofuran functionalization (**Figure 5.26**). One possible explanation is the chemical properties of benzofuran and indoles, the former being an electron donor and the latter an -acceptor. This difference has either an influence on the clickmer structure or folding or an influence on the target molecule and thus on the binding. In order to obtain a clear explanation, further binding analyses must be carried out, such as a crystal structure.

Further characterizations are explained in the next section (**section 6.3.3**).

Table 6.1 Multiple sequence alignment of the most abundant sequences in the click-selections targeting C3-GFP. The shared motif "CXXXG" is shown in red and "GXAXGAXGCC" in blue.

Name	Sequence random region (41-44 nt; X=EdU)
I10	CGCGXAGGXACCCGG**CXXXG**AA**XAXG**XA**G**GGGACCXAGAGA----------ACA--
F8	----XCGGGCCGGAGC--GAG**GXAXGAXGCC**AXCCXXCACAGCXCCA----------
F20	----------CCGCC--CGC**GXAXGAXGCC**GXCXXACGGGCAGCCGXAACCACAAC
B33	GGC---------GXA**CXXXG**--**X**C**X**C**A**CCXACACAXXCXAACCACCACXACGCCA--

6.3.2. Identification of clickmers in the multiplexed click-SELEX targeting C3-GFP and streptavidin

The multiplexed click-SELEX resulted in a strong enrichment of the unique sequences due to the high degree of selection rigour. When using the different azides in the deconvolution cycle, the percentage of each sequence changes. In the selections targeting C3-GFP with indole and benzofuranazides, the number of unique sequences was kept constant. The number of the other three azides increased (**Figure 5.34**). This effect is even stronger for the second deconvolution cycle of the selection targets streptavidin (**Figure 5.44**). However, the increase in the frequency of the unique sequences means that the complexity of these libraries has increased so that fewer sequences bind specifically. One possible explanation could be that errors are built in during amplification, thus generating more unique sequences. It has been observed that the amplification of homogeneous templates, such as complex oligonucleotide libraries, is very complicated[170]. Polz *et al*. have shown that bias can be reduced by using a high template concentration, as fewer cycles are required to complete amplification[170]. All deconvolution cycles performed in the multiplexed click selections showed different PCR cycles, probably due to the different number of sequences recovered after incubation during selection. The fewer sequences recovered, the more PCR cycles are required to complete amplification. In addition, Tolle *at el*. observed the formation of PCR by-products, which led to the prohibition of enrichment of certain target sequences[155]. This may be the case in deconvolution cycles with elevated single sequences, where the sequences obtained are amplified with PCR by-products, resulting in an increase of the single sequence (unique sequence frequency).

Furthermore, it is essential to sequence each deconvolution cycle for a clear hypothesis about the required functionalization for optimal interaction with the target molecule. The schematic representation of the sequence performance is shown in **Figure 5.33**. The first multiplexed click-SELEX targeting C3-GFP showed exactly what is shown in this schematic (**Figure 5.36**). When indole azide was used for DNA functionalization, all sequences that did not require this residue for interaction with C3-GFP decreased drastically in frequency in the deconvolution cycle. This is the case, for example, with F20 (**Figure 5.36 B**). The frequency of I10 increased strongly. From these data it seems obvious that I10 requires indole functionalization for optimal interaction with C3-GFP. This was demonstrated by flow cytometry (**Figure 5.26**). The other required functionalizations, such as benzofuran for F8 and F20, were evaluated in the same way.

The multiplexed click-SELEX targeting streptavidin required two deconvolution cycles. The hypothesis was that during the two deconvolution cycles the sequences that bind with several functionalizations are more clearly recognizable by the change in their frequency. Interestingly, the frequency for sequence B1 increased only after the second deconvolution cycle (selection cycle 10), but then above 15% (**Figure 5.45**). The frequency for sequence G1 showed a similar behavior,

increasing from cycle 8 to 9 from <1% to 7% and over 38% in selection cycle 10 (**Figure 5.45**). It is plausible that the more sequences are enriched with different chemical functionalizations during the multiplexed selection cycles, the more deconvolution cycles are required. The reason could be that up to the last multiplexed selection cycle all potential sequences with similar thermodynamic properties bind to the same epitope and compete with each other. All these sequences are enriched with a similar low frequency. This was the case with the multiplexed click selections targeting the peptide $Na_v1.6$ and streptavidin (**Figure 5.40**, **Figure 5.45**). Consequently, further deconvolution cycles are required to enrich the low frequency sequences to a high frequency in order to allow optimal differentiation of the overall enriched sequences.

All in all, we could confirm that the multiplexed click-SELEX works as expected. This new approach allows the selection of highly specific and highly affine clickmers or aptamers such as the click-SELEX. The great advantage of multiplexed click-SELEX is that several different modifications can be used in one selection, which increases the probability of a successful selection of an aptamer/clickmer. In addition, different modifications in a selection allow more competition between the sequences, which leads to a higher selection strength.

6.3.3. Evaluation of clickmers targeting C3-GFP

The click selections have enabled the enrichment of several sequences (**Figure 5.24 B**). The most common sequences were I10 (**1**), F8 (**2**), F20 (**2**) and B33 (**4**) (**Figure 5.24 A**, **Figure 5.36**). Using two different approaches, flow cytometry (C3-GFP immobilized on magnetic particles) (**Figure 5.24 B**) and SPR (C3-GFP in solution), it was shown that all these clickmers interact with C3-GFP (**Figure 5.28**). With flow cytometry it could be shown that all clickmers investigated need the original functionalization for optimal interaction with the target molecule (**Figure 5.26**). No to low interaction was observed without any functionalization. Consequently, functionalization of the functionalized DNA either interacts directly with the target molecule or functionalization has an effect on DNA folding. A structural analysis could provide clarity. To our knowledge, no **c**ickmer structures have been published.

Furthermore, it could be shown that all clickmers investigated are specific for C3-GFP compared to streptavidin or mE-GFP (**Figure 5.30**). C3-GFP and mE-GFP[171] are highly homologous and differ in only nine point mutations[29]. The fact that the clickmers do not interact with mE-GFP may indicate that one or all of these nine-point mutations are involved in the **c**lickmer-C3-GFP interaction. In addition, the first clickmer, C12, targeting C3-GFP may have the same epitope like I10 due to similar specificity[29]. Crystal structure analysis could confirm this hypothesis.

When comparing I10 with C12[26,29] and P5[26] there is no obvious sequence similarity (**Table 6.2**). Since all three clickmers show no unfunctionalized binding to C3-GFP and the only similarities in the

sequences do not contain the EdU, we can assume that these similarities (similar nucleotides) do not contribute to binding. But to exclude this for sure, further binding analyses should be performed (*e.g.* **c**rystal structure). That all three sequences have no sequence similarity could be due to the effect of using different libraries with different primer binding sites that are part of the **c**lickmer structure. The use of different competitors during selection (**section 6.3.1**) may be another reason.

Table 6.2 Multiple sequence alignment of the random region of the clickmers P5, C12, and I10.

The matching nucleotides are marked in bold.

Name	Random region (X=EdU)
P5	XAGGAG**G**G**AG**CA**A**GGXACGXXGC**A**GC**A**X**G**AC**GGG**AC**CC**G**A**C**A------
C12	------**G**XX**G**GA**A**GCGACGGGACGGX**A**A**G**GCXX**G**GG**CC**CCA**A**GGAGXG
I10	---CGC**G**X**AG**GX**A**CCCGGCXXXG**A**AX**A**X**G**XA**GGG**GA**CC**X**A**G**A**GAACA-

However, both clickmer I10 and C12 are highly specific and affine clickmers, and both require indole functionalization for their interaction with C3-GFP. It is interesting to note that when modified with benzofuran or benzothiophenazides[26], C12 has a higher binding (about 50-60%) than I10 (about 20%) compared to indole modification (**Figure 5.26**). For C12[26] no affinity difference could be observed between the three functionalizations. Since the three modifications in I10 showed interactions with C3-GFP to varying degrees, the affinity of modifications other than indole modifications for I10 was not investigated. It is plausible that an aromatic residue is involved in the interaction of I10 with the target molecule since the total functionalization of I10 with aromatic chemical units showed about 20% binding to C3-GFP compared to indole azide. The involvement of the aromatic residue can be excluded for C12, since the interaction of the functionalized C12 with *e.g.* ethylnaphthalene or ethylphenyl did not lead to a binding[26]. The same is true for P5[26]. Both clickmers, C12 and I10, show a similar K_D value for the indole modification, despite the difference in the method used (K_D (C12) = 59 ± 16 nM[26]; K_D (I10 at 37°C) = 26.5 ± 5.9 nM - **Table 5.3**). The other clickmers, F20, F8, and B33, showed a slight difference in affinity. While B33 has a low affinity (K_D (B33 at 37°C) = 153.8 ± 68.4 nM), F20 is the affine clickmer (K_D (F20 at 37°C) = 2.3 ± 0.6 nM) (**Table 5.3**). For all clickmers examined, the values for k_{on} and k_{off} rate at lower temperature become smaller, for I10, however, k_{on} rate. The k_{on} and k_{off} rate of C12 was not analyzed and cannot be compared. On the one hand, considering that thermodynamic activity is slower at lower temperatures, it is not surprising that the k_{off} rate at the lower temperature, 25°C, is significantly lower. On the other hand, Berezovski and Krylov suggest that either the protein or the aptamer or even both are exposed to a temperature-dependent conformational change of their structures[172]. The correct GFP folding required to form the chromophore[173] is temperature dependent[174,175]. In this study, however, the mutant C3-GFP was used, which can fold correctly even at 37°C. The consideration of this and the fact that the k_{on} rate of I10, but the other clickmers showed no temperature dependence, leads to the assumption that the clickmer structure could be more temperature dependent than that of C3-GFP. To confirm this hypothesis, structural studies of the complex C3-GFP clickmer might be useful.

In addition, benzylazide led to enrichment of clickmer B33 (**4**) (**Figure 5.24**), with a faster k_{off} rate and a higher K_D value than the other clickmers investigated (**Figure 5.29**). Against this background it can be explained why B33 (**4**) was not strongly enriched in multiplexed click-SELEX before the deconvolution cycle (**Figure 5.32**, **Figure 5.36 D**, **E**). Probably it was suppressed by the more affine clickmers I10 (**1**) and F20 (**2**), which have a slower k_{off} rate and a lower K_D value. In addition, the influence of different functionalizations on the binding of clickmers showed different binding behavior (**Figure 5.26**). While I10 and B33 showed a low binding functionalized with all tested aromatic residues, F20 and F8 showed a binding only with benzofuran (**2**) or benzothiophen (**3**) functionalization. This can be explained by the sequence similarity, the clickmer B33 and I10 have the motif "CXXXG", which is missing in F20 or F8 (**Table 6.1**). For a clear hypothesis a further analysis is necessary, *e.g.* a binding analysis with different variants in which the modification is changed to thymidine as it was done with the published clickmers C12[29] and C11.41[98].

Several scientific questions about these clickmers still need to be examined. An interesting point is the potential binding site and the interaction of the clickmers with the same or different epitopes on C3-GFP. I10 (**1**) and F20 (**2**) could bind different epitopes, as both clickmers have similar thermodynamic properties. On the one hand, F20 (**2**) has a faster k_{on} rate and a lower K_D value compared to I10 (**1**) (**Table 5.3**, **Figure 5.29**). If both clickmers interact with the same epitope, F20 (**2**) should have suppressed I10 (**1**) during the first eight selection cycle, as is the case with B33 (**4**). However, since I10 was the more dominant sequence in the first eight selection cycles, it can be concluded that F20 (**2**) and I10 (**1**) can interact with different epitopes. On the other hand, different sequences have different structural properties such as secondary structures, sequence order, melting temperature or their adaptation to polymerase[176]. In addition, some sequences adapt better to the PCR polymerases[176,177] used, which could influence the selection process. To confirm this hypothesis, further analyses are required, such as crystal structure studies.

6.3.4. Comparison of selection process targeting peptide $Na_v1.6$ and streptavidin

2014 Lee *et al*. have developed a monoclonal antibody that acts on the voltage sensor paddle of $Na_v1.7$[159]. The antibody prevents the function of $Na_v1.7$[159]. The group chose a peptide corresponding to the voltage sensor paddle located in domain II (S3 - S4 loop)[159] (**Figure 3.7 B**). Based on this strategy, we chose the same peptide sequence of the corresponding $Na_v1.6$ (**section 9.7**).

The unsuccessful multiplexed click-SELEX targeting peptide $Na_v1.6$ produced an enrichment for streptavidin, the matrix on which the peptide was immobilized. A possible explanation could be that the DNA could be rejected by the negatively charged peptide $Na_v1.6$ due to the fact that it is negatively charged, which reduced the possibility of enriching an aptamer or clickmer. However, after NGS analysis, three clickmers, I1, Ben1, and P2 were selected for further characterization. These clickmers bind to streptavidin with all investigated functionalizations (**Figure 5.42**), but not without

any functionalization. It may be that the triazole (**Figure 3.6**), which is formed during the click reaction and serves as a link between DNA and functionalization, interacts with streptavidin. Thus, no specific chemical residue is required for functionalization. In addition, the chemical residue can influence binding by affecting the π-system of triazole. To the best of our knowledge, however, no clickmer for streptavidin has yet been published.

It is also plausible that the selection procedure with the strong counter-SELEX step (**section 5.7**), which is intended to remove all binding sequences to the streptavidin beads, has a major influence on the resulting sequences. It is possible that all high-affinity clickmers for streptavidin were removed from the selection during the counter step and only the remaining clickmers were enriched.

We then performed a multiplexed click-SELEX targeting streptavidin directly. Surprisingly, the binding analyses after the first eight selection cycles showed a similar binding behaviour (**Figure 5.43**) as the previous selection (**Figure 5.37**). Nevertheless, the NGS analyses showed differences between the two selections: The number of unique sequences in the final cycle of the first selection (targeting peptide $Na_v1.6$) is higher (**Figure 5.38**, **Figure 5.44**), which means that this selection retains a higher library diversity and is not so enriched. This was also supported by the respective nucleotide distributions (**Figure 5.39**, **Supp. figure 13**). The most common sequences also differ (**Figure 5.40**, **Figure 5.45**). The counter-SELEX step in the first selection (targeting peptide $Na_v1.6$) greatly reduced the accumulation of sequence P2 (**Figure 5.40**) with a frequency of about 1% in the final selection cycle. P2 is the most abundant sequence in the second selection (targeting of streptavidin) with a frequency above 20% (**Figure 5.45**). Since P2 does not require specific functionalization for interaction with streptavidin, it has been functionalized with all five azides and interacts with the entire functionalization, resulting in a higher amount of template during PCR. In addition, P2 may adapt better to polymerase[176] (**section 6.3.3**) during selection compared to other sequences obtained, which explains the high frequency of P2 in selection.

From these data, we can assume that the counter-SELEX step, when performed as in the first selection targeting peptide $Na_v1.6$, has a large influence on the SELEX. The sequences generated most likely have a lower affinity to the matrix used for immobilizing the target molecule or used as the target molecule in the counter-SELEX step. In general, the affinity of the sequences and the selection success depend strongly on the target molecule and whether it can be addressed by the aptamer or clickmer, i.e. whether it can be bound.

6.3.5. Characterization of clickmers targeting streptavidin

Interestingly, the sequences (I1, Ben1 and P2) from the first selection (targeting peptide $Na_v1.6$) bind with each tested functionalization (**Figure 5.42**). This may be an effect of the selection procedure (**section 6.3.4**). The second selection (targeting streptavidin) resulted in the enrichment of the three most common sequences P2, B1 and G1 (**Figure 5.45**). In the concentration-dependent binding test

(**Figure 5.46 B**) B1 (**4**) showed the highest affinity. B1 only binds to streptavidin if it is functionalized with benzyl (**4**), chlorobenzyl (**5**) or methylbenzyl (**6**), but the last two functionalizations led to a lower affinity (Figure 5.49 B). This may be caused by the "additional" group (chlorine or methyl), which may interrupt binding to the target by steric hindrance. Furthermore, no binding with ethylphenol (**7**) was observed. The reason could be the linker - the ethyl group (**Figure 5.11**). All three other compounds contain a shorter linker - methyl group. The longer ethyl group provides more space for the rotation of the phenol group, which could interfere with binding or affect clickmer folding and thus prevent binding to the target molecule. In addition, the hydroxy group of phenol (**7**) can also influence the interaction. No binding was found for the further functionalization of clickmer B1. It can be assumed that benzyl is involved in the interaction with streptavidin, but with the available data it cannot be confirmed with certainty. To confirm this hypothesis, structural studies at clickmers would probably elucidate the reason.

The next sequence studied was G1, which showed interaction with streptavidin in the unfunctionalized version (**Figure 5.46**). For this reason, further analyses with canonical DNA were performed.

For comparison, the published aptamer 33[17] of SPR was examined together with B1 (**4**) and G1. The published K_D value of aptamer 33 is 59.0 ± 7.5 nM and was determined with fluorescein-labeled aptamer targeting streptavidin coated magnetic beads[17]. Due to the fact that SPR is another method[177-179], the K_D value obtained in this study (11.76 ± 0.73 nM at 21°C in the TRIS buffer) differs from the published K_D value (59.0 ± 7.5 nM)[17]. Moreover, it is not surprising that the higher the temperature, the higher the SPR data values (k_{on} and k_{off} rate, K_D) due to the faster kinetics (**Figure 5.51**, **Table 5.4**). Several publications have shown that kinetic data depend on buffer, ionic strength, pH and temperature[178-181]. This could explain the fact that G1 has a slower k_{on} rate and k_{off} rate than Aptamer 33, caused by the different selection procedures, the buffers used or the selection temperature. However, the selection of G1 shows that multiplexed click-SELEX also allows the selection of DNA aptamers.

Furthermore, as explained in **section 6.3.3** for clickmers targeting C3-GFP, the structures of aptamer/clickmer and/or streptavidin may depend on temperature. Since streptavidin has no temperature dependence[182], it can be assumed that the clickmer/aptamer structure of the investigated sequences is temperature-dependent and influences the interaction with streptavidin.

Clickmer B1 (**4**) was the most affine clickmer of all tested sequences targeting streptavidin with the fastest k_{on} rate, the slowest k_{off} rate and the lowest K_D value at all investigated temperatures and in all buffer systems (**Figure 5.51**). This may be caused by benzyl functionalization, which confers hydrophobicity to DNA. Crystal structure analyses of SOMAmers showed that the increase in hydrophobicity increases the interaction of SOMAmers and proteins[79].

Since the multiplexed click-SELEX targeting streptavidin was performed as proof-of-concept for the selection strategy, no further investigations were performed. However, some scientific questions remain unanswered. With regard to B1, which contains ten EdUs, it would be interesting to investigate which EdU position needs to be functionalized for interaction with streptavidin. Furthermore, a crystal structure analysis of P2 (**7**) and streptavidin could confirm the interaction of triazole with streptavidin.

7. Outlook

This work shows that voltage-gated sodium channels (VGSC) expressed in HEK293 cells are not addressable by DNA aptamers using today's selection methods (**section 5.1**). In addition, the modified aptamer approach, click-SELEX[29], has not generated clickmers for VGSC either. A possible explanation could be the small number of channels on the cell. In addition, the cells express numerous different proteins, which can also be specifically used, but are not of interest. In spite of all the selections targeting VGSC, it is still unclear whether an aptamer or clickmer can interact with VGSC.

In order to overcome the low expression of VGSC, another expression model might be helpful. An interesting alternative might be the cell-free expression of membrane proteins[183]. The most common cell-free expression is achieved by adding detergents such as dihexanoylphosphatidylcholine (DHPC) or dodecylmaltoside (DDM)[184]. Experiments with bacteriorhodopsin suggest that an α-helical membrane protein could be transferred to lipids or micelles[185]. However, it is uncertain how well the micelle structures mimic the natural membrane protein environment[161].

Other possibilities are nanodisks or nanolipoprotein particles (NLPs). These are nanoscale particles consisting of amphipathic helical proteins that form a lipid bilayer. The approach was validated by the expression of bacteriorhodopsin, a seven-transmembrane segment protein. The protein was co-purified with histidine-labelled particles, followed by folding into its native conformation[186]. One limitation should be mentioned: the absence of a translocone and transmembrane potential, in the case where the aptamer/clickmer requires a specific binding site. Nevertheless, the expression of VGSC in a cell-free system might allow the selection of an aptamer or clickmer, since the cell-free environment offers far fewer possible targets than a normal cell surface.

The applied cell-SELEX approach could lead to the generation of aptamers/clickmers targeting VGSC and expressed in a cell-free system. The investigation in the present study showed that even with a non-complex target molecule, such as a protein, the selection may not be successful.

In this work it was shown that the multiplexed click-SELEX approach facilitates the selection of nucleotide-modified aptamers that are highly affinity and specific. Nevertheless, it could be further optimized: In addition to EdU, a second alkyne-modified nucleotide, EdA, is commercially available. This second nucleotide should enable DNA functionalisation with different modifications in each sequence. For SOMAmers, the advantages of two modified bases have recently been demonstrated. They enable the generation of aptamers with higher affinities and stability than those with only one modification[91]. The integration of two modifiable nucleotides into the library in combination with the multiplex click-SELEX approach should be investigated, as the chemical diversity increases massively during a SELEX process, which could lead to a higher selection success of clickmers. It could allow the selection of very high affinity clickmers with unique properties.

8. Methods

8.1. Working with nucleic acids

8.1.1. Agarose gel electrophoresis

Usually, 4% agarose gels were used to monitor PCR products or ssDNA. For a 4% agarose gel, 4 g agarose was dissolved in 100 mL TBE-buffer and boiled for several minutes in the microwave. Then ethidium bromide solution was added at a 1:10000 dilution to 40 mL gel and after mixing the gel was poured. The electrophoresis was done in TBE buffer at 150V for 10-12 min. Before loading, the samples were mixed 1:6 with 6x DNA loading buffer. Ethidium bromide is intercalating into the DNA, by which the bands were visualized on a UV transilluminator (VWR) and compared and evaluated to the DNA ultra-low range ladder (Life Technologies).

Table 8.1 Buffer for agarose gel electrophoresis.

TBE buffer	6x DNA loading buffer
90 mM Tris, pH 8.0	60% Glycerol
90 mM Borat	10 mM Tris
2 mM Na_2EDTA	60 mM Na_2EDTA
	0,01% Bromophenol Blue

8.1.2. Polymerase Chain Reaction (PCR)

8.1.2.1. Taq polymerase

The PCR was done in a Mastercycler® Personal (Eppendorf), and in Personal Cycler from (Biometra®). For the amplification of ssDNA and dsDNA, the following cycles were usually performed several times.

Table 8.2 PCR program for Tag polymerase.

Step	T [°C]	t [s]
Denaturation	95	30
Annealing	64	30
Elongation	72	45

Table 8.3 Pipetting scheme for 100µL PCR reaction.

Reagent	Stock concentration	final concentration	V [µL]
Taq reaction buffer	5x	1x	20
$MgCl_2$	25 mM	2 mM	8
dNTP Mix	25 mM	200 µM	0.8
D3 fw primer	100 µM	1 µM	1
D3 rev phosphate primer	100 µM	1 µM	1
Taq Polymerase	5 U/µL	0.5 U/µL	2.5
ddH_2O	-	-	fill up to 100µL

8.1.2.2. PWO polymerase

The PCR was done in a Mastercycler® Personal (Eppendorf), and in Personal Cycler from (Biometra®). For the amplification of ssDNA and dsDNA of the FT2 or OW1 libraries, the following cycles were usually performed several times.

Table 8.4 PCR program for PWO polymerase.

Step	T [°C]	t [s]
Denaturation	95	30
Annealing	62	30
Elongation	72	60

To reduce the risk of by-product formation, the PCR samples were prepared on ice and the thermocycler was preheated to 95°C.

Table 8.5 Pipetting scheme for 100µL PCR reaction.

Reagent	Stock concentration	final concentration	V [µL]
PWO reaction buffer	5x	1x	10
dN*TP Mix	25 mM	200 µM	1
fw primer	100 µM	1 µM	1
rev phosphate primer	100 µM	1 µM	1
PWO Polymerase	2.5 U/µL	0.25 U/µL	1
ddH_2O	-	-	fill up to 100µL

8.1.3. Purification

8.1.3.1. Silica spin columns

If not indicated otherwise, DNA purifications were performed with NucleoSpin® Clean-Up kit (Macherey-Nagel) according to the manufacturers' recommendation. Briefly, two PCRs were pooled and loaded on one column, after washing with NT3 buffer, the PCR product was eluted twice with 25 µL ddH_2O.

8.1.3.2. Phenol-chloroform extraction

To isolate the ssDNA from cells lysate, phenol-chloroform extraction was performed. For this reason, one volume of phenol was added to the sample and vortexed well. After centrifugation at maximum speed for 3 min., the aqueous, upper phase was transferred to a new 2 mL tube. Two volumes of chloroform were added and vortexed. After centrifugation at maximum speed for 3 min., the upper phase was separated in a new 1.5 mL tube. The sample was mixed with 1/10 µL volume of 3M NaOAc pH 5.4, 1 µL glycogen and three volumes of cold (-20°C) abs. EtOH, after inverting several times, the samples were incubated at -80°C for 20 min. Afterward, the samples were centrifuged at 20.000 rcf at 4°C (Eppendorf centrifuge) for 30 min. The supernatant was discarded and the pellet was washed twice with 1/10 µL volume of 70% cold (-20°C) EtOH and centrifuged for 5 min at 4°C and 20.000 rcf. Finally, the pellet was dried at 95°C and dissolved in a desired volume of ddH_2O.

8.1.4. Concentration measurement

The DNA concentration in solution was done by UV absorbance (NanoDrop™ 2000/2000c Spectrophotometers) and for calculation, the Lambert-Beer law ($c=Abs_{260} \cdot d \cdot \varepsilon$) was used, where ε is the absorption coefficient, d is the path length and Abs260 is the absorbance at a given wavelength.

8.1.5. λ-Exonuclease digestion

In order to generate single-stranded DNA (ssDNA), λ-exonuclease digestion was performed. λ-Exonuclease [187] is a highly processive 5' to 3' exodeoxyribonuclease, which digests selectively the 5'-a phosphorylated strand of ds DNA and exhibits low activity on ssDNA and non-phosphorylated DNA. Subsequently, 1/10 volume of the supplied 10x λ-exonuclease reaction buffer was added to the purified PCR product. After addition of 1/100 volume λ-exonuclease (5000 U/mL), the samples were incubated for 20-30 min at 37°C, 1000 rpm. Afterward, the samples were purified with the NucleoSpin® Clean-Up kit using the NTC buffer, according to the manufacturer's recommendation.

8.1.6. TOPO-TA cloning

The enriched libraries of the selections were cloned into vectors and transformed into competent cells with the TOPO™ TA Cloning™ Kit for Subcloning (ThermoFisher) according to the manufacturer's recommendation. A crucial step for the cloning strategy is the use of the Taq polymerase for the amplification, for the addition of a 3' overhang deoxyadenosine. It is also very important to use unmodified primers. Finally, the plasmid was purified with NucleoSpin® Plasmid kit according to the manufacturers' recommendation, and the purified plasmid DNA was sent to GATC-Biotech for Sanger sequencing, which used the M13 reverse primer for the procedure.

8.1.7. Sanger sequencing

An amount of 30 µL plasmid-DNA (30-50 ng/µL) was sent to GATC-Biotech for Sanger sequencing with the M13 reverse primer.

8.1.8. Next-generation sequencing (NGS)

NGS was performed using the Illumina HiSeq1500 platform. The sample was prepared following the protocol from Tolle *et al.*[44]. Briefly, twelve different indices were introduced using PCR to multiplex several samples. Those indices allow loading twelve different samples into one sequencing run. Therefore, the PCR was performed using a set of 24 primers with twelve different indices sequences. The index sequences are listed in. Several SELEX cycles of enriched selections were amplified with these different set of primers and twelve samples were mixed and Illumina adapters were ligated.

Table 8.6 Sequences indices used for NGS.

Index	Sequence	Index	Sequence	Index	Sequence
Index 1	ATCACG	Index 5	ACAGTG	Index 9	GATCAG
Index 2	CGATGT	Index 6	GCCAAT	Index 10	TAGCTT
Index 3	TTAGGC	Index 7	CAGATC	Index 11	GGCTAC
Index 4	TGACCA	Index 8	ACTTGA	Index 12	CTTGTA

For this adaptation, the TruSeq DNA PCR-Free Sample Preparation Kit LT (Ref. 15037063, Illumina) was used. Afterward, the sample was purified via 2% agarose gel and NucleoSpin® Clean-Up kit (Macherey-Nagel) and was eluted in resuspension buffer. For library validation, a quantitative PCR and the quantification using the KAPA library quantification kit (Sigma-Aldrich) was performed prior to the sequencing.

The sequencing was done in collaboration with the group of Prof. Joachim Schultze (LIMES, Bonn) on an Illumina HiSeq 1500 instrument. A seventy-five bp single-end reads were performed. The Data analysis of demultiplexed raw data was done using the COMPAS (COMmonPAtternS) software[46] from AptaIT GmbH (Planegg-Martinsried, Germany).

8.2. Click chemistry

8.2.1. Reaction conditions in solution

A Cu(I)-catalyst solution was prepared. Accordingly, 100 mM sodium ascorbate, 1 mM CuSO4, and 4 mM THPTA were dissolved in a total volume of 100 µL ddH_2O. The click reaction was performed in a total volume of 100 µL. Corresponding, 10 µL of a 10 mM azide solution in DMSO, 10 µL of 10x PBS (pH7), and 80 µL DNA in ddH_2O were mixed and incubated for 60 min at 37°C and 650 rpm. Finally, the samples were purified with the NucleoSpin® Clean-Up kit from Macherey-Nagel (Düren) according to the manufacturer's recommendation.

8.2.2. Determination of reaction yield

The click reaction yield of test-oligos was determined via HPLC-MS as described in section 8.3 and was performed by Julia Siegl. The click reaction yield of libraries cannot be analyzed by HPLC-MS. Instead, the library strands were enzymatically digested to the individual nucleosides. These nucleosides were analyzed by RP-HPLC as described in section 8.3.2.

8.2.3. Enzymatic digestion to nucleosides

To 100 pmol DNA in 45 µL, 10 µL of the supplied 5x S1 nuclease reaction buffer (Life Technologies) was added. After addition of 0.5 µL S1 nuclease (100 U/µL), the samples were incubated for 60 min at 37°C, 800 rpm. Afterwards, 5.7 µL 10x alkaline phosphatase buffer (Promega) and 0.5 µL of alkaline phosphatase (CIAP) (1 U/µL), 0.5 µL snake venom phosphodiesterase I (1 U/µL) and 0.5 µL Benzonase nuclease (250 U/µL) were added, and the samples were incubated for 120 min at 37°C, 800

rpm. Next, the samples were heated to 95°C for 3 min and centrifuged for 3 min at 12000 rcf, 20 µL of the supernatant were used for further analysis by HPLC.

8.3. High-performance liquid chromatography and mass spectrometry (HPLC-MS)

8.3.1. HPLC-MS

The analyses by HPLC-MS were performed by Julia Siegl. Separation and analysis of DNA strands were performed with reversed-phase ion-pairing chromatography. 100 pmol of test-oligo (5'-GCACTGTXCATTCGCG -3') were functionalized as described previously. For separation of DNA (10 pmol), an analytical 1100 series HPLC system with an Agilent Zorbax 2.1x50mm, 5µm (SB-C18) 2.1x100 mm reverse phase column was used. An aqueous solution of 10 mM triethylammonium (TEA) and 100 mM hexafluoroisopropanol (HFIP) was used as mobile phase. A gradient from 0% to 30% acetonitrile in 20 min, 0.5 ml/min flow was used. Mass spectrometry was performed with an HTC Esquire (Brucker). Settings for measuring the samples with the ultrascan in the negative mode are the following: 50 psi, dry gas: 10 l/min, dry temperature: 365°C, SPS: 1000 m/z, ICC: 70000, scan: 500-1500 m/z.

8.3.2. RP-HPLC

For the analysis of the nucleosides after enzymatic digestion, the analytical 1260 Infinity series HPLC system (Agilent Technologies) with NUCLEODUR® C_{18} Pyramid 100 mm, 5 µm reverse phase column was used (Macherey Nagel). As the mobile phase, a gradient of ammonium acetate (NH_4OAc) in water (pH 4.5) and acetonitrile (CAN) was used (flow: 0.3 L/min). The program details are listed in **Table 8.7**.

Table 8.7 HPLC solvent gradient.

Time [min]	Solvent A (NH_4OAc) [%]	Solvent B (ACN) [%]
0	100	0
3	100	0
20	80	20
21	0	100
24	0	100
25	100	0
40	100	0

8.4. Working with eukaryotic cells

8.4.1. Cultivation

Cell lines were cultivated in DMEM (ThermoFisher) supplemented with 10% FCS (Sigma), MEM non-essential amino acids (ThermoFisher), and 1 mM sodium pyruvate (ThermoFisher) at 37°C, 5% CO_2. The cells were cultivated to 70-80% confluency and then they were split every 2-3 days.

8.4.2. Freezing and thawing

An amount of $5 \cdot 10^6$ cells were collected per cryotube. Next, the supernatant was discarded and the cells-pellet was resuspended in 1 mL cryomedia (1:1 cultivating media (see section 8.4.1) and cryoprotective medium (Lonza). The cells were immediately frozen at -80°C, after 24 hours the cells were transferred into the liquid nitrogen tank.

For thawing, one cryovial was thawed in the water bath and the cells were transferred into 10 mL cultivating media, then centrifuged for 5 min at 200 rcf, and finally resuspended in fresh 15 mL media and transferred into a new 75-cm²-flask.

8.4.3. Mycoplasma test

Mycoplasm tests were routinely performed according to the manufacturer's protocol (Minerva Biolabs).

8.4.4. Transfection with DNA plasmids

Plasmid:

pEGFPC1-GluR1Ctail was a gift from Robert Malinow (Addgene plasmid # 32441 ; http://n2t.net/addgene:32441 ; RRID:Addgene_32441)[158].

For plasmid transfection by lipofectamine 2000, 10^6 cells were seeded in 24 well plates 24 hours prior to transfection in standard media (DMEM, 10% FCS, MEM non-essential amino acids, and 1 mM sodium pyruvate). The next day, the media was exchanged with 5 mL of fresh media and the cells were transfected. The transfection mix (**Table 8.8**) was incubated for 15 min at room temperature and then added drop-wise to the cells. After incubation for 5 hours at 37°C and 5% CO_2, the transfection mix was removed and 4 mL of fresh standard media was added. The cells were incubated for 24 hours and then cultivated as described in section 8.4.1.

Table 8.8 Pipetting scheme for DNA transfection.

Transfection mix	
600 ng	Plasmid GluR1
250 µL	Opti-MEM
16 µL	Lipofectamine 2000

8.5. SELEX

8.5.1. Cell-SELEX

8.5.1.1. SELEX targeting $Na_v1.5$-HEK293 and $Na_v1.6$-HEK293 using D3-library

The cells were thawed as described in section 8.4.2. After cultivating for 10 days, the cells were used for the selection. The expression of the VGSCs was confirmed via the patch-clamp technique in the cooperation work with the group or Prof. Heinz Beck (Universität Bonn). In a 12.5cm² or 25cm² tissue culture flask, $0.5 \cdot 10^6$ or $1 \cdot 10^6$ cells were seeded and incubated for 24h at 37°C and 5% CO_2. Then the cells were washed twice with 10mL DMEM and then incubated with the DNA-library in binding buffer (DMEM, 10%FCS, MEM Non-Essential Amino Acids (NEAA), and sodium pyruvate) for 30 min at 37°C and 5% CO_2. Afterward, the supernatant was discard and the cells were washed with DMEM. Finally, the cells were scraped in 500 µL ddH_2O and transferred to a 2 mL tube. The bound DNA sequences were recovered by heating for 5 min to 95°C followed by phenol/chloroform extraction (section 8.1.3.2). The purified DNA was used as the template in the PCR. The detailed selection conditions are summarized in Table 8.9.

Table 8.9 Summary of cell-SELEX targeting $Na_v1.5$-HEK293 and $Na_v1.6$-HEK293 conditions.

SELEX cycle	D3-DNA-library	HEK293 cells	$Na_v1.x$-HEK293 cells	Wash at 37°C, 5%CO_2
1	1 nmol	$6.9 \cdot 10^6$	$4.8 \cdot 10^6$	2x 60 sec
2	500 pmol	2x $6.9 \cdot 10^6$	$4.8 \cdot 10^6$	3x 60 sec
3	200 pmol	2x $6.9 \cdot 10^6$	$4.8 \cdot 10^6$	4x 60 sec
4	100 pmol	3x $6.9 \cdot 10^6$	$4.8 \cdot 10^6$	5x 60 sec
5	100 pmol	3x $6.9 \cdot 10^6$	$4.8 \cdot 10^6$	6x 60 sec
6	100 pmol	3x $6.9 \cdot 10^6$	$4.8 \cdot 10^6$	7x 60 sec
7	100 pmol	3x $6.9 \cdot 10^6$	$4.8 \cdot 10^6$	7x 60 sec
8	100 pmol	4x $6.9 \cdot 10^6$	$4.8 \cdot 10^6$	7x 60 sec
9	100 pmol	5x $6.9 \cdot 10^6$	$4.8 \cdot 10^6$	7x 60 sec
10	100 pmol	5x $6.9 \cdot 10^6$	$4.8 \cdot 10^6$	7x 60 sec

8.5.1.2. SELEX targeting $Na_v1.1$-HEK293 and $Na_v1.2$-HEK293 using D3-library

The selection was carried out in a selection buffer (DMEM, 10% FCS, NEAA, sodium pyruvate, and 1mg/mL salmon sperm DNA). As a target, the $Na_v1.1$-HEK293 or $Na_v1.2$-HEK293 cells were used. The D3-DNA library was incubated with the cells for 30 min at 37°C and 5% CO_2. From the fourth selection cycle onwards, a counter selection step was introduced. The library was incubated first with the HEK293 cells in a T75 flask, followed by further incubations with fresh HEK293 cells, and finally the incubation with $Na_v1.x$-HEK293 cells for 30 min at 37°C and 5% CO_2. Afterward, the supernatant was discard and the cells were washed with DMEM. Finally, the cells were scraped in 500 µL ddH_2O and transferred to a 2 mL tube. The bound DNA sequences were recovered by heating for 5 min to 95°C followed by phenol/chloroform extraction (section 8.1.3.2). The purified DNA was used as the template in the PCR. The detailed selection conditions are summarized in Table 8.10.

Table 8.10 Summary of cell-SELEX targeting $Na_v1.1$-HEK293 and $Na_v1.2$-HEK293 conditions.

SELEX cycle	D3-DNA-library	HEK293 cells in T75 flask	Incubation time for each HEK293[min]	$Na_v1.x$-HEK293 cells in T25 flask	Wash at 37°C, 5%CO_2
1	500 pmol	-	30	$2 \cdot 10^6$	1x 10 sec 1x 120 sec
2	20 pmol	-	30	$4 \cdot 10^6$	1x 10 sec 1x 120 sec
3	20 pmol	-	30	$4 \cdot 10^6$	1x 30 sec 2x 120 sec
4	20 pmol	5x $5 \cdot 10^6$	30	$3 \cdot 10^6$	1x 30 sec 2x 120 sec
5	5 pmol	5x $4 \cdot 10^6$	30	$3 \cdot 10^6$	1x 30 sec 2x 120 sec
6	0.05 pmol	5x $4 \cdot 10^6$	60	$3 \cdot 10^6$	1x 30 sec 2x 120 sec
7	5 fmol	7x $4 \cdot 10^6$	3x 60 4x 30	$3 \cdot 10^6$	1x 30 sec 2x 120 sec
8	1 fmol	7x $4 \cdot 10^6$	3x 60 4x 30	$3 \cdot 10^6$	1x 30 sec 2x 120 sec
9	1 fmol	10x $4 \cdot 10^6$	1x 60 9x 30	$3 \cdot 10^6$	1x 30 sec 2x 120 sec

8.5.1.3. Click–SELEX targeting $Na_v1.6$-HEK293 using TTX-Elution

The selection was carried out in a selection buffer (DMEM, 10% FCS, NEAA, sodium pyruvate, and 1mg/mL salmon sperm DNA). As a target, the $Na_v1.6$-HEK293 cells were used. The FT2 library was functionalized with guanidine azide (11) like in section 8.2.1 and 8.2.2 described. This functionalized library was incubated first with the HEK293 and finally the incubation with $Na_v1.6$-HEK293 cells for 30 min at 37°C and 5% CO_2. Afterward, the supernatant was discard and the cells were washed with DMEM. Finally, the elution buffer (D-PBS with 5mM $MgCl_2$ and 1 mM $CaCl_2$, 20 µM TTX) was added to the cells and incubated for 5 min at RT. The supernatant was transferred to an Amicon 10K column and centrifuged for 5 min at 1400 rpm, the flowthrough was discard and the column was washed 4x 500 µL ddH_2O. Then the column was flipped into a fresh tube and centrifuged for 2 min at 1000 rpm. The recovered solution was used as the template in the PCR. The detailed selection conditions are summarized in Table 8.11.

Table 8.11 Summary conditions of click-SELEX targeting $Na_v1.6$-HEK293.

SELEX cycle	clicked-library	HEK293 cells in T75 flask	$Na_v1.6$-HEK293 cells in T75 flask	Wash at RT
1	500 pmol	$15 \cdot 10^6$	$15 \cdot 10^6$	2x 30 sec
2	150 pmol	$15 \cdot 10^6$	$15 \cdot 10^6$	2x 30 sec
3	50 pmol	2x $15 \cdot 10^6$	$15 \cdot 10^6$	1x 30 sec 1x 5 min 1x 30 sec
4	30 pmol	2x $15 \cdot 10^6$	$15 \cdot 10^6$	1x 30 sec 1x 5 min 1x 30 sec
5	30 pmol	3x $15 \cdot 10^6$	$15 \cdot 10^6$	1x 30 sec 1x 5 min 1x 30 sec
6	25 pmol	3x $15 \cdot 10^6$	$15 \cdot 10^6$	1x 30 sec 1x 5 min 1x 30 sec
7	25 pmol	4x $15 \cdot 10^6$	$15 \cdot 10^6$	1x 30 sec 1x 5 min 1x 30 sec

8.5.1.4. Click–SELEX targeting $Na_v1.6$-HEK293

The selection was carried out in a selection buffer (DMEM, 10% FCS, NEAA, sodium pyruvate, 1mg/mL salmon sperm DNA, and 500 pmol functionalized click-competitor). As a target, the $Na_v1.6$-HEK293 cells were used. The FT2 library and the click-competitor was functionalized with indole azide (**1**) or guanidine azide (**11**) like in section 8.2.1 and 8.2.2 described. This functionalized library was incubated first with the HEK293 and finally the incubation with $Na_v1.6$-HEK293 cells for 30 min at 37°C and 5% CO_2. Afterward, the supernatant was discard and the cells were washed with DMEM. Finally, the cells were scraped in 500 µL ddH_2O and transferred to a 2 mL tube. The bound DNA sequences were recovered by heating for 5 min to 95°C followed by phenol/chloroform extraction (section 8.1.3.2). The purified DNA was used as the template in the PCR. The detailed selection conditions are summarized in Table 8.12.

After eight selection cycle, a branch point was introduced. The enriched library was aliquoted in two samples. With one sample the selection was continued like before, and with the other sample, the target molecule was switched, meaning that for the counter selection step the $Na_v1.6$-HEK293 cells were used and as target cell the HEK293 cells.

Table 8.12 Summary conditions of click-SELEX targeting $Na_v1.6$-HEK293 using guanidine (11) and indole azides (1).

SELEX cycle	clicked-library	HEK293 cells in T75 flask	$Na_v1.6$-HEK293 cells in T25 flask	Incubation time [min]	Wash at RT
1	500 pmol	$10 \cdot 10^6$	$4.5 \cdot 10^6$	30	2x 30 sec
2	40 pmol	$10 \cdot 10^6$	$4.5 \cdot 10^6$	30	1x 30 sec, 1x 3 min, 1x 30 sec
3	80 pmol	$10 \cdot 10^6$	$4.5 \cdot 10^6$	25	1x 30 sec, 1x 3 min, 1x 30 sec
4	50 pmol	$10 \cdot 10^6$	$4.5 \cdot 10^6$	25	1x 30 sec, 1x 3 min, 1x 30 sec
5	50 pmol	$10 \cdot 10^6$	$4.5 \cdot 10^6$	20	1x 30 sec, 1x 3 min, 1x 30 sec
6	50 pmol	$10 \cdot 10^6$	$4.5 \cdot 10^6$	20	1x 30 sec, 1x 5 min, 1x 30 sec
7	50 pmol	$10 \cdot 10^6$	$4.5 \cdot 10^6$	15	1x 30 sec, 1x 5 min, 1x 30 sec
8	30 pmol	$10 \cdot 10^6$	$4.5 \cdot 10^6$	15	1x 30 sec, 1x 5 min, 1x 30 sec
9	20 pmol	$10 \cdot 10^6$	$4.5 \cdot 10^6$	15	1x 30 sec, 1x 5 min, 2x 30 sec
10	20 pmol	$10 \cdot 10^6$	$4.5 \cdot 10^6$	15	1x 30 sec, 1x 5 min, 2x 30 sec
11	20 pmol	$10 \cdot 10^6$	$4.5 \cdot 10^6$	15	1x 30 sec, 1x 5 min, 2x 30 sec
12	20 pmol	$10 \cdot 10^6$	$4.5 \cdot 10^6$	15	1x 30 sec, 1x 5 min, 2x 30 sec

8.5.1.5. Click–SELEX targeting GluR1-HEK293

The selection was carried out in a selection buffer (DMEM, 10% FCS, 1mg/mL salmon sperm DNA, and 500 pmol functionalized click-competitor). As a target, the GluR1-HEK293 cells were used. The OW1 library and the click-competitor was functionalized with indole azide (**1**), benzyl azide (**2**), or guanidine azide (**11**) like in section 8.2.1 and 8.2.2 described. This functionalized library was incubated first with the HEK293 and followed by the incubation with GluR1-HEK293 cells for 30 min at 37°C and 5% CO_2. Afterward, the supernatant was discard and the cells were washed with DMEM. Finally, the cells were scraped in 500 µL ddH_2O and transferred to a 2 mL tube. The bound sequences were recovered by heating for 5 min to 95°C followed by phenol/chloroform extraction (section 8.1.3.2). The purified DNA was used as the template in the PCR. The detailed selection conditions are summarized in Table 8.13 and Table 8.14.

Table 8.13 Summary conditions of click-SELEX targeting GluR1-HEK293 using indole azides (1).

SELEX cycle	clicked-library	HEK293 cells in T75 flask	GluR1-HEK293 cells in T25 flask	Wash at RT
1	500 pmol	-	$2.5 \cdot 10^6$	2x 30 sec
2	70 pmol	-	$2.5 \cdot 10^6$	2x 60 sec
3	30 pmol	$5 \cdot 10^6$	$2.5 \cdot 10^6$	2x 60 sec
4	30 pmol	3x $5 \cdot 10^6$	$2.5 \cdot 10^6$	2x 60 sec

Table 8.14 Summary conditions of click-SELEX targeting GluR1-HEK293 using benzyl azide (2) and guanidine (11).

SELEX cycle	clicked-library	HEK293 cells in T75 flask	GluR1-HEK293 cells in T25 flask	Wash at RT
1	500 pmol	$5 \cdot 10^6$	$2.5 \cdot 10^6$	2x 30 sec
2	60 pmol	$5 \cdot 10^6$	$2.5 \cdot 10^6$	2x 60 sec
3	30 pmol	2x $5 \cdot 10^6$	$2.5 \cdot 10^6$	2x 60 sec
4	30 pmol	2x $5 \cdot 10^6$	$2.5 \cdot 10^6$	2x 60 sec
5	30 pmol	3x $5 \cdot 10^6$	$2.5 \cdot 10^6$	2x 60 sec

8.5.2. Click-SELEX targeting cycle3-GFP

8.5.2.1. Beads preparation for recombinant proteins with His-Tag

For immobilization of the recombinant proteins, Dynabeads® His-Tag Isolation and Pulldown were used. These beads are functionalized with Co^{2+}-ions by which proteins with a His-Tag can be caught. Accordingly, 25 µL beads were washed three times with 500 µL washing buffer (1xPBS, 1 mg/mL BSA, 0.1% TWEEN 20) and resuspended in 500 µL of 3.5 µM protein solution in PBS. After, incubation for 30 min at 37°C and 800 rpm the protein-beads were washed three times with 500 µL and then resuspended in 500 µL washing buffer. They were stored at 4°C up to a maximum of two weeks.

8.5.2.2. SELEX targeting C3-GFP

The selections were performed following the protocol in the previous work[29]. Briefly, the SELEX buffer (SB1) contained D-PBS (Sigma D1283: NaCl (137.9 mM), Na_2HPO_4 (8.1 mM), KCl (2.7 mM), KH_2PO_4 (1.5 mM), $CaCl_2$ (0.9 mM), $MgCl_2$ (0.5 mM), pH 5.3), 1 mg/mL bovine serum albumin (BSA), 0.1% TWEEN 20, and 0.1 mg/mL UltraPure™ salmon sperm DNA (ThermoFisher). The target protein, C3-GFP was immobilized by His6 tag on magnetic beads, as described in section 8.5.2.1. After the incubation of the functionalized library with C3-GFP loaded magnetic beads for 30 min at 37°C, 800 rpm, the beads were washed three times with 200 µL of 1x SB1. The bound sequences were eluted by the addition of 100 µL of 300 mM imidazole solution, and incubating for 15 min at 37°C, 800 rpm. The supernatant was used as a template for the 800 µL PCR reaction. The PCR-product was visualized on a 4% agarose gel. After purification via NucleoSpin® Clean-Up kit from Macherey-Nagel (Düren) according to the manufacturer's recommendation, lambda exonuclease digestion (section 8.1.5) was performed to produce single-stranded DNA (ssDNA). For this purpose, the 180 µL of the purified PCR product was mixed with 20 µL of the supplied 10x λ-exonuclease

reaction buffer and 3 µL λ-exonuclease (5000 U/mL) were added. After incubating for 20 min at 37°C, 1000 rpm, the samples were purified with the NucleoSpin® Clean-Up kit using the NTC buffer, according to the manufacturer's recommendation. Eventually, the click reaction of the corresponding azide was performed as described in section 8.2.1, and the functionalized library was used for the next selection cycle. The selection details are listed in Table 8.15.

Table 8.15 Overview of the SELEX conditions targeting C3-GFP.

SELEX cycle	Unmodified beads [µL]	C3-GFP beads [µL]	Wash at 37°C, 800 rpm	Wash Vol [µL]	Competitor [pmol]
1	-	50	3x 30 sec	200	-
2	-	50	3x 30 sec	200	-
3	50	50	1x 30 sec 1x 5 min 1x 30 sec	200	-
4	50	35	1x 30 sec 1x 5 min 1x 30 sec	200	-
5	50	35	1x 30 sec 1x 5 min 1x 30 sec	200	100
6	50	25	3x 5 min	200	250
7	50	15	3x 5 min	500	500
8	50	5	3x 5 min	750	500
9	50	5	1x 30 sec 3x 5 min 1x 30 sec	1000	500
10	50	5	2x 30 sec 3x 5 min 1x 30 sec	1000	600

8.5.2.3. Multiplexed click-SELEX targeting C3-GFP

The multiplexed click-selection were performed like the click selection targeting C3-GFP (section 8.5.2.2), with slight changes. The library was aliquoted in five samples, and each sample was functionalized with another azide-containing compound. After the purification, the functionalized libraries were mixing all together. This combined functionalized library was supplied to the incubation with the target molecule for 30 min at 37°C, and 800 rpm. Afterward, the beads were washed and the elution solution was added. The further steps were performed like described in section 8.5.2.2.

After performing eight selection cycle, the enriched library was analyzed regarding the binding towards the C3-GFP beads. For this reason, the DNA of the eighth selection cycle was amplified and digested to ssDNA. This ssDNA was aliquoted in six samples and functionalized with the used azides for the selection. One sample was used unfunctionalized

for the analysis. Each functionalization was analyzed for itself for binding. After the binding to C3-GFP was confirmed, the deconvolution cycle was performed, meaning for each functionalization one selection cycle was performed analogously to the 8th selection cycle separately. Briefly, the functionalized library was incubated first with 50 µL unmodified beads at 37°C, 800 rpm, followed by the incubation with 5 µL C3-GFP modified beads for 30 min at 37°C, 800 rpm. Afterward, the beads were washed and the bound sequences were eluted by using 300mM imidazole (100µL) solution for 15 min at 37°C, 800 rpm. The recovered DNA was used as a template for PCR.

8.5.3. SELEX targeting peptide-$Na_v1.6$

8.5.3.1. Beads preparation for peptide $Na_v1.6$

The peptide $Na_v1.6$ was immobilized via the biotin at the N-terminus on streptavidin-coated magnetic beads (Dynabeads^{TM} M-280 streptavidin). Accordingly, 500 µL beads were washed three times with 500 µL washing buffer (PBS) and resuspended in 500 µL of 2 nmol (3.9 µM) peptide $Na_v1.6$ in PBS. After incubation for 30 min at room temperature and 800 rpm, the beads were washed three times with 500 µL washing buffer. The beads were stored at 4°C up to a maximum of one week.

8.5.3.2. Multiplexed click-SELEX targeting peptide $Na_v1.6$

The multiplexed click-SELEX targeting peptide $Na_v1.6$ was performed like the multiplexed click-SELEX targeting C3-GFP (section 8.5.2.3) with slight changes. Briefly, the selection was performed in a selection buffer SB2 (D-PBS, 1 mM $MgCl_2$, 1 mg/mL BSA, pH 7.4). The selection details are listed in Table 8.16.

Table 8.16 Overview of the SELEX conditions targeting peptide $Na_v1.6$.

SELEX cycle	streptavidin beads [µL]	peptide $Na_v1.6$ beads [µL]	Wash at 37°C, 800 rpm	Wash Vol [µL]	Competitor of each functionalization [pmol]
1	50	50	3x 30 sec	200	100
2	50	40	3x 30 sec	200	100
3	100	40	1x 30 sec 1x 5 min 1x 30 sec	200	100
4	100	30	1x 30 sec 1x 5 min 1x 30 sec	200	100
5	150	30	1x 30 sec 2x 5 min	200	100
6	150	30	1x 30 sec 2x 5 min	200	100
7	200	20	3x 5 min	200	100
8	200	15	3x 5 min	500	100

8.5.4. SELEX targeting streptavidin

The multiplexed click-SELEX targeting streptavidin was performed like the multiplexed click-SELEX peptide $Na_v1.6$ (section 8.5.3.2). The selection details are listed in Table 8.17.

Table 8.17 Overview of the SELEX conditions targeting streptavidin.

SELEX cycle	streptavidin beads [µL]	Wash at 37°C, 800 rpm	Wash Vol [µL]	Competitor of each functionalization [pmol]
1	50	3x 30 sec	200	100
2	50	3x 30 sec	200	100
3	35	1x 30 sec 1x 5 min 1x 30 sec	200	100
4	25	1x 30 sec 1x 5 min 1x 30 sec	200	100
5	20	1x 30 sec 2x 5 min	200	100
6	5	3x 5 min	200	100
7	5	3x 5 min	200	100
8	5	3x 5 min	500	100

8.6. Interaction analyses

8.6.1. Kinasation

For the kinasation of ssDNA, the T4 polynucleotide kinase (PNK) with the correspondent T4 PNK buffer and γ-^{32}P-ATP was used. The kinasation mixture (**Table 8.18**) was incubated for 60 min at 37°C and 300 rpm. The labeled DNA was passed through a G25 spin column (GE Healthcare) to remove the unreacted γ-^{32}P-ATP.

The click-DNA was functionalized with the appropriate azide-containing compound and purified with the NucleoSpin® Clean-Up kit from Macherey-Nagel (Düren) according to the manufacturer's recommendation.

Table 8.18 Pipetting scheme for one ^{32}P-kinasation reaction.

Reagent	Stock concentration	Final concentration	Volume [µL]
ssDNA	1 µM	10 pmol	10
ddH2O	-	-	5
T4 PNK reaction buffer	10x	1x	2
γ-32P-ATP	10 µCi/µL	10 µCi	1
T4 PNK	10 U/µL	20 U	2

8.6.2. Cell binding assay using Cherenkov protocol

In this study, liquid scintillation counting was used. It is a technique to measure the activity of a radioactive sample, which relies on the Cherenkov radiation. For such a Cherenkov binding assay, the aptamer was labeled with γ^{32}P and incubated with the target cells, followed by washing steps and

recovery of the cells. The radioactivity on the cells indicates the percentage of aptamer bound to or internalized into the cells. The assay sensitivity is much higher when compared to other validation methods such as flow cytometry.

The cells were seeded in a 25cm² tissue culture flask and cultivated under standard conditions for 24 hours. The cells were washed twice with 10 mL washing buffer (DMEM) and incubated for 30 min at 37°C with γ-^{32}P-DNA in 1mL standard media, containing 1 mg/mL Salmon Sperm DNA. The incubation buffer was transferred to 1.5 mL tube as fraction I. Then the cells were washed three times with 1 mL washing buffer, and all three fractions were collected in separate 1.5 mL tubes (fraction II, III and IV). Finally, the cells were detached by adding 500 µL trypsin/EDTA, and the tissue culture flask was washed once with 500 µL DMEM. Both volumes were pulled together (fraction V). Using the Cherenkov protocol, the radioactivity was measured on the Liquid scintillation counter WinSpectral (Perkin Elmer). The percentage of bound γ-^{32}P-DNA was calculated with the following formula:

$$\%\ \text{bound DNA} = \frac{\text{fraction V}}{\sum all\ fractions} \cdot 100$$

8.6.3. Flow cytometry

The binding interaction of proteins and peptide immobilized on magnetic beads were measured using a FACSCanto II (BD Biosciences). 5 µL of the respective magnetic beads were incubated for 30 min at 37°C, 800 rpm, with the Cy5-labeled and functionalized DNA in the respective SELEX buffer in a total volume of 20 µL. Afterward, the beads were washed twice with 200 µL and resuspended in 200 µL SELEX buffer. 50000 events were measured in the flow cytometer and the mean Cy5 fluorescence intensity (MFI) was analyzed by using the FlowJo software. The calculation and visualization of the experiments were performed with Prims 5.0f (GraphPad Software).

8.6.4. Surface plasmon resonance spectroscopy (SPR)

The surface plasmon resonance spectroscopy measurements were performed in the Biacore 3000. The clickmers targeting C3-GFP (I10, F8, F20, and B33) were immobilized via biotin on streptavidin-coated SPR sensor chip (SAD500L - Xantec) according to the manufacturer's recommendation. The C3-GFP was used as an analyte in different concentrations (1000 nM, 360 nM, 100 nM, 36 nM, 10 nM, 3.6 nM, 1 nM) and was injected for 120-225 s at a flow of 40µL/min. The dissociation time was 300 s, afterward, 5mM EDTA solution was injected to ensure a total dissociation of the protein. The measurements were performed at two different temperatures, 25°C and 37°C. The binding buffer (SB1) was prepared always fresh but without salmon sperm DNA (**section 8.5.2.2**). To reduce the unspecific binding of the C3-GFP to the sensor chip matrix, dextran sulfate (0.01 mg/mL at 25°C and 0.05 mg/mL at 37°C) was added to the running buffer.

The clickmer/aptamers targeting streptavidin (B1, G1, and Aptamer 33) were immobilized according to the manufacturer's recommendation on CMDP sensor chip from Xantec. Streptavidin in different concentrations (360 nM, 100 nM, 36 nM, 10 nM, 3.6 nM, 1 nM) was injected for 120 s at a flow of 40µL/min. The dissociation time was 300 s, afterward, regeneration solution (5 mM EDTA, 0.1% SDS, 0.5 M NaCl, 25 mM NaOH) was injected to ensure a total dissociation of the protein.

The analyses were performed with the software BIAevaluation 4.1 (Biacore). The data were fitted by using the 1:1 Langmuir model. The visualization of the experiments was performed with Prims 5.0f (GraphPad Software).

9. Materials

9.1. Reagents and chemicals

Table 9.1 Reagents and chemicals.

Reagent	Supplier
10x DPBS, with Mg/Ca	Sigma Aldrich
4',6-diamidino-2-phenylindole (DAPI)	Sigma Aldrich
Acetonitrile	Fluka
Agarose	Merck / Genaxxon
Agarose	Sigma Aldrich
Ammonium acetate	Gruessing
Ampicillin sodium salt	AppliChem
Benzonase	Sigma Aldrich
Bovine serum albumin (BSA, nuclease and protease free)	Calbiochem
Bromophenol blue	Merck
Chloroform	AppliChem
DMEM	Gibco
DMSO	Sigma Aldrich
dNTPs	Larova, Genaxxon
DPBS	Gibco
Dynabeads His-Tag Isolation and Pulldown	ThermoFisherScientific
Dynabeads M-280 streptavidin	TermoFisherScientific
EdU	Base click
EdUTP	BaseClick
Ethanol abs.	Sigma Aldrich
Ethidium bromide	Roth
FCS	SigmaAldrich
Imidazole	AppliChem
Lambda Exonuclease	ThermoFisherScientific
Magnesium chloride-hexahydrate	AppliChem
N,N,N',N'-tetramethylethylendiamide (TEMED)	Roth
Nuclease S1	ThermoFisherScientific
Phenol	Roth
Potassium chloride (KCl)	Gruessing
PWO DNA polymerase	Genaxxon
RNase T/A1	ThermoFisherScientific
Sodium acetate	Gruessing
Sodium ascorbate	Gruessing
Sodium Ethylendiamintetraacetic acid (EDTA)	AppliChem
SPR sensor chip CMDP	Xantec
SPR sensor chip SAD500L	Xantec
streptavidin	Sigma Aldrich

T4 polynucleotide kinase (PNK)	NEB
Tag polymerase	Promega
THPTA	BaseClick
Tris	Roth
Trypsin [0.05%]/EDTA [0.5M]	Gibco
TWEEN-20	Calbiochem
Ultra low ladder	ThermoFisherScientific
γ-^{32}P-ATP	Perkin Elmer

9.2. Commercial kits

Table 9.2 Commercial kits.

Application	Kit	Supplier
Adapter ligation	TruSeq DANN PCR-Free (LT)	Illumina
PCR purification	NucleoSpin Gel and PCR Clean-Up	Macherey-Nagel
Plasmid purification	NucleoSpin Plasmid	Macherey-Nagel
TOPO TA cloning	TOPO TA cloning kit for sequencing	Life Technologies
Mycoplasma test	VenorGeM Classic Mycoplasma PCR Detection Kit	Promega

9.3. Equipment

Table 9.3 Equipment.

Equipment	Manufacturer
Agarose chamber equipment	In house construction
Analytic balance	Sartorius
Autoclave	Systec
Cell scraper	TPP
Centrifuges	Eppendorf
Culture dishes, flask, plates	Sarstedt
FACS Canto II	BD
G25 columns	GE Healthcare
Hood (bacteria)	Antares
Hood (eukaryotic cell lines)	Hera
HPLC 1100 series, C18 Hypersil ODS	Agilent
Incubator (cell culture)	Hera
Liquid Scintillation counter	PerkinElmer
LSM 710 confocal laser scanning microscope	Zeiss
Magnetic rack	Life Technologies
Microwave	Bosch
Nanodrop 2000c Spectrophotometer	Thermo Scientific
PCR Mastercycler personal	Eppendorf
PCR Thermocycler	Biometra
pH meter	Inolab
pH Paper	Macherey-Nagel
Phosphorimager FLA-3000	Fujifilm
Pipet tips	Sarstedt
Pipets	Eppendorf
Plastic consumables	Sarstedt
Radioactive protection shield	Nalgene

Reaction tubes (2 ml, 1.5 ml, 0.5 ml)	Sarstedt
Thermomixer	Eppendorf
UV Transilluminator	VWR
Vortex mixer	Neolab
Water bath	GFL
Water purification system	TKA/Thermo Scientific/Merck Millipore

9.4. Buffers and solutions

Table 9.4 Buffers and solutions.

Name	Composition	Concentration
Agarose plates with ampicillin (250 mL)	Agarose	3.8 g
	LB broth	5 g
	Ampicillin	250 µL
CuAAC catalyst solution	THPTA	4 mM
	$CuSO_4$	1 mM
	Sodium ascorbate	25 mM
DNA loading buffer (6x)	Glycerol	60%
	Tris	10 mM
	Na_2EDTA (pH 8.0)	60 mM
	Bromophenol blue	0.03%
D-PBS (pH 5.3)	NaCl	137.9 mM
	Na_2HPO_4	8.1 mM
	KCl	2.7 mM
	KH_2PO_4	1.5 mM
	$CaCl_2$	0.9 mM
	$MgCl_2$	0.5 mM
D-PBS (pH 7.4)	NaCl	137.9 mM
	Na_2HPO_4	8.1 mM
	KCl	2.7 mM
	KH_2PO_4	1.5 mM
LB medium with ampicillin (500 mL)	LB broth	10 g
	Ampicillin	100 mg/mL
SELEX buffer SB1	D-PBS (pH5.3)	1x
	BSA	0.1%
	TWEEN-20	0.1%
	Salmon-Sperm	0.1 mg/mL
SELEX buffer SB2	D-PBS (pH7.4)	1x
	BSA	0.1%
	TWEEN-20	0.1%
TBE buffer	Tris	90 mM
	Boric acid	90 mM
	Na_2EDTA (pH8.0)	2 mM

9.5. Nucleic acids

All nucleic acids were purchased HPLC-purified and lyophilized from Ella Biotech GmbH (Martinsried).

Table 9.5 Nucleic acids.

Oligo	Sequence [5'- … -3']
D3-library	GCTGTGTGACTCCTGCAA -N43- GCAGCTGTATCTTGTCTCC
D3-forward primer	GCTGTGTGACTCCTGCAA
D3-reverse primer	GGAGACAAGATACAGCTGC
FT2-library	CACGACGCAAGGGACCACAGG -N42- CAGCACGACACCGCAGAGGCA (N= dA:dC:dG:EdU = 1:1:1:1)
FT2-forward primer	CACGACGCAAGGGACCACAGG
FT2-forward primer_Cy5	Cy5 – CACGACGCAAGGGACCACAGG
FT2-reverse primer	Phosphate – TGCCTCTGCGGTGTCGTGCTG
click-competitor	-N42-A-
OW1-library	AGCCACGGAAGAACCAGA -N44- GCAGAAGCGACAGCAACA (N= dA:dC:dG:EdU = 1:1:1:1)
OW1_forward primer	AGCCACGGAAGAACCAGA
OW1_forward primer_Cy5	Cy5 - AGCCACGGAAGAACCAGA
OW1_reverse primer	Phosphate - TGTTGCTGTCGCTTCTGC
I10	AGCCACGGAAGAACCAGACGCGXAGGXACCCGGCXXXGAAXAXGXAGGGGACCXA GAGAACAGCAGAAGCGACAGCAACA
B33	AGCCACGGAAGAACCAGAGGCGXACXXXGXCXCACCXACACAXXCXAACCACCAC XACGCCAGCAGAAGCGACAGCAACA
B15	AGCCACGGAAGAACCAGAAAGGGXGAGCAAAACCGGGCGGXGXXCCXAGGCXXXC ACGGCGGGCAGAAGCGACAGCAACA
B10	AGCCACGGAAGAACCAGACCXCCXACCCAXXXXACAACCCCXAGXACCCCXAXGG CACACACGCAGAAGCGACAGCAACA
F8	AGCCACGGAAGAACCAGAXCGGGCCGGAGCGAGGXAXGAXGCCAXCCXXCACAGC XCCAGCAGAAGCGACAGCAACA
F20	AGCCACGGAAGAACCAGACCGCCCGCGXAXGAXGCCGXCXXACGGGCAGCCGXAA CCACAACGCAGAAGCGACAGCAACA
F20sc	AGCCACGGAAGAACCAGAGXCGCGCXCCAGACGCXAACCGCCAXACACAGCXGCC GXGXCGAGCAGAAGCGACAGCAACA
C1	AGCCACGGAAGAACCAGAAGCACCATAACGTGGCGTCGGCGACCTCACTCCTCCA TGCCCCAGCAGAAGCGACAGCAACA
Sa	GCTGTGTGACTCCTGCAATGGGGGGTTGGGGAGTTGGGGATCCTTTGGTAGAGAT TGAGTTGCAGCTGTATCTTGTCTCC
392	GCTGTGTGACTCCTGCAACCCCCCGCGATTGGATTTGTGTTTGCTTTTCTCGTAC TCATGGGCAGCTGTATCTTGTCTCC
595	GCTGTGTGACTCCTGCAACCCGATTAGTTCCTCCCCGTTTGTGCTCGAGTTATTT TCCTGGGCAGCTGTATCTTGTCTCC
654	GCTGTGTGACTCCTGCAACCCGGGCGTTCTTGTTACTTTTGGATAGTGGTAGTTT TTCTGGGCAGCTGTATCTTGTCTCC
448	GCTGTGTGACTCCTGCAACCCCGAACTGTGATACGACGCTTTTTACCCTTTCTCT GTGTGGGCAGCTGTATCTTGTCTCC
545	GCTGTGTGACTCCTGCAATCTCCTCACAACAGCGAGCTGGAGCTTAGACCGGGTT TTAGGGGCAGCTGTATCTTGTCTCC
523	GCTGTGTGACTCCTGCAATAGTTAGGAACAGCGTCAAAAGCCCCCACTCGTCCCC

	CTTTTGGCAGCTGTATCTTGTCTCC
GN1	CACGACGCAAGGGACCACAGGCGGXGAAGXCAACAGGCGXAXXAGXACCXCAXAC AAAGAXAGCAGCACGACACCGCAGAGGCA
I1	CACGACGCAAGGGACCACAGGGCGGXACGGXXXGACCGXCCGAAGAGCXXCAAGC GAXXGAGGCAGCACGACACCGCAGAGGCA
Ben1	CACGACGCAAGGGACCACAGGGGXGGAGGXGGGXXXGAGAGAGAGGGGXGGXAGG AXGGGGXXCAGCACGACACCGCAGAGGCA
P2	CACGACGCAAGGGACCACAGGGGGXCAXGCCGGGXXGGAGXXXAAGGGGXXGGGG CAGGACCCCAGCACGACACCGCAGAGGCA
P2sc	CACGACGCAAGGGACCACAGGGXAGAGCCGGXCAGCXGGAGXGCGCGGXCGGXAX GGXAGGXGCAGCACGACACCGCAGAGGCA
G1	CACGACGCAAGGGACCACAGGTTTTGCGAACGCGGGTAGGCGCACCCTTCGCACA AACGTCCCCAGCACGACACCGCAGAGGCA
G1 sc	CACGACGCAAGGGACCACAGGGCGGCXCGXXAGCXGGCCACACCAGGCGACGCAX XCACCXXACAGCACGACACCGCAGAGGCA
B1	CACGACGCAAGGGACCACAGGCCAGGXXCGGXAXAXXCGGXCGCAGAXACGAACC AGGGXAXACAGCACGACACCGCAGAGGCA
Aptamer 33	ATACCAGCTTATTCAATTACAATGTCGCTCTCCGCCGCAGGAGCATTGTCTGTCT TTATGCTTCTCTTTTTTGTTGCAGATAGTAAGTGCAATCT

(X=EdU)

9.6. Proteins

Cycle 3 GFP (C3-GFP), 13105-S07E, Life Technologies

MSKGEELFTGVVPILVELDGDVNGHKFSVSGEGEGDATYGKLTLKFICTTGKLPVPWPTLVTTFSYGV
QCFSRYPDHMKRHDFFKSAMPEGYVQERTISFKDDGNYKTRAEVKFEGDTLVNRIELKGIDFKEDGNI
LGHKLEYNYNSHNVYITADKQKNGIKANFKIRHNIEDGSVQLADHYQQNTPIGDGPVLLPDNHYLSTQ
SALSKDPNEKRDHMVLLEFVTAAGITHGMDELYK

Monomeric E-GFP (mE-GFP), kindly provided by Volkmar Fieberg (Caesar, Bonn)

MGSHHHHHHENLYFQGSMVSKGEELFTGVVPILVELDGDVNGHKFSVSGEGEGDATYGKLTLKFICTT
GKLPVPWPTLVTTLTYGVQCFSRPDHMKQHDFFKSAMPEGYVQERTIFFKDDGNYKTRAEVKFEGDTL
VNRIELKGIDFKEDGNILGHKLEYNYNSHNVYIMADKQKNGIKVNFKIRHNIEDGSVQLADHYQQNTP
IGDGPVLLPDNHYLSTQSKLSKDPNEKRDHMVLLEFVTAAGITLGMDELYK

9.7. Peptide

Peptide Nav1.6, Bachem Distribution Services GmbH

Biotinyl-Met-Glu-Ser-Leu-Ala-Asp-Val-Glu-Gly-Leu-OH trifluoroacetate salt (purity > 95%)

9.8. Software

Table 9.6 Software.

Software	Manufacture
Adobe Illustrator	Adobe Systems
AIDA Biopackage	Raytest
ChemDraw	PerkinElmer
GraphPad Prism	GraphPad Software
Microsoft office package	Microsoft
Bioevaluation	Biacore
FlowJo	BD

10. Appendix

Supp. table 1 DNA sequences selected in cell-SELEX targeting HEK293 of the selectioncycle eight. Die Sequenzierung wurde mit Sanger Sequencing durchgeführt.

The nomenclature of the sequences was random.

Name	Random region
H8-1	CTGTCCCCCACTATGCAAAGAGGAGCCTCACACCTCTACGATGG
H8-2	CCCCGCGGCATACCGGAAATAATGGGTCTGAGTTTCTTTTTGG
H8-3	CCTCGAAGAAGGCGTCCCCCACTCATTCCTCCTTATACGAGG
H8-4	CGTGGGTGGGTTTATATTCGGTGGTGGTGGGGGTGGTACTGTT
H8-5	CGCGAGTAGTGATCCAATCGTCCCCCACTCATTCCCACTACTA
H8-6	CGAGACGGATCTTTAGTCCCCCACTCGCCCCATCCGTTCGAGG
H8-7	CGGAAAAAGGAAATGGTCGGCATGTCGTAAGGTTCTGTG
H8-8	TGCGTTTTCCTTGGGGTTCAGGGTAGGATGGGGGTGGAGGTGG
H8-9	CGGCAATTATTCGTCCCCCACTCCTACCTTCTTTATTGCCCGT
H8-10	TCCTATAACGTCCCCCACTGAACTAAAAAAGTAGGAGTTGGTG
H8-11	CGTGGGTGGGTTTATTTNNGGGGGGGGGGGGGGGGGACTGGT
H8-12	CGCATTTGGGTGGGATTGTTATTTGGGTCGGGATTGGCAGTT
H8-13	AGGTGTCACGGGCAGCCGTATCTGTCTCCNANGGAGAATTCCA GCACACTGGCGGCCGTTACTAGNGGANCCGAG
H8-14	CGGTTGCGGGCCGGCTAATCGCTCTGATTTGGTTCNTTTGGGG
H8-15	CCCGGCGTCGCGTTGGGTTATACCCATGATACTTTCTCACTGG
H8-16	TGAATACCTACCTGTCCCCCACTCCTACCTGTGCGTGTTCATG
H8-17	CAGTAGTGCCAAGCATTCGTCCCCCACTTTCTTTAGTGCTTGG
H8-18	GCGGAAAGTATGCTAACCCTAGGCGAGTGGTAGAGTTGTGAGG
H8-19	CTAGAGAGCTGGCCCGGTACCGTCCCCCACTATCATTACTGTG
H8-20	GCTATGGCCCTTGTCCCCCACTACGCCACCAGAGTTTGATGAG
H8-21	GGGAAGCAGTAAGATGTCGCGTCCCCCACTAATTTCGACTCGT
H8-22	GCAGACTGCCGTGTTCTTGTCCCCCACTTTCGTGCACTCG
H8-23	TCTCGAGGGTTGTTCCGTCCCCCACTCATATGCAAATCTCGGG

Supp. table 2 DNA sequences selected in cell-SELEX targeting HEK293 of the 12th selectioncycle. Die Sequenzierung wurde mit Sanger Sequencing durchgeführt.

The nomenclature of the sequences was random.

Name	Random region
H12-1	CGTGGGTGGGTTTATATTCGGTGGTGGTGGGGGTGGTACTGTT
H12-2	CGTGGGTGGGTTTATATTCGGTGGTGGTGGGGGTGGTACTGTT
H12-3	CGTGGGTGGGTTTATATTCGGTGGTGGTGGGGGTGGTACTGTT
H12-4	CGTGGGCGGGTTTATATTTGGTGGTGGTGGGGGTGGTACTGTT
H12-5	TCGGTTCCTGTTAGTTCGCTGGTGGTTGGTGGGGTGGCGGATG
H12-6	CGAGACGGATCTTTAGTCCCCCACTCGCCCCATCCGTTCGAGG
H12-7	TGCGTTTTCCTTGGGGTTTAGGGTAGGATGGGGGTGGAGGTGG
H12-8	TGGGGGGTTGGGGAGTTGGGGATCCTTTGGTAGAGATTGAGTT
H12-9	CGTGGGCGGGTTTATATTTGGTGGTGGTGGGGGTGGTACTGTT
H12-10	CGTGGGTGGGTTTATATTCGGTGGTGGTGGGGGTGGTACTGTT
H12-11	CGTGGGTGGGTTTATATTCGGTGGTGGTGGGGGTGGTACTGTT

H12-13	CGGGGTTAGATCCGTCCCCCACTAAACTTCTAACCCTAGGTCA
H12-14	TCGGTTCCTGTTAATTCGCTGGTGGTTGGTGGGGTGGCGGATG
H12-15	CGTGGGCGGGTTTATATTTGGTGGTGGTGGGGGTGGTACTGTT
H12-16	GGCCTTCAGTTGTTGAGAGCCTGTCCCCCACTTGTTACTCTCA
H12-17	CGTGGGCGGGTTTTATTTGGTGGTGGTGGGGGTGGTACTGTT
H12-18	CGTGGGTGGGTTTATATTCGGTGGTGGTGGGGGTGGTACTGTT
H12-19	GGTCTCCCGTCCCCCACTACAACCTCTCCTCAAGGTGTCACGG
H12-20	CGTGGGTGGGTTTATATTCGGTGGTGGTGGGGGTGGTACTGTT
H12-21	GTGAATTGTAATACGACTCNCTATAGGGCGAATTGGGCCCTNTA
H12-22	CCTCGAAGAAGGCGTCCCCCACTCATTCCTCCTTATACGAGG

Supp. table 3 DNA sequences selected in cell-SELEX targeting Nav1.5-HEK293. Listed are the sequence and their frequency according to the selections.

The nomenclature of the sequences was random.

Name	**Random region**
Na1.5-R8-1	CCTCGAAGAAGGCGTCCCCCACTCATTCCTCCCTATACGAGG
Na1.5-R8-2	GCTGAGTTCCTCTCCTCCGAAGTGTTGTGCGGTTTAATCGTGG
Na1.5-R8-3	CCTCGAAGAAGGCGTCCCCCACTCATTCCTCCTTATACGAGG
Na1.5-R8-4	TGGGGGGTTGGGGAGTTGGGGATCCTTTGGTAGAGATTGAGTT
Na1.5-R8-5	TGGGGGGTTGGGGAGTTGGGGATCCTTTGGTAGAGATTGAGTA
Na1.5-R8-6	TGGGGGGTTGGGGAGTTGGGGATCCTTTGGTAGAGATTGAGTT
Na1.5-R8-7	CGGGGTTAGATCCGTCCCCCACTAAACTTCTAACCCTAGGTCA
Na1.5-R8-8	TGGGGGGTTGGGGAGTTGGGGATCCTTTGGTAGAGATTGAGTA
Na1.5-R8-9	CCTCGAAGAAGGCGTCCCCCACTCATTCCTCCTTATACGAGG
Na1.5-R8-10	CCTCGAAGAAGGCGTCCCCCACTCACTCCTCCTTATACGAGG
Na1.5-R8-11	TGGAGGGTTGGGGAGTTGGGGATCCTTTGGTAGAGATTGAGTA
Na1.5-R8-12	TGGGGGGTTGGGGAGTTGGGGATCCTTTGGTAGAGATTGAGTT
Na1.5-R8-13	TGGGGGGTTGGGGAGTTGGGGATCCTTTGGCAGAGATTGAGTA
Na1.5-R8-14	CCGTGGCCGTTAGGCGTATCGTCCCCCACTACTACTTTGGGTT
Na1.5-R8-15	TGGGGTTGGGGAGTTGGGGATCCTTTGGTAGAGATTGAGTA
Na1.5-R8-16	CCTCGAAGAAGGCGTCCCCCACTCATTCCTCCTTATACGAGG
Na1.5-R8-17	CCTCGAAGAAGGCGTCCCCCACTCATTCCTCCTTATACGAGG
Na1.5-R8-18	TGGGGGGTTGGGGAGTTGGGGATCCTTTGGTAGAGATTGAGTA
Na1.5-R8-19	CCTCGAAGAAGGCGTCCCCCACTCATTCCTCCTTATACGAGG
Na1.5-R8-20	TGGGGGGTTGGGGAGTTGGGGATCCTTTGGTAGAGATTGAGTA
Na1.5-R8-21	TGGGGGGTTGGGGAGTTGGGGATCCTTTGGCAGAGATTGAGTT
Na1.5-R8-22	CCTCGAAGAAGGCGTCCCCCACTCATTCCTCCTTATACGAGG
Na1.5-R8-23	CCTCGAAGAAAGCGTCCCCCACTCATTCCTCCTTATACGAGG
Na1.5-R8-24	TGGGGGGTTGGGGAGTTGGGGATCCTTTGGTAGAGATTGAGTA
Na1.5-R8-25	TGGGGGGTTGAGGAGTTGGGGATCCTTTGGTAGAGATTGAGTA
Na1.5-R8-26	TGGGGGGTTGGGGAGTTGGGGATCCTTTGGTAGAGATTGAGTT
Na1.5-R8-27	TGGGGGGTTGGGGAGTTGGGGATCCTTTGGTAGAGATTGAGTA
Na1.5-R8-28	TGGGGGGTTGGGGAGTTGGGGATCCTTTGGTAGAGATTGAGTA
Na1.5-R8-29	TGGGGGGTTGGGGAGTTGGGGATCCTTTGGTAGAGATTGAGTA
Na1.5-R8-30	TGGGGGGTTGGGGAGTTGGGGATCCTTTGGTAGAGATTGAGTT
Na1.5-R8-31	CCTCGAAGAAGGCGTCCCCCACTCATTCCTCCTTATACGAGG

Na1.5-R8-32	CCTCGAAGAAGGCGTCCCCCACTCATTCCTCCTTATACGAGG
Na1.5-R8-33	CCTCGAAGAAGGCGTCCCCCACTCATTCCTCCTTATACGAGG
Na1.5-R8-34	CGAGACGGATCTTTAGTCCCCCACTCGCCCCATCCGTTCGAGG
Na1.5-R8-35	TGGGGGGTTGGGGAGTTGGGGATCCTTTGGTAGAGATTGAGTT
Na1.5-R8-36	TGGGGGGTTGGGGAGTTGGGGATCCTTTGGTAGAGATTGAGTT
Na1.5-R8-37	TGGGGGGTTGGGGAGTTGGGGATCCTTTGGTAGAGATTGAGTA
Na1.5-R8-38	CCTCGAAGAAGGCGTCCCCCACTCATTCCTCCTTATACGAGG
Na1.5-R8-39	TGGGGGGTTGGGGAGTTGGGGATCCTTTGGTAGAGATTGAGTT

Supp. table 4 DNA sequences selected in cell-SELEX targeting Nav1.6-HEK293. Listed are the sequence and their frequency according to the selections.

The nomenclature of the sequences was random.

Name	Random region
Na1.6-R8-1	TGGGGGGTTGGGGAGTTGGGGATCCTTTGGTAGAGATTGAGTT
Na1.6-R8-2	CGTAGACGAATCGATGGAAGGTTGCGTTCCTTTATTCACCGGG
Na1.6-R8-3	CCTTTTAATGCTAGCCACTGTGCCAACTGTCCCCCCACATGTG
Na1.6-R8-4	GCCCATCGGATTCCTTCGTTCCTCTCAGCCGGGAAAGTTTCCA
Na1.6-R8-5	CCAACCCTCGTATGTCAACTAATGTGGGGGTCTTTTATCGTTG
Na1.6-R8-6	CCAAGAAGAAATCCCAACGAAAGAAAGGCATCTGGATCTATTG
Na1.6-R8-7	CGCAGAGGATGATCGAGCAGTCCCCCACTATGTCCTTATTCGA
Na1.6-R8-8	CCACTGTCCCCCAGGTGTCTCACCGAGTTGGAGAACTTCTAAG
Na1.6-R8-9	TGGGGGGTTGGGGAGTTGGGGATCCTTTGGTAGAGATTGAGTT
Na1.6-R8-10	GGACGGCACTTCTCATTTACTCCTGCGATGGTCATGGTGAGGG
Na1.6-R8-11	CGAGACGGATCTTTAGTCCCCCACTCGCCCCATCCGTTCGAGG
Na1.6-R8-12	TGGGGGGTTGGGGAGTTGGGGATCCTTTGGTAGAGATTGAGTT
Na1.6-R8-13	CTAAGAGGATAGCCTGCCACTCCGTCCCCCACTATCGAATATG
Na1.6-R8-14	CGAGACTTTTGCATAAATTGAAGAGCAGTCAGTAAAATCGGGGG
Na1.6-R8-15	TGGGGGGTTGGGGAGTTGGGGATCCTTTGGTAGAGATTGAGTT
Na1.6-R8-16	CGTATCGATANGCCGTCTTTTTACTNNTGGTTCGCGTTTCCTG
Na1.6-R8-17	TGGGGGGTTGGGGAGTTGGGGATCCTTTGGTAGAGATTGAGTT
Na1.6-R8-18	CGAGACGGATCTTTAGTCCCCCACTCGCCCCATCCGTTCGAGG
Na1.6-R8-19	CCTCGAAGAAGGCGTCCCCCACTCATTCCTCCTTATACGAGG
Na1.6-R8-20	CGAGACGGATCTTTAGTCCCCCACTCGCCCCATCCGTTCGAGG
Na1.6-R8-21	CCTCGAAGAAGGCGTGCCCCACTCATTCCTCCTTATACGAGG
Na1.6-R8-22	CCCCGGGTCTTTCGTTTTTACCTATCCCCTTTGTTAGCGTTGG
Na1.6-R8-23	CCCAGCCAGCTGAACGATTTACGTCCCCCGCTTATACTCACCG
Na1.6-R8-24	AGGGCGAATTCCA
Na1.6-R8-25	CCTCGAAGAAGGCGTCCCCCACTCATTCCTCCTTATACGAGG
Na1.6-R8-26	TGGGGGGTTGGGGAGTTGGGGATCCTTTGGTAGAGATTGAGTT
Na1.6-R8-27	CCTCGAAGAAGGCGTCCCCCACTCATTCCTCCTTATACGAGG
Na1.6-R8-28	GGGAGGTTCGGAGTGTTTAGGGGATCATTACATGTGGGTGTGG
Na1.6-R8-29	CGGCCAGAAATGTTCTAGTCCCCCACTTTTCCTCCTCATTTCG
Na1.6-R8-30	CGAGACGGATCTTTAGTCCCCCACTCGCCCCATCCGCTCGAGG
Na1.6-R8-31	CGGGGTTAGATCCGTCCCCCACTAAACTTCTAACCCTAGGTCA
Na1.6-R8-32	TGGGGGGTTGGGGAGTTGGGGATCCTTTGGTAGAGATTGAGTT
Na1.6-R8-33	TGGGGGGTTGGGGAGTTGGGGATCCTTTGGTAGAGATTGAGTT

Na1.6-R8-34	CGTGGGTGGGTTTATATTCGGTGGTGGTGGGGGTGGTACTGTT

Supp. table 5 DNA sequences selected in cell-SELEX targeting $Na_v1.5$-HEK293 sequenced by NGS. Listen are the 15 most abundant sequence patterns and their frequency in the final selection cycle 10.

The nomenclature of the sequences was random.

pattern	random region	NGS frequency (last selection cycle)
1	TGGGGGGTTGGGGAGTTGGGGATCCTTTGGTAGAGATTGAGTA	5.11%
2	CCTCGAAGAAGGCGTCCCCCACTCATTCCTCCTTATACGAGG	1.01%
3	CGAGACGGATCTTTAGTCCCCCACTCGCCCCATCCGTTCGAGG	0.13%
4	TGGGGGGTTGGGGAGTTGGGGATCCTTTGTAGAGATTGAGTA	0.09%
5	GGTCTCCCGTCCCCCACTACAACCTCTCCTCAAGGTGTCACGG	0.02%
6	CGGGGTTAGATCCGTCCCCCACTAAACTTCTAACCCTAGGTCA	0.01%
7	CCGTGGCCGTTAGGCGTATCGTCCCCCACTACTACTTTGGGTT	0.01%
8	TGGGGGGTTGGGAGTTGGGGATCCTTTGGTAGAGATTGAGTA	0.01%
9	GTACAGGTGCGCGTTGCCCTTGTCCCCCACTAATCTTACCTCG	<0.01%
10	CGGCTGGCCGGTTCACGTCCCCCACTATTTCCCCATTCCGCGG	<0.01%
11	CCTCGAAGAAGGCGTCCCCACTCATTCCTCCTTATACGAGG	<0.01%
12	TGGGGGGTTGGGGAGTTGGATCCTTTGGTAGAGATTGAGTA	<0.01%
13	CGATAATAGCGGCCAGAAAGTCCAACTGTCCCCCCTTTTGTG	<0.01%
14	CGCGCGGGAGGTCGTAGATAACTGTCCCCCCGTAGACATCCCA	<0.01%
15	CCCGAGCGTCCCCCACTCTTTCTTTTCAAGGTTGCATGTTCGG	<0.01%

Supp. table 6 DNA sequences selected in cell-SELEX targeting $Na_v1.6$-HEK293 sequenced by NGS. Listen are the 15 most abundant sequence patterns and their frequency in the final selection cycle 10.

The nomenclature of the sequences was random.

pattern	random region	NGS frequency (last selection cycle)
1	CCTCGAAGAAGGCGTCCCCCACTCATTCCTCCTTATACGAGG	2.23%
2	TGGGGGGTTGGGGAGTTGGGGATCCTTTGGTAGAGATTGAGTT	1.63%
3	CGAGACGGATCTTTAGTCCCCCACTCGCCCCATCCGTTCGAGG	0.66%
4	CGTGGGCGGGTTTATATTTGGTGGTGGTGGGGGTGGTACTGTT	0.40%
5	CGTGGGTGGGTTTATATTCGGTGGTGGTGGGGGTGGTACTGTT	0.38%
6	CGAGACCAGCTGCACGCCTACGTCCCCCACTAGTTTATTCTGG	0.26%
7	CGGGGTTAGATCCGTCCCCCACTAAACTTCTAACCCTAGGTCA	0.25%
8	CAGTAGTGCCAAGCATTCGTCCCCCACTTTCTTTAGTGCTTGG	0.08%
9	GGTCTCCCGTCCCCCACTACAACCTCTCCTCAAGGTGTCACGG	0.08%
10	CGGCCAGAAATGTTCTAGTCCCCCACTTTTCC	0.07%
11	CGGCCAGAAATGTTCTAGTCCCCCACTTTTCCTCCTCATTTCG	0.07%
12	CGACGGAAATTGTTCTGTCCCCCACTATAATCCCT	0.07%
13	CGACGGAAATTGTTCTGTCCCCCACTATAATCCCTGTCTGTCG	0.06%
14	CCGTAAACGTCCCCCACTCTCCCACAAGGTTGCTTAACATCTG	0.06%
15	CCCGGGAAGTAAAGGTCCCCCACTCTATATTCTCTGACAGGGG	0.05%

Supp. table 7 DNA sequences selected in cell-SELEX targeting HEK293 sequenced by NGS. Listen are the 15 most abundant sequence patterns and their frequency in the final selection cycle 12.

The nomenclature of the sequences was random.

pattern	random region	NGS frequency (last selection cycle)
1	CGTGGGTGGGTTTATATTCGGTGGTGGTGGGGGTGGTACTGTT	2.84%
2	TCGGTTCCTGTTAATTCGCTGGTGGTTGGTGGGGTGGCGGATG	0.55%
3	CGTGGGTGGGTTTTATTCGGTGGTGGTGGGGGTGGTACTGTT	0.52%
4	GGTCTCCCGTCCCCCACTACAACCTCTCCTCAAGGTGTCACGG	0.11%
5	CGTGGGTGGGTTTATTCGGTGGTGGTGGGGGTGGTACTGTT	0.11%
6	CGTGGGTGGGTTATATTCGGTGGTGGTGGGGGTGGT	0.09%
7	CGTGGGTGGGTTATATTCGGTGGTGGTGGGGGTGGTACTGTT	0.09%
8	GCCAATCAATTCCGCGTCAGTTTATCCGTCTTTCTTATTCCGG	0.08%
9	TGGGGGGTTGGGGAGTTGGGGATCCTTTGGTAGAGATTGAGTT	0.06%
10	TCTATCGCTACCCGCGTGTCGTCTTTAGCTATCCGTTCCCCGA	0.05%
11	CGTGGGTGGGTTTATATTCGGTGGTGGTGGGGGG	0.04%
12	CGAGACGGATCTTTAGTCCCCCACTCGCCCCATCCGTTCGAGG	0.04%
13	CCTCGAAGAAGGCGTCCCCCACTCATTCCTCCTTATACGAGG	0.04%
14	CGTGGGTGGGTTTATTTCGGTGGTGGTGGGGGTGGTACTGTT	0.04%
15	CGTGGGTGGGTTTTATTTCGGTGGTGGTGGGGGTGGTACTGTT	0.03%

Supp. table 8 The remaining sequences and their frequency [%] in starting library (SL) and selection cycles (C2-C10) of the NGS analysis of the SELEX targeting $Na_v1.6$-HEK293 after hiding patterns, which are present in the SELEX targeting HEK293.

The nomenclature of the sequences was random.

Sequence name and the random region		SL	C2	C3	C4	C5	C6	C7	C8	C9	C10
392	CCCCCCGCGATTGGATTTGTGTTTGCTTTTCTCGTACTCATGG	0.00	0.00	0.00	0.00	$2.50 \cdot 10^{-1}$	$4.73 \cdot 10^{-2}$	$9.54 \cdot 10^{-2}$	$4.72 \cdot 10^{-2}$	$3.98 \cdot 10^{-2}$	$1.19 \cdot 10^{-1}$
595	CCCGATTAGTTCCTCCCCGTTTGTGCTCGAGTTATTTTCCTGG	0.00	0.00	$2.88 \cdot 10^{-1}$	0.00	$2.50 \cdot 10^{-1}$	$6.62 \cdot 10^{-1}$	$4.53 \cdot 10^{-1}$	$1.53 \cdot 10^{-1}$	$5.97 \cdot 10^{-2}$	$1.78 \cdot 10^{-1}$
654	CCCGGGCGTTCTTGTTACTTTTGGATAGTGGTAGTTTTTCTGG	0.00	0.00	0.00	$3.61 \cdot 10^{-1}$	$2.19 \cdot 10^{-1}$	$4.26 \cdot 10^{-1}$	$2.62 \cdot 10^{-1}$	$9.43 \cdot 10^{-2}$	$9.96 \cdot 10^{-2}$	$5.93 \cdot 10^{-2}$
448	CCCCGAACTGTGATACGACGCTTTTTACCCTTTCTCTGTGTGG	0.00	0.00	0.00	$2.41 \cdot 10^{-1}$	$9.39 \cdot 10^{-2}$	$4.73 \cdot 10^{-2}$	$1.67 \cdot 10^{-2}$	$1.18 \cdot 10^{-2}$	$1.99 \cdot 10^{-2}$	$5.93 \cdot 10^{-2}$

Supp. table 9 The remaining sequences and their frequency [%] in starting library (SL) and selection cycles (C4-C10) of the NGS analysis of the SELEX targeting $Na_v1.5$-HEK293 after hiding patterns, which are present in the SELEX targeting HEK293.

The nomenclature of the sequences was random.

Sequence name and the random region		SL	C4	C6	C8	C10
545	TCTCCTCACAACAGCGAGCTGGAGCTTAGACCGGGTTTTAGGG	0.00	0.00	0.00	5.01 · 10-2	1.24 · 10-2
523	TAGTTAGGAACAGCGTCAAAAGCCCCCACTCGTCCCCCTTTTG	0.00	0.00	0.00	1.67 · 10-2	5.29 · 10-2

Supp. table 10 DNA sequences selected in click-SELEX with indole azide for DNA functionalization targeting C3-GFP sequenced by NGS. Listed are the 15 most abundant sequence patterns and their frequency in the final selection cycle 10.

The nomenclature of the sequences was random.

pattern	random region	NGS frequency (last selection cycle)
I10	CGCGTAGGTACCCGGCTTTGAATATGTAGGGGACCTAGAGAACA	60,40%
8	CCCACTGCGCAGGCTTTCGATATGTAGCACAGAGGG	2,92%
3	CCCACTGCGCAGGCTTTCGATATGTAGCACAGAGGGAATACTGG	2,78%
20	TAGAAGAAACACCCAACCTGCGAGACTTTCGATATGT	0,09%
10	TAGAAGAAACACCCAACCTGCGAGACTTTCGATATGTGACCGAA	0,08%
12	GACCCGACTTTCGATATGTAAGGTCCGAGGGGACGAACG	0,05%
11	CTCGGCCCGGCTTTGCATATGTAAGGCCCATCACCTCGAACAAG	0,03%
7	TCATAGACCCGACTTTCGATATGTAAGGTCCGAGGGGACGAACG	0,03%
15	ACGTAAACGTGGGCGGCTTTCAATATGTAACCCACAGGACCGCG	0,01%
14	GCCCGGCTTTCAATACTTAGGGATCAGTATACTGGAAGGGGCAA	0,01%
5	CGCGTAGGTACCCGGCTTGAATATGTAGGGGACCTAGAGAACA	0,01%
4	CGCGTAGGTACCCGGTTTGAATATGTAGGGGACCTAGAGAACA	0,01%
16	CTCGAGCTTTCGATATGTACGAGCCGTTCCGACCTCCCA	0,01%
17	CGCTGAGGCCCCATACTCTGTTAACCCCCCTAAGGTCTTCCCCG	0,00%
22	TCGGGTATCGCGCCTTTCGATATGTAGCGATACAAATCCAACCT	0,00%

Supp. table 11 DNA sequences selected in click-SELEX with benzyl azide for DNA functionalization targeting C3-GFP sequenced by NGS. Listed are the 15 most abundant sequence patterns and their frequency in the final selection cycle 8.

The nomenclature of the sequences was random.

pattern	random region	NGS frequency (last selection cycle)
9	GGCGTACTTTGTCTCACCTACACATTCTAACCACCACT	18,93%
B10	CCTCCTACCCATTTTGCAACCCCTAGTACCC	17,35%
B33	GGCGTACTTTGTCTCACCTACACATTCTAACCACCACTACGCCA	14,38%
B15	AAGGGTGAGCAAAGCCGGGCGGTGTTCCTAGGCTTTCACGGCGG	13,12%
1	CCTCCTACCCATTTTGCAACCCCTAGTACCCCTATGGCACACAC	9,44%
6	CCCTCTCCCTAAATAACCCTCGCCCATTTTGTACGTGTCCAGAA	1,01%
12	GGTATGAACATTGGTAGTGGGGGACCTACTTAGGGGAGGGTGGG	0,68%
10	CCATATGTCCCGTATACGCCCTCCCCTTATACGCCACTTGGCA	0,36%
11	CCATATGCCCCGTATACGCCCTCCCCTTATACGCCACTTGGCA	0,32%
17	GGTAAACATCCGGTTACACCCTTCATGCCCTCTCCCCGTTCATT	0,29%
18	CCGAATATCATCAGTCTAGACGTTTCAGGTCACCCTGTTTCACA	0,18%
22	CCATCATTGTCCCTAGTCAAATTGTCCCCTGAACTAATATCTGA	0,13%
26	CCTTGACCCAATAATGTCCCATACCTTTATCCCACGTTTACA	0,12%
23	ATCATGGGGGGTGGTGGGGAGTAGGTGGGAGGGTGCCACATCTA	0,11%
21	GGCTACGTCTCGCCGCTCCCTGTATCGCCGTTTACCCCCGTCCA	0,09%
20	GCGCCCTCGCCTCCGTTAACGCCCTATTCCCCACACTCAGAACA	0,09%

Supp. table 12 DNA sequences selected in click-SELEX with benzofuran azide for DNA functionalization targeting C3-GFP sequenced by NGS. Listed are the 15 most abundant sequence patterns and their frequency in the final selection cycle 8.

The nomenclature of the sequences was random.

pattern	random region	NGS frequency (last selection cycle)
F20	CCGCCCGCGTATGATGCCGTCTTACGGGCAGCCGTAACCACAAC	33,70%
F8	TCGGGCCGGAGCGAGGTATGATGCCATCCTTCACAGCTCCA	14,48%
3	CAGGTATGATGCCATCTTCGGAGGGAAATGCGGCAGTGGAAG	2,10%
4	AGCACCATAACGTGACGTCGGCGACCTCACTCCTCCATGCCCCA	1,89%
5	CTGGGGGTATGGTGCCGTCTTACCCATAGGCGGATCTCAGACGA	0,83%
6	CGCCGGACGTATAATGCCATCTTGCCCGACTGCGACTAACACAA	0,16%
7	TGGTGGGCCAGGTATAATGCCATCCTTCGGACCCCTCGGCATAG	0,02%
9	TCGGGCCGGAGCGAGGTATGATGCCATCTTCACAGCTCCA	0,02%
11	CCGCCCGCGTATGATGCCATCCTTCACAGCTCCA	0,01%
8	GGGAGCTTATGAGGCACGGGGTATAGTCACGTCTTACCGCACCA	0,01%
12	CCGCCCGCGTATGATGCCGTCTTACGGGCAGCCGTACCACAAC	0,01%
10	GCGGGGTATGGTGCCGTCTTACCGCTCCTTGACCATAACGCGGG	0,01%
13	GCGGGGTATGGTACCGTCTTACCGCTCCTTGACCATAACGCGGG	0,01%
14	CGCGTAGGTACCCGGCTTTGAATATGTAGGGGACCTAGAGAACA	0,01%

Supp. table 13 DNA sequences selected in multiplexed click-SELEX targeting C3-GFP sequenced by NGS. Listed are the 15 most abundant sequence patterns and their frequency in the final multiplexed selection cycle 8 (multiplexed C8).

The nomenclature of the sequences was random.

pattern	random region	NGS frequency (multiplexed C8)
46	CGCGTAGGTACCCGGCTTTGAATATGTAGGGGACCTA	38,97%
I10_11	CGCGTAGGTACCCGGCTTTGAATATGTAGGGGACCTAGAG	36,22%
I10_26	CGCGTAGGTACCCGGCTTTGAATATGTAGGGGACCTAGAGA	36,17%
I10	CGCGTAGGTACCCGGCTTTGAATATGTAGGGGACCTAGAGAACA	35,58%
F20_2	CCGCCCGCGTATGATGCCGTCTTACGGGCAGCCGCAACCACAAC	14,20%
F20	CCGCCCGCGTATGATGCCGTCTTACGGGCAGCCGTAACCACAAC	13,53%
F8	TCGGGCCGGAGCGAGGTATGATGCCATCCTTCACAGCTCCA	0,99%
4	AGCACCATAACGTGGCGTCGGCGACCTCACTCCTCCATGCCCCA	0,92%
I10_23	CGCGTAGGTACCCGGCTTTGAATATGTAGGGGACCTAGAAA	0,90%
7	CTGGGGGTATGGTGCCGTCTTACCCATAGGCGGATCTCAGACGA	0,41%
10	GGGAGCTTATGAGGCACGGGGTATAGTCACGTCTTACCGCACCA	0,15%
9	GCGACGCTGGCGTGCAGGTAAAGAATCTATAGCGCACCACACA	0,10%
I10_6	CGCGTAGGTACCCGGCTTTGAATATGTAGGGGACCTGAGAACA	0,09%
40	CCGCCCGCGTATGATGCCGTCTTACGGGCAACCACAAC	0,07%
I10_25	CGCGTAGGTACCCGGCTTTGAATATGTAGGGGACCTAAGAACA	0,06%

Supp. table 14 DNA sequences selected in multiplexed click-SELEX targeting C3-GFP sequenced by NGS. Listed are the 15 most abundant sequence patterns and their frequency in the final multiplexed selection cycle 8 (multiplexed C8) and the deconvolution cycle 9 using only indole for DNA functionalization.

The nomenclature of the sequences was random.

pattern	random region	NGS frequency (multiplexed C8)	NGS frequency (indole C9)
I10	CGCGTAGGTACCCGGCTTTGAATATGTAGGGGACCTAGAGAACA	35,58%	65,91%
I10_26	CGCGTAGGTACCCGGCTTTGAATATGTAGGGGACCTAGAA	0,93%	1,99%
I10_24	CGCGTAGGTACCCGGCTTTGAATATGTAGGGGACCTAGAAA	0,90%	1,93%
I10_23	CGCGTAGGTACCCGGCTTTGAATATGTAGGGGACCTAGAAAA	0,88%	1,86%
I10_2	CGCGTAGGTACCCGGCTTTGAATATGTAGGGGACCTGAGAACA	0,09%	0,22%
I10_12	CGCGTAGGTACCCGGCTTTGAATATGTAGGGGACCTAAGAACA	0,06%	0,14%
I10_3	CGCGTGGTACCCGGCTTTGAATATGTAGGGGACCTAGAGAACA	0,05%	0,13%
I10_7	CGCGTAGGTACCCGGCTTTGAATATGTAGGGGACCAGAGAACA	0,04%	0,09%
I10_13	CGCGTAGGTACCCGGCTTTGAATATGTAGGGGACCTAGAACA	0,02%	0,05%
F20_5	CCGCCCGCGTATGATGCCGTCTTACGGGCAGCCGCAACCACAAC	14,20%	0,05%
F20	CCGCCCGCGTATGATGCCGTCTTACGGGCAGCCGTAACCACAAC	13,53%	0,05%
I10_21	CGCGTAGGTACCCGGCTTTGAATATGTAGGGGACTAGAGAACA	0,03%	0,05%
I10_29	CGCGTAGGTACCCGGCTTTGAATATGTAGGGGACCTAGAGAAA	0,02%	0,04%
I10_10	CGCTAGGTACCCGGCTTTGAATATGTAGGGGACCTAGAGAACA	0,02%	0,03%
I10_18	CGCGAGGTACCCGGCTTTGAATATGTAGGGGACCTAGAGAACA	0,02%	0,03%
I10_4	CGCGTAGGTACCCGGCTTTGAATATGTAGGGGACCTGAACA	0,01%	0,02%

Supp. table 15 DNA sequences selected in multiplexed click-SELEX targeting C3-GFP sequenced by NGS. Listed are the 15 most abundant sequence patterns and their frequency in the final multiplexed selection cycle 8 (multiplexed C8) and the deconvolution cycle 9 using only benzofuran for DNA functionalization.

The nomenclature of the sequences was random.

pattern	random region	NGS frequency (multiplexed C8)	NGS frequency (benzofuran C9)
F20	CCGCCCGCGTATGATGCCGTCTTACGGGCAGCCGTAACCACAAC	13,53%	30,21%
F20_2	CCGCCCGCGTATGATGCCGTCTTACGGGCAGCCGCAACCACAAC	14,20%	29,07%
3	CTGGGGGTATGGTGCCGTCTTACCCATAGGCGGATCTCAGACGA	0,41%	0,74%
F8	TCGGGCCGGAGCGAGGTATGATGCCATCCTTCACAGCTCCA	0,99%	0,46%
4	AGCACCATAACGTGGCGTCGGCGACCTCACTCCTCCATGCCCCA	0,92%	0,31%
31	CCGCCCGCGTATGATGCCGTCTTACGGGCAACCACAAC	0,07%	0,15%
I10	CGCGTAGGTACCCGGCTTTGAATATGTAGGGGACCTAGAGAACA	35,58%	0,12%
9	GGGAGCTTATGAGGCACGGGGTATAGTCACGTCTTACCGCACCA	0,15%	0,02%
F20_30	CCGCCCGCGTATGATGCCGTCTTACGGGCAGCCGTACCACAAC	0,01%	0,02%
F20_8	CCGCCCGCGTATGATGCCGTCTTACGGGCAGCCGCACCACAAC	0,01%	0,01%
F8_10	TCGGGCCGGAGCGAGGTATGATGCCATCTTCACAGCTCCA	0,01%	0,01%
13	CGCCGGACGTATAATGCCATCTTGCCCGACTGCGACTAACACAA	0,05%	0,00%
F20_11	CCGCCCGCGTATGATGCCGTCTTACGGGCAGCCGAACCACAAC	0,00%	0,00%
14	GCGACGCTGGCGTGCAGGTAAAGAATCTATAGCGCACCACACA	0,10%	0,00%
20	GCGGGGTATGGTGCCGTCTTACCGCTCCTTGACCATAACACGGG	0,00%	0,00%

Supp. table 16 DNA sequences selected in multiplexed click-SELEX targeting C3-GFP sequenced by NGS. Listed are the 15 most abundant sequence patterns and their frequency in the final multiplexed selection cycle 8 (multiplexed C8) and the deconvolution cycle 9 using only benzene for DNA functionalization.

The nomenclature of the sequences was random.

pattern	random region	NGS frequency (multiplexed C8)	NGS frequency (benzene C9)
I10_23	CGCGTAGGTACCCGGCTTTGAATATGTAGGGGACCTAGAGA	36,17%	13,11%
C1	AGCACCATAACGTGGCGTCGGCGACCTCACTCCTCCATGCCCCA	0,92%	13,09%
I10	CGCGTAGGTACCCGGCTTTGAATATGTAGGGGACCTAGAGAACA	35,58%	12,84%
F20_3	CCGCCCGCGTATGATGCCGTCTTACGGGCAGCCGCAACCACAAC	14,20%	5,74%
F20	CCGCCCGCGTATGATGCCGTCTTACGGGCAGCCGTAACCACAAC	13,53%	4,74%
F8	TCGGGCCGGAGCGAGGTATGATGCCATCCTTCACAGCTCCA	0,99%	0,39%
6	CTGGGGGTATGGTGCCGTCTTACCCATAGGCGGATCTCAGACGA	0,41%	0,34%
69	CCGCCCGCGTATGATGCCGTCTTACGGGCAACCACAAC	0,07%	0,15%
7	GGGAGCTTATGAGGCACGGGGTATAGTCACGTCTTACCGCACCA	0,15%	0,12%
I10_8	CGCGTAGGTACCCGGCTTTGAATATGTAGGGGACCTGAGAACA	0,09%	0,04%
9	GCGACGCTGGCGTGCAGGTAAAGAATCTATAGCGCACCACACA	0,10%	0,03%
I10_16	CGCGTAGGTACCCGGCTTTGAATATGTAGGGGACCTAAGAACA	0,06%	0,03%
I10_10	CGCGTGGTACCCGGCTTTGAATATGTAGGGGACCTAGAGAACA	0,05%	0,02%
12	CGCCGGACGTATAATGCCATCTTGCCCGACTGCGACTAACACAA	0,05%	0,02%
I10_13	CGCGTAGGTACCCGGTTTGAATATGTAGGGGACCTAGAGAACA	0,01%	0,02%

Supp. table 17 DNA sequences selected in multiplexed click-SELEX targeting C3-GFP sequenced by NGS. Listed are the 15 most abundant sequence patterns and their frequency in the final multiplexed selection cycle 8 (multiplexed C8) and the deconvolution cycle 9 using only chlorobenzene for DNA functionalization.

The nomenclature of the sequences was random.

pattern	random region	NGS frequency (multiplexed C8)	NGS frequency (chlorobenzene C9)
C1	AGCACCATAACGTGGCGTCGGCGACCTCACTCCTCCATGCCCCA	0,92%	24,31%
I10	CGCGTAGGTACCCGGCTTTGAATATGTAGGGGACCTAGAGAACA	35,58%	5,19%
F20_3	CCGCCCGCGTATGATGCCGTCTTACGGGCAGCCGCAACCACAAC	14,20%	2,02%
F20	CCGCCCGCGTATGATGCCGTCTTACGGGCAGCCGTAACCACAAC	13,53%	1,53%
6	CTGGGGGTATGGTGCCGTCTTACCCATAGGCGGATCTCAGACGA	0,41%	0,14%
F8	TCGGGCCGGAGCGAGGTATGATGCCATCCTTCACAGCTCCA	0,99%	0,11%
7	GGGAGCTTATGAGGCACGGGGTATAGTCACGTCTTACCGCACCA	0,15%	0,05%
I10_8	CGCGTAGGTACCCGGCTTTGAATATGTAGGGGACCTGAGAACA	0,09%	0,02%
I10_15	CGCGTAGGTACCCGGTTTGAATATGTAGGGGACCTAGAGAACA	0,01%	0,01%
I10_12	CGCGTGGTACCCGGCTTTGAATATGTAGGGGACCTAGAGAACA	0,05%	0,01%
14	CGCCGGACGTATAATGCCATCTTGCCCGACTGCGACTAACACAA	0,05%	0,01%
I10_10	CGCGAGGTACCCGGCTTTGAATATGTAGGGGACCTAGAGAACA	0,02%	0,01%
11	GCGACGCTGGCGTGCAGGTAAAGAATCTATAGCGCACCACACA	0,10%	0,01%
I10_17	CGCGTAGGACCCGGCTTTGAATATGTAGGGGACCTAGAGAACA	0,02%	0,01%
I10_13	CGCGTAGGTACCCGGCTTTGAATATGTAGGGGACCAGAGAACA	0,04%	0,01%

Supp. table 18 DNA sequences selected in multiplexed click-SELEX targeting C3-GFP sequenced by NGS. Listed are the 15 most abundant sequence patterns and their frequency in the final multiplexed selection cycle 8 (multiplexed C8) and the deconvolution cycle 9 using only ethanamine for DNA functionalization.

The nomenclature of the sequences was random.

pattern	random region	NGS frequency (multiplexed C8)	NGS frequency (ethanamine C9)
I10_38	GCGTAGGTACCCGGCTTTGAATATGTAGGGGACCTAGAGAACA	35,73%	18,95%
I10	CGCGTAGGTACCCGGCTTTGAATATGTAGGGGACCTAGAGAACA	35,58%	18,83%
F20_2	CCGCCCGCGTATGATGCCGTCTTACGGGCAGCCGCAACCACAAC	14,20%	8,36%
F20	CCGCCCGCGTATGATGCCGTCTTACGGGCAGCCGTAACCACAAC	13,53%	6,86%
85	ACGTGACGTCGGCGACCTCACTCCTCCATGCCCCA	0,63%	3,70%
4	AGCACCATAACGTGACGTCGGCGACCTCACTCCTCCATGCCCCA	0,41%	2,46%
5	AGCACCATAACGTGGCGTCGGCGACCTCACTCCTCCATGCCCCA	0,92%	2,23%
F8	TCGGGCCGGAGCGAGGTATGATGCCATCCTTCACAGCTCCA	0,99%	0,70%
I10_52	CGCGTAGGTACTCGGCTTTGAATATGTAGGGGACCTAGAGAACA	0,17%	0,66%
I10_47	CGCGTAGATACCCGGCTTTGAATATGTAGGGGACCTAGAGAACA	0,40%	0,40%
7	CTGGGGGTATGGTGCCGTCTTACCCATAGGCGGATCTCAGACGA	0,41%	0,25%
8	GGGAGCTTATGAGGCACGGGGTATAGTCACGTCTTACCGCACCA	0,15%	0,18%
75	CCGCCCGCGTATGATGCCGTCTTACGGGCAACCACAAC	0,07%	0,15%
9	GCGACGCTGGCGTGCAGGTAAAGAATCTATAGCGCACCACACA	0,10%	0,06%
I10_10	CGCGTAGGTACCCGGCTTTGAATATGTAGGGGACCTGAGAACA	0,09%	0,06%

Supp. table 19 DNA sequences selected in multiplexed click-SELEX targeting streptavidin sequenced by NGS. Listed are the 15 most abundant sequence patterns and their frequency in the final multiplexed selection cycle 8 (multiplexed C8).

The nomenclature of the sequences was random.

pattern	random region	NGS frequency (multiplexed C8)
P2	GGGTCATGCCGGGTTGGAGTTTAAGGGGTTGGGGCAGGACCC	21,77%
P2_1	GGGTCATGCCGGGTTGGAGTTTAAGGGGTTGGGGCAAGACCC	1,44%
P2_2	GGGTCATGCCGGGTTGGAGTTTAAGGGGTTGGGGCAGAACCC	1,36%
P1	AGGGGCGCTTTGGGGGAAATATGGGAGGTGGGGGGGGTCCCG	1,09%
P2_3	GGGTCATGCCGGGTTGGAGTTTAAGGGGTTGGGACAGGACCC	1,05%
P2_4	GGGTCATGCCGGGTTGGAGTTTAAGAGGTTGGGGCAGGACCC	1,04%
P2_5	GGGTCATGTCGGGTTGGAGTTTAAGGGGTTGGGGCAGGACCC	0,74%
P1_2	AGGGACGCTTTGGGGGGAATGTGGGAGGTGGGGGGGGTCCCG	0,68%
P2_6	GGATCATGCCGGGTTGGAGTTTAAGGGGTTGGGGCAGGACCC	0,63%
P2_7	GGGCCATGCCGGGTTGGAGTTTAAGGGGTTGGGGCAGGACCC	0,59%
P1_3	AGGGGCACTTTGGGGGAAATATGGGAGGTGGGGGGGGTCCCG	0,59%
P2_8	GGGTCATGCCGGGTTGGAGTTTAAGGGGTTGGGGTAGGACCC	0,46%
B2	GGACGGGCAAGATGGCTTCGGGGCTTGGGCGTTTTAAGGGGA	0,43%
P1_4	AGGGACGCTTTGGGGGAAATATGGGAGGTGGGGGGGGTCCCG	0,37%
I1	GCGGTACGGTTTGACCGTCCGAAGAGCTTCAAGCGATTGAGG	0,36%

Supp. table 20 DNA sequences selected in multiplexed click-SELEX targeting streptavidin sequenced by NGS. Listed are the 15 most abundant sequence patterns and their frequency in the final multiplexed selection cycle 8 (multiplexed C8) and the deconvolution cycle 9 using only phenol for DNA functionalization.

The nomenclature of the sequences was random.

pattern	random region	NGS frequency (multiplexed C8)	NGS frequency (phenol C10)
P2	GGGTCATGCCGGGTTGGAGTTTAAGGGGTTGGGGCAGGACCC	21,77%	20,99%
P1	AGGGGCGCTTTGGGGGAAATATGGGAGGTGGGGGGGGTCCCG	1,09%	2,18%
P1_3	AGGGGCACTTTGGGGGAAATATGGGAGGTGGGGGGGGTCCCG	0,59%	1,45%
P2_4	GGGTCATGCCGGGTTGGAGTTTAAGAGGTTGGGGCAGGACCC	1,04%	1,02%
P2_1	GGGTCATGCCGGGTTGGAGTTTAAGGGGTTGGGGCAAGACCC	1,44%	0,98%
P1_4	AGGGACGCTTTGGGGGAAATATGGGAGGTGGGGGGGGTCCCG	0,37%	0,92%
P1_5	AGGGACGCTTTGGGGGGAATTTGGGAGGTGGGGGGGGTCCCG	0,39%	0,90%
P2_3	GGGTCATGCCGGGTTGGAGTTTAAGGGGTTGGGACAGGACCC	1,05%	0,77%
P2_2	GGGTCATGCCGGGTTGGAGTTTAAGGGGTTGGGGCAGAACCC	1,36%	0,74%
P2_5	GGGTCATGTCGGGTTGGAGTTTAAGGGGTTGGGGCAGGACCC	0,74%	0,64%
P1_5	AGGGACGCTTTGGGGGAAATTTGGGAGGTGGGGGGGGTCCCG	0,10%	0,48%
P1_!4	AGGGACGCTTTGGGGGAAATGTGGGAGGTGGGGGGGGTCCCG	0,35%	0,46%
P_9	GGGTCATGCCGGGTTGGAGTTTAAGGGGTTGGGGCATGACCC	0,34%	0,45%
P1_10	AGGGACGCTTTGGGGGGAATGTGGGAGGTGGGGGGGGTCCCG	0,68%	0,43%
P1_11	AGGGACACTTTGGGGGAAATATGGGAGGTGGGGGGGGTCCCG	0,14%	0,42%

Supp. table 21 DNA sequences selected in multiplexed click-SELEX targeting streptavidin sequenced by NGS. Listed are the 15 most abundant sequence patterns and their frequency in the final multiplexed selection cycle 8 (multiplexed C8) and the deconvolution cycle 9 using only indole for DNA functionalization.

The nomenclature of the sequences was random.

pattern	random region	NGS frequency (multiplexed C8)	NGS frequency (indole C10)
I1_1	GCGGTACGGTTTGACCGTCCGAAGAGCTTTAAGCGATTGAGG	0,25%	7,80%
P2	GGGTCATGCCGGGTTGGAGTTTAAGGGGTTGGGGCAGGACCC	21,77%	6,85%
I2	GGCGGGCGTTTTGCGCCCGAGTGTTAACGACACAAGGGACCA	0,07%	4,74%
I2_1	GGCGGGCGTTTTGCGCCCGAGTGTTAACGACGCAAGGGACCA	0,04%	3,42%
I1_2	GCGGTACGGTTTTGACCGTCCGAAGAGCTTCAAGCGATTGAG	0,04%	3,29%
I1_3	GCGGTACGGTTTGACCGTCCGAAGAGCTTCAAGCGATTGAGG	0,36%	3,11%
I1_4	GCGGTACGGTTTTACCGTCCGAAGAGCTTCAAGCGATTGAGG	0,07%	2,46%
B2_1	GGGCGGGCAAGATGGCTTCGGGGCTTGGGCGTTTTAAGGGGA	0,12%	2,20%
I1_5	GCGGTACGGTTTTGACCGTCCGAAGAGCTTCAAGCGATTGAGG	0,03%	2,13%
B2	GGACGGGCAAGATGGCTTCGGGGCTTGGGCGTTTTAAGGGGA	0,43%	1,61%
P1	AGGGGCGCTTTGGGGGAAATATGGGAGGTGGGGGGGGTCCCG	1,09%	1,09%
B2_2	TGACGGGCAAGATGGCTTCGGGGCTTGGGCGTTTTAAGGGGA	0,06%	0,98%
I1_6	GCGGTACGGTTTTACCGTCCGAAGAGCTTTAAGCGATTGAGG	0,01%	0,84%
I1_7	GCGGTACGGTTTTGACCGTCCGAAGAGCTTTAAGCGATTGAG	0,01%	0,77%
I2_2	GGCGGGCGTTTTGCGCCCGAGTGTTAACGACACAAGGAACCA	0,01%	0,74%

Supp. table 22 DNA sequences selected in multiplexed click-SELEX targeting streptavidin sequenced by NGS. Listed are the 15 most abundant sequence patterns and their frequency in the final multiplexed selection cycle 8 (multiplexed C8) and the deconvolution cycle 9 using only benzene for DNA functionalization.

The nomenclature of the sequences was random.

pattern	random region	NGS frequency (multiplexed C8)	NGS frequency (benzene C10)
B1	CCAGGTTCGGTATATTCGGTCGCAGATACGAACCAGGGTATA	0,01%	15,52%
P1_5	AGGGACGCTTTGGGGGGAATTTGGGAGGTGGGGGGGGTCCCG	0,39%	3,51%
P1_2	AGGGGCGCTTTGGGGGAAATATGGGAGGTGGGGGGGGTCCCG	1,09%	2,78%
P2	GGGTCATGCCGGGTTGGAGTTTAAGGGGTTGGGGCAGGACCC	21,77%	2,51%
P1_3	AGGGGCACTTTGGGGGAAATATGGGAGGTGGGGGGGGTCCCG	0,59%	1,84%
B2	GGACGGGCAAGATGGCTTCGGGGCTTGGGCGTTTTAAGGGGA	0,43%	1,69%
B2_1	GGGCGGGCAAGATGGCTTCGGGGCTTGGGCGTTTTAAGGGGA	0,12%	1,54%
P1_5	AGGGACGCTTTGGGGGAAATTTGGGAGGTGGGGGGGGTCCCG	0,10%	1,52%
P1_6	AGGGGCGCTTTGGGGGAAATTTGGGAGGTGGGGGGGGTCCCG	0,06%	1,07%
P1_7	AGGGACACTTTGGGGGGAATTTGGGAGGTGGGGGGGGTCCCG	0,11%	0,96%
P1_8	AGGGGCACTTTGGGGGAAATTTGGGAGGTGGGGGGGGTCCCG	0,04%	0,68%
B2	TGACGGGCAAGATGGCTTCGGGGCTTGGGCGTTTTAAGGGGA	0,06%	0,60%
P1_4	AGGGACGCTTTGGGGGAAATATGGGAGGTGGGGGGGGTCCCG	0,37%	0,53%
P1_9	AGGGACACTTTGGGGGAAATTTGGGAGGTGGGGGGGGTCCCG	0,04%	0,48%
P1_10	AGGGGCGCTTTGGGGGGAATTTGGGAGGTGGGGGGGGTCCCG	0,07%	0,43%

Supp. table 23 DNA sequences selected in multiplexed click-SELEX targeting streptavidin sequenced by NGS. Listed are the 15 most abundant sequence patterns and their frequency in the final multiplexed selection cycle 8 (multiplexed C8) and the deconvolution cycle 9 using only guanidine for DNA functionalization.

The nomenclature of the sequences was random.

pattern	random region	NGS frequency (multiplexed C8)	NGS frequency (guanidine C10)
G1	TTTTGCGAACGCGGGTAGGCGCACCCTTCGCACAAACGTCCC	0,04%	38,87%
G2	ATTCCGCACGCTCCGGTCGCAGGATGAGGAATCGTAATTTGA	0,00%	5,67%
G1_1	TTTTGCGAACGCGGGTAGGCGCACCCTTCGCACAAACGTTCC	0,00%	3,57%
G1_2	TTTTGCGAACGCGGGTAGGCGCACCCTTTGCACAAACGTCCC	0,00%	2,91%
G1_3	TTTTGCGAACGCGGGTAGGCACACCCTTCGCACAAACGTCCC	0,00%	2,02%
G1_4	TTTTGCGAACGCGGGTAGGCGCACCCTTCACACAAACGTCCC	0,00%	1,14%
G1_5	TTTTGTGAACGCGGGTAGGCGCACCCTTCGCACAAACGTCCC	0,00%	1,13%
G1_6	TTTTGCGAACGCGAGTAGGCGCACCCTTCGCACAAACGTCCC	0,00%	0,96%
G1_7	TTTTGCGAACGCGGGTAGGCGCACCCTTCGCACAAATGTCCC	0,00%	0,87%
G1_8	TTTTGCAAACGCGGGTAGGCGCACCCTTCGCACAAACGTCCC	0,00%	0,81%
G1_9	TTTTGCGAACGCGGGTAGGCGCACCCTTCGCACAAACATCCC	0,00%	0,77%
G1_10	TTTTGCGAACGCGGGTAGGCGCACCCTTCGCATAAACGTCCC	0,00%	0,65%
G1_11	TTTTGCGAACGCGGGTAGGTGCACCCTTCGCACAAACGTCCC	0,00%	0,59%
G1_12	TTTTGCGAATGCGGGTAGGCGCACCCTTCGCACAAACGTCCC	0,00%	0,51%
G1_13	TTTTGCGAACGCGGGTAGGCGCACTCTTCGCACAAACGTCCC	0,00%	0,51%

Supp. table 24 DNA sequences selected in multiplexed click-SELEX targeting streptavidin sequenced by NGS. Listed are the 15 most abundant sequence patterns and their frequency in the final multiplexed selection cycle 8 (multiplexed C8) and the deconvolution cycle 9 using only methylpropane for DNA functionalization.

The nomenclature of the sequences was random.

pattern	random region	NGS frequency (multiplexed C8)	NGS frequency (methylpropane C10)
P2	GGGTCATGCCGGGTTGGAGTTTAAGGGGTTGGGGCAGGACCC	21,77%	8,25%
P1_2	AGGGGCGCTTTGGGGGAAATATGGGAGGTGGGGGGGGTCCCG	1,09%	3,70%
P1_3	AGGGGCACTTTGGGGGAAATATGGGAGGTGGGGGGGGTCCCG	0,59%	2,35%
P1_5	AGGGACGCTTTGGGGGGAATTTGGGAGGTGGGGGGGGTCCCG	0,39%	1,53%
P1_4	AGGGACGCTTTGGGGGAAATATGGGAGGTGGGGGGGGTCCCG	0,37%	1,10%
P2_4	GGGTCATGCCGGGTTGGAGTTTAAGAGGTTGGGGCAGGACCC	1,04%	0,77%
P1_5	AGGGACGCTTTGGGGGAAATTTGGGAGGTGGGGGGGGTCCCG	0,10%	0,61%
P1_10	AGGGACGCTTTGGGGGGAATGTGGGAGGTGGGGGGGGTCCCG	0,68%	0,54%
P1_11	AGGGACACTTTGGGGGAAATATGGGAGGTGGGGGGGGTCCCG	0,14%	0,49%
P1_12	AGGGACGCTTTGGGGGAAATGTGGGAGGTGGGGGGGGTCCCG	0,35%	0,47%
P2_1	GGGTCATGCCGGGTTGGAGTTTAAGGGGTTGGGGCAAGACCC	1,44%	0,47%
P1_13	AGGGGCGCTTTGGGGGAAATATGGGAGGTGGGGGAGGTCCCG	0,13%	0,46%
P1_7	AGGGACACTTTGGGGGGAATTTGGGAGGTGGGGGGGGTCCCG	0,11%	0,36%
P1_6	AGGGGCGCTTTGGGGGAAATTTGGGAGGTGGGGGGGGTCCCG	0,06%	0,35%
P2_5	GGGTCATGTCGGGTTGGAGTTTAAGGGGTTGGGGCAGGACCC	0,74%	0,29%

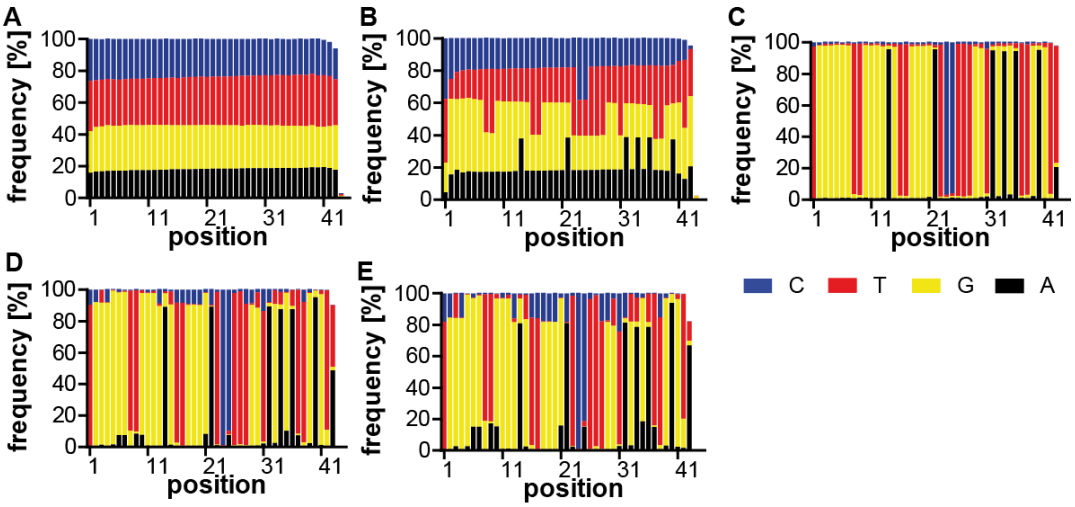

Supp. figure 1: Nucleotide distribution of the NGS analysis of $Na_v1.5$ D3 SELEX.

Nucleotide distribution at the different positions of the random region in the DNA of the starting library D3 (**A**). selection cycle 4 (**B**), selection cycle 6 (**C**), selection cycle 8 (**D**), and selection cycle 10 (**E**) of the selection targeting Nav1.5-HEK293. The alterations of nucleotide distribution were investigated by using the COMPAS (COMmonPAtternS) software from AptaIT GmbH (Planegg-Martinsried, Germany).

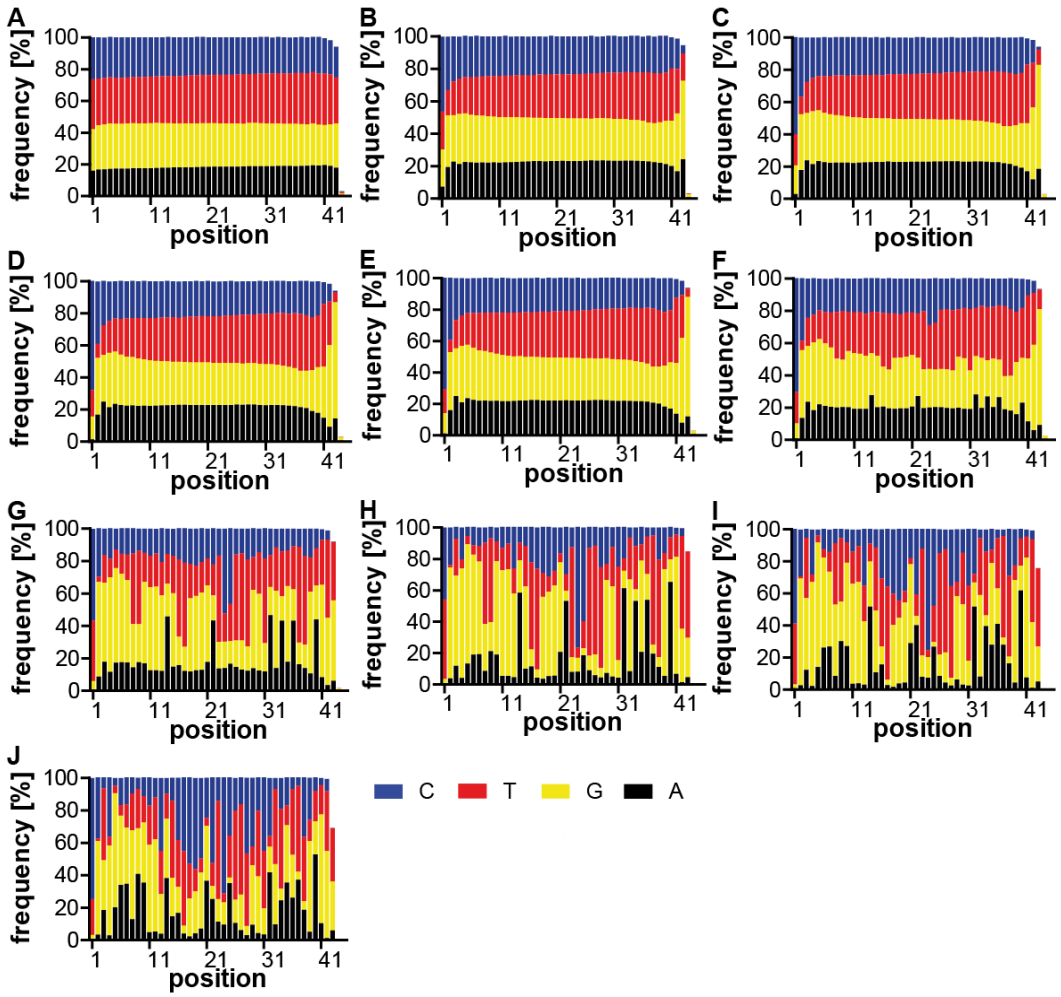

Supp. figure 2: Nucleotide distribution of the NGS analysis of $Na_v1.6$ D3 SELEX

Nucleotide distribution at the different positions of the random region in the DNA of the starting library D3 (**A**). selection cycle 2 (**B**), selection cycle 3 (**C**), selection cycle 4 (**D**), selection cycle 5 (**E**), selection cycle 6 (**F**), selection cycle 7 (**G**), selection cycle 8 (**H**), selection cycle 9 (**I**), and selection cycle 10 (**J**) of the selection targeting Nav1.6-HEK293. The alterations of nucleotide distribution were investigated by using the COMPAS (COMmonPAtternS) software from AptaIT GmbH (Planegg-Martinsried, Germany).

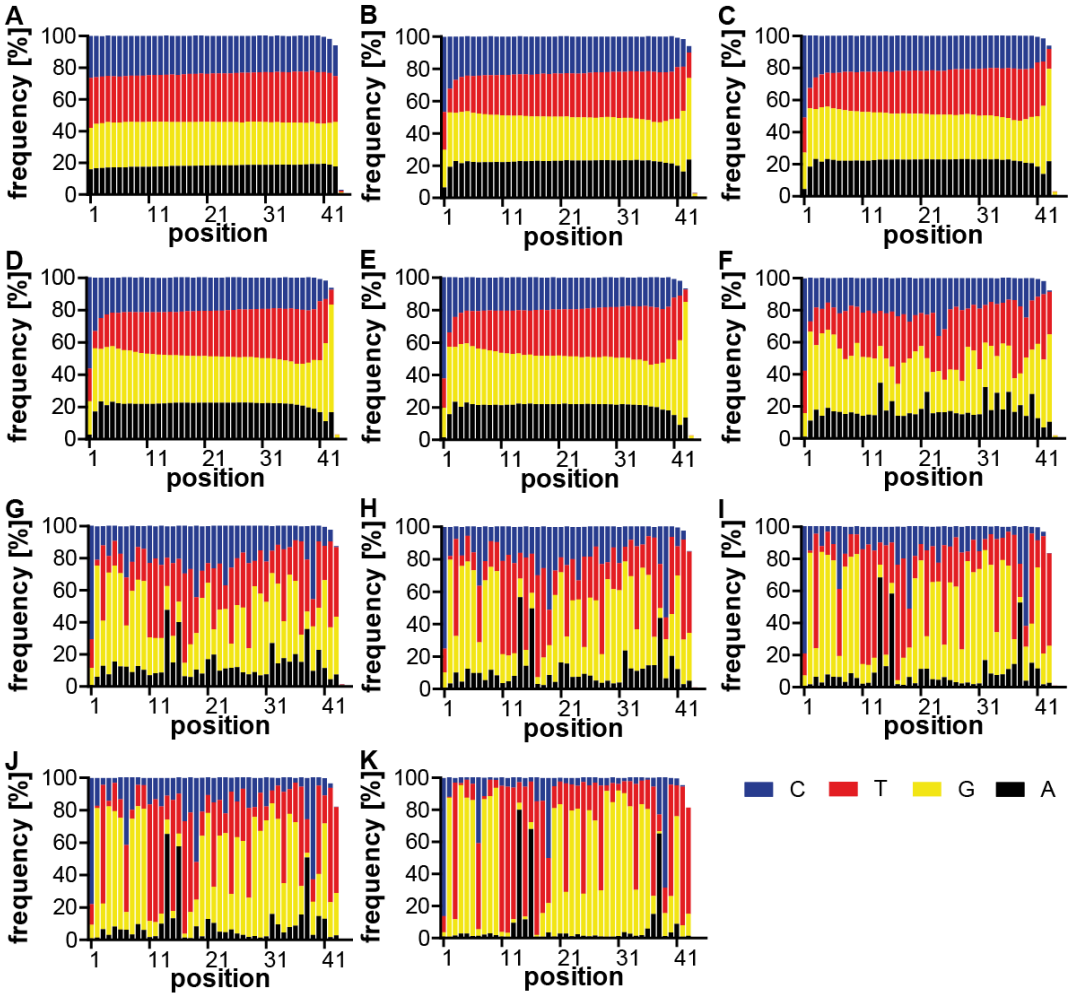

Supp. figure 3: Nucleotide distribution of the NGS analysis of HEK293 D3 SELEX

Nucleotide distribution at the different positions of the random region in the DNA of the starting library D3 (**A**). selection cycle 3 (**B**), selection cycle 4 (**C**), selection cycle 5 (**D**), selection cycle 6 (**E**), selection cycle 7 (**F**), selection cycle 8 (**G**), selection cycle 9 (**H**), selection cycle 10 (**I**), selection cycle 11 (**J**), and selection cycle 12 (**K**) of the branch point selection targeting HEK293. The alterations of nucleotide distribution were investigated by using the COMPAS (COMmonPAtternS) software from AptaIT GmbH (Planegg-Martinsried, Germany).

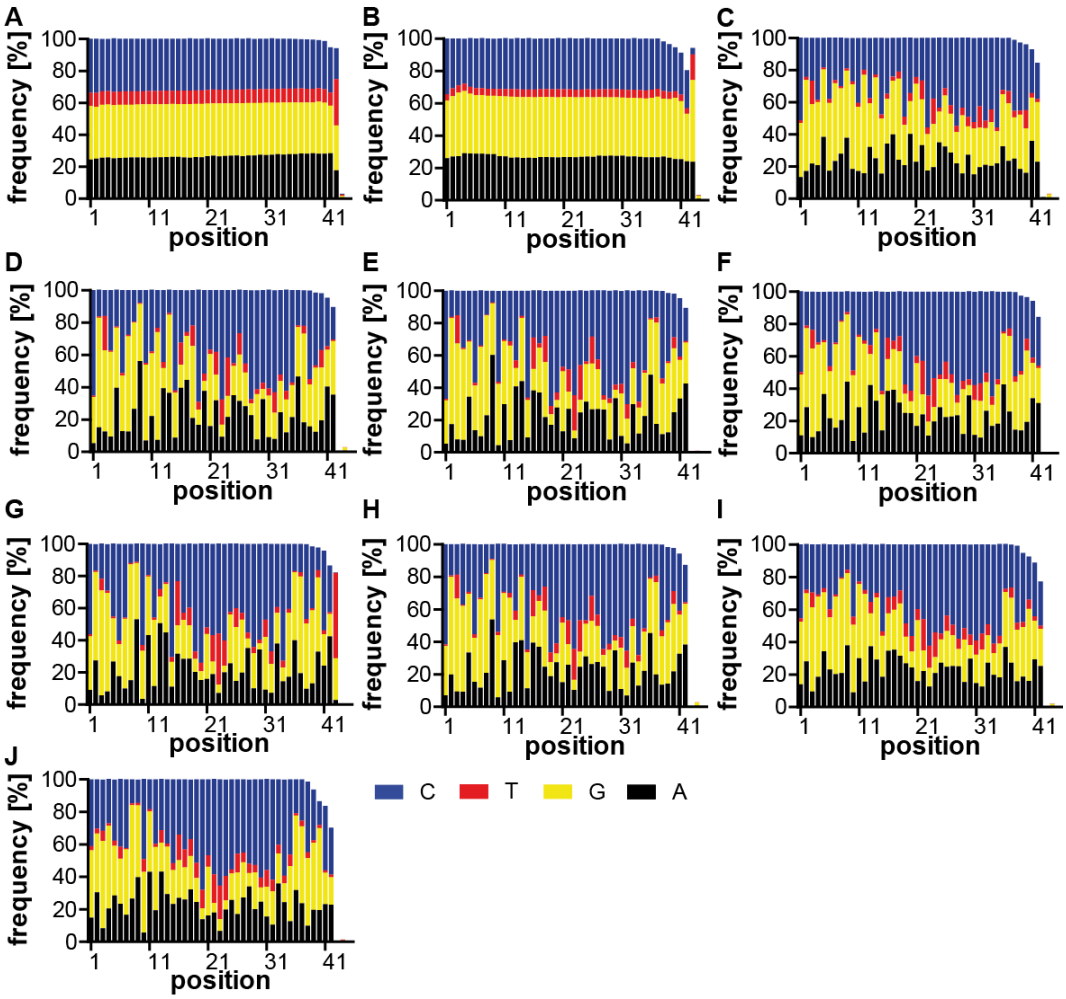

Supp. figure 4: Nucleotide distribution of the NGS analysis of cell-click-selection targeting $Na_v1.6$-HERK293. The DNA was functionalized with indole azide.

Nucleotide distribution at the different positions of the random region in the DNA of the starting library FT-0.35 (**A**). selection cycle 4 (**B**), selection cycle 6 (**C**), selection cycle 8 (**D**), selection cycle 9 (**E**), selection cycle 10 (**F**), selection cycle 12 (**G**) targeting $Na_v1.6$-HEK293. The selection cycle 9 (**H**), selection cycle 10 (**I**), and selection cycle 12 (**J**) targeting HEK293. The alterations of nucleotide distribution were investigated by using the COMPAS (COMmonPAtternS) software from AptaIT GmbH (Planegg-Martinsried, Germany).

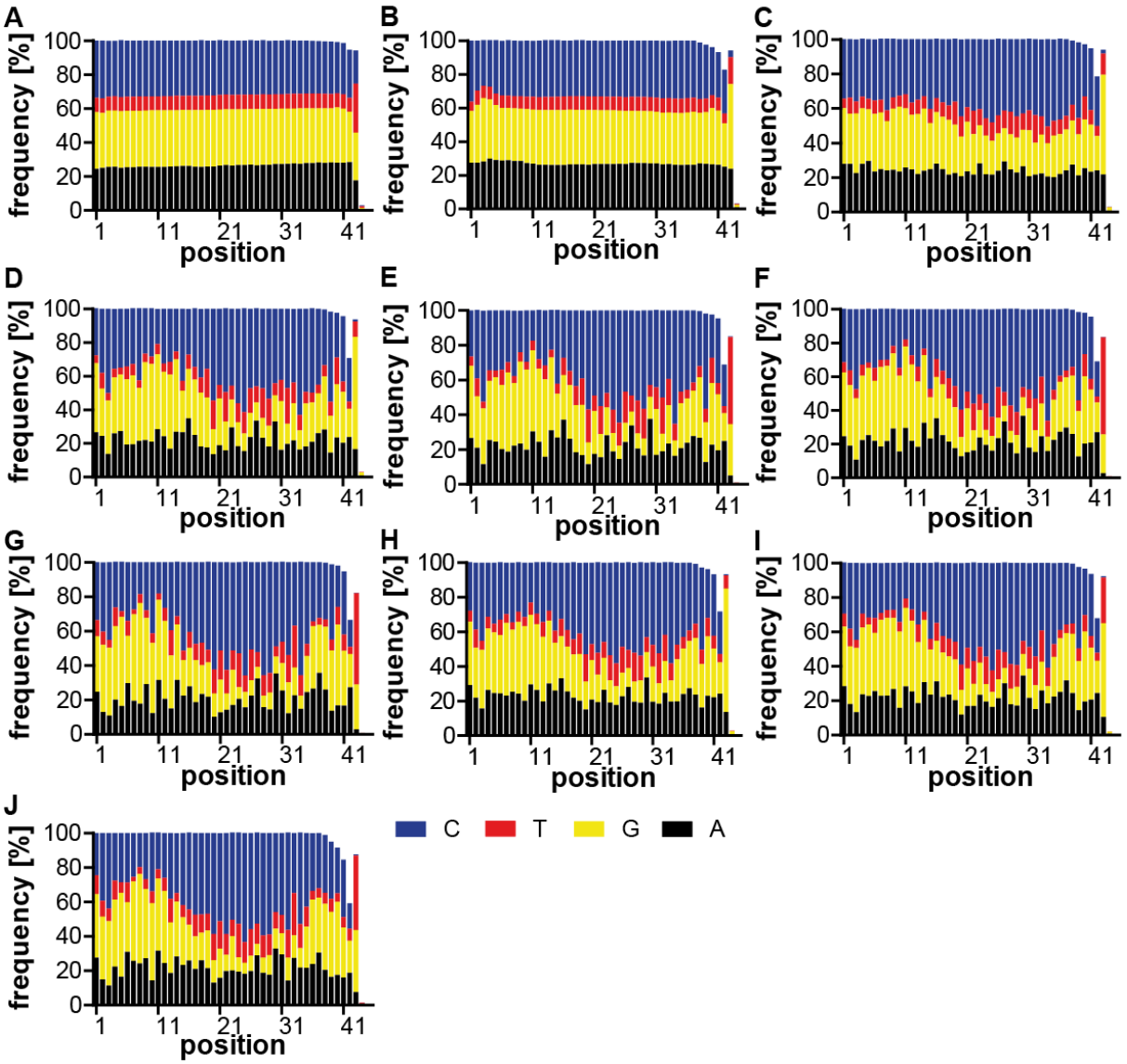

Supp. figure 5 Nucleotide distribution of the NGS analysis of cell-click-selection targeting $Na_v1.6$-HERK293. The DNA was functionalized with guanidine azide.

Nucleotide distribution at the different positions of the random region in the DNA of the starting library FT-0.35 (**A**). selection cycle 4 (**B**), selection cycle 6 (**C**), selection cycle 8 (**D**), selection cycle 9 (**E**), selection cycle 10 (**F**), selection cycle 12 (**G**) targeting $Na_v1.6$-HEK293. The selection cycle 9 (**H**), selection cycle 10 (**I**), and selection cycle 12 (**J**) targeting HEK293. The alterations of nucleotide distribution were investigated by using the COMPAS (COMmonPAtternS) software from AptaIT GmbH (Planegg-Martinsried, Germany).

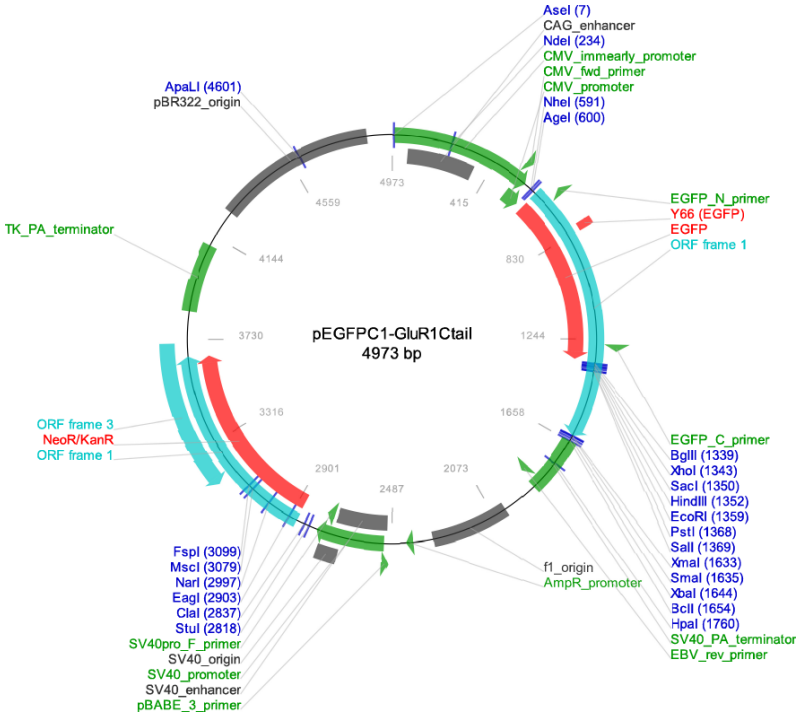

Supp. figure 6: Vector of pEGFPC1-GluR1 C tail plasmid (Addgene plasmid #32441, RRID:Addgene_32441)[158].

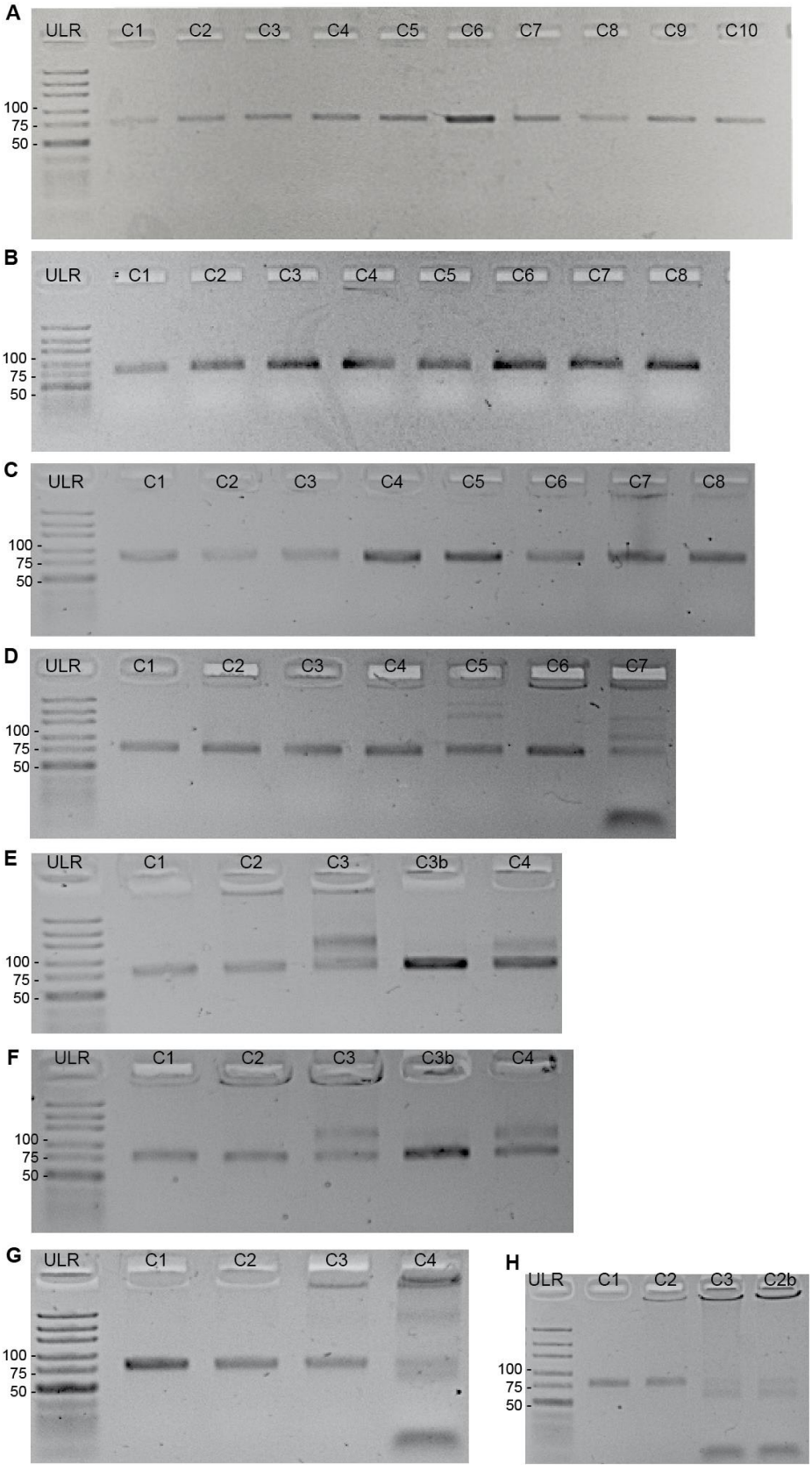

Supp. figure 7 Agarose gel electrophoresis analyses of the PCR products from all selections targeting C3-GFP.

(**A**) Indole azide (**1**) SELEX, (**B**) benzyl azide (**4**) SELEX, (**C**) benzofuran azide (**2**) SELEX, (**D**) azideethanamine (**10**) SELEX, (**E**) methylbenzyl azide (**6**) SELEX, (**F**) chlorobenzyl azide (**5**) SELEX, (**G**) methylpropane azide (**9**) SELEX, (**H**) naphthaline azide (**8**) SELEX.

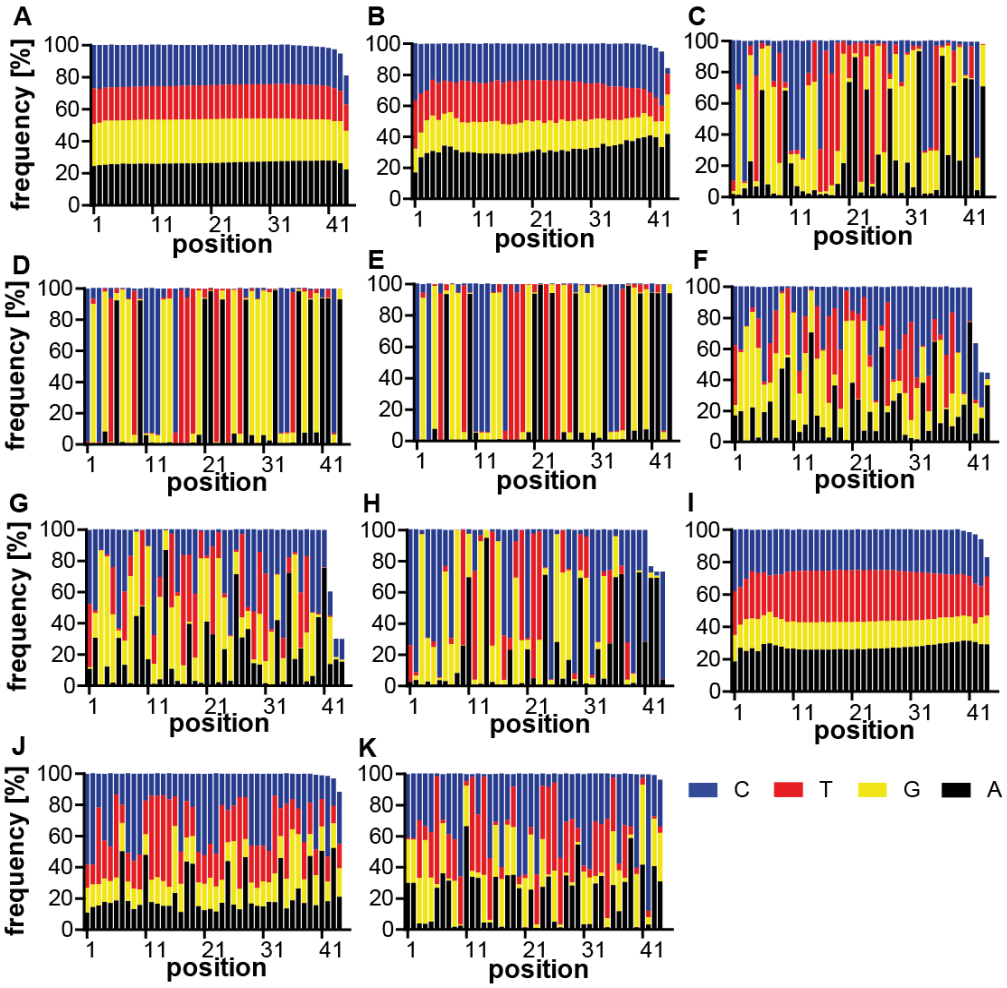

Supp. figure 8: Nucleotide distribution of the NGS analyses of click-selections targeting C3-GFP.

Nucleotide distribution at the different positions of the random region in the DNA of the starting library OW1 (**A**), selection cycle 4 (**B**), selection cycle 6 (**C**), selection cycle 8 (**D**), and selection cycle 6 (**E**) using indole (**1**) for DNA functionalization. The selection cycle 4 (**F**), selection cycle 6 (**G**), selection cycle 8 (**H**) using benzofuran (**2**). The selection cycle 4 (**I**), selection cycle 6 (**J**), selection cycle 8 (**K**) using benzyl (**4**).

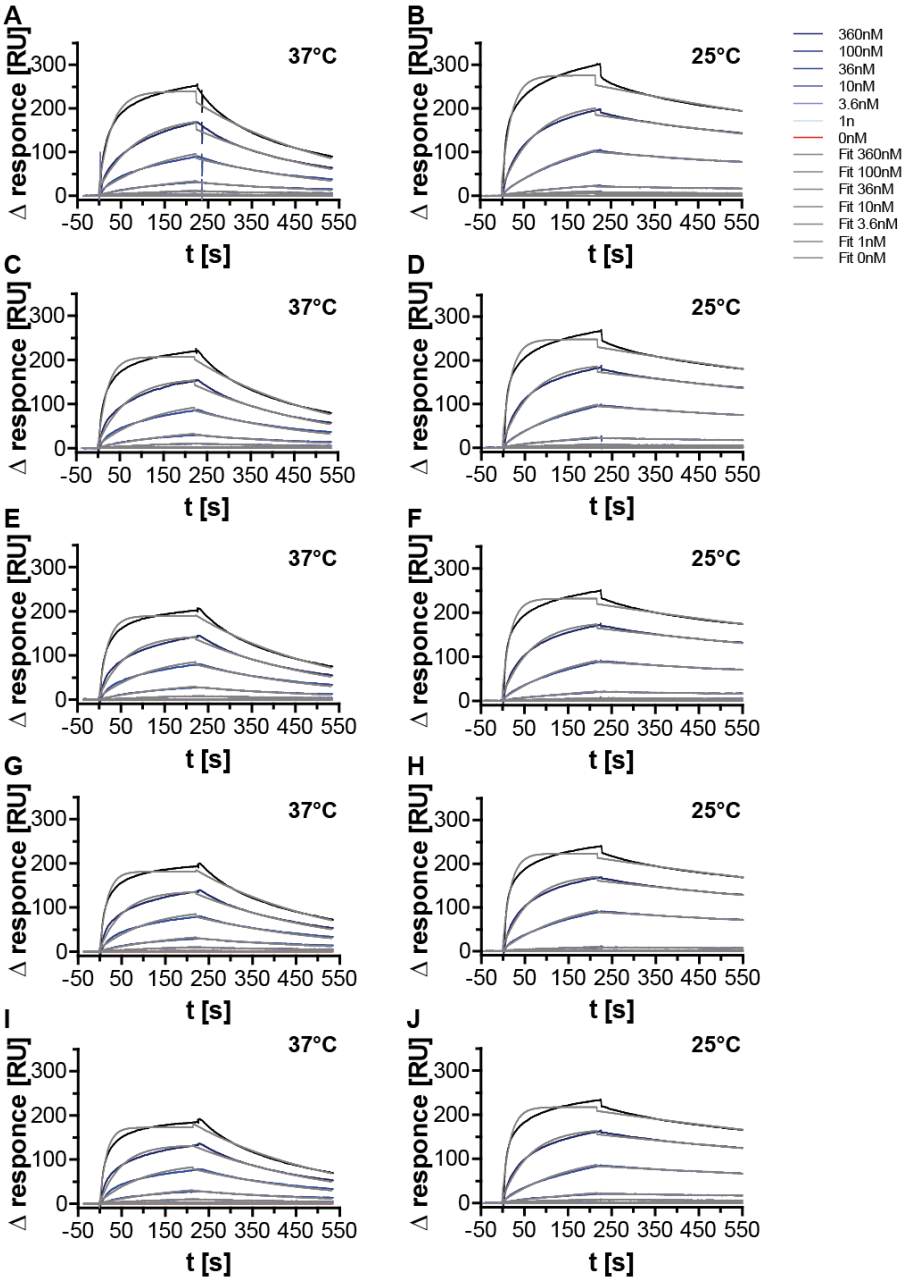

Supp. figure 9 Surface plasmon resonance spectroscopy (SPR) measurements of the clickmers I10 (1) at 37°C and 25°C.

Shown are the surface plasmon resonance spectroscopy (SPR) measurements of the clickmer I10 (**1**) at 37°C (**A**, **C**, **E**, **G**, **I**) and at 25°C (**B**, **D**, **F**, **H**, **J**) targeting C3-GFP. The biotinylated clickmer were immobilized on a streptavidin-coated SPR sensor chip and C3-GFP in different concentration was used as the analyte.

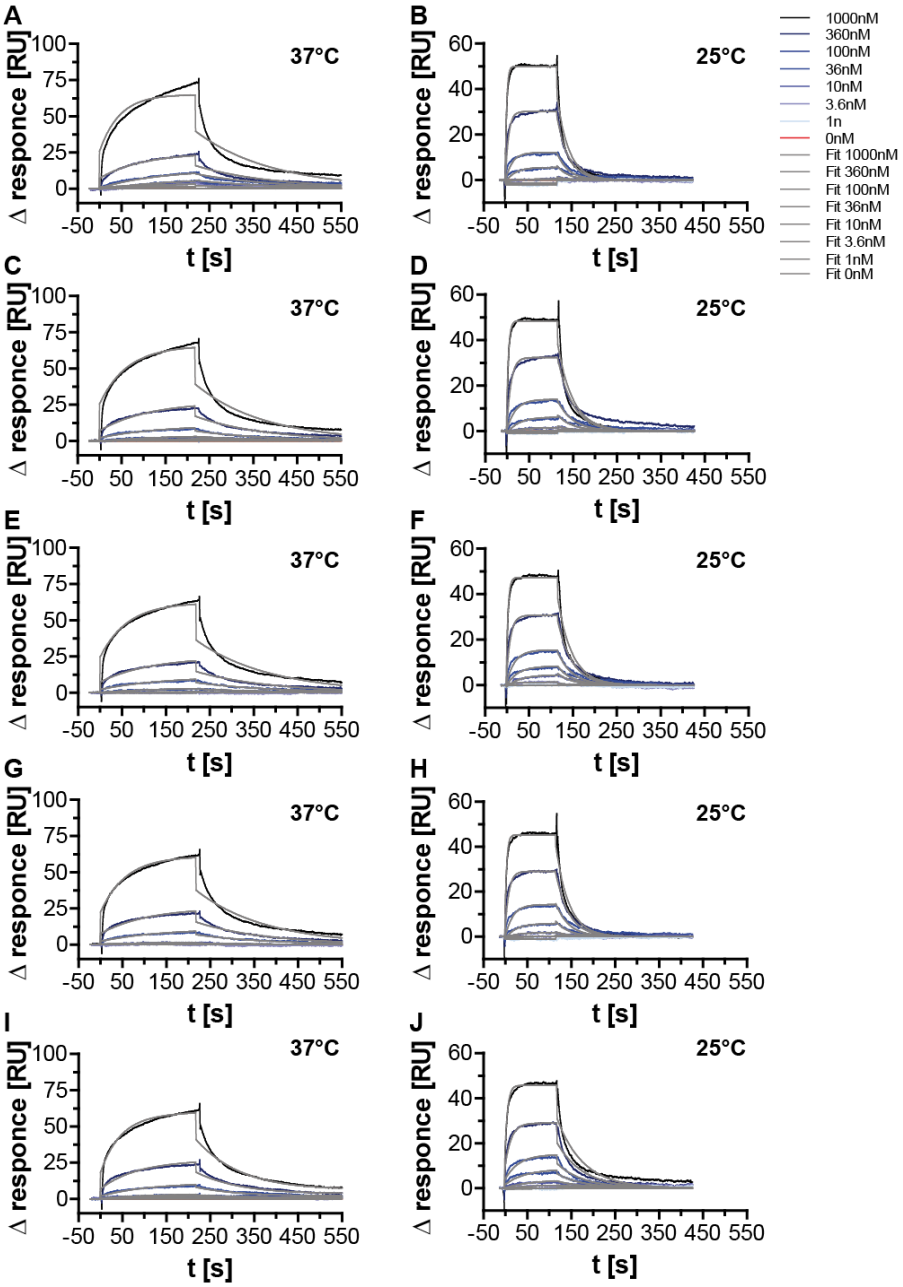

Supp. figure 10 Surface plasmon resonance spectroscopy (SPR) measurements of the clickmers B33 (4) at 37°C and 25°C.

Shown are the surface plasmon resonance spectroscopy (SPR) measurements of the clickmer B33 (**4**) at 37°C (**A**, **C**, **E**, **G**, **I**) and at 25°C (**B**, **D**, **F**, **H**, **J**) targeting C3-GFP. The biotinylated clickmer were immobilized on a streptavidin-coated SPR sensor chip and C3-GFP in different concentration was used as the analyte.

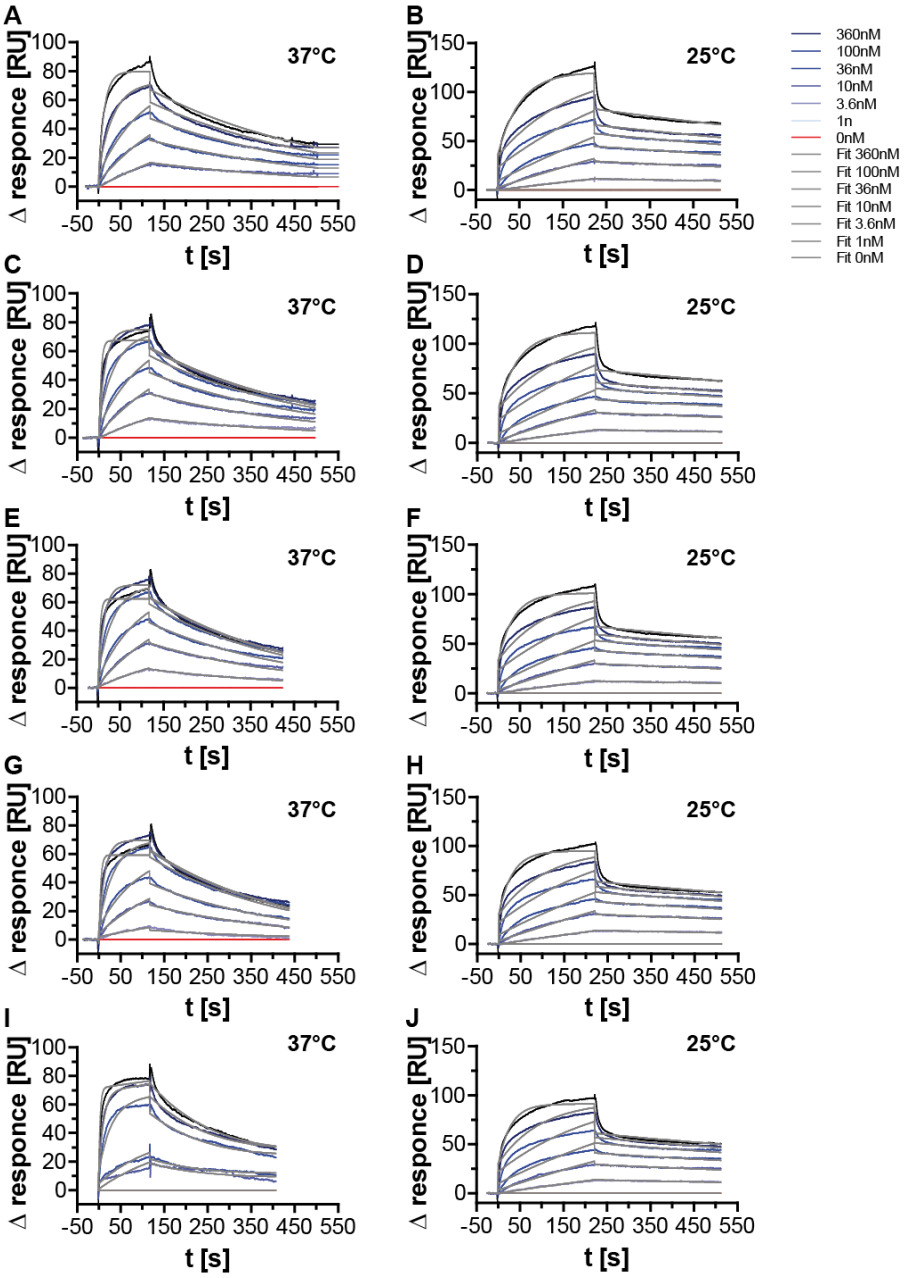

Supp. figure 11 Surface plasmon resonance spectroscopy (SPR) measurements of the clickmers F8 (2) at 37°C and 25°C.

Shown are the Surface Plasmon Resonance spectroscopy (SPR) measurements of the clickmer F8 (**2**) at 37°C (**A**, **C**, **E**, **G**, **I**) and at 25°C (**B**, **D**, **F**, **H**, **J**) targeting C3-GFP. The biotinylated clickmer were immobilized on a streptavidin-coated SPR sensor chip and C3-GFP in different concentration was used as the analyte.

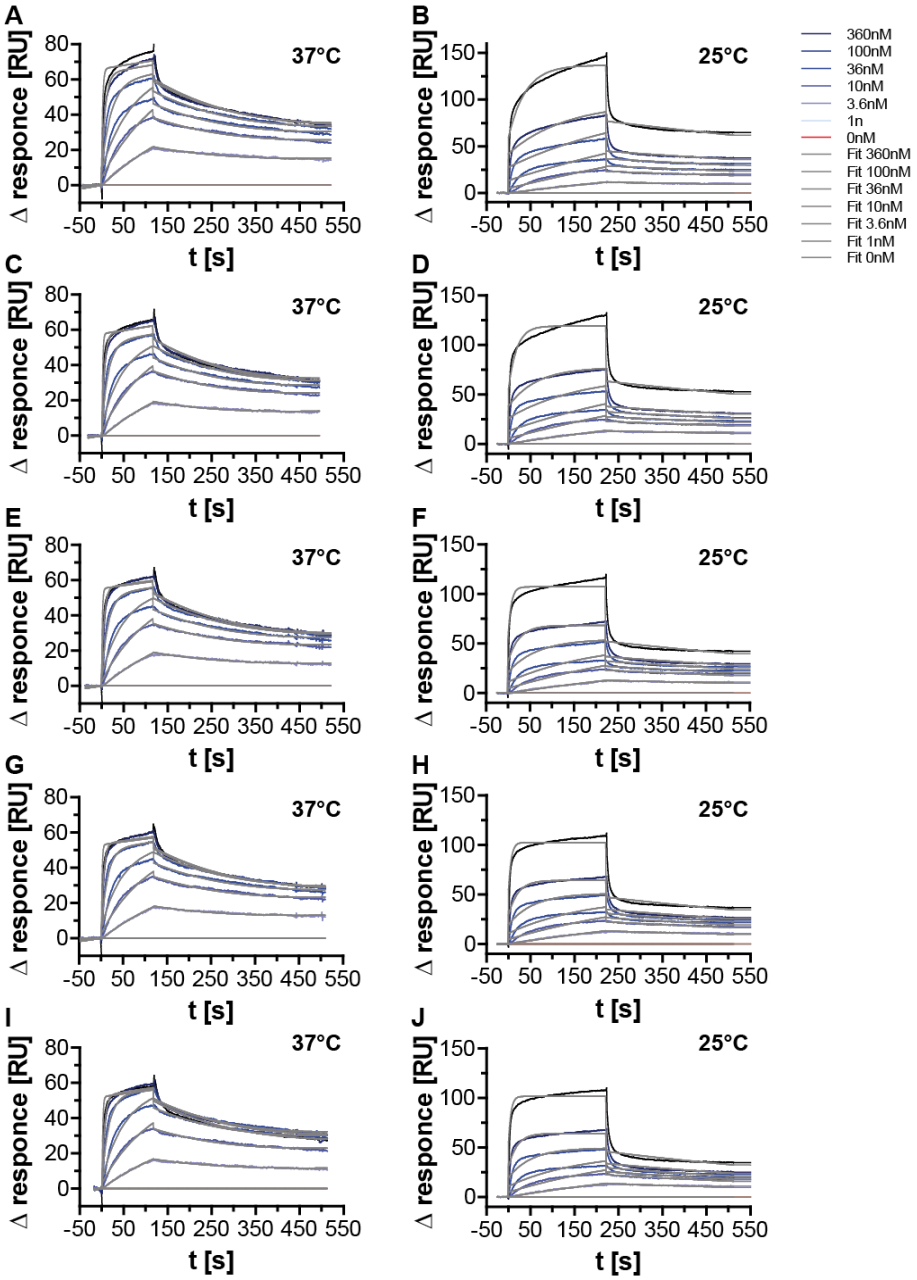

Supp. figure 12 Surface plasmon resonance spectroscopy (SPR) measurements of the clickmers F20 (2) at 37°C and 25°C.

Shown are the Surface Plasmon Resonance spectroscopy (SPR) measurements of the clickmer F20 (**2**) at 37°C (**A**, **C**, **E**, **G**, **I**) and at 25°C (**B**, **D**, **F**, **H**, **J**) targeting C3-GFP. The biotinylated clickmer were immobilized on a streptavidin-coated SPR sensor chip and C3-GFP in different concentration was used as the analyte.

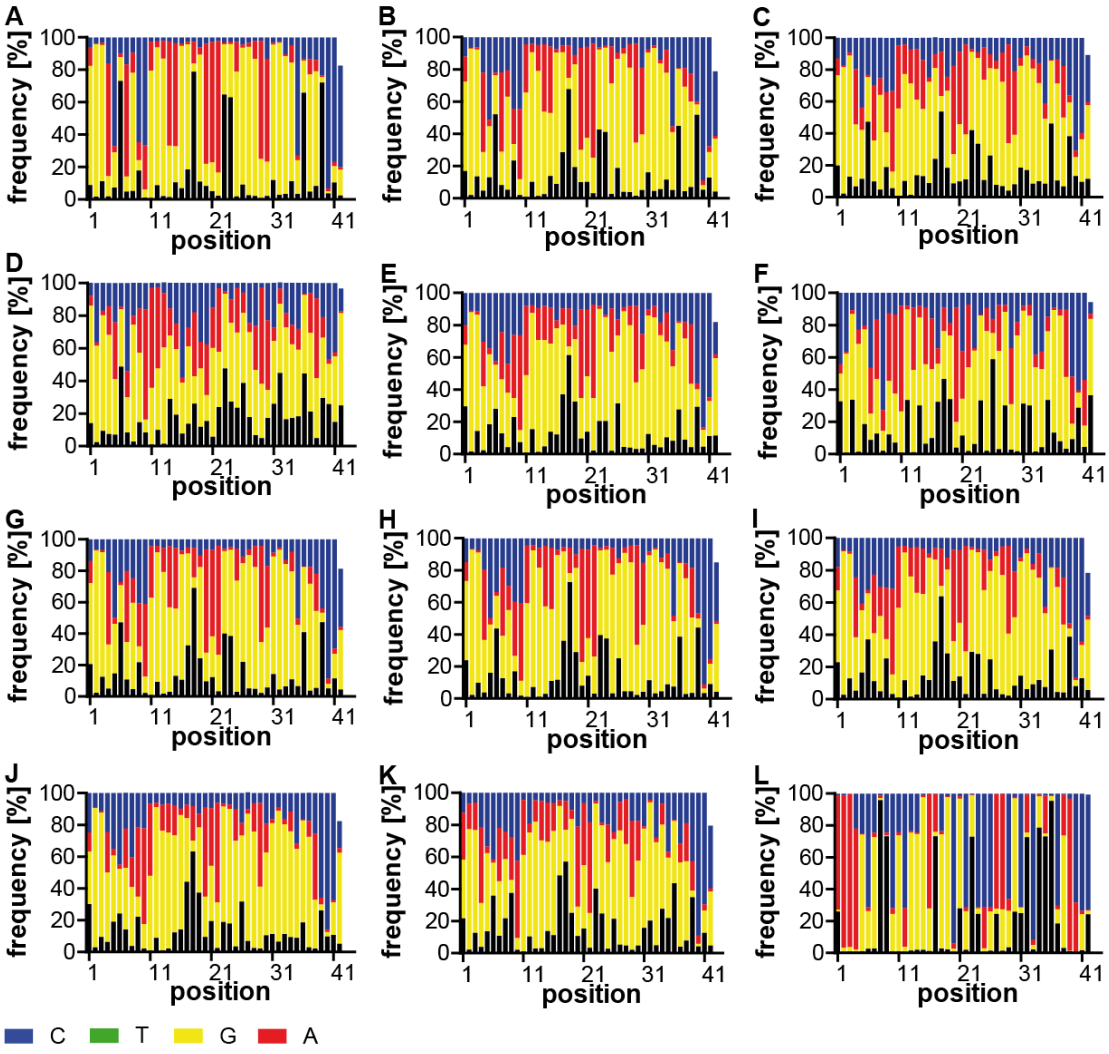

Supp. figure 13: Nucleotide distribution of the NGS analysis of multiplex click-SELEX targeting streptavidin.

Nucleotide distribution at the different positions of the random region in the DNA of the selection cycle 6 (**A**), cycle 8 (**B**), and deconvolution cycle 9 (**C**) and 10 (**D**) using the azides indole (**1**), and deconvolution cycle 9 (**E**) and 10 (**F**) using benzyl (**4**), and deconvolution cycle 9 (**G**) and 10 (**H**) using phenol (**7**), and deconvolution cycle 9 (**I**) and 10 (**J**) using methylpropane (**9**), and deconvolution cycle 9 (**K**) and 10 (**L**) using guanidine (**11**).

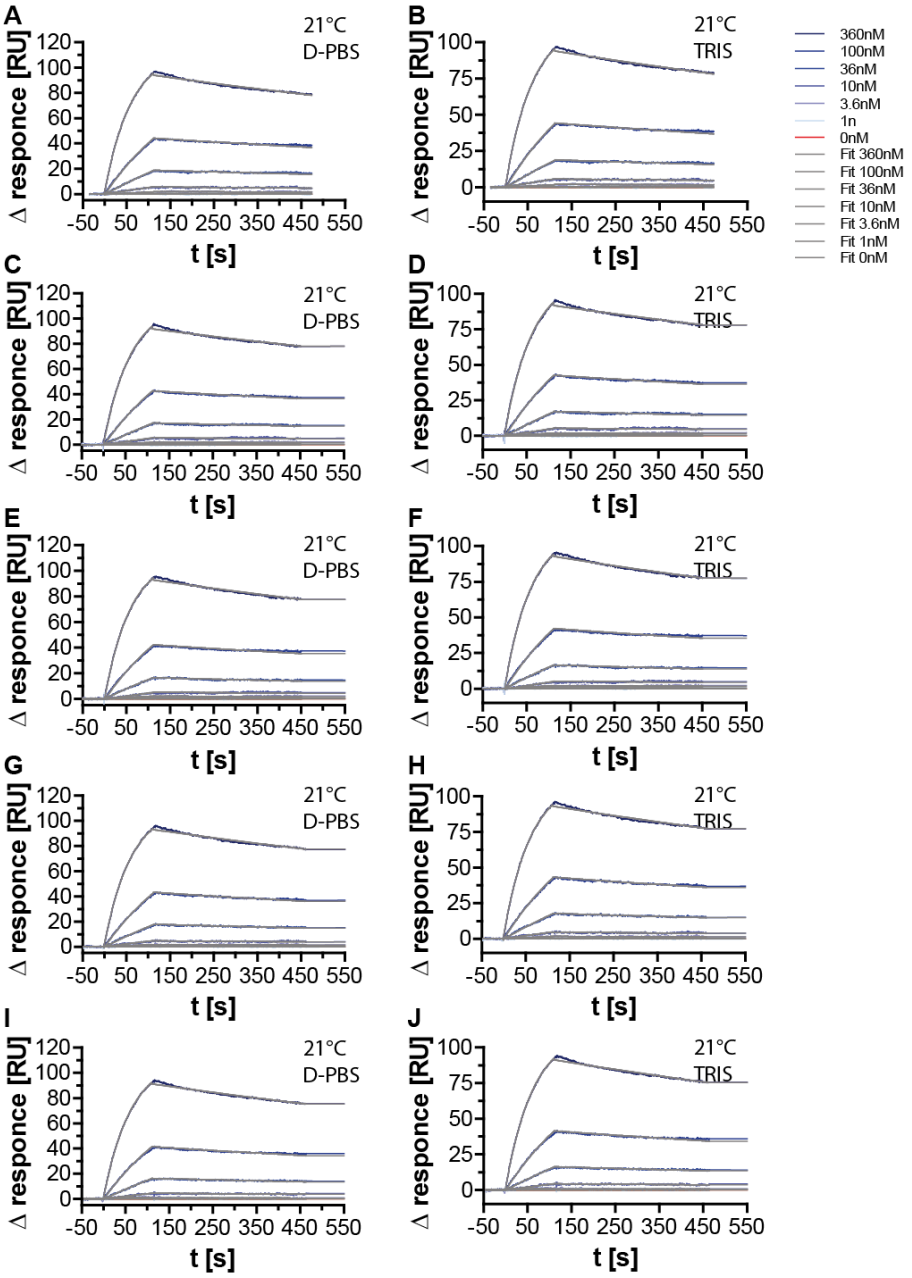

Supp. figure 14 Surface plasmon resonance spectroscopy (SPR) measurements of the clickmers Aptamer33 at 21°C in D-PBS and TRIS buffer.

Shown are the surface plasmon resonance spectroscopy (SPR) measurements of the aptamer 33 at 21°C in D-PBS buffer system (**A**, **C**, **E**, **G**, **I**) and in TRIS buffer system (**B**, **D**, **F**, **H**, **J**) targeting streptavidin. The aptamer was immobilized on an SPR sensor chip and streptavidin in different concentration was used as the analyte.

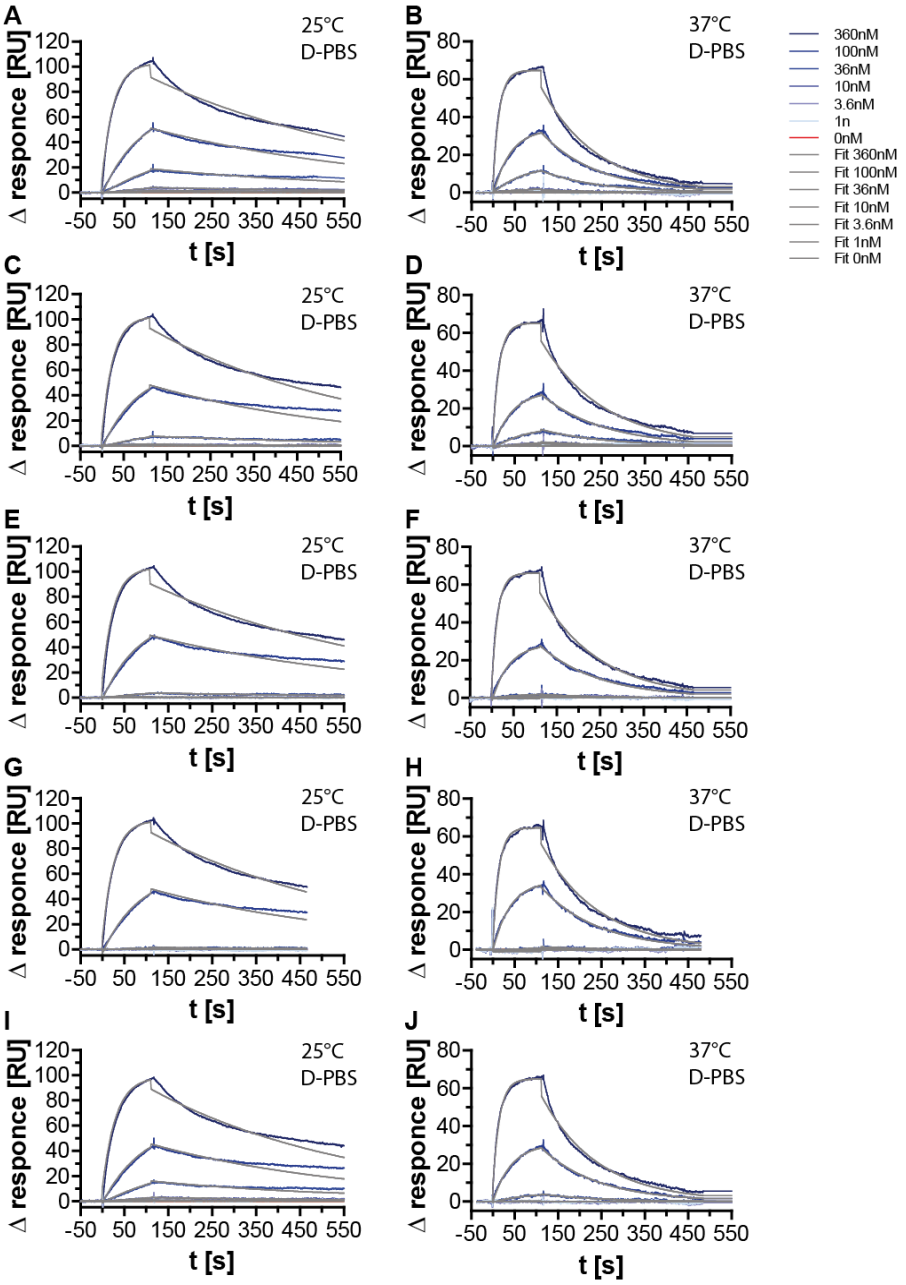

Supp. figure 15 Surface plasmon resonance spectroscopy (SPR) measurements of the clickmers Aptamer33 at 25°C and 37°C in D-PBS buffer.

Shown are the Surface Plasmon Resonance spectroscopy (SPR) measurements of the aptamer 33 in D-PBS buffer system at 25°C (**A**, **C**, **E**, **G**, **I**) and at 37°C (**B**, **D**, **F**, **H**, **J**) targeting streptavidin. The aptamer was immobilized on an SPR sensor chip and streptavidin in different concentration was used as the analyte.

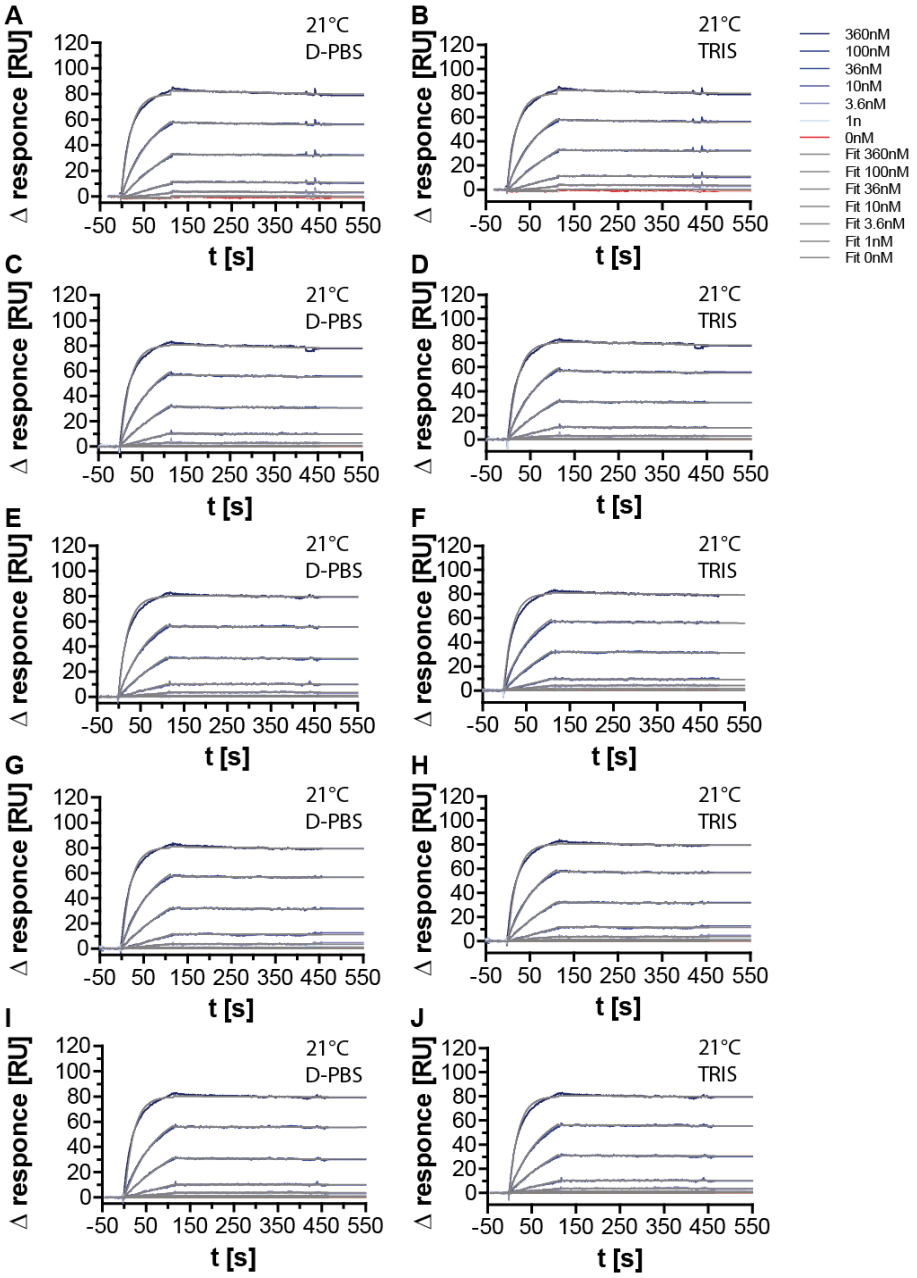

Supp. figure 16 Surface plasmon resonance spectroscopy (SPR) measurements of the clickmers B1 (4) at 21°C in D-PBS and TRIS buffer.

Shown are the Surface Plasmon Resonance spectroscopy (SPR) measurements of the clickmer B1 (**4**) at 21°C in D-PBS buffer system (**A**, **C**, **E**, **G**, **I**) and in TRIS buffer system (**B**, **D**, **F**, **H**, **J**) targeting streptavidin. The aptamer was immobilized on an SPR sensor chip and streptavidin in different concentration was used as the analyte.

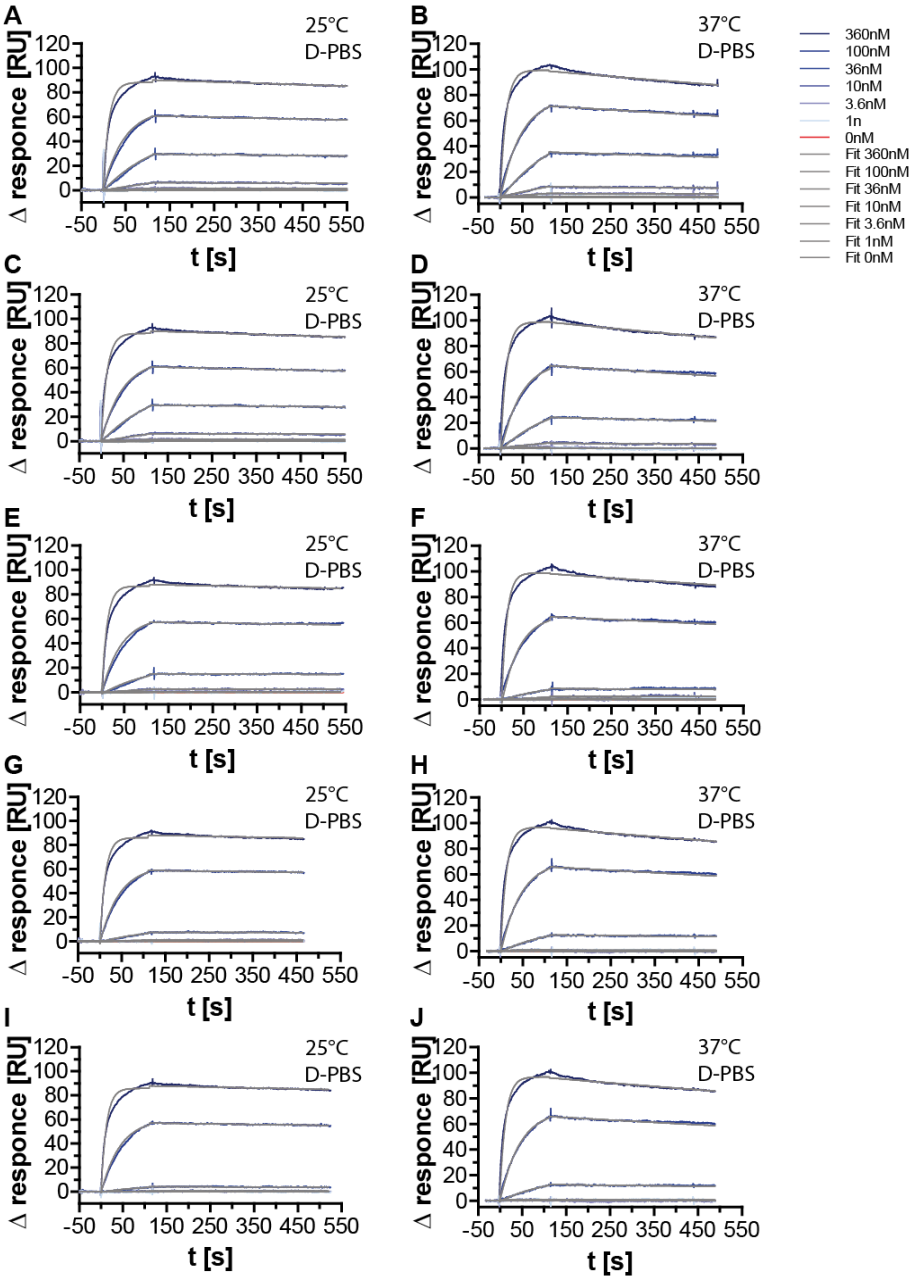

Supp. figure 17 Surface plasmon resonance spectroscopy (SPR) measurements of the clickmers B1 (4) at 25°C and 37°C in D-PBS buffer.

Shown are the Surface Plasmon Resonance spectroscopy (SPR) measurements of the clickmer B1 (**4**) in D-PBS buffer system at 25°C (**A**, **C**, **E**, **G**, **I**) and at 37°C (**B**, **D**, **F**, **H**, **J**) targeting streptavidin. The aptamer was immobilized on an SPR sensor chip and streptavidin in different concentration was used as the analyte.

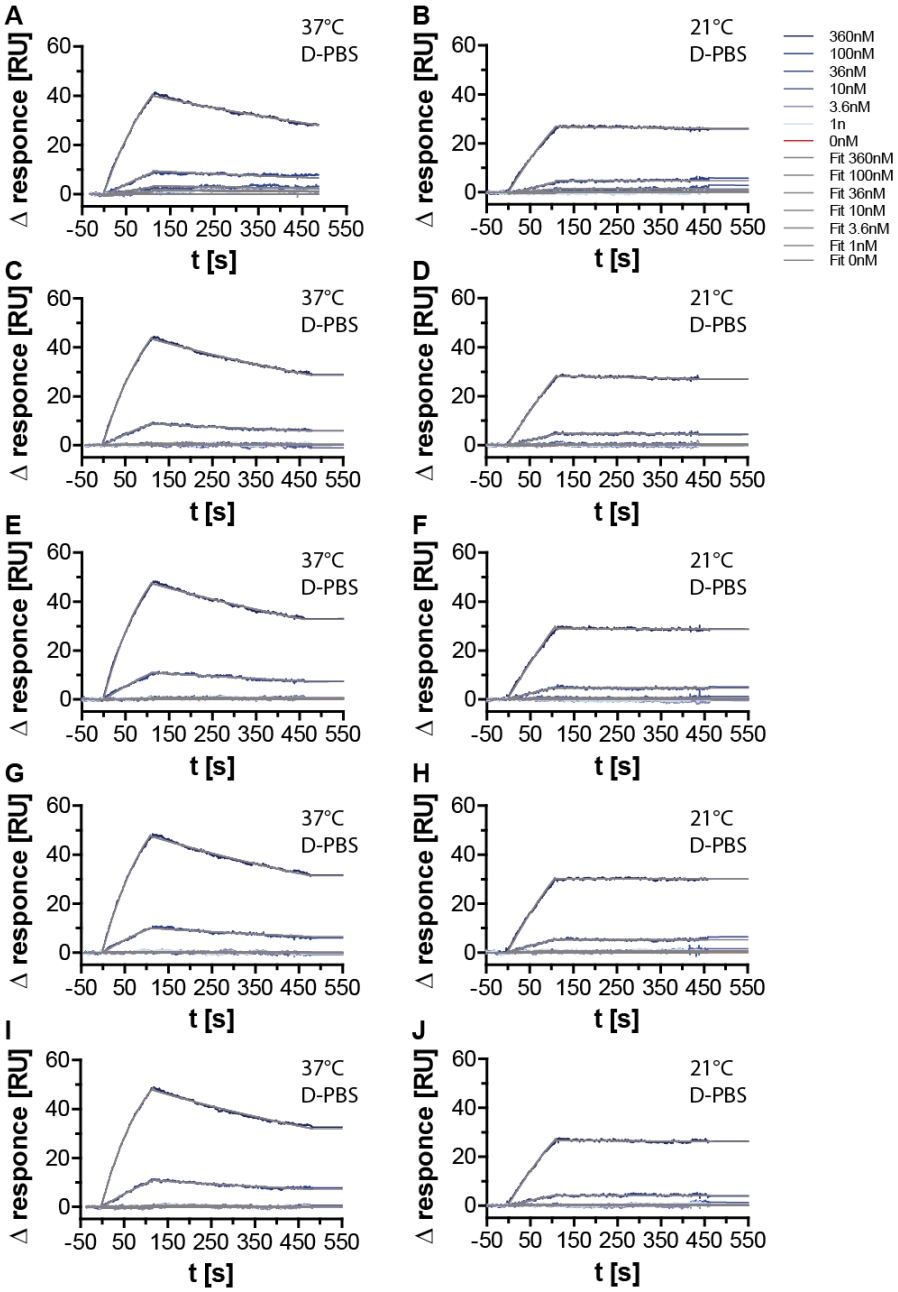

Supp. figure 18 Surface plasmon resonance spectroscopy (SPR) measurements of the clickmers G1 at 37°C and 21°C in D-PBS buffer.

Shown are the Surface Plasmon Resonance spectroscopy (SPR) measurements of the aptamer G1 in D-PBS buffer system at 37°C (**A**, **C**, **E**, **G**, **I**) and at 21°C (**B**, **D**, **F**, **H**, **J**) targeting streptavidin. The aptamer was immobilized on an SPR sensor chip and streptavidin in different concentration was used as the analyte.

11. List of abbreviations

Table 11.1 List of abbreviations.

Abbreviation	Explanation
BSA	bovine serum albumin
bp	base pairs
C3-GFP	cycle3-green fluorescent protein
$CaCl_2$	calcium chloride
DAPI	4',6-diamidino-2-phenylindole
ddH_2O	distilled water
DNA	deoxyribonucleic acid
dNTP	deoxyribonucleoside triphosphate
e.g.	exempli gratia (for example)
EDTA	ethylenediaminetetraacetic acid
EdU	5-ethynyl-2'-deoxyuridine
EdUTP	5-ethynyl-5'-O-triphosphate-2'-deoxyuridine
EtOH	ethanol
FACS	fluorescence-activated cell sorting
g	gram
HEK293	human embryonic kidney 293 cells
HPLC	high-performance liquid chromatography
K_D	dissociation constant
k_{off} rate	dissociation rate constant
k_{on} rate	association rate constant
L	liter
LC-MS	liquid chromatography-mass spectrometry
M	molar
MFI	mean fluorescence intensity
$MgCl_2$	magnesium chloride
NaCl	sodium chloride
NaOAc	sodium acetate
NMR	nuclear magnetic resonance spectroscopy
nt	nucleotide
NTC	no template control of PCR reactions
PBS	phosphate-buffered saline
PCR	polymerase chain reaction
pH	negative decade logarithm of the hydrogen ion concentration
PNK	polynucleotide kinase
rpm	rounds per minute
RT	room temperature (25°C)
SD	standard deviation
sec	second
SELEX	systematic evolution of ligands by exponential enrichment
SPR	surface plasmon resonance
TBE	Tris-Borate-EDTA buffer
THPTA	Tris(4-(3-hydroxy-propyl)-[1,2,3]triazol-1-ylmethyl)amine
UV	ultraviolet
V	volt

12. List of figures

13. List of Tables

14. Bibliography

1 LeDoux, J. *The emotional brain*. (SIMON & SCHUSTER PAPERBACKS, 1996).

2 Alexander, S. P. *et al.* THE CONCISE GUIDE TO PHARMACOLOGY 2017/18: Overview. *British journal of pharmacology* **174 Suppl 1**, S1-S16, doi:10.1111/bph.13882 (2017).

3 Alexander, S. P. *et al.* THE CONCISE GUIDE TO PHARMACOLOGY 2017/18: Voltage-gated ion channels. *British journal of pharmacology* **174 Suppl 1**, S160-S194, doi:10.1111/bph.13884 (2017).

4 Pendergrast, P. S., Marsh, H. N., Grate, D., Healy, J. M. & Stanton, M. Nucleic acid aptamers for target validation and therapeutic applications. *Journal of biomolecular techniques : JBT* **16**, 224-234 (2005).

5 Ellington, A. D. & Szostak, J. W. In vitro selection of RNA molecules that bind specific ligands. *Nature* **346**, 818-822, doi:10.1038/346818a0 (1990).

6 Tuerk, C. & Gold, L. Systematic evolution of ligands by exponential enrichment: RNA ligands to bacteriophage T4 DNA polymerase. *Science* **249**, 505-510 (1990).

7 Mayer, G. The chemical biology of aptamers. *Angewandte Chemie* **48**, 2672-2689, doi:10.1002/anie.200804643 (2009).

8 Robertson, D. L. & Joyce, G. F. Selection in vitro of an RNA enzyme that specifically cleaves single-stranded DNA. *Nature* **344**, 467-468, doi:10.1038/344467a0 (1990).

9 Liu, J. *et al.* Recent developments in protein and cell-targeted aptamer selection and applications. *Current medicinal chemistry* **18**, 4117-4125 (2011).

10 Hermann, T. & Patel, D. J. Adaptive recognition by nucleic acid aptamers. *Science* **287**, 820-825 (2000).

11 Rowsell, S. *et al.* Crystal structures of a series of RNA aptamers complexed to the same protein target. *Nature structural biology* **5**, 970-975, doi:10.1038/2946 (1998).

12 Nagai, K. RNA-protein complexes. *Current opinion in structural biology* **6**, 53-61 (1996).

13 Uhlenbeck, O. C., Pardi, A. & Feigon, J. RNA structure comes of age. *Cell* **90**, 833-840 (1997).

14 Cho, E. J., Lee, J. W. & Ellington, A. D. Applications of aptamers as sensors. *Annual review of analytical chemistry* **2**, 241-264, doi:10.1146/annurev.anchem.1.031207.112851 (2009).

15 Ellington, A. D. & Szostak, J. W. Selection in vitro of single-stranded DNA molecules that fold into specific ligand-binding structures. *Nature* **355**, 850-852, doi:10.1038/355850a0 (1992).

16 Tuerk, C., MacDougal, S. & Gold, L. RNA pseudoknots that inhibit human immunodeficiency virus type 1 reverse transcriptase. *Proceedings of the National Academy of Sciences of the United States of America* **89**, 6988-6992 (1992).

17 Stoltenburg, R., Reinemann, C. & Strehlitz, B. FluMag-SELEX as an advantageous method for DNA aptamer selection. *Analytical and bioanalytical chemistry* **383**, 83-91, doi:10.1007/s00216-005-3388-9 (2005).

18 Dickinson, H., Lukasser, M., Mayer, G. & Huttenhofer, A. Cell-SELEX: In Vitro Selection of Synthetic Small Specific Ligands. *Methods in molecular biology* **1296**, 213-224, doi:10.1007/978-1-4939-2547-6_20 (2015).

19 Meyer, C., Hahn, U. & Rentmeister, A. Cell-specific aptamers as emerging therapeutics. *Journal of nucleic acids* **2011**, 904750, doi:10.4061/2011/904750 (2011).

20 Mayer, G. *et al.* From selection to caged aptamers: identification of light-dependent ssDNA aptamers targeting cytohesin. *Bioorganic & medicinal chemistry letters* **19**, 6561-6564, doi:10.1016/j.bmcl.2009.10.032 (2009).

21 Seyfried, P., Eiden, L., Grebenovsky, N., Mayer, G. & Heckel, A. *Photo-Tethers for the (Multi-)Cyclic, Conformational Caging of Long Oligonucleotides* (2016).

22 Pinto, A. *et al.* Functional detection of proteins by caged aptamers. *ACS chemical biology* **7**, 360-366, doi:10.1021/cb2003835 (2012).

23 Stoltenburg, R., Reinemann, C. & Strehlitz, B. SELEX--a (r)evolutionary method to generate high-affinity nucleic acid ligands. *Biomolecular engineering* **24**, 381-403, doi:10.1016/j.bioeng.2007.06.001 (2007).

24 Majumder, P., Gomes, K. N. & Ulrich, H. Aptamers: from bench side research towards patented molecules with therapeutic applications. *Expert opinion on therapeutic patents* **19**, 1603-1613, doi:10.1517/13543770903313746 (2009).

25 Oehler, S., Alex, R. & Barker, A. Is nitrocellulose filter binding really a universal assay for protein-DNA interactions? *Analytical biochemistry* **268**, 330-336, doi:10.1006/abio.1998.3056 (1999).

26 Pfeiffer, F. *et al.* Identification and characterization of nucleobase-modified aptamers by click-SELEX. *Nature protocols* **13**, 1153-1180, doi:10.1038/nprot.2018.023 (2018).

27 Soldevilla, M. M. *et al.* Identification of LAG3 high affinity aptamers by HT-SELEX and Conserved Motif Accumulation (CMA). *PloS one* **12**, e0185169, doi:10.1371/journal.pone.0185169 (2017).

28 Kowalska, E., Bartnicki, F., Pels, K. & Strzalka, W. The impact of immobilized metal affinity chromatography (IMAC) resins on DNA aptamer selection. *Analytical and bioanalytical chemistry* **406**, 5495-5499, doi:10.1007/s00216-014-7937-y (2014).

29 Tolle, F., Brandle, G. M., Matzner, D. & Mayer, G. A Versatile Approach Towards Nucleobase-Modified Aptamers. *Angewandte Chemie* **54**, 10971-10974, doi:10.1002/anie.201503652 (2015).

30 Bruno, J. G. In vitro selection of DNA to chloroaromatics using magnetic microbead-based affinity separation and fluorescence detection. *Biochemical and biophysical research communications* **234**, 117-120, doi:10.1006/bbrc.1997.6517 (1997).

31 Darmostuk, M., Rimpelova, S., Gbelcova, H. & Ruml, T. Current approaches in SELEX: An update to aptamer selection technology. *Biotechnology advances*, doi:10.1016/j.biotechadv.2015.02.008 (2015).

32 Turcheniuk, K., Tarasevych, A. V., Kukhar, V. P., Boukherroub, R. & Szunerits, S. Recent advances in surface chemistry strategies for the fabrication of functional iron oxide based magnetic nanoparticles. *Nanoscale* **5**, 10729-10752, doi:10.1039/C3NR04131J (2013).

33 Yildirim, M. A., Goh, K. I., Cusick, M. E., Barabasi, A. L. & Vidal, M. Drug-target network. *Nature biotechnology* **25**, 1119-1126, doi:10.1038/nbt1338 (2007).

34 Rahimizadeh, K. *et al.* Development of Cell-Specific Aptamers: Recent Advances and Insight into the Selection Procedures. *Molecules* **22**, doi:10.3390/molecules22122070 (2017).

35 Sefah, K., Shangguan, D., Xiong, X., O'Donoghue, M. B. & Tan, W. Development of DNA aptamers using Cell-SELEX. *Nature protocols* **5**, 1169-1185, doi:10.1038/nprot.2010.66 (2010).

36 Ye, M. *et al.* Generating aptamers by cell-SELEX for applications in molecular medicine. *International journal of molecular sciences* **13**, 3341-3353, doi:10.3390/ijms13033341 (2012).

37 Dua, P., Kim, S. & Lee, D. K. Nucleic acid aptamers targeting cell-surface proteins. *Methods* **54**, 215-225, doi:10.1016/j.ymeth.2011.02.002 (2011).

38 Zhou, J. & Rossi, J. J. Evolution of Cell-Type-Specific RNA Aptamers Via Live Cell-Based SELEX. *Methods in molecular biology* **1421**, 191-214, doi:10.1007/978-1-4939-3591-8_16 (2016).

39 Cerchia, L., Esposito, C. L., Jacobs, A. H., Tavitian, B. & de Franciscis, V. Differential SELEX in human glioma cell lines. *PloS one* **4**, e7971, doi:10.1371/journal.pone.0007971 (2009).

40 Sanger, F., Nicklen, S. & Coulson, A. R. DNA sequencing with chain-terminating inhibitors. *Proceedings of the National Academy of Sciences of the United States of America* **74**, 5463-5467 (1977).

41 Beier, R. *et al.* Selection of a DNA aptamer against norovirus capsid protein VP1. *FEMS microbiology letters* **351**, 162-169, doi:10.1111/1574-6968.12366 (2014).

42 Zimmermann, B., Gesell, T., Chen, D., Lorenz, C. & Schroeder, R. Monitoring genomic sequences during SELEX using high-throughput sequencing: neutral SELEX. *PloS one* **5**, e9169, doi:10.1371/journal.pone.0009169 (2010).

43 Beier, R., Boschke, E. & Labudde, D. New strategies for evaluation and analysis of SELEX experiments. *BioMed research international* **2014**, 849743, doi:10.1155/2014/849743 (2014).

44 Tolle, F. & Mayer, G. Preparation of SELEX Samples for Next-Generation Sequencing. *Methods in molecular biology* **1380**, 77-84, doi:10.1007/978-1-4939-3197-2_6 (2016).

45 Cho, M. *et al.* Quantitative selection of DNA aptamers through microfluidic selection and high-throughput sequencing. *Proceedings of the National Academy of Sciences of the United States of America* **107**, 15373-15378, doi:10.1073/pnas.1009331107 (2010).

46 Blank, M. Next-Generation Analysis of Deep Sequencing Data: Bringing Light into the Black Box of SELEX Experiments. *Methods in molecular biology* **1380**, 85-95, doi:10.1007/978-1-4939-3197-2_7 (2016).

47 Hoinka, J., Backofen, R. & Przytycka, T. M. AptaSUITE: A Full-Featured Bioinformatics Framework for the Comprehensive Analysis of Aptamers from HT-SELEX Experiments. *Molecular therapy. Nucleic acids* **11**, 515-517, doi:10.1016/j.omtn.2018.04.006 (2018).

48 Ruan, S., Joshua Swamidass, S. & Stormo, G. D. BEESEM: Estimation of Binding Energy Models Using HT-SELEX Data. *Bioinformatics*, doi:10.1093/bioinformatics/btx191 (2017).

49 Hoinka, J. & Przytycka, T. AptaPLEX - A dedicated, multithreaded demultiplexer for HT-SELEX data. *Methods* **106**, 82-85, doi:10.1016/j.ymeth.2016.04.011 (2016).

50 Thiel, W. H. & Giangrande, P. H. Analyzing HT-SELEX data with the Galaxy Project tools--A web based bioinformatics platform for biomedical research. *Methods* **97**, 3-10, doi:10.1016/j.ymeth.2015.10.008 (2016).

51 Fox, E. J., Reid-Bayliss, K. S., Emond, M. J. & Loeb, L. A. Accuracy of Next Generation Sequencing Platforms. *Next generation, sequencing & applications* **1**, doi:10.4172/jngsa.1000106 (2014).

52 Pfeiffer, F. *et al.* Systematic evaluation of error rates and causes in short samples in next-generation sequencing. *Scientific reports* **8**, 10950, doi:10.1038/s41598-018-29325-6 (2018).

53 Lapa, S. A., Chudinov, A. V. & Timofeev, E. N. The Toolbox for Modified Aptamers. *Molecular biotechnology* **58**, 79-92, doi:10.1007/s12033-015-9907-9 (2016).

54 Diafa, S. & Hollenstein, M. Generation of Aptamers with an Expanded Chemical Repertoire. *Molecules* **20**, 16643-16671, doi:10.3390/molecules200916643 (2015).

55 Chen, T., Hongdilokkul, N., Liu, Z., Thirunavukarasu, D. & Romesberg, F. E. The expanding world of DNA and RNA. *Current opinion in chemical biology* **34**, 80-87, doi:10.1016/j.cbpa.2016.08.001 (2016).

56 Nimjee, S. M., White, R. R., Becker, R. C. & Sullenger, B. A. Aptamers as Therapeutics. *Annual review of pharmacology and toxicology* **57**, 61-79, doi:10.1146/annurev-pharmtox-010716-104558 (2017).

57 Pfeiffer, F., Rosenthal, M., Siegl, J., Ewers, J. & Mayer, G. Customised nucleic acid libraries for enhanced aptamer selection and performance. *Current opinion in biotechnology* **48**, 111-118, doi:10.1016/j.copbio.2017.03.026 (2017).

58 Aschenbrenner, J. & Marx, A. DNA polymerases and biotechnological applications. *Current opinion in biotechnology* **48**, 187-195, doi:10.1016/j.copbio.2017.04.005 (2017).

59 Aschenbrenner, D., Baumann, F., Milles, L. F., Pippig, D. A. & Gaub, H. E. C-5 Propynyl Modifications Enhance the Mechanical Stability of DNA. *Chemphyschem : a European journal of chemical physics and physical chemistry* **16**, 2085-2090, doi:10.1002/cphc.201500193 (2015).

60 Kimoto, M., Yamashige, R., Matsunaga, K., Yokoyama, S. & Hirao, I. Generation of high-affinity DNA aptamers using an expanded genetic alphabet. *Nature biotechnology* **31**, 453-457, doi:10.1038/nbt.2556 (2013).

61 Pinheiro, V. B. & Holliger, P. Towards XNA nanotechnology: new materials from synthetic genetic polymers. *Trends in biotechnology* **32**, 321-328, doi:10.1016/j.tibtech.2014.03.010 (2014).

62 Keefe, A. D., Pai, S. & Ellington, A. Aptamers as therapeutics. *Nature reviews. Drug discovery* **9**, 537-550, doi:10.1038/nrd3141 (2010).

63 Jellinek, D. *et al.* Potent 2'-amino-2'-deoxypyrimidine RNA inhibitors of basic fibroblast growth factor. *Biochemistry* **34**, 11363-11372 (1995).

64 Pagratis, N. C. *et al.* Potent 2'-amino-, and 2'-fluoro-2'-deoxyribonucleotide RNA inhibitors of keratinocyte growth factor. *Nature biotechnology* **15**, 68-73, doi:10.1038/nbt0197-68 (1997).

65 Burmeister, P. E. *et al.* Direct in vitro selection of a 2'-O-methyl aptamer to VEGF. *Chemistry & biology* **12**, 25-33, doi:10.1016/j.chembiol.2004.10.017 (2005).

66 Pinheiro, V. B. & Holliger, P. The XNA world: progress towards replication and evolution of synthetic genetic polymers. *Current opinion in chemical biology* **16**, 245-252, doi:10.1016/j.cbpa.2012.05.198 (2012).

67 Darfeuille, F., Hansen, J. B., Orum, H., Di Primo, C. & Toulme, J. J. LNA/DNA chimeric oligomers mimic RNA aptamers targeted to the TAR RNA element of HIV-1. *Nucleic acids research* **32**, 3101-3107, doi:10.1093/nar/gkh636 (2004).

68 Elle, I. C. *et al.* Selection of LNA-containing DNA aptamers against recombinant human CD73. *Molecular bioSystems* **11**, 1260-1270, doi:10.1039/c5mb00045a (2015).

69 Schmidt, K. S. *et al.* Application of locked nucleic acids to improve aptamer in vivo stability and targeting function. *Nucleic acids research* **32**, 5757-5765, doi:10.1093/nar/gkh862 (2004).

70 Eckstein, F. Phosphorothioate oligodeoxynucleotides: what is their origin and what is unique about them? *Antisense & nucleic acid drug development* **10**, 117-121, doi:10.1089/oli.1.2000.10.117 (2000).

71 Pinheiro, V. B. *et al.* Synthetic genetic polymers capable of heredity and evolution. *Science* **336**, 341-344, doi:10.1126/science.1217622 (2012).

72 Houlihan, G., Arangundy-Franklin, S. & Holliger, P. Engineering and application of polymerases for synthetic genetics. *Current opinion in biotechnology* **48**, 168-179, doi:10.1016/j.copbio.2017.04.004 (2017).

73 Houlihan, G., Arangundy-Franklin, S. & Holliger, P. Exploring the Chemistry of Genetic Information Storage and Propagation through Polymerase Engineering. *Accounts of chemical research* **50**, 1079-1087, doi:10.1021/acs.accounts.7b00056 (2017).

74 Taylor, A. I. *et al.* Catalysts from synthetic genetic polymers. *Nature* **518**, 427-430, doi:10.1038/nature13982 (2015).

75 Taylor, A. I. & Holliger, P. Selecting Fully-Modified XNA Aptamers Using Synthetic Genetics. *Current protocols in chemical biology* **10**, e44, doi:10.1002/cpch.44 (2018).

76 Alves Ferreira-Bravo, I., Cozens, C., Holliger, P. & DeStefano, J. J. Selection of 2'-deoxy-2'-fluoroarabinonucleotide (FANA) aptamers that bind HIV-1 reverse transcriptase with picomolar affinity. *Nucleic acids research* **43**, 9587-9599, doi:10.1093/nar/gkv1057 (2015).

77 Ni, S. *et al.* Chemical Modifications of Nucleic Acid Aptamers for Therapeutic Purposes. *International journal of molecular sciences* **18**, doi:10.3390/ijms18081683 (2017).

78 Kuwahara, M. & Sugimoto, N. Molecular evolution of functional nucleic acids with chemical modifications. *Molecules* **15**, 5423-5444, doi:10.3390/molecules15085423 (2010).

79 Gold, L. *et al.* Aptamer-based multiplexed proteomic technology for biomarker discovery. *PloS one* **5**, e15004, doi:10.1371/journal.pone.0015004 (2010).

80 Keefe, A. D. & Cload, S. T. SELEX with modified nucleotides. *Current opinion in chemical biology* **12**, 448-456, doi:DOI 10.1016/j.cbpa.2008.06.028 (2008).

81 Eaton, B. E. The joys of in vitro selection: chemically dressing oligonucleotides to satiate protein targets. *Current opinion in chemical biology* **1**, 10-16 (1997).

82 Sefah, K. *et al.* In vitro selection with artificial expanded genetic information systems. *Proceedings of the National Academy of Sciences of the United States of America* **111**, 1449-1454, doi:10.1073/pnas.1311778111 (2014).

83 Eid, C., Palko, J. W., Katilius, E. & Santiago, J. G. Rapid Slow Off-Rate Modified Aptamer (SOMAmer)-Based Detection of C-Reactive Protein Using Isotachophoresis and an Ionic Spacer. *Analytical chemistry* **87**, 6736-6743, doi:10.1021/acs.analchem.5b00886 (2015).

84 Gupta, S. *et al.* Chemically modified DNA aptamers bind interleukin-6 with high affinity and inhibit signaling by blocking its interaction with interleukin-6 receptor. *The Journal of biological chemistry* **289**, 8706-8719, doi:10.1074/jbc.M113.532580 (2014).

85 Mian, I. S., Bradwell, A. R. & Olson, A. J. Structure, function and properties of antibody binding sites. *Journal of molecular biology* **217**, 133-151 (1991).

86 Ramaraj, T., Angel, T., Dratz, E. A., Jesaitis, A. J. & Mumey, B. Antigen-antibody interface properties: composition, residue interactions, and features of 53 non-redundant structures. *Biochimica et biophysica acta* **1824**, 520-532, doi:10.1016/j.bbapap.2011.12.007 (2012).

87 Gold, L. SELEX: How It Happened and Where It will Go. *Journal of molecular evolution* **81**, 140-143, doi:10.1007/s00239-015-9705-9 (2015).

88 Davies, D. R. *et al.* Unique motifs and hydrophobic interactions shape the binding of modified DNA ligands to protein targets. *Proceedings of the National Academy of Sciences of the United States of America* **109**, 19971-19976, doi:10.1073/pnas.1213933109 (2012).

89 Gelinas, A. D. *et al.* Crystal structure of interleukin-6 in complex with a modified nucleic acid ligand. *The Journal of biological chemistry* **289**, 8720-8734, doi:10.1074/jbc.M113.532697 (2014).

90 Rohloff, J. C. *et al.* Nucleic Acid Ligands With Protein-like Side Chains: Modified Aptamers and Their Use as Diagnostic and Therapeutic Agents. *Molecular therapy. Nucleic acids* **3**, e201, doi:10.1038/mtna.2014.49 (2014).

91 Gawande, B. N. *et al.* Selection of DNA aptamers with two modified bases. *Proceedings of the National Academy of Sciences of the United States of America* **114**, 2898-2903, doi:10.1073/pnas.1615475114 (2017).

92 Gierlich, J., Burley, G. A., Gramlich, P. M., Hammond, D. M. & Carell, T. Click chemistry as a reliable method for the high-density postsynthetic functionalization of alkyne-modified DNA. *Organic letters* **8**, 3639-3642, doi:10.1021/ol0610946 (2006).

93 El-Sagheer, A. H. & Brown, T. Click chemistry with DNA. *Chemical Society reviews* **39**, 1388-1405, doi:10.1039/b901971p (2010).

94 Nikic, I., Kang, J. H., Girona, G. E., Aramburu, I. V. & Lemke, E. A. Labeling proteins on live mammalian cells using click chemistry. *Nature protocols* **10**, 780-791, doi:10.1038/nprot.2015.045 (2015).

95 Sirbu, B. M., Couch, F. B. & Cortez, D. Monitoring the spatiotemporal dynamics of proteins at replication forks and in assembled chromatin using isolation of proteins on nascent DNA. *Nature protocols* **7**, 594-605, doi:10.1038/nprot.2012.010 (2012).

96 Shui, B. *et al.* RNA aptamers that functionally interact with green fluorescent protein and its derivatives. *Nucleic acids research* **40**, e39, doi:10.1093/nar/gkr1264 (2012).

97 Stanlis, K. K. & McIntosh, J. R. Single-strand DNA aptamers as probes for protein localization in cells. *The journal of histochemistry and cytochemistry : official journal of the Histochemistry Society* **51**, 797-808, doi:10.1177/002215540305100611 (2003).

98 Rosenthal, M., Pfeiffer, F. & Mayer, G. A Receptor-Guided Design Strategy for Ligand Identification. *Angewandte Chemie*, doi:10.1002/anie.201903479 (2019).

99 Gramlich, P. M., Wirges, C. T., Manetto, A. & Carell, T. Postsynthetic DNA modification through the copper-catalyzed azide-alkyne cycloaddition reaction. *Angewandte Chemie* **47**, 8350-8358, doi:10.1002/anie.200802077 (2008).

100 Wolter, O. & Mayer, G. Aptamers as Valuable Molecular Tools in Neurosciences. *The Journal of neuroscience : the official journal of the Society for Neuroscience* **37**, 2517-2523, doi:10.1523/JNEUROSCI.1969-16.2017 (2017).

101 Spill, F. *et al.* Controlling uncertainty in aptamer selection. *Proceedings of the National Academy of Sciences of the United States of America* **113**, 12076-12081, doi:10.1073/pnas.1605086113 (2016).

102 Antipova, O. M. *et al.* Advances in the Application of Modified Nucleotides in SELEX Technology. *Biochemistry. Biokhimiia* **83**, 1161-1172, doi:10.1134/S0006297918100024 (2018).

103 Takahashi, M. Aptamers targeting cell surface proteins. *Biochimie*, doi:10.1016/j.biochi.2017.11.019 (2017).

104 Hodgkin, A. L. & Huxley, A. F. Currents carried by sodium and potassium ions through the membrane of the giant axon of Loligo. *The Journal of physiology* **116**, 449-472 (1952).

105 Hodgkin, A. L. & Huxley, A. F. The components of membrane conductance in the giant axon of Loligo. *The Journal of physiology* **116**, 473-496 (1952).

106 Hodgkin, A. L. & Huxley, A. F. The dual effect of membrane potential on sodium conductance in the giant axon of Loligo. *The Journal of physiology* **116**, 497-506 (1952).

107 Hodgkin, A. L. & Huxley, A. F. A quantitative description of membrane current and its application to conduction and excitation in nerve. *The Journal of physiology* **117**, 500-544 (1952).

108 Hille, B. The permeability of the sodium channel to organic cations in myelinated nerve. *The Journal of general physiology* **58**, 599-619 (1971).

109 Hille, B. The permeability of the sodium channel to metal cations in myelinated nerve. *The Journal of general physiology* **59**, 637-658 (1972).

110 Hille, B. Ionic selectivity, saturation, and block in sodium channels. A four-barrier model. *The Journal of general physiology* **66**, 535-560 (1975).

111 Armstrong, C. M. Interaction of tetraethylammonium ion derivatives with the potassium channels of giant axons. *The Journal of general physiology* **58**, 413-437 (1971).

112 Hille, B. *Ionic Channels of Excitable Membranes*. Vol. 3rd ed. (Sinauer Associates Inc., Sunderland, MA., 2001).

113 Blumenthal, K. M. & Seibert, A. L. Voltage-gated sodium channel toxins: poisons, probes, and future promise. *Cell biochemistry and biophysics* **38**, 215-238, doi:10.1385/CBB:38:2:215 (2003).

114 Catterall, W. A. Voltage-gated sodium channels at 60: structure, function and pathophysiology. *The Journal of physiology* **590**, 2577-2589, doi:10.1113/jphysiol.2011.224204 (2012).

115 Corry, B. & Thomas, M. Mechanism of ion permeation and selectivity in a voltage gated sodium channel. *Journal of the American Chemical Society* **134**, 1840-1846, doi:10.1021/ja210020h (2012).

116 Bagal, S. K., Marron, B. E., Owen, R. M., Storer, R. I. & Swain, N. A. Voltage gated sodium channels as drug discovery targets. *Channels* **9**, 360-366, doi:10.1080/19336950.2015.1079674 (2015).

117 Bagal, S. K. *et al.* Ion channels as therapeutic targets: a drug discovery perspective. *Journal of medicinal chemistry* **56**, 593-624, doi:10.1021/jm3011433 (2013).

118 Harrison, D. C. Antiarrhythmic drug classification: new science and practical applications. *The American journal of cardiology* **56**, 185-187 (1985).

119 Narahashi, T., Anderson, N. C. & Moore, J. W. Comparison of tetrodotoxin and procaine in internally perfused squid giant axons. *The Journal of general physiology* **50**, 1413-1428 (1967).

120 Ragsdale, D. S., McPhee, J. C., Scheuer, T. & Catterall, W. A. Common molecular determinants of local anesthetic, antiarrhythmic, and anticonvulsant block of voltage-gated Na+ channels. *Proceedings of the National Academy of Sciences of the United States of America* **93**, 9270-9275 (1996).

121 Beneski, D. A. & Catterall, W. A. Covalent labeling of protein components of the sodium channel with a photoactivable derivative of scorpion toxin. *Proceedings of the National Academy of Sciences of the United States of America* **77**, 639-643 (1980).

122 Agnew, W. S., Moore, A. C., Levinson, S. R. & Raftery, M. A. Identification of a large molecular weight peptide associated with a tetrodotoxin binding protein from the electroplax of Electrophorus electricus. *Biochemical and biophysical research communications* **92**, 860-866 (1980).

123 Barchi, R. L. Protein components of the purified sodium channel from rat skeletal muscle sarcolemma. *Journal of neurochemistry* **40**, 1377-1385 (1983).

124 Noda, M. *et al.* Expression of functional sodium channels from cloned cDNA. *Nature* **322**, 826-828, doi:10.1038/322826a0 (1986).

125 Noda, M. *et al.* Primary structure of Electrophorus electricus sodium channel deduced from cDNA sequence. *Nature* **312**, 121-127 (1984).

126 Goldin, A. L. *et al.* Messenger RNA coding for only the alpha subunit of the rat brain Na channel is sufficient for expression of functional channels in Xenopus oocytes. *Proceedings of the National Academy of Sciences of the United States of America* **83**, 7503-7507 (1986).

127 Bezanilla, F. The voltage sensor in voltage-dependent ion channels. *Physiological reviews* **80**, 555-592, doi:10.1152/physrev.2000.80.2.555 (2000).

128 Catterall, W. A. Ion channel voltage sensors: structure, function, and pathophysiology. *Neuron* **67**, 915-928, doi:10.1016/j.neuron.2010.08.021 (2010).

129 Stuhmer, W. *et al.* Structural parts involved in activation and inactivation of the sodium channel. *Nature* **339**, 597-603, doi:10.1038/339597a0 (1989).

130 Kontis, K. J., Rounaghi, A. & Goldin, A. L. Sodium channel activation gating is affected by substitutions of voltage sensor positive charges in all four domains. *The Journal of general physiology* **110**, 391-401 (1997).

131 Catterall, W. A. & Zheng, N. Deciphering voltage-gated Na(+) and Ca(2+) channels by studying prokaryotic ancestors. *Trends Biochem Sci* **40**, 526-534, doi:10.1016/j.tibs.2015.07.002 (2015).

132 Payandeh, J., Scheuer, T., Zheng, N. & Catterall, W. A. The crystal structure of a voltage-gated sodium channel. *Nature* **475**, 353-358, doi:10.1038/nature10238 (2011).

133 Catterall, W. A. From ionic currents to molecular mechanisms: the structure and function of voltage-gated sodium channels. *Neuron* **26**, 13-25 (2000).

134 Zhang, X. *et al.* Crystal structure of an orthologue of the NaChBac voltage-gated sodium channel. *Nature* **486**, 130-134, doi:10.1038/nature11054 (2012).

135 McCusker, E. C. *et al.* Structure of a bacterial voltage-gated sodium channel pore reveals mechanisms of opening and closing. *Nature communications* **3**, 1102, doi:10.1038/ncomms2077 (2012).

136 Lenaeus, M. J. *et al.* Structures of closed and open states of a voltage-gated sodium channel. *Proceedings of the National Academy of Sciences of the United States of America*, doi:10.1073/pnas.1700761114 (2017).

137 Moreland, J. L., Gramada, A., Buzko, O. V., Zhang, Q. & Bourne, P. E. The Molecular Biology Toolkit (MBT): a modular platform for developing molecular visualization applications. *BMC Bioinformatics* **6**, 21, doi:10.1186/1471-2105-6-21 (2005).

138 Xu, D. & Zhang, Y. Generating triangulated macromolecular surfaces by Euclidean Distance Transform. *PloS one* **4**, e8140, doi:10.1371/journal.pone.0008140 (2009).

139 Pan, X. *et al.* Structure of the human voltage-gated sodium channel Nav1.4 in complex with beta1. *Science* **362**, doi:10.1126/science.aau2486 (2018).

140 Shen, H. *et al.* Structural basis for the modulation of voltage-gated sodium channels by animal toxins. *Science* **362**, doi:10.1126/science.aau2596 (2018).

141 Catterall, W. A., Goldin, A. L. & Waxman, S. G. International Union of Pharmacology. XLVII. Nomenclature and structure-function relationships of voltage-gated sodium channels. *Pharmacological reviews* **57**, 397-409, doi:10.1124/pr.57.4.4 (2005).

142 Catterall, W. A. Sodium channels, inherited epilepsy, and antiepileptic drugs. *Annual review of pharmacology and toxicology* **54**, 317-338, doi:10.1146/annurev-pharmtox-011112-140232 (2014).

143 Hille, B. The receptor for tetrodotoxin and saxitoxin. A structural hypothesis. *Biophysical journal* **15**, 615-619, doi:10.1016/S0006-3495(75)85842-5 (1975).

144 Kasteel, E. E. & Westerink, R. H. Comparison of the acute inhibitory effects of Tetrodotoxin (TTX) in rat and human neuronal networks for risk assessment purposes. *Toxicology letters* **270**, 12-16, doi:10.1016/j.toxlet.2017.02.014 (2017).

145 Furukawa, T., Sasaoka, T. & Hosoya, Y. Effects of tetrodotoxin on the neuromuscular junction. *The Japanese journal of physiology* **9**, 143-152 (1959).

146 Woodward, R. B. The structure of tetrodotoxin. *Pure Appl. Chem.* **9**, 49-74 (1964).

147 Narahashi, T., Moore, J. W. & Scott, W. R. Tetrodotoxin Blockage of Sodium Conductance Increase in Lobster Giant Axons. *The Journal of general physiology* **47**, 965-974 (1964).

148 Noda, M., Suzuki, H., Numa, S. & Stuhmer, W. A single point mutation confers tetrodotoxin and saxitoxin insensitivity on the sodium channel II. *FEBS letters* **259**, 213-216 (1989).

149 Terlau, H. *et al.* Mapping the site of block by tetrodotoxin and saxitoxin of sodium channel II. *FEBS letters* **293**, 93-96 (1991).

150 Stevens, M., Peigneur, S. & Tytgat, J. Neurotoxins and their binding areas on voltage-gated sodium channels. *Frontiers in pharmacology* **2**, 71, doi:10.3389/fphar.2011.00071 (2011).

151 Shamah, S. M., Healy, J. M. & Cload, S. T. Complex target SELEX. *Accounts of chemical research* **41**, 130-138, doi:10.1021/ar700142z (2008).

152 Su, Z. *et al.* Next-generation sequencing and its applications in molecular diagnostics. *Expert review of molecular diagnostics* **11**, 333-343, doi:10.1586/erm.11.3 (2011).

153 Balasubramanian, S. Sequencing nucleic acids: from chemistry to medicine. *Chemical communications* **47**, 7281-7286, doi:10.1039/c1cc11078k (2011).

154 Lipkind, G. M. & Fozzard, H. A. A structural model of the tetrodotoxin and saxitoxin binding site of the Na+ channel. *Biophysical journal* **66**, 1-13, doi:10.1016/S0006-3495(94)80746-5 (1994).

155 Tolle, F., Wilke, J., Wengel, J. & Mayer, G. By-product formation in repetitive PCR amplification of DNA libraries during SELEX. *PloS one* **9**, e114693, doi:10.1371/journal.pone.0114693 (2014).

156 Tolle, F., Rosenthal, M., Pfeiffer, F. & Mayer, G. Click Reaction on Solid Phase Enables High Fidelity Synthesis of Nucleobase-Modified DNA. *Bioconjugate chemistry* **27**, 500-503, doi:10.1021/acs.bioconjchem.5b00668 (2016).

157 Liu, Y. *et al.* Targeting inhibition of GluR1 Ser845 phosphorylation with an RNA aptamer that blocks AMPA receptor trafficking. *Journal of neurochemistry* **108**, 147-157, doi:10.1111/j.1471-4159.2008.05748.x (2009).

158 Rumpel, S., LeDoux, J., Zador, A. & Malinow, R. Postsynaptic receptor trafficking underlying a form of associative learning. *Science* **308**, 83-88, doi:10.1126/science.1103944 (2005).

159 Lee, J. H. *et al.* A monoclonal antibody that targets a NaV1.7 channel voltage sensor for pain and itch relief. *Cell* **157**, 1393-1404, doi:10.1016/j.cell.2014.03.064 (2014).

160 Raddatz, M. S. *et al.* Enrichment of cell-targeting and population-specific aptamers by fluorescence-activated cell sorting. *Angewandte Chemie* **47**, 5190-5193, doi:10.1002/anie.200800216 (2008).

161 Katzen, F., Peterson, T. C. & Kudlicki, W. Membrane protein expression: no cells required. *Trends in biotechnology* **27**, 455-460, doi:10.1016/j.tibtech.2009.05.005 (2009).

162 Takahashi, M., Sakota, E. & Nakamura, Y. The efficient cell-SELEX strategy, Icell-SELEX, using isogenic cell lines for selection and counter-selection to generate RNA aptamers to cell surface proteins. *Biochimie* **131**, 77-84, doi:10.1016/j.biochi.2016.09.018 (2016).

163 Kim, E. Y. *et al.* Selection of aptamers for mature white adipocytes by cell SELEX using flow cytometry. *PloS one* **9**, e97747, doi:10.1371/journal.pone.0097747 (2014).

164 Milo, R., Phillips, R. & Orme, N. *Cell biology by the numbers*. (2015).

165 Takahashi, M. Aptamers targeting cell surface proteins. *Biochimie* **145**, 63-72, doi:10.1016/j.biochi.2017.11.019 (2018).

166 Pestourie, C. *et al.* Comparison of different strategies to select aptamers against a transmembrane protein target. *Oligonucleotides* **16**, 323-335, doi:10.1089/oli.2006.16.323 (2006).

167 Wang, J., Rudzinski, J. F., Gong, Q., Soh, H. T. & Atzberger, P. J. Influence of target concentration and background binding on in vitro selection of affinity reagents. *PloS one* **7**, e43940, doi:10.1371/journal.pone.0043940 (2012).

168 Tahiri-Alaoui, A. *et al.* High affinity nucleic acid aptamers for streptavidin incorporated into bi-specific capture ligands. *Nucleic acids research* **30**, e45 (2002).

169 Wang, C., Yang, G., Luo, Z. & Ding, H. In vitro selection of high-affinity DNA aptamers for streptavidin. *Acta biochimica et biophysica Sinica* **41**, 335-340 (2009).

170 Polz, M. F. & Cavanaugh, C. M. Bias in template-to-product ratios in multitemplate PCR. *Applied and environmental microbiology* **64**, 3724-3730 (1998).

171 Tsien, R. Y. The green fluorescent protein. *Annual review of biochemistry* **67**, 509-544, doi:10.1146/annurev.biochem.67.1.509 (1998).

172 Berezovski, M. & Krylov, S. N. Thermochemistry of protein-DNA interaction studied with temperature-controlled nonequilibrium capillary electrophoresis of equilibrium mixtures. *Analytical chemistry* **77**, 1526-1529, doi:10.1021/ac048577c (2005).

173 Fukuda, H., Arai, M. & Kuwajima, K. Folding of green fluorescent protein and the cycle3 mutant. *Biochemistry* **39**, 12025-12032, doi:10.1021/bi000543l (2000).

174 Leiderman, P., Huppert, D. & Agmon, N. Transition in the temperature-dependence of GFP fluorescence: from proton wires to proton exit. *Biophysical journal* **90**, 1009-1018, doi:10.1529/biophysj.105.069393 (2006).

175 Ogawa, H., Inouye, S., Tsuji, F. I., Yasuda, K. & Umesono, K. Localization, trafficking, and temperature-dependence of the Aequorea green fluorescent protein in cultured vertebrate cells. *Proceedings of the National Academy of Sciences of the United States of America* **92**, 11899-11903, doi:10.1073/pnas.92.25.11899 (1995).

176 Wang, T., Chen, C., Larcher, L. M., Barrero, R. A. & Veedu, R. N. Three decades of nucleic acid aptamer technologies: Lessons learned, progress and opportunities on aptamer development. *Biotechnology advances* **37**, 28-50, doi:10.1016/j.biotechadv.2018.11.001 (2019).

177 Head, S. R. *et al.* Library construction for next-generation sequencing: overviews and challenges. *BioTechniques* **56**, 61-64, 66, 68, passim, doi:10.2144/000114133 (2014).

178 Kumar, N. & Maiti, S. Quadruplex to Watson-Crick duplex transition of the thrombin binding aptamer: a fluorescence resonance energy transfer study. *Biochemical and biophysical research communications* **319**, 759-767, doi:10.1016/j.bbrc.2004.05.052 (2004).

179 Hianik, T., Ostatna, V., Sonlajtnerova, M. & Grman, I. Influence of ionic strength, pH and aptamer configuration for binding affinity to thrombin. *Bioelectrochemistry* **70**, 127-133, doi:10.1016/j.bioelechem.2006.03.012 (2007).

180 Bini, A., Minunni, M., Tombelli, S., Centi, S. & Mascini, M. Analytical performances of aptamer-based sensing for thrombin detection. *Analytical chemistry* **79**, 3016-3019, doi:10.1021/ac070096g (2007).

181 Hall, B., Cater, S., Levy, M. & Ellington, A. D. Kinetic optimization of a protein-responsive aptamer beacon. *Biotechnology and bioengineering* **103**, 1049-1059, doi:10.1002/bit.22355 (2009).

182 Holmberg, A. *et al.* The biotin-streptavidin interaction can be reversibly broken using water at elevated temperatures. *Electrophoresis* **26**, 501-510, doi:10.1002/elps.200410070 (2005).

183 Junge, F. *et al.* Advances in cell-free protein synthesis for the functional and structural analysis of membrane proteins. *New biotechnology* **28**, 262-271, doi:10.1016/j.nbt.2010.07.002 (2011).

184 Rouse, S. L. & Sansom, M. S. Interactions of lipids and detergents with a viral ion channel protein: molecular dynamics simulation studies. *The journal of physical chemistry. B* **119**, 764-772, doi:10.1021/jp505127y (2015).

185 Berrier, C. *et al.* Cell-free synthesis of a functional ion channel in the absence of a membrane and in the presence of detergent. *Biochemistry* **43**, 12585-12591, doi:10.1021/bi049049y (2004).

186 Katzen, F. *et al.* Cell-free protein expression of membrane proteins using nanolipoprotein particles. *BioTechniques* **45**, 469, doi:10.2144/000112996 (2008).

187 Kujau, M. J. & Wolfl, S. Efficient preparation of single-stranded DNA for in vitro selection. *Molecular biotechnology* **7**, 333-335, doi:10.1007/BF02740823 (1997).

188 Tolle, F. *Click-SELEX - A versatile approach towards nucleobase-modified aptamers*, Rheinischen Friedrich-Wilhelms-Universität Bonn, (2016).

189 Pfeiffer, F. *Click-SELEX enables the selection of Δ9-tetrahydrocannabinol-binding nucleic acids*, RheinischenFriedrich-Wilhelms-Universität Bonn, (2018).

190 Haßel, S. K. *Aptamers for targeted activation of T cell-mediated immunity*, Rheinischen Friedrich-Wilhelms-Universität Bonn, (2016).